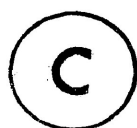


RELAXATION PROCESSES OF POLAR MOLECULES
IN SOME ORGANIC GLASSES

A Thesis Submitted to
LAKEHEAD UNIVERSITY
Thunder Bay, Ontario, Canada

by



MUHAMMED ABUL KASHEM

in partial fulfillment of the requirements for the

Degree of

MASTER OF SCIENCE

1982

ProQuest Number: 10611675

All rights reserved

INFORMATION TO ALL USERS

The quality of this reproduction is dependent upon the quality of the copy submitted.

In the unlikely event that the author did not send a complete manuscript and there are missing pages, these will be noted. Also, if material had to be removed, a note will indicate the deletion.



ProQuest 10611675

Published by ProQuest LLC (2017). Copyright of the Dissertation is held by the Author.

All rights reserved.

This work is protected against unauthorized copying under Title 17, United States Code
Microform Edition © ProQuest LLC.

ProQuest LLC.
789 East Eisenhower Parkway
P.O. Box 1346
Ann Arbor, MI 48106 - 1346

THESES

M.Sc.

1982

K11



(c) Muhammed A. Kashem 1982

TO MY FATHER

ABSTRACT

Dielectric absorption studies of a variety of polar solutes containing rotatable groups and of some analogous rigid molecules dispersed in (i) an atactic polystyrene matrix, (ii) glassy o-terphenyl and polyphenyl ether have been carried out. Sample preparations and the dielectric measurements using General Radio 1615-A and 1621 capacitance bridges with appropriate temperature-controllable cells have been described. The glass transition temperature measurements using the Glass Transition Temperature Measurement Apparatus have also been described. The experimental data as a function of frequency at different temperatures were subject to analysis by a series of computer programmes written in APL language. The activation energy barriers opposing the dielectric relaxation processes were obtained by the application of the Eyring rate equation.

Different types of polar rigid molecules have been studied mainly to provide sources of relaxation data and activation parameters in the three media for comparison with those of flexible molecules of analogous size.

The results of these rigid molecules have been used to obtain a correlation between enthalpy and entropy of activation; enthalpy of activation and volume needed for the reorientation of the rigid molecules. The activation parameters for the rigid molecules were found to depend on the nature of the solvent.

Of the flexible molecules, a variety of anisoles and acetophenones have been studied in the three media. Intramolecular processes involving the rotations of the methoxy and acetyl groups have been observed with enthalpies of $\sim 8 \text{ kJ mol}^{-1}$ and $\sim 30 \text{ kJ mol}^{-1}$ respectively.

A wide variety of aliphatic esters, $R_1C^*OOR_2$, has been examined in the three media and the rotation of groups around the central C-C* and/or C*-O bond was found. The barrier to rotation about the central C-C* bond in simple cases was found to be significantly lower (about $6-10 \text{ kJ mol}^{-1}$ in the absence of conjugative effect) than that about the C*-O bond ($\sim 22 \pm 2 \text{ kJ mol}^{-1}$ for methoxy group rotation in methyl chloroformate).

Rotation of the ester group has also been examined in a number of aromatic and some related esters. The intramolecular processes involving the rotation of both the ester group around the C-C* bond and the alkoxy group around the C*-O bond have been observed. The enthalpy of activation for methoxy group rotation around the C*-O bond in methyl salicylate is found to be 21 and 24 kJ mol⁻¹ in the pure compressed solid and polyphenyl ether, respectively.

In all the systems, the activation parameters for intramolecular motions were found to be independent of the media within the limits of experimental error.

ACKNOWLEDGEMENTS

The work described in this thesis was conducted at Lakehead University, Thunder Bay, Ontario, Canada, during the period from September 1980 to August 1982. I wish to express my deepest sense of gratitude and indebtedness to my research supervisor, Professor S. Walker for his indispensable guidance, generous help, invaluable suggestions and constant encouragement throughout this work.

I am also grateful to Dr. M.A. Saleh, Dr. J.P. Shukla, Dr. M.A. Desando and Mr. D.L. Gourlay for their occasional help and suggestions. I greatly acknowledge the co-operation of Mr. B.K. Morgan for his considerable technical assistance throughout the course of this work.

I am also thankful to Mrs. Joan Parnell for helping me in typing this thesis. Thanks are also due to Lakehead University for providing financial support for the research work.

Finally, I wish to express my gratitude
to my wife, Shahana Akter, for her keen interest and
inspiration in my work.

Thunder Bay,
August, 1982.

Author

TABLE OF CONTENTS

	<u>PAGE</u>
ABSTRACT.....	i
ACKNOWLEDGEMENTS.....	iv
TABLE OF CONTENTS.....	vi
LIST OF TABLES.....	viii
LIST OF FIGURES.....	x
CHAPTER I.....	1
Introduction.....	1
References.....	8
CHAPTER II.....	10
Basic Theory.....	11
References.....	22
CHAPTER III.....	23
Experimental.....	23
III.1 Introduction.....	24
III.2 Dielectric Measurement with GR Bridge.....	26
General Radio Bridge.....	26
The Capacitance Cells.....	28
Sample Preparations and Dielectric Measurements.....	30
Evaluation of Results.....	34
III.3 Glass Transition Temperature Measurement.....	40
References.....	46

TABLE OF CONTENTS continued...

	<u>PAGE</u>
CHAPTER IV.....	47
Dielectric Relaxation Processes of Rigid Polar Molecules in Some Organic Glasses.....	47
IV.1 Introduction.....	48
IV.2 Experimental Results.....	52
IV.3 Discussion.....	55
References.....	75
CHAPTER V.....	98
Relaxation Processes of Some Anisoles and Acetophenones.....	98
V.1 Introduction.....	99
V.2 Experimental Results.....	101
V.3 Discussion.....	103
References.....	114
CHAPTER VI.....	136
Dielectric Relaxation of Aliphatic Esters.....	136
VI.1 Introduction.....	137
VI.2 Experimental Results.....	142
VI.3 Discussion.....	145
References.....	172
CHAPTER VII.....	202
Dielectric Relaxation of Aromatic and Related Esters.....	202
VII.1 Introduction.....	203
VII.2 Experimental Results.....	207
VII.3 Discussion.....	210
References.....	230

LIST OF TABLES

		<u>PAGE</u>
TABLE IV.1	Eyring Analysis Results for Rigid Polar Molecules in Some Organic Glasses.....	77
TABLE IV.2	Fuoss-Kirkwood Analysis Parameters, ϵ_{∞} , and Effective Dipole Moments (μ) of Rigid Polar Molecules in Some Organic Glasses.....	80
TABLE V.1	Eyring Analysis Results for Some Anisoles and Acetophenones in Organic Glasses.....	116
TABLE V.2	Fuoss-Kirkwood Analysis Parameters, ϵ_{∞} , and Effective Dipole Moments (μ) of Some Anisoles and Acetophenones in Organic Glasses.....	118
TABLE V.3	Table Showing the Relationship Between Dielectric Loss and Molar Concentration for Acetophenone in Some Organic Glasses.....	124
TABLE VI.1	Infrared Stretching Frequencies and Dielectric Relaxation Data of Aliphatic Esters.....	175
TABLE VI.2	Tabulated Summary of Fuoss-Kirkwood Analysis Parameters and Effective Dipole Moments (μ) for Aliphatic Esters.....	180

LIST OF TABLES continued...

	<u>PAGE</u>
TABLE VII.1 Eyring Analysis Results for a Variety of Aromatic and Related Esters in Some Organic Glasses.....	232
TABLE VII.2 Tabulated Summary of Fuoss-Kirkwood Analysis Parameters, ϵ_{∞} , and Effective Dipole Moments (μ) for a variety of Aromatic and Related Esters.....	234

LIST OF FIGURES

		<u>PAGE</u>
FIGURE III.1	Three-terminal coaxial cell (Cell A).....	29
FIGURE III.2	Three terminal coaxial cell (Cell B).....	29
FIGURE III.3	Parallel-plate capacitance cell.....	29
FIGURE III.4	Glass Transition Temperature Measurement Apparatus.....	42
FIGURE III.5	A typical plot showing the measurement of glass transition temperature (T_g) of the sample containing methyl formate in polyphenyl ether.....	45
FIGURE IV.1	Structural formulae of some rigid molecules.....	53
FIGURE IV.2	Plot of ΔH_E versus ΔS_E for rigid molecules in polystyrene matrices.....	58

LIST OF FIGURES continued...

		<u>PAGE</u>
FIGURE IV.3	Plot of ΔH_E versus ΔS_E for rigid molecules in o-terphenyl.....	59
FIGURE IV.4	Plot of ΔH_E versus ΔS_E for rigid molecules in polyphenyl ether.....	60
FIGURE IV.5	Representation of molecular axes and the position of the molecular dipole in rigid molecules, as well as the possible rotational axes	62
FIGURE IV.6	Volume swept out by a rotating molecule.....	64
FIGURE IV.7	Plot of ΔH_E versus \bar{V}_{mean} of rigid molecules in polystyrene matrices.....	66
FIGURE IV.8	Plot of ΔH_E versus \bar{V}_{mean} of rigid molecules in o-terphenyl..	67
FIGURE IV.9	Plot of ΔH_E versus \bar{V}_{mean} of rigid molecules in poly- phenyl ether.....	68

LIST OF FIGURES continued...

		<u>PAGE</u>
FIGURE IV.10	ϵ'' versus T(K) plots for o-dichlorobenzene in a polystyrene matrix, o- terphenyl and polyphenyl ether.....	89
FIGURE IV.11	ϵ'' versus $\log_{10}f$ plot for o-dichlorobenzene in a polystyrene matrix.....	90
FIGURE IV.12	ϵ'' versus $\log_{10}f$ plot for chlorobenzene in o-terphenyl...	91
FIGURE IV.13	ϵ'' versus $\log_{10}f$ plot for benzonitrile in polyphenyl ether.....	92
FIGURE IV.14	$\log_{10}(T\tau)$ versus $1/T$ plots for bromoform in a polystyrene matrix, o-terphenyl and poly- phenyl ether.....	93
FIGURE IV.15	$\log_{10}(T\tau)$ versus $1/T$ plots for trichloroethylene in a poly- styrene matrix, o-terphenyl and polyphenyl ether.....	94

LIST OF FIGURES continued...

		<u>PAGE</u>
FIGURE IV.16	Log ₁₀ (Tτ) versus 1/T plots for o-dichlorobenzene in a polystyrene matrix, o- terphenyl and polyphenyl ether.....	95
FIGURE IV.17	Log ₁₀ (Tτ) versus 1/T plots for nitrobenzene in a poly- styrene matrix, o-terphenyl and polyphenyl ether.....	96
FIGURE IV.18	Log ₁₀ (Tτ) versus 1/T plots for 1-chloronaphthalene in a polystyrene matrix, o-terphenyl and polyphenyl ether.....	97
FIGURE V.1	Structural formulae of some anisoles and acetophenones.....	102
FIGURE V.2	ε" versus log ₁₀ f plot for para- methylanisole in a polystyrene matrix.....	126
FIGURE V.3	ε" versus log ₁₀ f plot for acetophenone in polyphenyl ether.....	127

LIST OF FIGURES continued...

	<u>PAGE</u>
FIGURE V.4	ϵ'' versus $\text{Log}_{10} f$ plot for para-bromoacetophenone in o-terphenyl..... 128
FIGURE V.5	ϵ'' versus T(K) plot for para-methylacetophenone in o-terphenyl..... 129
FIGURE V.6	ϵ'' versus T(K) plot for para-nitroacetophenone in o-terphenyl..... 130
FIGURE V.7	$\text{Log}_{10}(\text{T}\tau)$ versus 1/T plot for anisole in o-terphenyl..... 131
FIGURE V.8	$\text{Log}_{10}(\text{T}\tau)$ versus 1/T plot for para-bromoanisole in o- terphenyl..... 132
FIGURE V.9	$\text{Log}_{10}(\text{T}\tau)$ versus 1/T plot for para-dimethoxybenzene in polyphenyl ether..... 133
FIGURE V.10	$\text{Log}_{10}(\text{T}\tau)$ versus 1/T plots for acetophenone in a polystyrene matrix, o-terphenyl and poly- phenyl ether..... 134

LIST OF FIGURES continued...

		<u>PAGE</u>
FIGURE V.11	Log ₁₀ (Tτ) versus 1/T plot . for para-bromoacetophenone in o-terphenyl.....	135
FIGURE VI.1	Enthalpy of activation diagram for an iso- merization of an aliphatic ester.....	146
FIGURE VI.2	ε" versus log ₁₀ f plot for propyl formate in a polystyrene matrix.....	190
FIGURE VI.3	ε" versus log ₁₀ f plot for methyl crotonate in poly- phenyl ether.....	191
FIGURE VI.4	ε" versus log ₁₀ f plot for methyl chloroformate in o-terphenyl.....	192
FIGURE VI.5	Log ₁₀ (Tτ) versus 1/T plot for methyl acrylate in a poly- styrene matrix.....	193
FIGURE VI.6	Log ₁₀ (Tτ) versus 1/T plots for methyl crotonate in a polystyrene matrix, o-terphenyl and poly- phenyl ether.....	194

LIST OF FIGURES continued...

	<u>PAGE</u>
FIGURE VI.7	$\text{Log}_{10}(\tau)$ versus $1/T$ plot for vinyl chloroacetate in o-terphenyl..... 195
FIGURE VI.8	$\text{Log}_{10}(\tau)$ versus $1/T$ plot for dimethyl oxalate in a polystyrene matrix..... 196
FIGURE VI.9	$\text{Log}_{10}(\tau)$ versus $1/T$ plots for methyl chloroformate in a polystyrene matrix, o- terphenyl and polyphenyl ether. 197
FIGURE VI.10	Cole-Cole plot for methyl acetate in a polystyrene matrix..... 198
FIGURE VI.11	Cole-Cole plot for methyl propiolate in a polystyrene matrix..... 198
FIGURE VI.12	Cole-Cole plot for methyl chloroformate in o-terphenyl... 198
FIGURE VI.13	ϵ'' versus $T(K)$ plot for methyl propiolate in o-terphenyl..... 199

LIST OF FIGURES continued...

		<u>PAGE</u>
FIGURE VI.14	ϵ'' versus T(K) plot for vinyl butyrate in o-terphenyl.....	200
FIGURE VI.15	$\ln(\epsilon'')$ versus $\ln T(K)$ plot for methyl chloroformate in polyphenyl ether.....	201
FIGURE VII.1	Structural formulae of some aromatic and related esters....	208-209
FIGURE VII.2	ϵ'' versus $\log_{10} f$ plot for methyl benzoate in polyphenyl ether.....	241
FIGURE VII.3	ϵ'' versus $\log_{10} f$ plot for methyl cinnamate in o-terphenyl.....	242
FIGURE VII.4	ϵ'' versus $\log_{10} f$ plot for dimethyl-2,6-naphthalene dicarboxylate in a polystyrene matrix...	243
FIGURE VII.5	ϵ'' versus T(K) plot for cyclohexyl acrylate in a polystyrene matrix.....	244

LIST OF FIGURES continued...

	<u>PAGE</u>
FIGURE VII.6	$\text{Log}_{10}(\text{T}\tau)$ versus $1/\text{T}$ plot for methyl benzoate in polyphenyl ether..... 245
FIGURE VII.7	$\text{Log}_{10}(\text{T}\tau)$ versus $1/\text{T}$ plots for methyl cinnamate in a polystyrene matrix, o- terphenyl and polyphenyl ether..... 246
FIGURE VII.8	$\text{Log}_{10}(\text{T}\tau)$ versus $1/\text{T}$ plot for dimethyl-2,6-naphthalene dicarboxylate in a poly- styrene matrix (high tempera- ture process)..... 247
FIGURE VII.9	$\text{Log}_{10}(\text{T}\tau)$ versus $1/\text{T}$ plot for α -naphthyl acetate in a poly- styrene matrix (low tempera- ture process)..... 248
FIGURE VII.10	$\text{Log}_{10}(\text{T}\tau)$ versus $1/\text{T}$ plot for α -naphthyl acetate in a poly- styrene matrix (high tempera- ture process)..... 249
FIGURE VII.11	$\text{Log}_{10}(\text{T}\tau)$ versus $1/\text{T}$ plot for cyclohexyl acrylate in a poly- styrene matrix (low tempera- ture process)..... 250

LIST OF FIGURES continued...

	<u>PAGE</u>
FIGURE VII.12	
$\text{Log}_{10}(\tau)$ versus $1/T$	
plot for cyclohexyl	
acrylate in a polystyrene	
matrix (high temperature	
process).....	251

CHAPTER I

I N T R O D U C T I O N

I. INTRODUCTION

The use of dielectric methods to study the composition of the materials and the structure of their constituent molecules has a long history and numerous experiments have been carried out since its inception as a useful technique. The rotary movements of molecules are studied through i.r. and Raman spectroscopy as well as by direct dielectric and magnetic-resonance measurements (1-3). Of these, the dielectric absorption technique has been the subject of considerable interest in dealing with a wide variety of problems: studies of (i) the properties and uses of commercial dielectric materials, and (ii) the structure and molecular forces in different types of systems. After the successful application of the technique to determine the dipole moment and other molecular parameters for simple solids and liquids attention was turned to study the molecular and/or intramolecular motions of numerous molecules containing rotatable polar groups.

Earlier investigations at microwave frequencies have provided an effective means of studying molecular

structure in liquids and solutions (4,5). Aromatic molecules containing rotatable polar groups have been studied extensively by the dielectric absorption technique (6). Information about the dielectric properties of agricultural materials (7,8) as well as systems of biological interest (9,10) have also been the subject of applied studies in this area. Considerable information has also been obtained from dielectric relaxation studies of polymers and their aqueous solutions (11). Dielectric measurements (12) have provided a sensitive means of investigating the properties and uses of commercial dielectric materials in the solid phase.

Because of the recent progress in the development of stable sources and sensitive methods of detection, together with the use of computers for the analysis of experimental data, it is now possible to obtain accurate values of relaxation parameters for certain types of molecular and/or intramolecular motions.

The dielectric absorption of dipolar molecules, which contain a rotatable polar group may contain contributions from whole molecule and intramolecular group

reorientations (6). In the vast majority of cases, however, the dielectric absorption of the flexible group and the molecule itself are nearly always overlapped (13) so that it is difficult to obtain reliable results for the energy barriers associated with the relaxations. Group relaxation times, obtained from Budó-type analyses of the loss data, and the activation enthalpies for internal rotation generally contain appreciable errors. Dielectric studies of a wide variety of polar solutes dispersed in non-polar solvents of varying viscosities have indicated that the molecular relaxation times are more sensitive to the viscosity of the medium than the group relaxation times. Consequently, attempts have been made to separate the two processes by increasing the solvent viscosity.

In recent years, the dielectric absorption studies of polar solutes dispersed in a polymer matrix such as in polystyrene have received considerable attention in the literature. This method has proved its success for determining the accurate intramolecular energy barriers (14,15) which can also be obtained with the other relaxation techniques (15). One of the great advantages

of the polymer-matrix technique is that for a system with a flexible polar molecule, where both the molecular and intramolecular processes overlap, the relaxation time for the former can be increased to such an extent that either it may be considerably slowed down or may even be eliminated owing to the highly viscous surrounding medium, so that either or both the processes may be studied independently. Such a technique appeared more straightforward in comparison to the dielectric solution approach, since in solution studies complications are frequently met owing to the overlap of the different types of processes which for their separation require a Budó analyses which in a number of cases, is now known to be unsatisfactory (13). Moreover, the frequency and temperature ranges accessible to the solution studies are fairly limited, and hence relaxation parameters cannot be obtained with reasonable accuracy. However, these limitations may be overcome in the polymer-matrix techniques, since different instruments can be used to cover a wide frequency range of investigations over a broad temperature range, i.e., from liquid nitrogen temperature (~ 80 K) to the glass transition temperature of the matrix system. Thus, it seemed that the technique can be used more reliably for determining the activation

parameters, comparable to those determined by other direct relaxation methods.

Polystyrene is one of the most extensively used solvents by polymer-matrix technique. It has very little dielectric loss of its own (less than 1×10^{-3} over the frequency range 100 Hz to 1 GHz) below its glass transition temperature and thus, its dielectric interference with the dispersed solute is negligible. And it is now well established that dielectric studies of solutes dispersed in a polystyrene matrix are especially suited to group relaxation studies and may lead to the accurate determination of intramolecular energy barriers, since this process can sometimes be separated from the molecular relaxation owing to the high viscosity of the medium.

Most recently, two other molecular glass-forming solvent systems, o-terphenyl and polyphenyl ether, have been used by polymer-matrix technique. o-Terphenyl is a non-polar which melts at 328.7 K and the liquid may be cooled to a glass with an apparent glass transition at ~ 243 K. Previous works (17-20) have demonstrated that many supercooled liquid o-terphenyl solutions

are sufficiently stable above T_g to allow reproducible dielectric measurements. Polyphenyl ether is six-ring meta-linked bis(m(m-phenoxy phenoxy)phenyl)ether with a glass transition at about 270 K (21). This solvent differs from o-terphenyl and polystyrene in that it is more polar since it contains polar ether linkages and has a comparatively large loss α -process just above its T_g , but the absorption in the glassy state is of the order of $(1-1.5) \times 10^{-3}$ which is quite small (22).

The present work is aimed at gaining basic information on the relaxation behaviour of dipolar solutes dispersed in the latter two glassy solvents since negligible literature data are available in these solvents. Moreover, in order to make possible comparisons between the Eyring parameters observed for molecular and intramolecular motions in different solvents we chose to study a number of dipolar solutes, both rigid and flexible, in a polystyrene matrix, o-terphenyl and polyphenyl ether. The values of activation parameters determined for an intramolecular process in a polystyrene matrix will be used as the standard, and the corresponding values obtained in o-terphenyl and also in polyphenyl ether will be compared with these.

REFERENCES

1. R.G. Gordon, *Adv. Magn. Resonance*, 3(1981)1.
2. R.P. Young and R.N. Jones, *Chem. Rev.*,
71(1971)219.
3. M. Davies, *Ann. Reports (A)*, 67(1970)65.
4. N.E. Hill, W.E. Vaughan, A.H. Price and M.
Davies, "Dielectric Properties
and Molecular Behaviour", Van
Nostrand-Reinhold, London, (1969).
5. C.P. Smyth, "Dielectric Behaviour and Structure"
McGraw-Hill, London, (1955).
6. C.P. Smyth, *Adv. Mol. Relax. Proc.*, 1(1967-68)1.
7. T.P. Corcoran, O.S. Nelson, E.L. Stetson, and
W.C. Schlaphoff, *Transactions of the
ASAE*, 13(No.3)(1970)348.
8. O.S. Nelson, *Transactions of the ASAE*, 16(2)
(1973)384.
9. E.H. Grant, S.E. Keefe and S. Takashima, *J. Phys.
Chem.*, 72(1968)4373.
10. J.L. Salefran, G. Delbos, C. Marzat, and A.M.
Bottreau, *Adv. Mol. Relax. Inter.
Proc.*, 10(1977)35.
11. G.P. South and E.H. Grant, *Biopolymers*,
13(1974)1777.
12. R.J. Meakins, *Progress in Dielectrics*,
3(1961)151.
13. J. Crossley, S.P. Tay and S. Walker, *Adv. Mol.
Relax. Proc.*, 6(1974)79.
14. M. Davies and J. Swain, *Trans. Faraday Soc.*,
67(1971)1637.

15. S.P. Tay, S. Walker and E. Wyn-Jones, Adv. Mol. Relax. Inter. Proc., 13(1978)47.
16. W.J. Orville-Thomas, (ed), "Internal Rotation in Molecules", John Wiley and Sons, New York (1974).
17. G. Williams and P.J. Haines, Faraday Symp. Chem. Soc., 6(1972)14.
18. M. Nakamura, H. Takahashi, and K. Higasi, Bull. Chem. Soc. Japan, 47(1974)1593.
19. J. Crossley, D. Gourlay, M. Rujimethabhas, S.P. Tay and S. Walker, J. Chem. Phys., 71(1979)4095.
20. D.L. Gourlay, M.Sc. Thesis, Lakehead University, Thunder Bay, Ontario, Canada, (1982).
21. A.J. Barlow, J. Lamb and N.S. Taskoprülü, J. Acoust. Soc. Am., 46(1969)569.
22. J. Crossley, A. Heravi and S. Walker, J. Chem. Phys., 75(1981)418.

CHAPTER II

B A S I C T H E O R Y

BASIC THEORY

The dielectric constant or permittivity, ϵ' , of a material is a frequency-dependent quantity which may be expressed in terms of its polarizability in an applied electric field. For most simple polar molecules in non-polar solvents, all types of polarization can reach their equilibrium value when the applied field is of the order of 10^8 Hz or less. But at higher frequencies, the dipoles lag behind the field and polarization falls off so that its contribution to total permittivity decreases. It is this fall of polarizability with its associated fall of permittivity accompanied by the absorption of energy which constitutes dielectric dispersion.

The basic principles and fundamental equations for dealing with dielectric absorptions are well established. The total polarization (P_T) of a polar molecule is given by the Clausius-Mossotti-Debye (1) theories as:

$$\begin{aligned}
 P_T &= P_E + P_A + P_O \\
 &= \frac{4\pi N}{3} \left(\alpha_E + \alpha_A + \frac{\mu^2}{3kT} \right) \\
 &= \frac{\epsilon_0 - 1}{\epsilon_0 + 2} \cdot \frac{M}{d} \qquad \qquad \qquad (II.1)
 \end{aligned}$$

where α is the polarizability, N is Avogadro's number, k is the Boltzmann constant, μ the dielectric dipole moment, T the absolute temperature, M the gram molecular weight, d the density (g ml^{-1}), and ϵ_0 the static dielectric constant of the material. The subscripts, E, A and O in P indicate the electronic, atomic and orientation polarizations, respectively.

The Clausius-Mossotti-Debye theories are applicable to gases but are often inadequate when applied to polar liquids due to the invalidity of the Lorentz field used in these theories as a measure of the local field in a dipolar dielectric.

Onsager (2) developed the following expression in an attempt to obtain the relationship between permittivity and dipole moment in liquids and solids:

$$\frac{(\epsilon_0 - \epsilon_\infty)(2\epsilon_0 + \epsilon_\infty)}{\epsilon_0(\epsilon_\infty + 2)^2} \cdot \frac{M}{d} = \frac{4\pi N\mu^2}{9kT} \quad (\text{II.2})$$

where ϵ_∞ is the very high frequency or optical dielectric

constant. At very high frequency when the orientation polarization vanishes equation (II.1) becomes:

$$\frac{\epsilon_{\infty} - 1}{\epsilon_{\infty} + 2} \cdot \frac{M}{d} = \frac{4\pi N}{3} (\alpha_E + \alpha_A) \quad (\text{II.3})$$

ivity

Combination of equations (II.1) and II.3) gives the Debye equation:

$$\frac{3(\epsilon_0 - \epsilon_{\infty})}{(\epsilon_0 + 2)(\epsilon_{\infty} + 2)} \cdot \frac{M}{d} = \frac{4\pi N\mu^2}{9kT} \quad (\text{II.4})$$

equations (II.2) and (II.4) allow a comparison of the values of μ^2 given by Onsager and Debye equations:

$$\frac{\mu^2(\text{Onsager})}{\mu^2(\text{Debye})} = \frac{(2\epsilon_0 + \epsilon_{\infty})(\epsilon_0 + 2)}{3\epsilon_0(\epsilon_{\infty} + 2)} \quad (\text{II.5})$$

For gases at low pressures the Onsager equation reduces to the Debye equation when ϵ_0 and ϵ_{∞} are practically identical.

The molecular polarization is dependent on

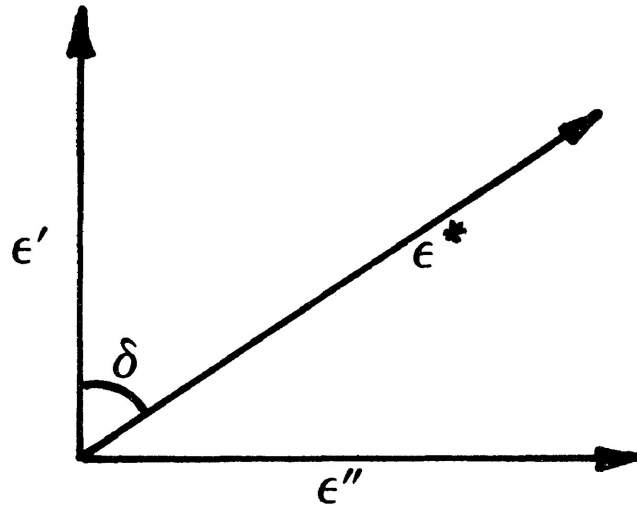
the frequency of the applied field. At low frequencies the dielectric constant is numerically equal to that obtained when a static field is employed. As the frequency of the applied field increases, the dipoles begin to lag behind and the orientation polarization (P_0) falls off so that its contribution to the total permittivity decreases. It is this decrease in polarization and permittivity and the resultant absorption of energy which describes the dielectric dispersion. The resulting phase displacement (δ) leads to a dissipation of energy, as Joule heating, in the medium, the measure of which is given by the dielectric loss (ϵ'') defined as:

$$\epsilon'' = \epsilon' \tan\delta \quad (\text{II.6})$$

where ϵ' is the real part of the dielectric constant and $\tan\delta$ is the loss tangent or energy dissipation factor. In this frequency region the dielectric constant is a complex quantity given by:

$$\epsilon^* = \epsilon' - i\epsilon'' \quad (i = \sqrt{-1}) \quad (\text{II.7})$$

The relationship between ϵ' , ϵ'' and δ is illustrated by the following diagram:



Dielectric relaxation is the exponential decay with time of the polarization in a dielectric when an external field is removed. The relaxation time, τ , is defined as the time in which the polarization is reduced to $1/e$ times its original value:

$$P(t) = P_0 \exp(-t/\tau) \quad (\text{II.8})$$

where $P(t)$ is the specific polarization at time t in an electromagnetic field.

The frequency dependence of the complex permittivity in the region of dielectric absorption for a

system characterized by a single discrete relaxation time is given by the Debye equation:

$$\epsilon^* = \epsilon_\infty + \frac{\epsilon_0 - \epsilon_\infty}{1 + i\omega\tau} \quad (\text{II.9})$$

where ω is the angular frequency in rad s^{-1} .

On combination of equations (II.7) and (II.9) followed by separation into real and imaginary parts lead to the Debye and Pellat equations:

$$\frac{\epsilon' - \epsilon_\infty}{\epsilon_0 - \epsilon_\infty} = \frac{1}{1 + (\omega\tau)^2} \quad (\text{II.10})$$

$$\frac{\epsilon''}{\epsilon_0 - \epsilon_\infty} = \frac{\omega\tau}{1 + (\omega\tau)^2} \quad (\text{II.11})$$

Elimination of $\omega\tau$ from these equations gives:

$$\left(\epsilon' - \frac{\epsilon_0 + \epsilon_\infty}{2}\right)^2 + (\epsilon'')^2 = \left(\frac{\epsilon_0 - \epsilon_\infty}{2}\right)^2 \quad (\text{II.12})$$

This is the equation of a circle with the centre lying on the abscissa. The locus of ϵ' and ϵ'' in an Argand diagram

is a semi-circle of radius $(\epsilon_0 - \epsilon_\infty)/2$ and is known as the Cole-Cole Plot (3).

For many systems these equations may be satisfactorily valid, but for the systems, where more than one relaxation process is involved in the dielectric absorption, the analysis of experimental data becomes more complicated. Cole and Cole (3) considered the case when there is a symmetrical distribution about the mean relaxation time, τ_0 , and obtained the relation:

$$\epsilon^* = \epsilon_\infty + \frac{\epsilon_0 - \epsilon_\infty}{1 + (i\omega\tau)^{1-\alpha}} \quad (\text{II.13})$$

where α is the distribution parameter whose values range $0 \leq \alpha \leq 1$, when $\alpha = 0$ the Debye equation is obtained.

A number of other functions has been considered for non-Debye type of absorption curves. Cole-Davidson (4) have formulated a function which describes right-skewed arcs. The equation is given by:

$$\epsilon^* = \epsilon' - i\epsilon'' = \epsilon_\infty + \frac{\epsilon_0 - \epsilon_\infty}{(1 + i\omega\tau)^\beta} \quad (\text{II.14})$$

where β is the asymmetric distribution co-efficient.

Fuoss and Kirkwood (5) also developed a theory regarding the distribution of relaxation times. These workers found that the dielectric loss of some polymers could be represented by the expression:

$$\epsilon'' = \epsilon''_{\max} \operatorname{sech}\left\{\beta \ln\left(\frac{f_{\text{obs}}}{f_{\max}}\right)\right\} \quad (\text{II.15})$$

The mean relaxation time characterizing the dipole motion giving rise to the absorption is represented by

$\tau = 1/\omega_{\max} = 1/2\pi f_{\max}$ where f_{\max} (Hz) is the frequency at which the maximum loss factor, ϵ''_{\max} , is observed.

β is itself a significant empirical parameter as its inverse measures the width of the absorption relative to the Debye process ($\beta = 1$), and f_{\max} are usually evaluated from the linear relationship:

$$\cosh^{-1}\left(\frac{\epsilon''_{\max}}{\epsilon''}\right) = 2.303(\log f_{\max} - \log f) \quad (\text{II.16})$$

For molecules, which contain a rotatable polar group, dielectric absorption may often be characterized by

two discrete relaxation times corresponding to molecular and intramolecular rotations. Budó (6) considered that for multiple discrete relaxation processes the complex dielectric constant could be represented by the superimposition of overlapping Debye absorptions. Thus, for systems having two discrete processes with relaxation times τ_1 and τ_2 the following equations can be deduced:

$$\frac{\epsilon' - \epsilon_\infty}{\epsilon_0 - \epsilon_\infty} = \frac{C_1}{1 + (\omega\tau_1)^2} + \frac{C_2}{1 + (\omega\tau_2)^2} \quad (\text{II.17})$$

$$\frac{\epsilon''}{\epsilon_0 - \epsilon_\infty} = \frac{C_1 \omega\tau_1}{1 + (\omega\tau_1)^2} + \frac{C_2 \omega\tau_2}{1 + (\omega\tau_2)^2} \quad (\text{II.18})$$

$$C_1 + C_2 = 1 \quad (\text{II.19})$$

where C_1 and C_2 are the weighting factors of the two contributing absorptions. When C_1/C_2 is small, an almost symmetrical Cole-Cole plot results. The dielectric absorp-

tion data for systems with significant τ_1/τ_2 and C_1/C_2 ratios may separate into two distinct absorption regions.

A number of models has been suggested to account for the mechanism of the molecular relaxation processes. Debye (1) has suggested a simple relaxation mechanism and according to his theory each dipole has two equilibrium positions separated by an energy barrier, ΔE . In such a situation the dipoles will oscillate within the potential minima, and sometimes acquire enough energy to jump the barrier.

The Eyring rate theory (7) is often applied to the reorientation of an electric dipole between two equilibrium positions. According to this treatment if ΔG_E is the free energy of activation for the dipole to reach the top of the barrier opposing reorientation, then the number of times such a reorientation occurs per second is given by the expression:

$$1/\tau = (\kappa kT/h) \exp(-\Delta G_E/RT) \quad (\text{II.20})$$

where T is the absolute temperature, h is Plank's constant, R is the universal gas constant, k the Boltzmann's

constant, and K is the transmission co-efficient normally taken to be 1; this corresponds with the case that each time the dipolar molecule is excited to the top of the energy barrier it continues to move in the same direction to the adjacent minimum position. Thus, the process is one of relaxation between two equilibrium positions but it is commonly referred to as rotation.

Since

$$\Delta G_E = \Delta H_E - T\Delta S_E$$

where ΔH_E is the heat of activation and ΔS_E the entropy of activation for this dipole relaxation process. Thus:

$$\tau = (h/kT) \exp(\Delta H_E/RT) \exp(-\Delta S_E/R) \quad (\text{II.21})$$

which on taking logarithms and rearrangement gives:

$$\ln \tau T = (\Delta H_E/RT) + \ln(h/k) - (\Delta S_E/R) \quad (\text{II.22})$$

Thus, it is evident from the above equations that a plot of $\ln(\tau T)$ versus $1/T$ is a straight line. The slope of the line therefore yields the ΔH_E value for the observed relaxation process.

References

1. P. Debye, "Polar Molecules", Chemical Catalog Co., New York, (1929).
2. L. Onsager, J. Am. Chem. Soc., 58(1936)1486.
3. K.S. Cole and R.H. Cole, J. Chem. Phys., 9(1941)341.
4. D.W. Davidson and R.H. Cole, J. Chem. Phys., 19(1951)1484.
5. R.M. Fuoss and J.G. Kirkwood, J. Am. Chem. Soc., 63(1941)385.
6. A. Budó, Z. Phys., 39(1938)706.
7. S. Glasstone, K.J. Laidler, and H. Eyring, "The Theory of Rate Processes", McGraw-Hill, New York, (1941).

CHAPTER III

E X P E R I M E N T A L

III.1 INTRODUCTION

When a material of dielectric constant ϵ completely fills the space between the two plates of an ideal capacitor, the dielectric constant is defined by the simple ratio:

$$\epsilon = \frac{C}{C_0} \quad (\text{III.1})$$

where C is the capacitance when the space is filled with the material, and C_0 is the capacitance measured when there is a perfect vacuum between the plates. In fact, however, ϵ is not a constant. It is a frequency-dependent complex quantity, and the complex dielectric permittivity, ϵ^* , defined as:

$$\epsilon^* = \epsilon' - i\epsilon'' \quad i = \sqrt{-1} \quad (\text{III.2})$$

If a sinusoidal potential of amplitude E and frequency $\omega \text{ rad s}^{-1}$ is applied to the capacitor, then the current I flowing through the circuit can be expressed as:

$$I = E\omega C = E\omega C_0(\epsilon' - i\epsilon'') \quad (\text{III.3})$$

in which the substitution for C and ω follows from equations (III.1) and (III.2), respectively. The real component, $E\omega C_0 \epsilon'$, known as the charging current is 90° out of phase with the applied potential and, therefore, does not need any electrical work to be done. If, however, the dielectric is a polar substance then the displacement current acquires an imaginary component, $E\omega C_0 \epsilon''$, in phase with the applied potential. This is known as the loss current, which is related to the energy dissipated as heat since it causes some electrical work to be done as given by the dot product, $EI = E^2 \omega C_0 \epsilon''$. Now, if we define δ as the angle between the total current and the charging current axis, i.e., the angle by which the charging current fails to become 90° out of phase with the potential, then:

$$\tan\delta = \frac{\text{loss current}}{\text{charging current}} = \frac{\epsilon''}{\epsilon'} \quad (\text{III.4})$$

where ϵ' is the observed dielectric constant according to equation (III.1) and ϵ'' is known as the loss factor, which is directly proportional to the concentration of the polar material in the dielectric. These principles are the basis of all dielectric measurements.

In this thesis most of the chemical systems studied were experimentally examined as solutes dissolved in (a) glassy o-terphenyl, (b) polyphenyl ether, commercially known as Santovac (1), and (c) polystyrene matrices. The solutes were either polar solids or liquids. Dielectric measurements were performed by the use of the General Radio 1615-A Capacitance bridge and the General Radio 1621 Precision Capacitance Measurement System. The glass transition temperature, T_g , of some of the chemical systems, were measured by the use of Glass Transition Measurement Apparatus. This instrument was designed by Mr. B. K. Morgan of this laboratory.

III.2 DIELECTRIC MEASUREMENT WITH GR BRIDGE

General Radio Bridge

The GR1615-A Capacitance bridge and the GR1621 Precision Capacitance Measurement system are manufactured by General Radio Company, Concord, Massachusetts, U.S.A. The GR1615-A bridge allows measurement of the capacitance and conductivity of a sample to be made at frequencies ranging from 50 Hz to 10^5 Hz. This system consists of GR1310-B sine wave signal generator and 1232A tuneable

amplifier-null detector. While the GR1621 system consists of the GR1616 Precision Capacitance bridge with the GR1316 Oscillator and the GR1238 Detector. This GR1621 system measures the capacitance and the conductivity of a capacitor more precisely in the frequency range of 10 Hz to 10^5 Hz. After warm up the frequency stability is typically within $\pm 0.001\%$ for a few minutes. Also, with the help of this later system a wide range of capacitance can be measured, extending from the resolution limit of 0.1 aF (10^{-7} picofarad) to a maximum of 10 μ F (10 microfarad), with internal standards, or farther with external standards.

The GR bridge measures the capacitance and conductivity of the capacitor, which can be related to the components of the complex permittivity by the following equations (2):

$$\epsilon' = C/C_0 \quad (\text{III.5})$$

and

$$\epsilon'' = G/\omega C_0 \quad (\text{III.6})$$

where G is the conductivity of the system and the other terms have their usual meaning, mentioned previously. Actual measurements were made by bringing the bridge into balance as indicated by null-detector for solutions studied in different three-terminal co-axial and parallel-plate capacitance cells.

The Capacitance Cells

The cells, designed by Mr. B. K. Morgan of this laboratory, described earlier by previous workers. However, the cells which were used for this work are illustrated in the following figures (reproduced by the courtesy of D. L. Gourlay (3)). Figure III.1 and Figure III.2 present the two three-terminal coaxial cells referred to as cell A and cell B, respectively. Cell B had been designed as a modification of cell A, to decrease the requisite volume of sample required for study but both operated on the same basic principle. The temperature stabilization time and also, the length of time required for the capacitance and dissipation factors of the bridge to reach constant values, have indeed been decreased by this modified cell design. Cell A and cell B were used for dielectric measurements of the samples (which are

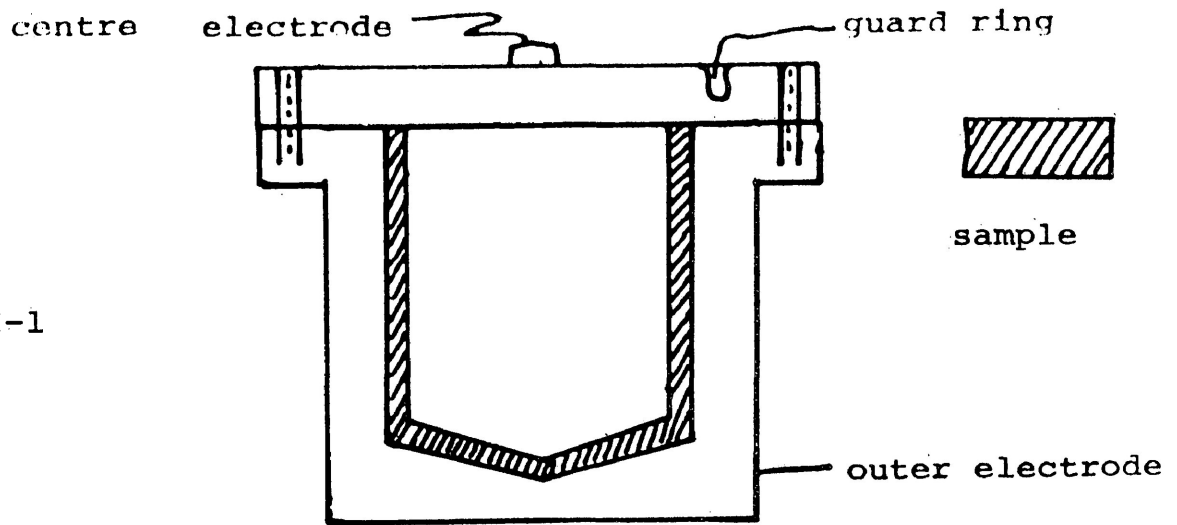


FIGURE III-1

Cell A: Three terminal coaxial cell

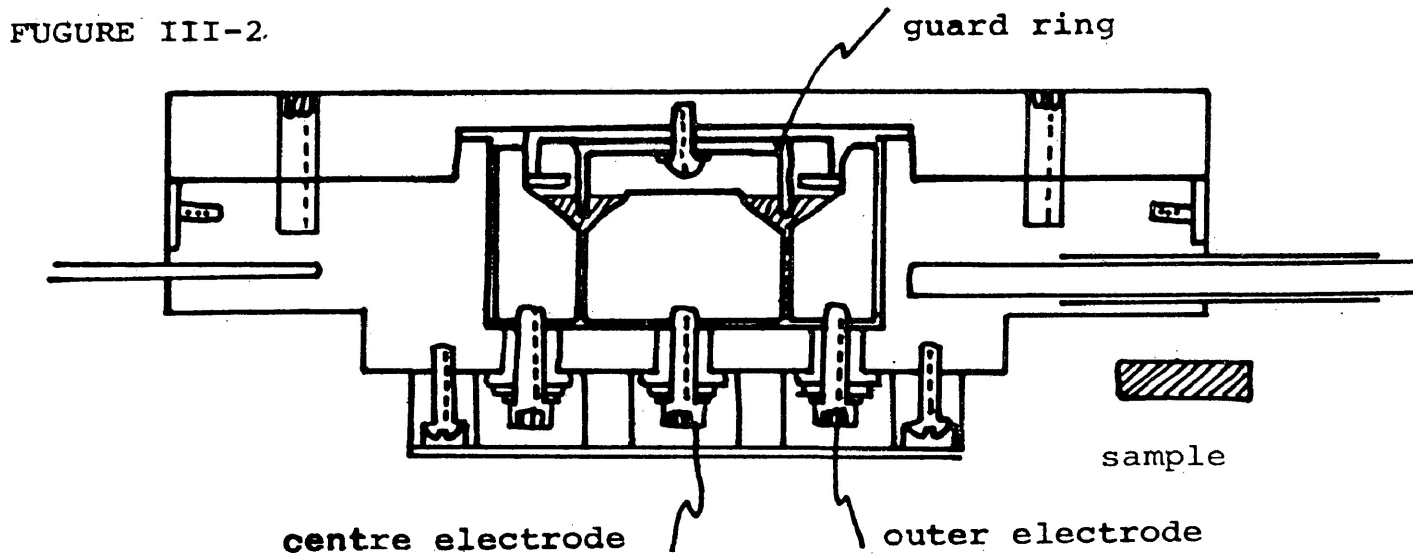
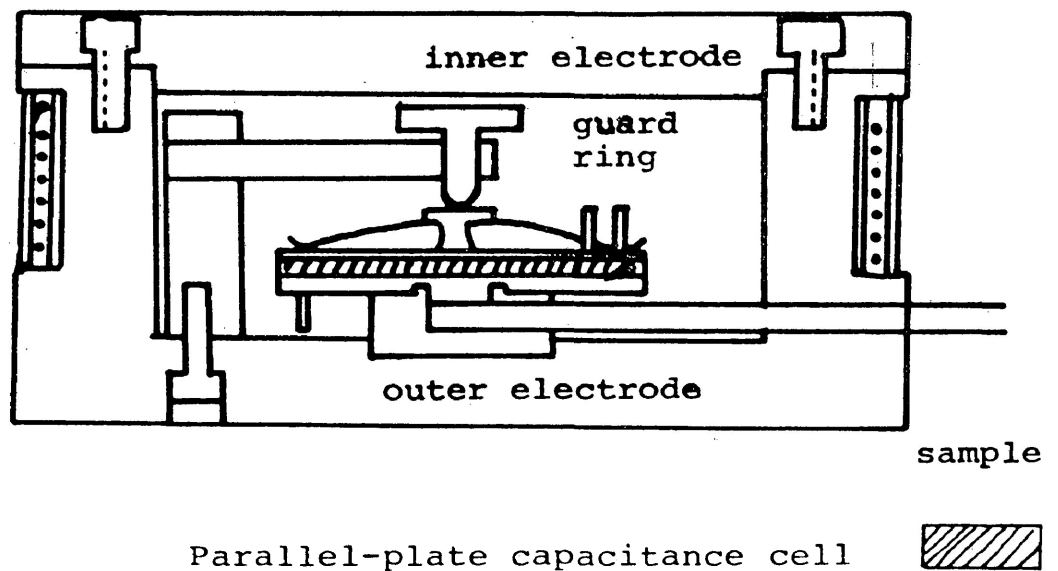


FIGURE III-2

Cell B: Three terminal coaxial cell

FIGURE III-3



Parallel-plate capacitance cell

liquid at room temperature) in o-terphenyl and polyphenyl ether. Figure III-3 presents the three-terminal circular parallel-plate capacitance cell which was used for dielectric measurements of samples dispersed in polystyrene matrices in the form of solid disc.

The capacitance cells, regardless of design, were encased in essentially the same type of air-tight aluminium chamber. Each cell was cooled from the top by conduction through a flat-bottomed, styrofoam insulated, liquid nitrogen container. Heating balance was accomplished through a temperature control circuit consisting of a thermocouple, and a thermoelectric temperature controller model 3814021133 unit (accuracy $\pm 0.1^{\circ}\text{C}$) using nichrome wire heating element surrounding the cell.

SAMPLE PREPARATIONS AND DIELECTRIC MEASUREMENTS

Samples placed in the coaxial cells were liquid solutions. The solutions were prepared by adding a given quantity of polar solute to a heated quantity of solvent such that the resultant solution had a weight/weight concentration of about 8% or less depending upon the magnitude of the dipole moment of the solute and, in

certain cases, on the solubility of the solute in the solvent. The two main solvents used in these studies were o-terphenyl and polyphenyl ether (1). The solvents were initially heated to about 333 K in order to facilitate the dissolution of the added solute and also in the case of o-terphenyl, to melt the solvent. The solutions were then left for about twenty-four hours to ensure a homogeneous solution. The cells were heated again to above 333 K, filled with the solution and then cooled quickly with an aluminium flat-bottomed liquid nitrogen vessel. The cooling rate was approximately 10 K per minute for cell A and about 18 K per minute for cell B.

For a chemical system, the dielectric characteristics of which were unknown, the sample was cooled down to near liquid nitrogen temperature and slowly heated up to the glass transition temperature while capacitance and dissipation (conductance in the case of GR1621) at recorded temperatures were taken periodically. From the resultant plot of $\tan\delta$ (as calculated from experimental data) versus temperature (K) at fixed frequency (usually 1 kHz), suspected areas of dielectric absorption were identified. The system was then heated again to 333 K and cooled quickly to some temperature well

below the temperature at which the absorption process was expected to begin from the lowest frequency of the measurement. Full frequency dielectric measurements at specific temperatures were then carried out so as to obtain a broad $\log f_{\max}$ range as possible. The temperature was recorded to an accuracy of $\pm 0.1^{\circ}\text{C}$ with the help of a Newport 264-3 platinum resistance thermometer.

In the case of solutions of polar solutes dispersed in atactic polystyrene, the samples were prepared by employing the procedure similar to that described by Davies and Swain (4). The desired amount of solute (0.2~0.4 g) and polystyrene pellets (nearly 4 g as required to make about 5 mol % of the former) were dissolved in ~10 ml of 1,2-transdichloroethylene, in a porcelain crucible. The mixture was stirred thoroughly, until it dissolved completely, followed by evaporation in a drying oven at about $85 - 100^{\circ}\text{C}$. The plastic mass was then placed in a stainless steel die, removed, trimmed to size, and its average thickness was measured. The weight of the disc was also noted, and the molar concentration of the solute in the matrix was calculated according to the formula given by Tay and Walker (5) as:

$$\text{Concentration} = \frac{\text{wt. of solute used}}{\text{mol wt. of solute}} \times \frac{\text{wt. of disc}}{\text{wt. of P.S.+ solute}}$$

$$\times \frac{1000}{\text{vol. of disc}}$$

The polystyrene matrix disc was then clamped between the electrodes of the parallel-plate capacitance cell and the dielectric measurement carried out in the previously described fashion.

Measurements made with the General Radio bridge were of dissipation or conductivity factors and capacitance. The product of the frequency and dissipation factor yields the loss tangent value, $\tan\delta$. With these values obtained experimentally and the following relations, it was possible to determine dielectric loss values for the parallel-plate capacitance cell.

$$\epsilon'' = \epsilon' \tan\delta \quad (\text{II .6})$$

$$\epsilon' = \frac{Cd}{0.08842A} \quad (\text{III.7})$$

and

$$\epsilon'' = \frac{\epsilon' G}{\omega C} \quad (\text{III.8})$$

where C is the capacitance of the cell with the sample in picofarads, d is the spacing of the capacitance plates (in cm), A is the effective area of the plates (in cm^2), G is the conductivity of the system in picomhos. The effective area of the electrode plates, A , had been determined by measuring the capacitance of the cell containing a standard quartz disc of diameter 2.0 inches, thickness 0.0538 inches (supplied by the Rutherford Research Products Co., New Jersey, U.S.A.) with a dielectric constant of 3.819.

The coaxial cells were also calibrated, to determine relevant constants, with purified cyclohexane at room temperature. Calibration studies were also carried out down to liquid nitrogen temperatures to see if there was any variation between values of ϵ' determined at room temperature and those at lower temperatures. Variation was considered negligible.

EVALUATION OF RESULTS

The experimental data, obtained by dielectric measurements, were analysed by the use of a series of calculator and computer programmes. The programmes were

written in the APL language. The dielectric loss of the sample solution was calculated using the Texas SR59 programmable calculator and the loss for the pure solute was then obtained by subtracting the values for the pure solvent at each frequency (obtained through similar measurements) from that observed for the sample solution, i.e.:

$$\epsilon''_{\text{solute}} = \epsilon''_{\text{solution}} - \epsilon''_{\text{solvent}}$$

For each measurement of temperature, the data of dielectric loss factor as a function of frequency were analysed by the computer according to the Fuoss-Kirkwood equation, (II.15), by a procedure employed by Davies and Swain (4). By iteration the computer programme finds that the value of ϵ''_{max} provides the best linear fit to the plot of $\cosh^{-1}(\epsilon''_{\text{max}}/\epsilon'')$ against $\ln(f)$. From the slope of this line the value of the distribution parameter, β , is deduced. The frequency of maximum dielectric loss, f_{max} , is obtained from this slope and the intercept of the line on the \cosh^{-1} -axis.

The Fuoss-Kirkwood equation does not consider the real part of the complex permittivity nor does it

deal with the limiting values at low and high frequencies, ϵ_0 , and ϵ_∞ , respectively, except that the total dispersion is given by the expression:

$$\Delta\epsilon' = \epsilon_0 - \epsilon_\infty = \frac{2\epsilon''_{\max}}{\beta} \quad (\text{III.9})$$

Therefore, the analysis was supplemented with the Cole-Cole equation (II.13) to obtain ϵ_∞ in conjunction with the following relation (6) for the value of α , the Cole-Cole distribution parameter:

$$\beta = \frac{1-\alpha}{\sqrt{2} \cos\left(\frac{\pi(1-\alpha)}{4}\right)} \quad (\text{III.10})$$

Several estimates of ϵ_∞ were obtained from the Cole-Cole equation given the experimental values of ϵ' at various frequencies. The average of these estimates was calculated, along with a value for ϵ' at the frequency of maximum loss.

The calculation of the effective dipole moments involved in the dielectric relaxation process was made by using the Debye (7) equation (III.11) and the Onsager (8) equation (III.12):

$$\mu^2 = \frac{2700 \text{ kT } (\epsilon_0 - \epsilon_\infty)}{4\pi Nc (\epsilon' + 2)^2} \quad (\text{III.11})$$

$$\mu^2 = \frac{900 \text{ kT } (2\epsilon_0 + \epsilon_\infty) (\epsilon_0 - \epsilon_\infty)}{4\pi Nc \epsilon_0 (\epsilon_\infty + 2)^2} \quad (\text{III.12})$$

where the value of $(\epsilon_0 - \epsilon_\infty)$ is given by the equation (III.9), ϵ' is the value of ϵ' at $\omega_{\text{max}} = 1/\tau_0 = 2\pi f_{\text{max}}$, ϵ_0 is the static dielectric constant derived from the estimated average of ϵ_∞ and equation (III.9), c is the concentration in moles.litre⁻¹, T is the temperature in K, N is the Avogadro's number, and k the Boltzmann constant. These equations yield μ in units of e.s.u.-cm, but commonly this parameter is expressed in Debye units, where:

$$1 \text{ D} = 1 \times 10^{-18} \text{ e.s.u. -cm}$$

The dipole moments observed at different temperatures were then fed into a separate computer programme to estimate the extrapolated values of the dipole moment at temperatures above those of measurement. This technique is similar to that employed by Davies and Swain (4) and was based on the assumption that the dipole

moment is a linear function of temperature. It seemed from their work that this method yielded reasonable results, although there is a little theoretical basis for such a procedure. However, in many cases it is well established that the variation of ϵ_0 and ϵ_∞ with temperature may be described by an equation of the form $\log(\epsilon) = aT+b$ (9).

The energy barrier which must be surmounted in the motion of the dipole was evaluated in terms of the Eyring enthalpy of activation, ΔH_E , by using the Eyring rate expression equation (II.21), a procedure commonly used in dielectric work (4,10):

$$\tau = \frac{1}{\text{rate}} = \frac{h}{kT} \left(\exp\left(\frac{-\Delta G_E}{RT}\right) \right)$$

$$\tau = \frac{h}{kT} \exp\left(\frac{\Delta H_E}{RT}\right) \exp\left(\frac{-\Delta S_E}{R}\right) \quad (\text{II.21})$$

which can be rearranged to the linear form as:

$$\ln(T\tau) = \frac{\Delta H_E}{R} - \left(\frac{\Delta S_E}{R} - \ln\left(\frac{h}{k}\right)\right) \quad (\text{II.22})$$

The plots of $\log(T\tau)$ against $1/T$ yielded good straight lines, and from the slope and intercept of this line, the

values of the enthalpy of activation, ΔH_E , and the entropy of activation, ΔS_E , respectively were evaluated with the help of a computer programme. The programme also calculates relaxation times ' τ ' and free energies of activation $\Delta G_E (= \Delta H_E - T\Delta S_E)$ at different temperatures.

The result of the analyses of dielectric data to obtain Fuoss-Kirkwood parameters, $\log_{10}(f_{\max})$, ϵ''_{\max} , and β , the relaxation time, τ , and the limiting high frequency dielectric constant, ϵ_{∞} , and the effective dipole moments, μ , are collected in tables in each chapter. The results of Eyring analyses of these data are also presented in each of the following chapters.

Standard statistical techniques (11) provide a means of estimating errors in fitting a straight line to a set of graph points. The FUOSSK computer programme calculated errors in $\log f_{\max}$ and β for the 90%, 95%, 98%, and 99% confidence intervals. The 95% confidence interval was chosen as a good representation of experimental error, typical values for $\log_{10}(f_{\max})$ being ± 0.05 to 0.10.

The same technique was adopted to calculate

the 95% confidence intervals for both ΔH_E and ΔS_E . In the present work, the maximum error in ΔH_E is hardly greater than $\pm 10\%$ or $\pm 3 \text{ kJ mol}^{-1}$ whichever be the greater .

The structural diagrams of some typical molecules investigated are given in the experimental section of each Chapter.

III.3 GLASS TRANSITION TEMPERATURE MEASUREMENT

The Glass Transition Temperature Measurement apparatus, shown in Figure III.4, designed by Mr. B. K. Morgan of this laboratory, detects linear expansion of solid or frozen liquid samples. Heating the sample N causes the inner pyrex tube to move upwards relative to the outer pyrex tube. This movement is transmitted from the cap of the inner tube to the core of the transducer C. Movement of the core causes a change in the electromagnetic coupling between the input and output coils of the transducer. The output coil is connected to a strip chart recorder which displays a rising trace as the sample is heated towards the glass transition temperature. Near the glass transition temperature the trace levels off and

KEY TO FIGURE III.4 ON FACING PAGE

A	24DC IN
B	VOLTAGE OUT TO CHART RECORDER
C	H.P. 24DC DT-100 TRANSDUCER
D	TRANSDUCER CORE WITH OFFSET WEIGHT
E	TRANSDUCER HEIGHT ADJUSTMENT SCREW
F	OUTER PYREX TUBE
G	INNER PYREX TUBE
H	INNER TUBE GUIDE ROD SUPPORT
J	INNER TUBE CAP
K	LIQUID NITROGEN FUNNEL
L	STYROFOAM INSULATION
M	HEATING BLOCK
N	LIQUID SAMPLE IN DISPOSABLE HOLDER
O	PYREX DISH
P	INSULATION
Q	THERMOMETER PROBE
R	THERMOREGULATOR PROBE
S	SOLID SAMPLE HOLDER
T	HEATING BLOCK

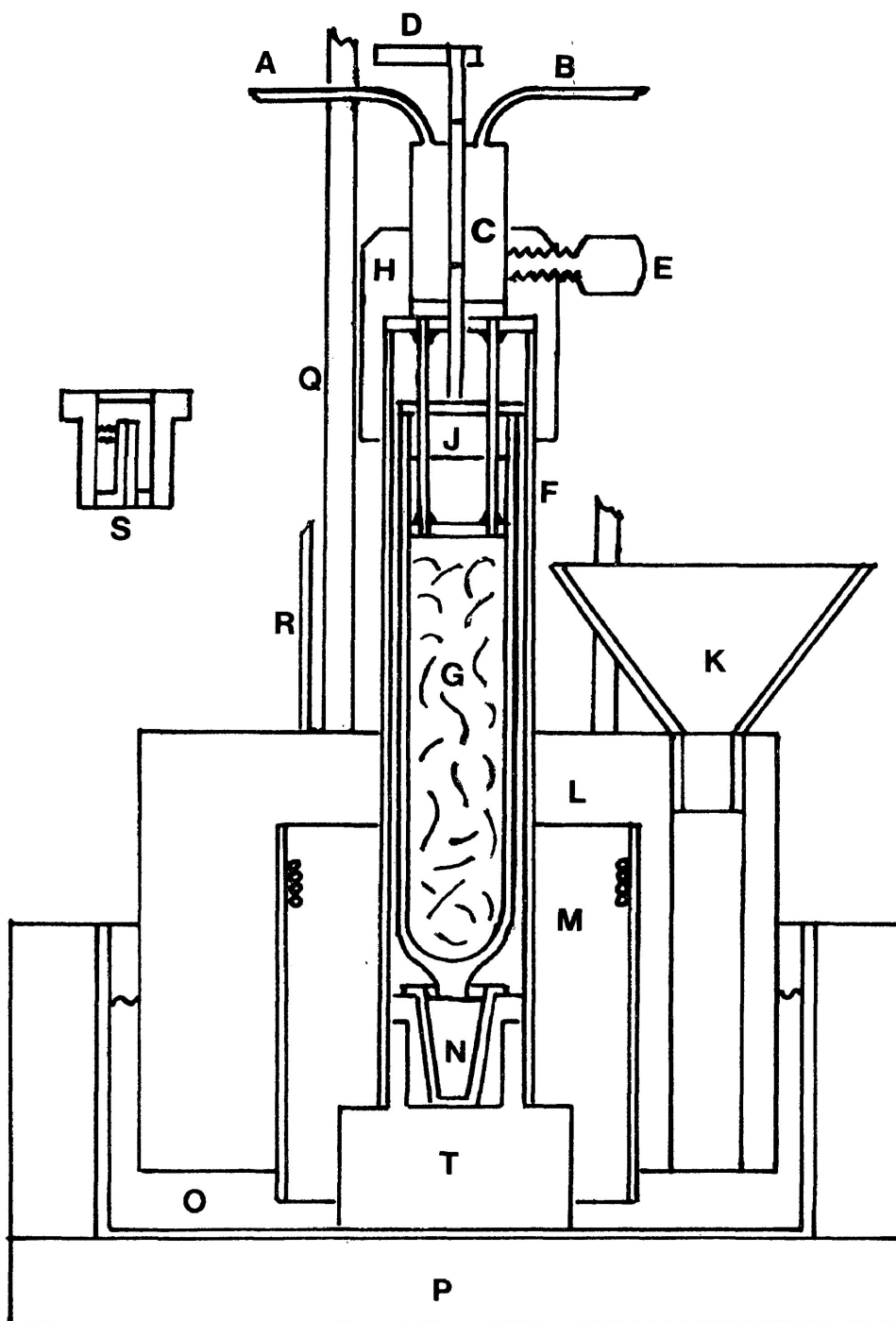


Figure : III-4 Glass Transition Temperature Measurement Apparatus.

and then begins to fall as the sample softens. There are two interchangeable sample holders with the apparatus. The sample holder S for the sample, solid at room temperature, and N for the samples which are liquid at room temperature. The idea for this instrument was suggested by Dr. N. Koizumi. His apparatus was much larger measuring the sample expansion and temperature changes under vacuum. Both changes being measured simultaneously on an X-Y recorder. He also employed a Hewlett Packard transducer, model #24DCDT-100.

The solid sample was prepared in the form of a strip roughly 20 mm x 8 mm and 1 to 2 mm thick. The sample was secured at one end by a small screw in a slotted rod which fits freely in sample holder S. The liquid sample was poured at room temperature into a disposable polyethylene cup. The cup was placed in its stainless steel holder under the central pyrex tube. The central tube was raised by the cap of the outer tube, to which it was connected by two sliding rods, it was not lowered until the sample had been frozen.

The sample holder, sitting within two interlocking circular blocks M and T, was cooled rapidly (where the sample needed to be frozen) by pouring liquid nitrogen

into funnel K. The funnel was held by the microcellular polystyrene insulation which surrounded block M. When the sample had been cooled to about 40°C below the expected glass transition temperature the transducer position was adjusted. With the central tube in contact with the sample, the transducer was carefully moved up and down until the pen of the chart recorder registers on the bottom of the scale. With a regulated voltage of 24 volts D.C. applied to the transducer, a recorder sensitivity of 500 mv, a chart speed of 8 inch per hr was selected. The temperature was controlled by a thermoelectric temperature controller, model 3814021133. The 110 volts output of the controller was reduced to about 60 volts through a variac transformer which was wired to the heating block M. The temperature of the sample was raised by manually raising the digital temperature setting of the controller in increments of 1°C per min. The temperature was recorded with the help of Newport 254-3 platinum resistance thermometer and the temperature was also periodically recorded by hand on the chart until the glass transition temperature passed. Figure III.5 shows a typical plot of glass transition temperature measurement results, which also demonstrate the working principle of the apparatus more clearly.

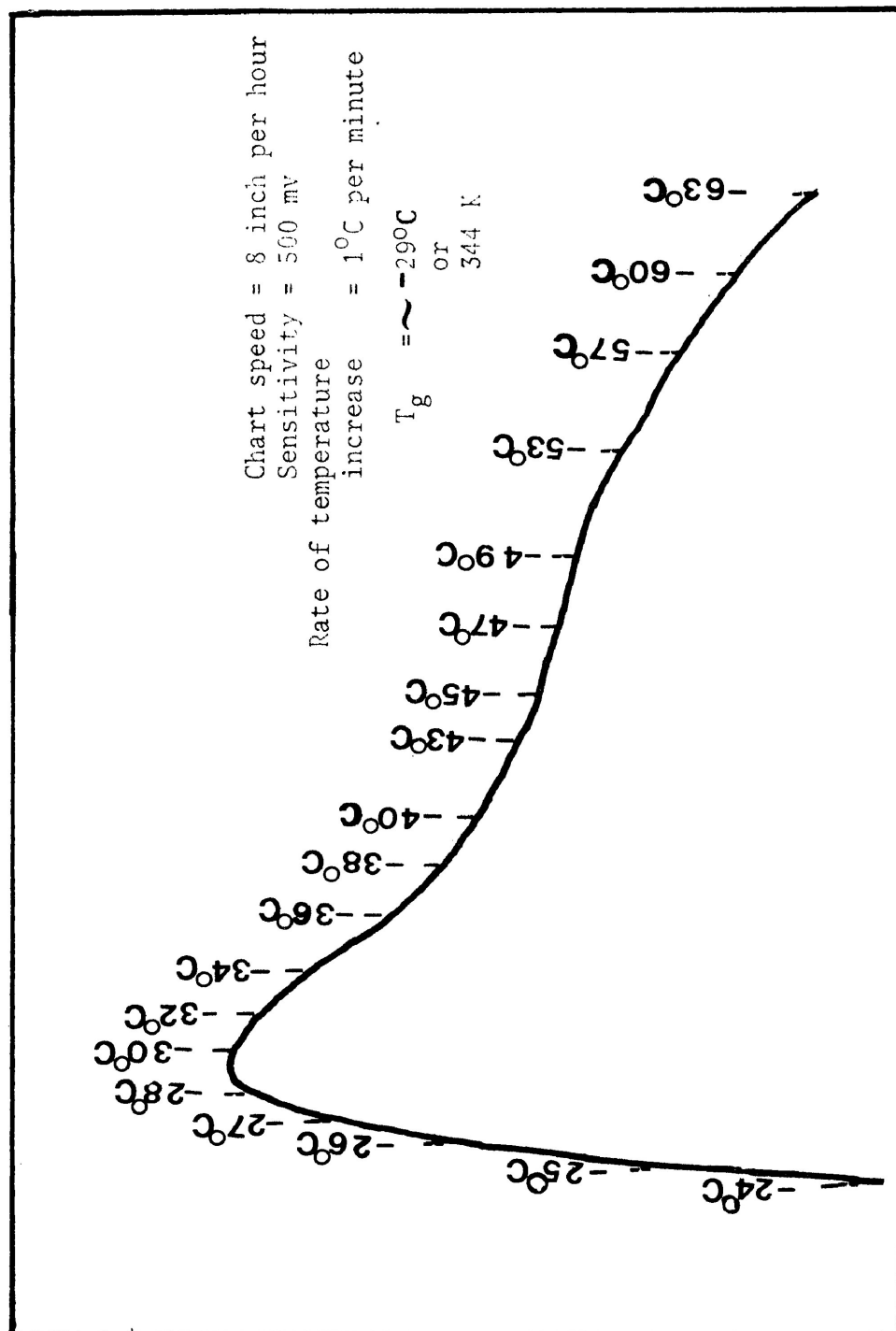


Figure : III-5 A typical plot showing the measurement of glass transition temperature (T_g) of the sample containing methyl formate in polyphenyl ether.

III

References

1. Santovac is the registered trademark of a six-ring meta-linked poly-phenyl ether, Bis m(m-phenoxy phenoxy)phenyl ether, which is a high vacuum medium produced and marketed by Monsanto, Ltd.
2. C.P. Smyth, "Dielectric Behaviour and Structure", McGraw-Hill Book Co., New York, (1955)203.
3. D.L. Gourlay, M.Sc. Thesis, Lakehead University, Thunder Bay, Ontario, Canada (1982).
4. M. Davies and J. Swain, Trans. Faraday Soc., 67(1971)1637.
5. S.P. Tay and S. Walker, J. Chem. Phys., 63(1975)1634.
6. N.E. Hill, W.E. Vaughan, A.H. Price and M. Davies, "Dielectric Properties and Molecular Structure", Van Nostrand-Reinhold, London, England, (1969)292.
7. Ibid., 235.
8. C.J.F. Böttcher, "Theory of Electric Polarization", Elsevier Publishing Co., Amsterdam, Netherlands, (1952)323.
9. A.A. Maryott and E.R. Smith, "Table of Dielectric Constants of Pure Liquids", National Bureau of Standards, Circular No. 514, U.S. Government printing office, Washington, 25, D.C., USA, (1951).
10. M. Davies and A. Edwards, Trans. Faraday Soc., 63(1967)2163.
11. B. Ostle, "Statistics in Research", (2nd ed.), Iowa State University Press, Ames, Iowa, USA, (1963).

CHAPTER IV

DIELECTRIC RELAXATION PROCESSES OF RIGID
POLAR MOLECULES IN ORGANIC GLASSES

IV.1

INTRODUCTION

A large number of rigid dipolar molecules have been extensively studied by various dielectric-absorption techniques in a variety of solvents. Attempts have been made to investigate the dependence of dielectric relaxation time (τ) and enthalpy of activation (ΔH_E) upon such factors as: entropy of activation (ΔS_E), the size and shape of rigid dipolar molecules, volume swept out by these molecules in their reorientation process, the direction of the dipoles within the molecules, moments of inertia, and also upon the viscosity of the medium.

Higasi (1) showed an almost linear dependence of entropy of activation (ΔS_E) upon the corresponding enthalpy of activation (ΔH_E) for a variety of organic molecules in p-xylene. He tentatively postulated that, "the entropy change is zero or has a small negative value, if ΔH_E is below 13.4 kJ mol^{-1} ". Davies and Edwards (2) also found a similar relationship between ΔH_E and ΔS_E for the molecular relaxation process of polar molecules of various sizes and shapes of the types: camphor, anthrone, cholest-4-ene-3-one, tetracyclone, and β -

naphthol. This linear dependence between ΔH_E and ΔS_E may be explained qualitatively if the activation energy is assumed to be largely needed to displace adjacent solvent molecules. Thus, the larger the energy required for ΔH_E the greater will be the local reorganizational entropy. Pitt and Smyth (3) demonstrated that for the three polar solutes, anthrone, fluorenone, and phenanthraquinone, in benzene solution the phenanthraquinone had a longer molecular relaxation time, and this was attributed to a greater volume being swept out by this molecule in orienting about its long axis. Crossley and Walker (4) examined quinoline, isoquinoline, and phthalazine in cyclohexane solution at 323 K. In these solute molecules of almost identical size and shape, the direction of the dipole moment varies. It appeared in these molecules that no significant variation of relaxation time was detectable within the limits of the accuracy of measurements.

Hassel (5) has examined some aromatic halides in p-xylene at 288 K. He reported the enthalpies of activation for the fluoro-, chloro-, bromo-, and iodo-benzenes as 5.9, 6.7, 8.4, and 9.2 kJ mol⁻¹, respectively.

This indicates a slight increase in ΔH_E with increase in the size of the molecule. Both Hassel (5) and Cooke (6), however, found reasonable correlation between activation energy and volume swept out by the molecule for dilute solutions of mono-halobenzenes, ortho- and meta-dihalo-benzenes, o-dibenzenes, m-dibenzenes, and naphthalenes in p-xylene. Other workers also attempted to explore the dependence of dielectric relaxation time and enthalpy of activation upon molecular rotational volume (7), position of the dipole moment within the solute molecule (8), moment of inertia (9), and viscosity of the medium (10,17).

In a recent attempt to investigate the effects of solvent on the relaxation characteristics of a molecule, a number of solutes measured in a variety of glass-forming solvents at temperatures below T_g . These solvents are polystyrene, o-terphenyl and polyphenyl ether.

Extensive studies of carefully selected dipolar solutes dispersed in a polystyrene matrix have been reported (9,14,15). Very broad loss curves were

observed for numerous rigid polar solutes, where dipole reorientation necessarily involves whole molecule rotations.

o-Terphenyl is a non-polar and melts at 328 K, but forms molecular glass when cooled below its T_g (~ 243 K) (12,13). Previous workers (12,13,16) have demonstrated that it was possible to make reproducible dielectric measurements with o-terphenyl as solvents from liquid nitrogen temperature up to above T_g .

Polyphenyl ether is another glass-forming solvent. It is bis(m(m-phenoxy phenoxy)phenyl)ether, a six-ring meta-linked polyphenyl ether with a glass transition at 270 K (17). This solvent differs from o-terphenyl and polystyrene in that it is more polar since it contains polar ether linkages and has a comparatively large loss α -process just above its T_g , but the absorption in the glassy state is quite small (18).

However, extensive dielectric studies in the latter two solvents (o-terphenyl and polyphenyl ether) has not been made. Moreover, detailed knowledge of the molecular relaxation parameters and the associated energy

barriers are essential for the assignment of a particular process in a similarly sized flexible molecule studied in these three media (polystyrene, o-terphenyl and polyphenyl ether) as will be seen in the following chapters. It is mainly for this second reason that different types of rigid dipolar molecules have been studied in these media which could also provide, at least, a qualitative interpretation of the activation parameters in terms of size, shape, and volume of the dipole units.

IV.2 EXPERIMENTAL RESULTS

The dielectric measurements of twelve dipolar rigid molecules (listed in Figure IV-1) have been made in the frequency range of 10^2 to 10^5 Hz by the use of a General Radio bridge, the procedure being described in Chapter III. The solvents used are: (a) polystyrene, (b) o-terphenyl, and (c) polyphenyl ether. All the molecules (Figure IV.1) were studied mainly for the use as rigid molecules providing reference values of molecular relaxation parameters in the above mentioned media. Some of these molecules studied in polystyrene matrices by several co-workers in this laboratory were also recorded

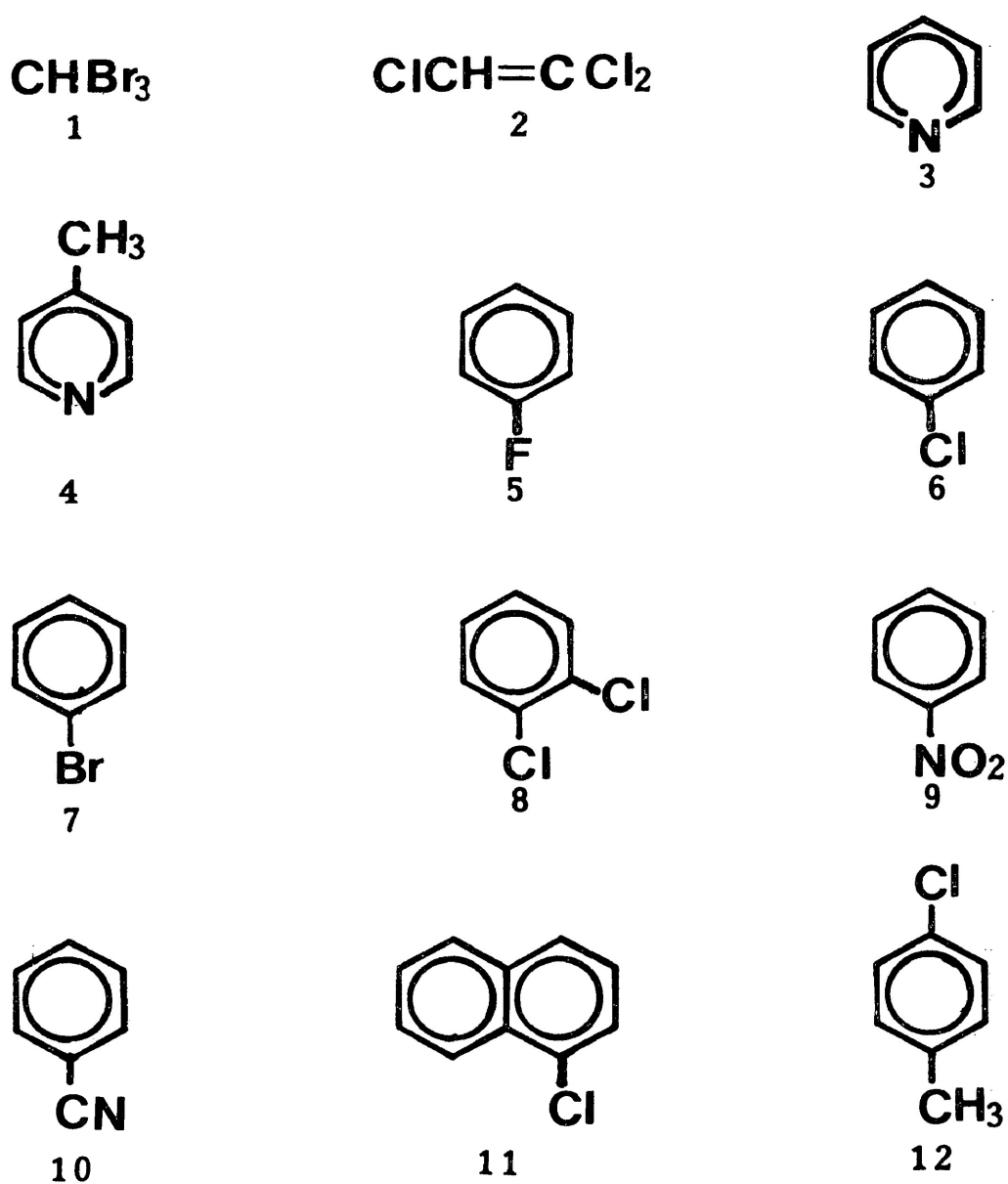


FIGURE IV.1

- | | | | |
|-----|---------------------|-----|-------------------|
| 1. | bromoform | 2. | trichloroethylene |
| 3. | pyridine | 4. | 4-methyl pyridine |
| 5. | fluorobenzene | 6. | chlorobenzene |
| 7. | bromobenzene | 8. | o-dichlorobenzene |
| 9. | nitrobenzene | 10. | benzonitrile |
| 11. | 1-chloronaphthalene | 12. | p-chlorotoluene |

in this chapter for comparison with the results obtained in the other two media (o-terphenyl and polyphenyl ether).

Figures IV.2-IV.4 show the plots of ΔH_E versus ΔS_E , while Figures IV.7 - IV.9 presents ΔH_E versus $\bar{V}(\frac{V_y + V_z}{2})$, in the mentioned medium. Sample plots of dielectric loss, $\epsilon''(=\epsilon''_{\text{observed}} - \epsilon''_{\text{solvent}})$ versus T(K) are shown in Figure IV.10 in the three media. Figures IV.11, IV.12, and IV.13 show the sample plots of ϵ'' versus $\log f$ in the polystyrene matrices, o-terphenyl, and in polyphenyl ether, respectively. Sample plots of $\log T\tau$ versus $1/T$ in three media are also presented in Figures IV.14-IV.18.

Table IV.1 lists the results from Eyring analyses, while Table IV.2 summarizes the Fuoss-Kirkwood analysis parameters together with the values of ϵ_∞ and the experimental dipole moments. The following symbols are employed:

PS	Polystyrene matrices
OTP	o-Terphenyl

Santovac	Polyphenyl ether
\bar{V} (\AA^3)	Mean volume swept by reorientation about centre of volume
ΔT (K)	Temperature range in the absolute scale
β -range	Range of variation in the Fuoss-Kirkwood distribution parameter β .
ΔG_E	Eyring free energy of activation
ΔH_E	Eyring enthalpy of activation
ΔS_E	Eyring entropy of activation
f	frequency in Hz
-	Relaxation times in seconds (s)

IV.3 DISCUSSION

The Eyring analysis results and the Fuoss-Kirkwood analysis parameters for twelve rigid dipolar molecules have been presented in Tables IV.1 and IV.2, respectively. Table IV.2 also collects the values of ϵ_∞ and apparent dipole moments corresponding to the dispersion at a particular temperature. The relaxation times and the free energies of activation have been shown at temperatures which are close to the individual absorptions, because for some molecules, the parameters

obtained by extrapolation may not be meaningful at all temperatures, but a more reasonable comparison can easily be made by choosing the one within or closest to the experimental observations.

Table IV shows that the values of the distribution parameter, β , for all the twelve rigid dipolar molecules in the three media (polystyrene, o-terphenyl and polyphenyl ether) range from 0.21 - 0.27. These low β -values (which imply a wide range of relaxation times) for the molecular motion in these media, agree well with the observations by earlier workers (2,9,14,23,24) for a series of rigid molecules in a polystyrene matrix. Table IV.2 also indicates that for each system studied, the temperature dependent ' β ' values do not seem to vary significantly over the temperature range in which the absorption curves have been observed.

Davies et al (2,24) obtained linear ΔH_E versus ΔS_E plots for various solutes dispersed in polystyrene matrices. Higasi (1) also showed a similar relationship for a variety of organic molecules in p-

xylene. Later workers (9,14,23) of this laboratory also found an almost linear relationship between ΔH_E and ΔS_E for different types of rigid dipolar molecules dispersed in polystyrene matrices. Figures IV.2, IV.3 and IV.4 show the plots of ΔS_E versus ΔH_E obtained from the present studies in polystyrene matrices, o-terphenyl, and polyphenyl ether, respectively, of different rigid molecules (listed in Table IV.1). These figures indicate clearly that the entropy of activation increases linearly with enthalpy of activation as the size of the molecule increases. Linear regression analysis for the results of molecular relaxation yielded the following equation:

(i) in polystyrene matrices

$$\Delta S_E \text{ (J K}^{-1} \text{ mol}^{-1}\text{)} = -70 + 2.2 \Delta H_E \text{ (kJ mol}^{-1}\text{)},$$

(ii) in o-terphenyl

$$\Delta S_E \text{ (J K}^{-1} \text{ mol}^{-1}\text{)} = -69 + 2.1 \Delta H_E \text{ (kJ mol}^{-1}\text{)},$$

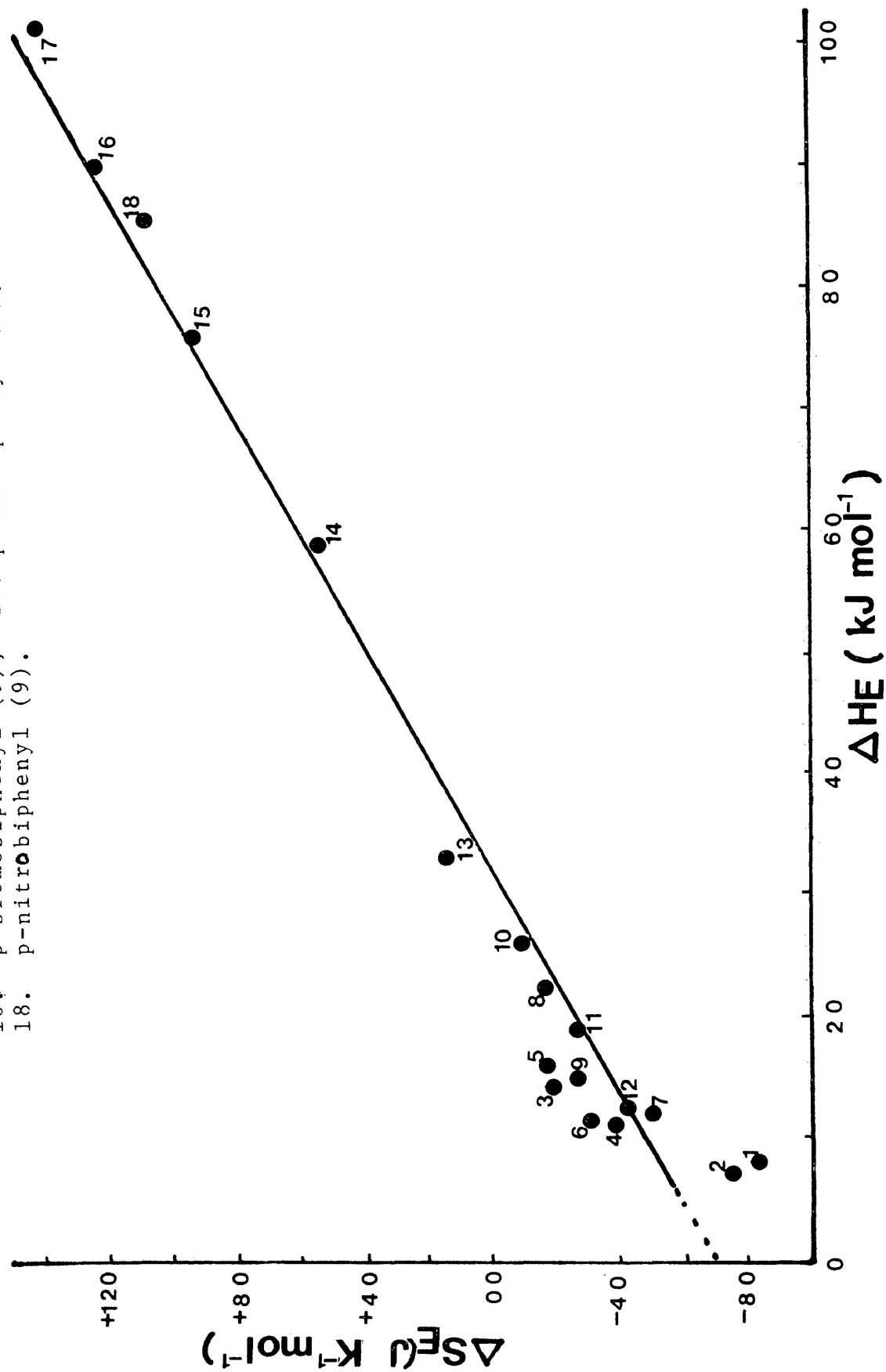
and (iii) in polyphenyl ether

$$\Delta S_E \text{ (J K}^{-1} \text{ mol}^{-1}\text{)} = -70 + 2.6 \Delta H_E \text{ (kJ mol}^{-1}\text{)}.$$

FIGURE IV.2

Plot of Eyring enthalpy of activation versus Eyring entropy of activation for the following rigid molecules in polystyrene matrices:

1. bromoform; 2. trichloroethylene; 3. 4-methyl pyridine (23);
4. chlorobenzene (23); 5. bromobenzene (23); 6. o-dichlorobenzene;
7. nitrobenzene; 8. benzonitrile (23); 9. 1-chloronaphthalene (14);
10. p-chlorotoluene (9); 11. iodobenzene (9); 12. p-fluorobenzene (9);
13. p-bromotoluene (9); 14. p-fluorobiphenyl (9); 15. p-chlorobiphenyl (9);
16. p-bromobiphenyl (9); 17. p-iodobiphenyl (9);
18. p-nitrobiphenyl (9).



1. bromoform; 2. trichloroethylene; 3. pyridine; 4. 4-methyl pyridine;
5. fluorobenzene; 6. chlorobenzene; 7. bromobenzene; 8. o-dichlorobenzene;
9. nitrobenzene; 10. benzonitrile; 11. 1-chloronaphthalene; 12. p-chlorotoluene;
13. p-fluorotoluene (13); 14. benzyl trichloride (13).

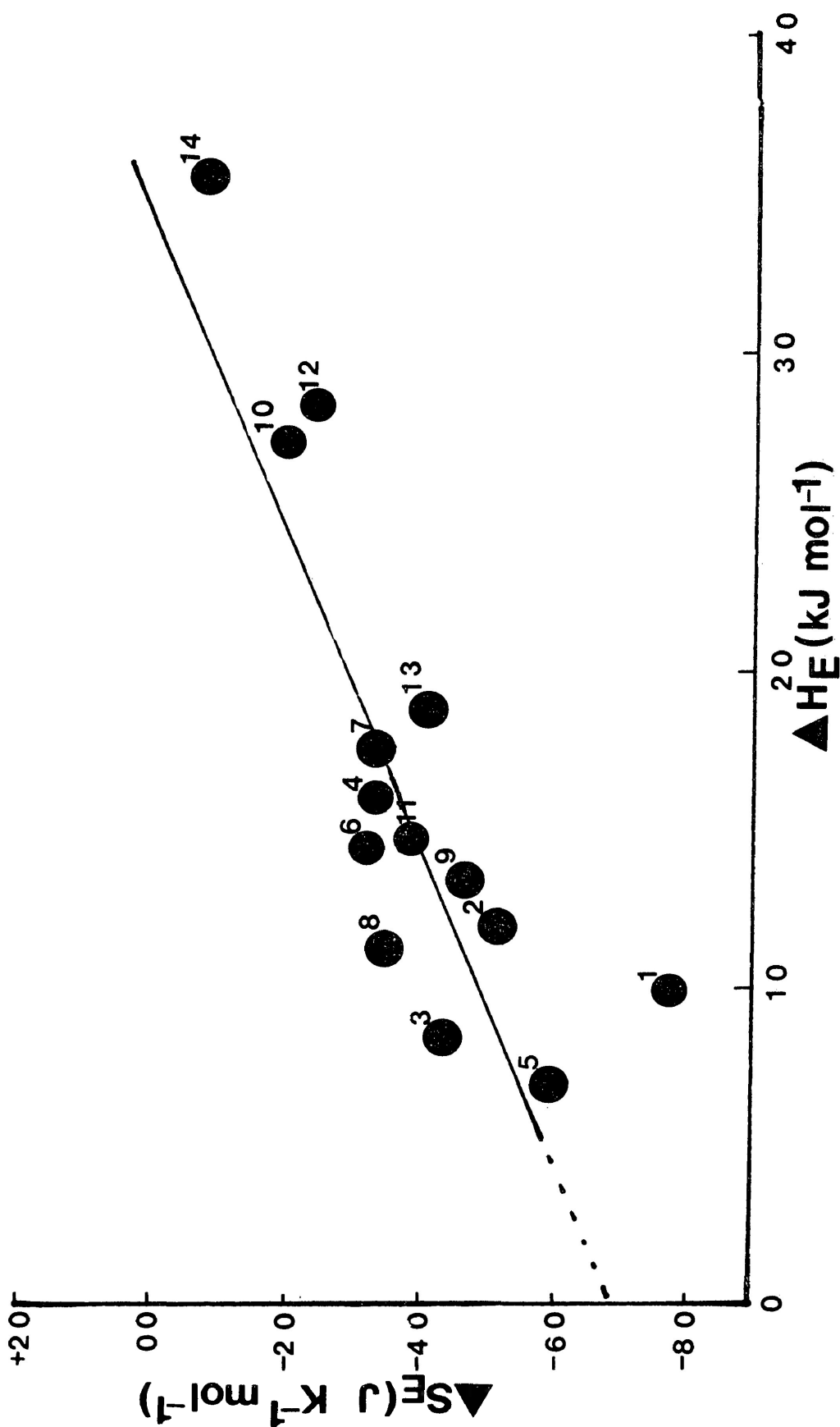


FIGURE IV.3 Plot of Eyring enthalpy of activation (ΔH_E^{\ddagger}) versus Eyring entropy of activation (ΔS_E^{\ddagger}) for several rigid molecules in o-terphenyl

1. bromoform; 2. trichloroethylene; 3. 4-methyl pyridine; 4. chlorobenzene;
5. bromobenzene; 6. o-dichlorobenzene; 7. nitrobenzene; 8. benzonitrile;
9. 1-chloronaphthalene; 10. p-chlorotoluene

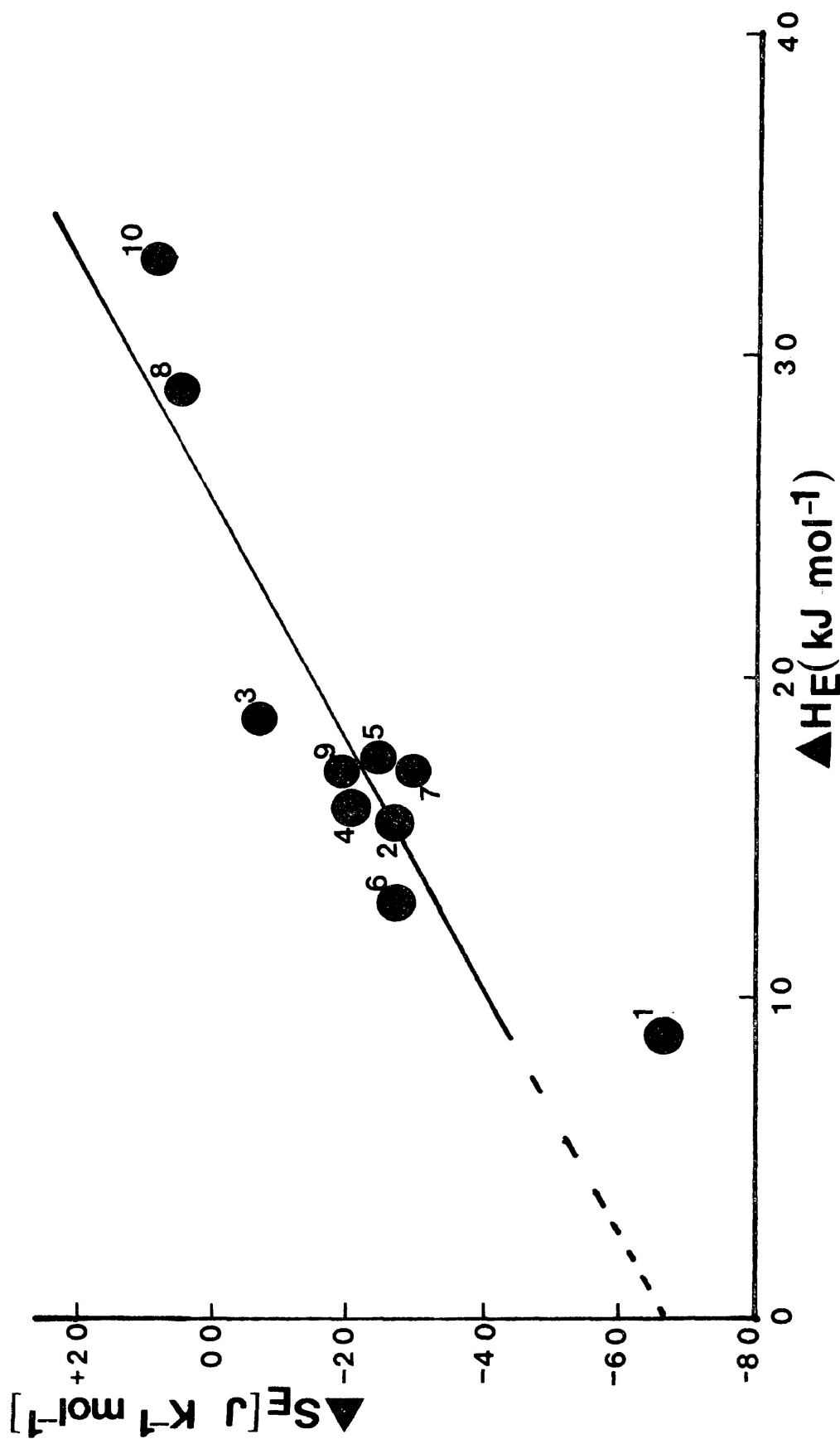


FIGURE IV.4 Plot of Eyring enthalpy of activation (ΔH^\ddagger) versus Eyring entropy of activation (ΔS^\ddagger) for several rigid molecules in polyphenyl ether.

The theoretical ground for this correlation is lacking. According to Davies and Edwards (2), such behaviour can be understood qualitatively if the activation energy is needed primarily to displace the adjacent solvent media so that the larger the energy required for ΔH_E the larger the local disorder, ΔS_E . However, the figures show that it was not possible to fit into the same plot the data for bromoform, which could be due to the probable hydrogen bonding in this molecule. Moreover, it appears from earlier investigations (9,14,23) that the linear ΔH_E versus ΔS_E relationship would be more reasonable for any series of molecules when the shape is quite similar and the inclination of the dipole to the principal axis is about the same. It is also necessary to point out that there is no absolute significance of the activation entropy determined by the Eyring expression since the exponential factor cannot be fully justified. As Davies and Edwards (2) say: "the entropy terms ΔS_E^* are best regarded as empirical corrections ($\exp(\Delta S_E^*/R)$) to a predetermined frequency value (kT/h) in the rate equation". Therefore, the deviation from a single linear ΔS_E versus ΔH_E relationship would not be surprising for a wide variety of dipolar molecules.

Tay and Walker (14), and also other workers (9,23) of this laboratory found a linear relationship between the enthalpy of activation and the volume swept out by the molecule for a variety of rigid molecules dispersed in polystyrene matrices. More recently, Gourlay (19) observed similar linear dependence of ΔH_E against mean volume swept out by certain rigid molecules for rotation about their centre of volume. All of these molecules have one thing in common: the dipole moment always lies along the long axis. The following diagram (Figure IV.5) illustrates the point. The molecular axes, x, y and z, are in the order of decreasing length. The molecular dipole lies along the x-axis. Arrows about the y and z axes describe possible molecular rotations:

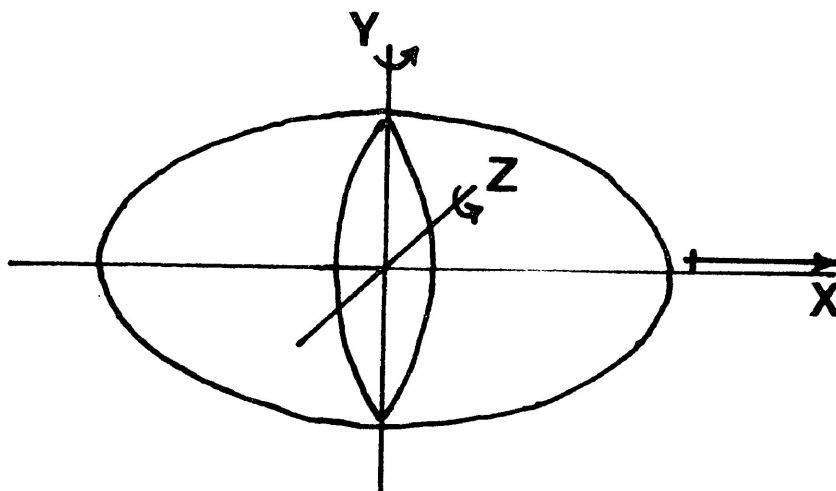


Figure: IV-5

Since the dipole moment lies along the longest x-axis, so the rotation of the molecule may give rise to two extreme types of swept volume: one involves large displacement of surrounding molecules, corresponding to out-of-plane rotation about the z-axis, the other, a rotation about the y-axis involves less displacement of adjacent molecules. The point through which the x, y and z axes pass is the centre of mass. However, unlike the case of a gas, the rotation relating to the jostling motion molecules experience in the liquid state may well result in the molecule rotating about its centre of volume.

The centre of mass or volume, effective radii, and the length of the rotating species were determined either from molecular models (9) or scale drawings constructed from known bond lengths and bond angles (26). The volumes of revolution were assumed to be cylinders. Hence, with the aid of known radius and length of rotating species, the volumes swept out by dipole reorientation about the two axes, perpendicular to the molecular moment, and also the volumes swept out for rotation about the centre of volume were calculated.

For rotation, either about the centre of mass or centre of volume, the swept volume is composed of two half cylinders, the radii of which were taken to be the maximum lengths of the molecule in each direction from the point of rotation and the cylinder lengths to be the length of the molecule in the direction parallel to the axis of rotation, Figure IV.6:

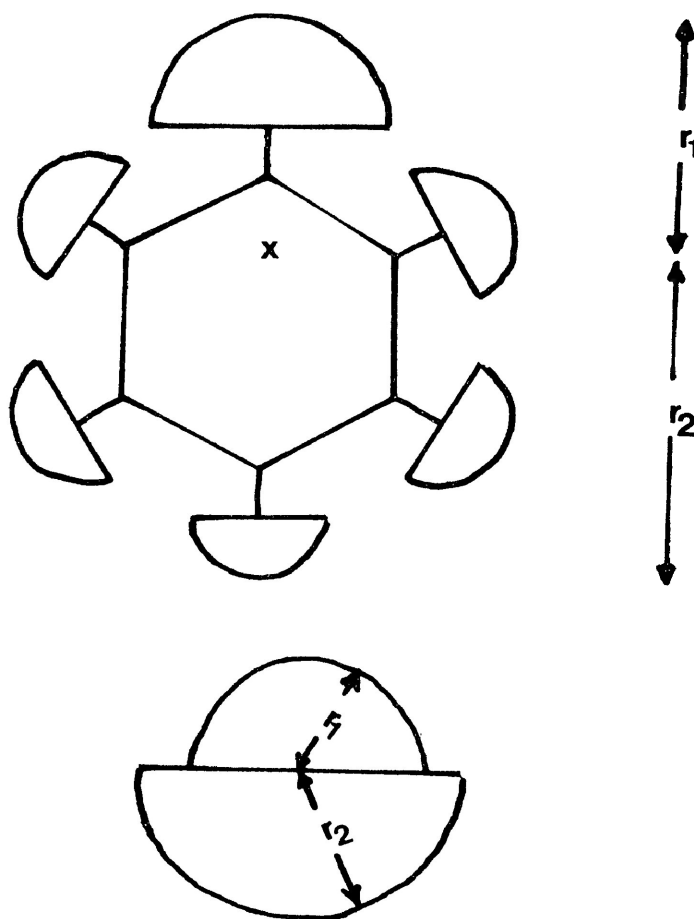


Figure: IV-6

The volumes are considered to be more accurate than $\pm 10\%$. The enthalpies of activation were plotted against mean volume ($\bar{V} = \frac{V_z + V_y}{2}$) for rotation about the centre of volume. It was found that within the limits of experimental error estimates, there is some linear relationship between the mean swept volumes and the activation energies as shown in Figures IV.7, IV.8 and IV.9 for the molecular process of different rigid molecules in polystyrene matrices, o-terphenyl and polyphenyl ether, respectively. However, it was found that some molecules deviate from this linear relation which may be due to their nonsimilarity in shape. Nevertheless, from these plots and earlier works (9,14, 23) it would seem more likely that at least a rough linear correlation exists between ΔH_E and the volume needed for reorientation of a given series of molecules having a similar shape factor.

Table IV.1 shows that for any particular molecule the relaxation times are longer and so the values of free energies of activation as well as enthalpies of activation are higher in polyphenyl ether than those in o-terphenyl, which in turn are higher in magnitude than the corresponding values in a polystyrene matrix.

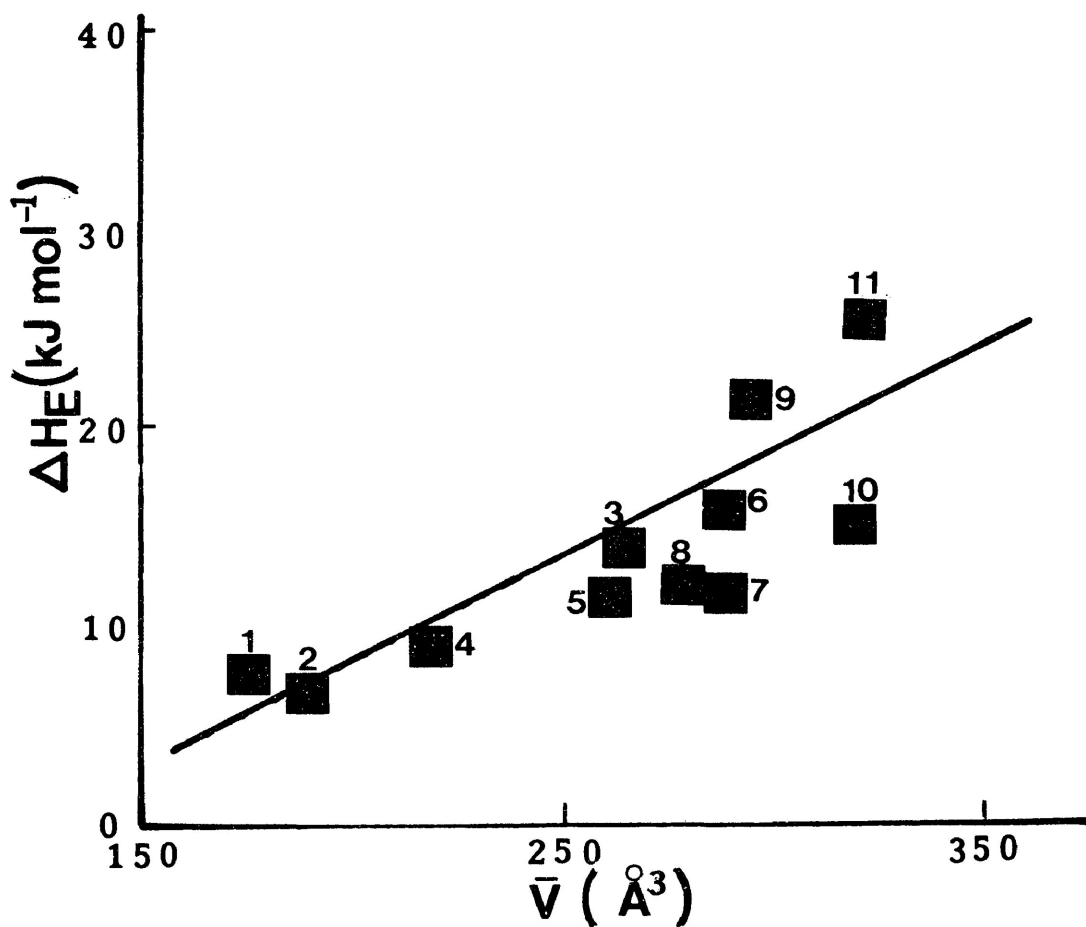


FIGURE IV.7 Plot of activation enthalpy (ΔH_E) versus mean volume swept out (\bar{V}) about the centre of volume in polystyrene matrices of the following molecules:

- | | |
|----------------------|-------------------------|
| 1. bromoform | 2. trichloroethylene |
| 3. 4-methyl pyridine | 4. fluorobenzene |
| 5. chlorobenzene | 6. bromobenzene |
| 7. o-dichlorobenzene | 8. nitrobenzene |
| 9. benzonitrile | 10. 1-chloronaphthalene |
| 11. p-chlorotoluene | |

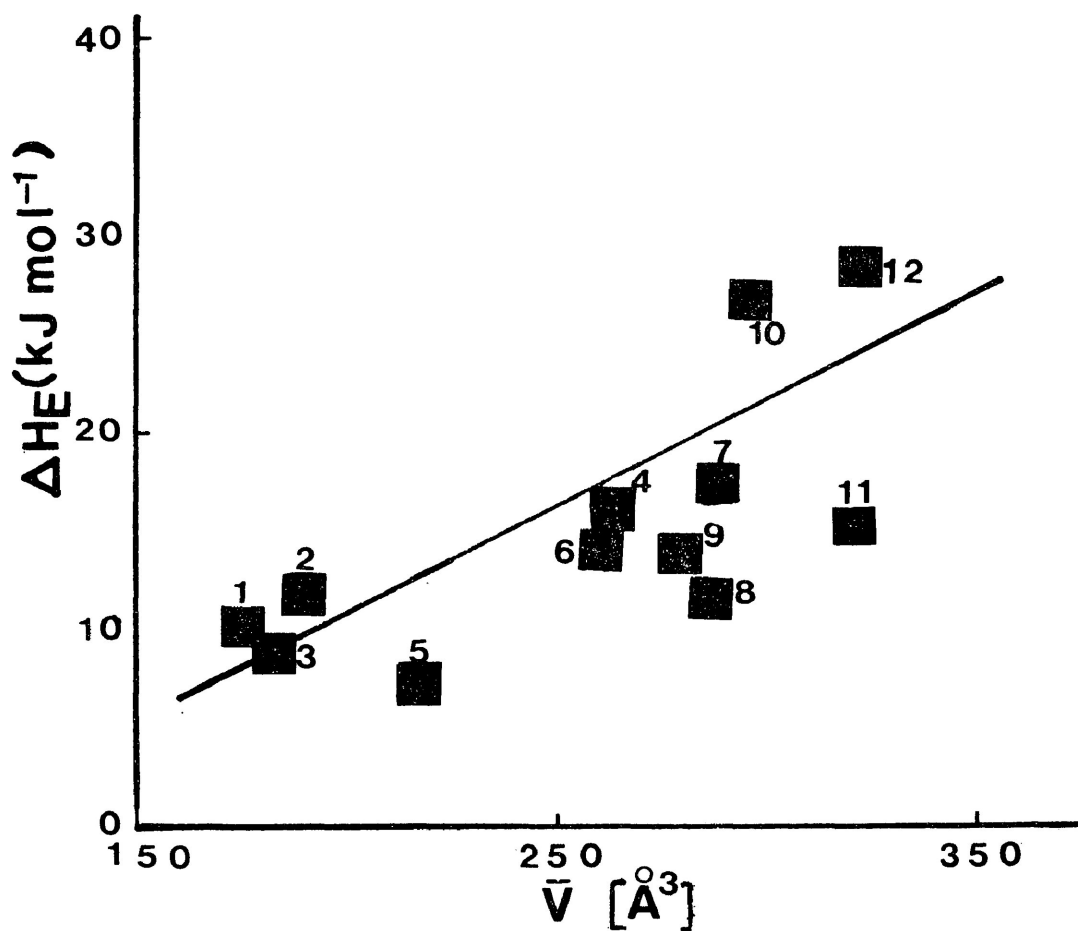


FIGURE IV.8 Plot of activation enthalpy (ΔH_E) versus mean volume swept out (\bar{V}) about the centre of volume in o-terphenyl of the following molecules:

- | | |
|-------------------------|----------------------|
| 1. bromoform | 2. trichloroethylene |
| 3. pyridine | 4. 4-methyl pyridine |
| 5. fluorobenzene | 6. chlorobenzene |
| 7. bromobenzene | 8. o-dichlorobenzene |
| 9. nitrobenzene | 10. benzonitrile |
| 11. 1-chloronaphthalene | 12. p-chlorotoluene |

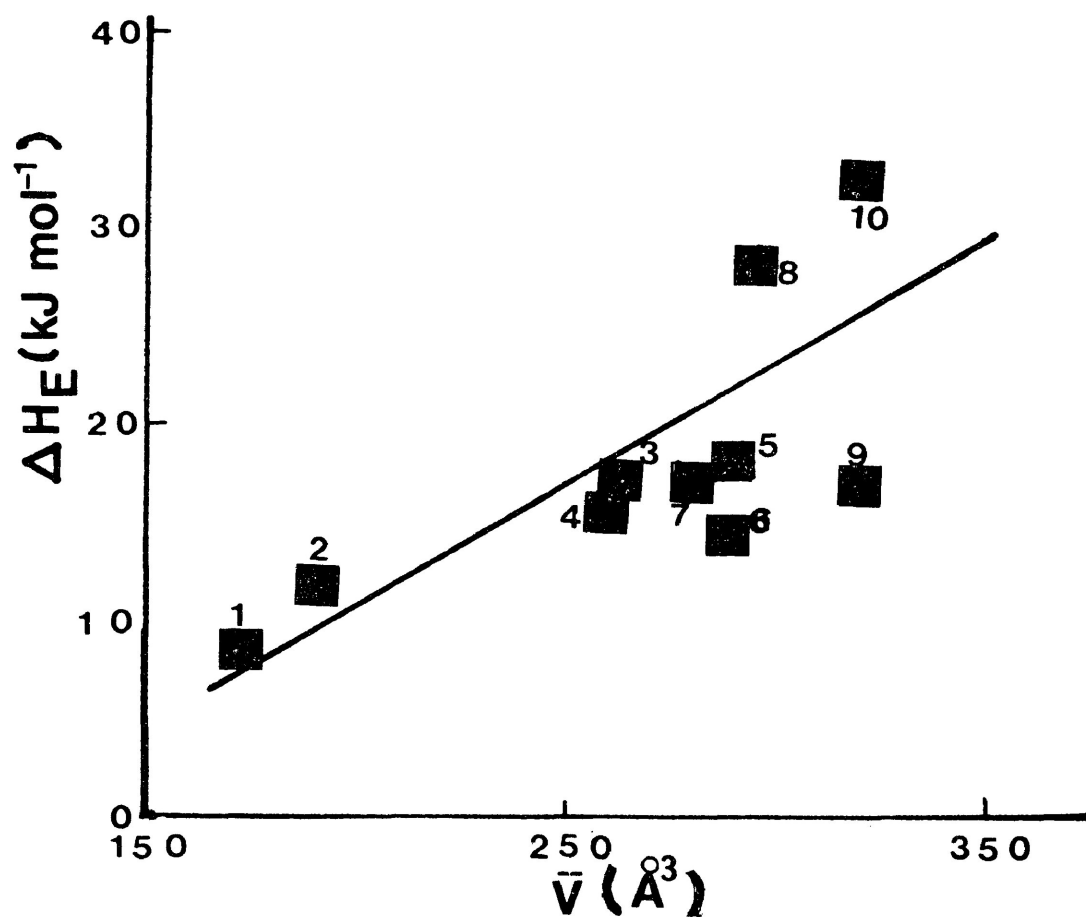


FIGURE IV.9 Plot of activation enthalpy (ΔH_E) versus mean volume swept out (\bar{V}) about the centre of volume in polyphenyl ether of the following molecules

- | | |
|------------------------|----------------------|
| 1. bromoform | 2. trichloroethylene |
| 3. 4-methyl pyridine | 4. chlorobenzene |
| 5. bromobenzene | 6. o-dichlorobenzene |
| 7. nitrobenzene | 8. benzonitrile |
| 9. 1-chloronaphthalene | 10. p-chlorotoluene |

This is mainly owing to an increase in viscosity of the medium from polystyrene to polyphenyl ether. However, the data for bromoform (Table IV.1) are not consistent with this solvent effect. Intermolecular hydrogen bonding, $\text{—}\overset{|}{\underset{|}{\text{C}}}\text{—H}\cdots\text{Br—}\overset{|}{\underset{|}{\text{C}}}\text{—H}\cdots$, may be the cause of this discrepancy. The enthalpies of activation of bromoform are 7.9 ± 0.7 , 10.4 ± 0.8 , and 8.8 ± 0.5 kJ mol^{-1} in a polystyrene matrix, o-terphenyl and polyphenyl ether respectively.

It can be seen (Table IV.1) that the increase in the values of Eyring parameters for trichloroethylene by changing the medium (i.e., from polystyrene to o-terphenyl, and from o-terphenyl to polyphenyl ether) are appreciably larger, the activation enthalpies for this molecule in a polystyrene matrix, o-terphenyl and polyphenyl ether being 7.0 ± 0.3 , 12.0 ± 0.5 , and 15.5 ± 1.7 , respectively. This may be explained, as the dipole moment of this molecule is directed along its long axis, and the molecule could have an appreciable contribution from an end-to-end tumbling motion. Such a relaxation contribution would lead the solute molecule to sweep out a larger volume, which could in turn lead to its experiencing a greater viscous drag from the more viscous solvents, and

hence reflects the larger ΔH_E and ΔS_E values for the molecule.

Pyridine and 4-methyl pyridine (*v*-picoline), nitrogen containing heterocyclic rigid molecules, received special consideration since this might give some information concerning molecular interaction with the solvent due to the hybridized lone pair electron of the hetero-atom or the π -electrons of the ring. The Eyring analysis results for these two molecules can be compared with those of analogous non-heterocyclic rigid molecules listed in the same Table IV.1. The results indicate that the Eyring parameters for pyridine in *o*-terphenyl are, within experimental error limits, identical to those observed for fluorobenzene in the same medium. Similarly, there is a small difference between the results for 4-methyl pyridine and chlorobenzene in the three media of investigation. On comparison of ΔH_E (kJ mol^{-1}) values, we find that they are for 4-methyl pyridine and chlorobenzene, (i) in a polystyrene matrix 14 (23) and 11 (23); (ii) in *o*-terphenyl 16.0 ± 0.9 and 14.4 ± 0.5 ; and (iii) in polyphenyl ether 17.2 ± 0.7 and 16.0 ± 0.9 , respectively.

A more extensive study of the effect of size, shape and the inclination of the dipole to the principal

axis of rotation would seem worthwhile. The data provided in Table IV.1 for mono- and disubstituted benzenes accomplishes this to a further extent. It can be seen that in the case of mono-halobenzenes there is almost a regular increase in the Eyring parameters in all the three media as we pass on from fluorobenzene to bromobenzene. This increase in the values of ΔH_E and other parameters with the increasing size of the molecules along the series of monohalobenzenes are consistent with the earlier observation in p-xylene (5) and in polystyrene matrices (9,23). But o-dichlorobenzene yielded lower values of ΔH_E and other parameters (Table IV.1) in all the three media than the corresponding values of similar-sized rigid molecule, e.g. bromobenzene. The ΔH_E values of o-dichlorobenzene are 11.2 ± 0.6 , 11.4 ± 0.6 , and 13.4 ± 0.8 kJ mol⁻¹ in a polystyrene matrix, o-terphenyl and polyphenyl ether, respectively. The values are within the limits of experimental error, identical to the corresponding values of chlorobenzene (Table IV.1). Previous workers studied ortho- and meta-dihalobenzenes as well as mono-halobenzenes in p-xylene at 25°C (19), p-xylene at 60°C (21) and benzene at 23°C (22). They also observed that the relaxation times of ortho- and meta-

dihalobenzenes differ very little and are only slightly longer than those of the mono-substituted compounds. Crossley (20) had accounted for this discrepancy by the suggestion that the mean relaxation time is more related to the length of the molecule than to its volume. It was also concluded by Mountain (21) that "within the limits of experimental error the relaxation times of *m*-compounds may be said to be the same as those of the *o*-derivative", and "similarly the enthalpies of activation are also equivalent and show no suggestion of increasing ΔH_E with larger molecular volume as was obtained by Hassel (5) with mono-substituted halobenzenes". Recently, Mazid (23), from dielectric studies in polystyrene matrices, observed that the enthalpies of activation for ortho-dihalobenzenes are about the same and the entropies of activation are generally negative.

Table IV.1 shows that although nitrobenzene gave an absorption process in a higher temperature range than chlorobenzene in the three media, yet the values of ΔH_E , within the limits of experimental error, are almost identical for these two molecules in the same medium.

The ΔH_E values for nitrobenzene are 12.1 ± 1.9 , 13.7 ± 0.6 and 17.2 ± 0.8 kJ mol⁻¹ in a polystyrene matrix, o-terphenyl and polyphenyl ether, respectively.

Benzonitrile, another mono-substituted benzene having its molecular dipole moment coincident with its principal axis yielded relatively higher values of ΔH_E and other parameters (Table IV.1) in harmony with its size. This is also apparent from the plots of ΔH_E versus mean volume swept, \bar{V} (\AA^3), about the centre of volume (Figures IV.7-IV.9). The enthalpies of activation in a polystyrene matrix, o-terphenyl and polyphenyl ether for benzonitrile are 22 (23), 27.4 ± 1.5 , and 28.7 ± 0.6 kJ mol⁻¹, respectively. The values of ΔH_E and other parameters in o-terphenyl for this molecule agree well with those obtained by earlier workers in this laboratory (13).

Table IV.1 shows that p-chlorotoluene has considerably higher values of temperature range, enthalpy of activation, and entropy of activation, than those for 1-chloronaphthalene. This indicates that ΔH_E and other relaxation parameters of a rigid polar molecule are very sensitive to the length of its long axis. The enthalpies of activation for p-chlorotoluene are 26 (9), 28.8 ± 3.0 ,

and $32.9 \pm 2.6 \text{ kJ mol}^{-1}$ in a polystyrene matrix, o-terphenyl, and polyphenyl ether, respectively. While the ΔH_E values of 1-chloronaphthalene in these media are 14.7 ± 0.7 , 14.8 ± 0.8 , and $17.0 \pm 0.8 \text{ kJ mol}^{-1}$, respectively. Tay et al (14), from their dielectric studies in a polystyrene matrix, reported that the ΔH_E values for the 1-halonaphthalenes and those for cyclohexyl chloride (24), cyclohexyl bromide (24), o-dichlorobenzene (24), and meta-dibromobenzene are of the same order whereas their rotational volumes vary appreciably. They suggested that 1-halonaphthalene could have an appreciable contribution from the cylindrical barrel-like motion about the longest axis. They also noted that 2-halonaphthalenes have longer relaxation times than the corresponding 1-halonaphthalenes, which agrees well with the observation by Grubb and Smyth (25) for similar molecules in dilute liquid solutions.

REFERENCES

1. K. Higasi, "Dielectric Relaxation and Molecular Structure Monograph Series of the Research Institute of Applied Electricity", No. 9(1961).
2. M. Davies and A. Edwards, Trans. Faraday Soc., 63(1967)2163.
3. D.A. Pitt and C.P. Smyth, J. Am. Chem. Soc., 80(1958)1061.
4. J. Crossley and S. Walker, Can. J. Chem., 46(1968)2639.
5. W.F. Hassel, Ph.D. Thesis, University of Aston, Birmingham, England, (1966).
6. B. F. Cooke, M.Sc. Thesis, Lakehead University, Thunder Bay, Ontario, Canada, (1969).
7. E.N. Dicarilo and C.P. Smyth, J. Am. Chem. Soc., 66(1962)1105.
8. D.A. Pitt and C.P. Smyth, J. Phys. Chem., 63(1959)582.
9. H.A. Khwaja, M.Sc. Thesis, Lakehead University, Thunder Bay, Ontario, Canada, (1978).
10. J. Crossley and S. G. Srivastava, Can. J. Chem., 54(1976)1418.
11. G.A. Bologun and C.W.N. Cumper, J. Chem. Soc., Faraday II, (1973)1172.
12. J. Crossley, D. Gourlay, M. Rujimethalhas, S.P. Tay, and S. Walker, J. Chem. Phys., 71(1979)10.
13. D.L. Gourlay, M.Sc. Thesis, Lakehead University, Thunder Bay, Ontario, Canada, (1982).

14. S.P. Tay and S. Walker, J. Chem. Phys., 63(1975)1634.
15. J. Crossley, M.A. Mazid, C.K. McLellan, P.F. Mountain and S. Walker; Can. J. Chem., 56(1978)567.
16. M. Nakamura, H. Takahashi, and K. Higasi, Bull. Chem. Soc., Japan, 47(1974)1593.
17. A.J. Barlow, J. Lamb and N.S. Taskoprlü, J. Acoust. Soc. Am., 46(1969)569.
18. J. Crossley, A. Heravi and S. Walker, J. Chem. Phys., 75(1981)418.
19. J. Crossley, W.F. Hassel and S. Walker, J. Chem. Phys., 48(1968)1261.
20. J. Crossley, Ph.D. Thesis, University of Aston, Birmingham, England, (1967).
21. P.F. Mountain, Ph.D. Thesis, University of Aston, Birmingham, England, (1969).
22. B. Sinha, S.B. Roy and G.S. Kastha, Ind. J. Phys., 40(1966)101.
23. M.A. Mazid, M.Sc. Thesis, Lakehead University, Thunder Bay, Ontario, Canada, (1977).
24. M. Davies and J. Swain, Trans. Faraday Soc., 67(1971)1637.
25. E.L. Grubb and C.P. Smyth, J. Am. Chem. Soc., 83(1961)4122.
26. L.E. Sutton, "Tables of Interatomic Distances", Special Publications No. 11, Chemical Society, (1958).

TABLE IV.1: EYRING ANALYSIS RESULTS FOR RIGID POLAR MOLECULES IN SOME ORGANIC CLASSES

MOLECULE	MEDIUM	ΔT (K)	Relaxation Time τ (s)				ΔG_E (kJ mol ⁻¹)				ΔH_E kJ mol ⁻¹	ΔS_E J K ⁻¹ mol ⁻¹
			100 K	150 K	200 K	200 K	100 K	150 K	200 K	200 K		
Bromoform	Polystyrene matrix	99-135	1.6×10^{-4}	4.5×10^{-6}		16.3	20.5		7.9 ± 0.7	-84.3 ± 6.2		
	o-Terphenyl	107-144	1.7×10^{-3}	1.7×10^{-5}		18.2	22.2		10.4 ± 0.8	-78.4 ± 6.2		
	Polyphenyl ether	100-139	2.1×10^{-4}	4.0×10^{-6}		16.5	20.4		8.8 ± 0.5	-77.1 ± 4.6		
Trichloroethylene	Polystyrene matrix	79-117	2.4×10^{-5}	9.9×10^{-7}		14.8	18.6		7.0 ± 0.3	-77.7 ± 3.4		
	o-Terphenyl	107-144	5.4×10^{-4}	2.9×10^{-6}		17.3	20.0		12.0 ± 0.5	-52.9 ± 4.0		
	Polyphenyl ether	102-138	1.2×10^{-3}	1.7×10^{-6}		18.0	19.3		15.5 ± 1.7	-25.7 ± 10.6		
Pyridine	o-Terphenyl	78-99	2.3×10^{-6}	5.3×10^{-8}		12.8	15.0		8.4 ± 1.1	-43.9 ± 12.9		
4-Methyl pyridine	Polystyrene matrix	88-124 (23)	8.5×10^{-5}	2.1×10^{-7}		15.8	16.7		14	-19		
	o-Terphenyl	105-154	5.8×10^{-3}	6.3×10^{-6}		19.3	20.9		16.0 ± 0.9	-33.0 ± 7.5		
	Polyphenyl ether	110-152	1.0×10^{-2}	2.0×10^{-6}		18.9	19.8		17.2 ± 0.7	-25.8 ± 6.0		

TABLE IV.1: continued...

MOLECULE	MEDIUM	ΔT (K)	Relaxation Time τ (s)				ΔG_E (kJ mol ⁻¹)			ΔH_E kJ mol ⁻¹	ΔS_E J K ⁻¹ mol ⁻¹
			100 K	150 K	200 K	200 K	100 K	150 K	200 K		
Fluorobenzene	Polystyrene matrix	94-118 (9)		9.1×10^{-9}		13			~ 9	--	
	o-Terphenyl	79-99	2.8×10^{-6}	1.1×10^{-7}		12.9	15.9		7.0 \pm 0.4	-59.2 \pm 5.2	
Chlorobenzene	Polystyrene matrix	89-125 (9)		4.3×10^{-7}		18			9	-60	
		81-111 (23)	2.3×10^{-5}	1.9×10^{-7}		14.8	16.7		11	-40	
	o-Terphenyl	99-140	7.7×10^{-4}	1.6×10^{-6}		17.6	19.2		14.4 \pm 0.5	-32.1 \pm 4.5	
	Polyphenyl ether	104-139	1.1×10^{-3}	1.2×10^{-6}		17.9	18.8		16.0 \pm 0.9	-18.9 \pm 7.9	
Bromobenzene	Polystyrene matrix	101-136 (23)	5.5×10^{-4}	6.9×10^{-7}		17.3	18.2		16	-17	
		115-164	3.3×10^{-2}	2.0×10^{-5}		20.7	22.4		17.4 \pm 1.1	-33.3 \pm 8.1	
		113-160	1.6×10^{-2}	1.2×10^{-5}		20.1	21.7		18.1 \pm 0.7	-31.3 \pm 5.2	
o-Dichlorobenzene	Polystyrene matrix	80-103	4.3×10^{-6}	3.3×10^{-8}		13.3	14.4		11.2 \pm 0.6	-21.4 \pm 6.9	
		81-114	2.4×10^{-5}	1.7×10^{-7}		14.4	16.4		11.4 \pm 0.6	-33.8 \pm 6.3	
		81-115	3.7×10^{-5}	1.2×10^{-7}		15.1	16.0		13.4 \pm 0.8	-17.5 \pm 7.7	

TABLE IV.1: continued...

MOLECULE	MEDIUM	ΔT (K)	Relaxation Time τ (s)					ΔG_E (kJ mol ⁻¹)			ΔH_E kJ mol ⁻¹	ΔS_E J K ⁻¹ mol ⁻¹
			100 K	150 K	200 K	100 K	150 K	200 K				
Nitrobenzene	Polystyrene matrix	93-145	4.0×10^{-4}	2.1×10^{-6}		17.1	19.6	12.1 \pm 1.9	-49.8 \pm 7.0			
		118-161	7.2×10^{-3}	2.0×10^{-5}		19.5	22.4	13.7 \pm 0.6	-47.7 \pm 4.4			
		110-152	1.0×10^{-2}	6.9×10^{-6}		19.8	21.1	17.2 \pm 0.8	-25.8 \pm 6.1			
Benzonitrile	Polystyrene matrix	133-175 (23)		7.3×10^{-5}	7.1×10^{-7}		24.0	24.8	22	-16		
		166-219		1.3×10^{-2}	3.9×10^{-5}		30.4	31.4	27.4 \pm 1.5	-20.3 \pm 8.2		
		160-209		5.2×10^{-3}	1.2×10^{-5}		29.3	29.6	28.7 \pm 0.6	-4.2 \pm 3.5		
1-Chloro- naphthalene	Polystyrene matrix	103-133 (14)	9.0×10^{-7}					19	14.7 \pm 0.7	-25.6 \pm 6.0		
		100-146	1.9×10^{-3}	3.7×10^{-6}		18.4	20.3	14.8 \pm 0.8	-37.6 \pm 7.1			
		103-145	3.2×10^{-3}	2.3×10^{-6}		18.8	19.7	17.0 \pm 0.8	-18.5 \pm 6.7			
p-Chlorotoluene	Polystyrene matrix	163-196 (9)		1.6×10^{-3}	5.8×10^{-6}		28	29	26	-9		
		205-241		8.5×10^{-1}	2.0×10^{-3}		35.7	38.0	28.8 \pm 3.0	-24.9 \pm 11.6		
		197-240		8.8×10^{-1}	9.1×10^{-4}		35.7	36.7	32.9 \pm 2.6	9.8 \pm 8.2		

TABLE IV.2: Fuoss-Kirkwood Analysis Parameters, ϵ_{∞} , and Effective Dipole Moments (μ) of Rigid Polar Molecules in Some Organic Glasses.

T(K)	$10^6 \tau$ (s)	$\log f_{\max}$	β	$10^3 \epsilon''_{\max}$	ϵ_{∞}	μ (D)
<u>0.35 M Bromoform in a Polystyrene matrix</u>						
98.6	183	2.94	0.21	0.97	2.49	0.26
105.1	100	3.20	0.22	1.04	2.49	0.26
113.9	43.4	3.56	0.25	1.10	2.49	0.26
119.9	28.8	3.74	0.19	1.15	2.49	0.31
126.8	15.2	4.02	0.17	1.20	2.49	0.35
134.6	11.0	4.16	0.15	1.20	2.49	0.39
<u>0.34 M Bromoform in o-Terphenyl</u>						
107.0	655	2.39	0.18	0.80	2.75	0.25
112.4	372	2.63	0.20	0.85	2.75	0.25
118.9	232	2.86	0.19	0.90	2.75	0.26
126.0	103	3.19	0.20	0.96	2.76	0.27
132.4	55.1	3.46	0.20	1.02	2.76	0.29
137.7	45.6	3.59	0.23	1.08	2.76	0.29
144.2	24.3	3.82	0.24	1.16	2.76	0.30
<u>0.49 M Bromoform in Polyphenyl Ether</u>						
100.2	186	2.93	0.18	3.36	2.92	0.39
105.2	126	3.10	0.16	3.67	2.92	0.44
110.5	88.4	3.36	0.14	3.87	2.92	0.51
117.5	37.8	3.62	0.15	4.05	2.92	0.50
122.8	22.4	3.85	0.17	4.19	2.93	0.49
129.2	14.7	4.03	0.19	4.31	2.93	0.50
139.2	7.39	4.33	0.18	4.43	2.93	0.53
<u>0.71 M Trichloroethylene in a Polystyrene Matrix</u>						
78.5	287	2.74	0.22	1.02	2.54	0.16
82.2	191	2.92	0.19	1.07	2.54	0.17
91.1	62.7	3.40	0.20	1.15	2.54	0.19
95.4	39.8	3.60	0.22	1.17	2.54	0.18
100.0	31.6	3.80	0.23	1.20	2.54	0.18
106.8	12.7	4.10	0.21	1.22	2.54	0.19
116.5	6.24	4.41	0.19	1.17	2.54	0.20

TABLE IV.2 continued...

T(K)	$10^6 \tau$ (s)	$\log f_{\max}$	β	$10^3 \epsilon''_{\max}$	ϵ_{∞}	μ (D)
<u>0.62 M Trichloroethylene in o-Terphenyl</u>						
107.2	610	2.91	0.20	2.70	2.73	0.32
111.7	196	3.15	0.21	2.89	2.73	0.33
116.7	113	3.44	0.19	2.99	2.73	0.36
120.5	58.0	3.63	0.19	3.09	2.73	0.37
124.7	37.1	3.84	0.21	3.19	2.73	0.37
128.8	23.3	4.01	0.22	3.30	2.73	0.37
133.4	15.7	4.19	0.23	3.36	2.74	0.37
138.2	10.3	4.32	0.24	3.41	2.74	0.37
144.2	4.71	4.53	0.25	3.31	2.74	0.37
<u>0.72 M Trichloroethylene in Polyphenyl Ether</u>						
101.1	775	2.31	0.18	5.15	2.88	0.40
105.8	551	2.46	0.16	5.36	2.88	0.44
110.9	172	2.96	0.18	5.56	2.88	0.44
115.2	103	3.19	0.22	5.76	2.89	0.41
121.3	33.6	3.67	0.19	6.03	2.89	0.45
125.5	17.5	3.96	0.19	6.19	2.89	0.48
130.9	11.2	4.15	0.22	6.37	2.89	0.46
137.9	6.81	4.37	0.25	6.39	2.89	0.45
<u>0.91 M Pyridine in o-Terphenyl</u>						
78.4	50.6	3.50	0.18	21.91	2.81	0.66
84.0	19.6	3.91	0.18	23.02	2.81	0.69
89.6	7.52	4.33	0.21	23.77	2.78	0.68
93.0	5.27	4.48	0.23	24.25	2.79	0.67
99.2	2.78	4.76	0.27	25.16	2.81	0.65

TABLE IV.2: continued...

T(K)	$10^6 \tau$ (s)	$\log f_{\max}$	β	$10^3 \epsilon''_{\max}$	ϵ_{∞}	μ (D)
<u>0.90 M 4,Methyl Pyridine in o-Terphenyl</u>						
105.1	1703	1.98	0.17	11.44	2.76	0.58
112.3	666	2.38	0.19	12.64	2.76	0.59
118.6	311	2.73	0.17	13.46	2.76	0.66
123.7	131	3.08	0.17	14.17	2.76	0.69
128.6	60.8	3.42	0.17	14.87	2.76	0.73
135.2	27.5	3.76	0.19	15.80	2.76	0.73
141.1	14.5	4.04	0.20	16.54	2.76	0.74
148.3	7.37	4.33	0.23	17.66	2.77	0.73
154.3	3.92	4.61	0.23	18.14	2.77	0.76

0.85 M 4,Methyl Pyridine in Polyphenyl Ether

104.1	1609	2.00	0.16	12.64	2.89	0.63
110.6	388	2.61	0.17	13.02	2.89	0.67
116.3	204	2.89	0.17	13.84	2.89	0.68
120.7	80.4	3.30	0.18	14.51	2.89	0.70
133.8	6.83	4.37	0.22	17.01	2.90	0.72
145.5	2.61	4.79	0.25	18.92	2.91	0.73
155.5	1.23	5.11	0.27	19.73	2.93	0.75

0.89 M Fluorobenzene in o-Terphenyl

79.1	32.8	3.68	0.17	19.15	2.75	0.65
84.0	16.5	3.98	0.19	20.09	2.76	0.65
88.8	8.57	4.27	0.21	20.35	2.74	0.64
94.1	5.13	4.49	0.24	20.86	2.74	0.63
98.8	3.10	4.71	0.26	21.15	2.75	0.62

TABLE IV.2: continued...

T (K)	$10^6 \tau$ (s)	$\log f_{\max}$	β	$10^3 \epsilon''_{\max}$	ϵ_{∞}	μ (D)
<u>0.72 M Chlorobenzene in o-Terphenyl</u>						
98.6	979	2.21	0.18	8.89	2.74	0.54
104.9	361	2.64	0.16	9.76	2.73	0.62
110.9	127	3.10	0.18	10.36	2.74	0.62
117.2	47.8	3.52	0.17	10.97	2.73	0.67
126.6	14.8	4.03	0.20	12.03	2.74	0.68
134.1	7.49	4.33	0.22	12.74	2.74	0.68
139.3	4.33	4.57	0.22	13.04	2.75	0.70
<u>0.41 M Chlorobenzene in Polyphenyl Ether</u>						
104.2	890	2.57	0.20	5.61	2.91	0.54
109.9	426	2.90	0.18	6.35	2.91	0.62
116.0	65.3	3.39	0.20	7.17	2.91	0.64
121.3	27.5	3.76	0.19	7.47	2.91	0.68
127.2	13.4	4.08	0.21	7.75	2.92	0.69
133.0	6.92	4.36	0.23	8.07	2.92	0.68
138.6	3.65	4.64	0.23	8.28	2.92	0.70
<u>0.57 M Bromobenzene in o-Terphenyl</u>						
115.2	1226	2.01	0.18	4.87	2.73	0.49
119.7	833	2.28	0.17	5.26	2.73	0.53
124.5	521	2.49	0.18	5.53	2.73	0.54
130.6	170	2.87	0.21	5.80	2.73	0.53
136.2	98.3	3.21	0.17	6.14	2.73	0.61
141.0	55.4	3.46	0.17	6.39	2.72	0.64
146.4	22.1	3.76	0.17	6.77	2.72	0.67
151.8	13.0	4.09	0.18	7.01	2.72	0.67
157.0	8.36	4.18	0.19	7.36	2.72	0.68
163.7	6.48	4.39	0.22	7.61	2.72	0.66

TABLE IV.2: continued...

T(K)	$10^6 \tau$ (s)	$\log f_{\max}$	β	$10^3 \epsilon''_{\max}$	ϵ_{∞}	μ (D)
<u>0.58 M Bromobenzene in Polyphenyl Ether</u>						
113.0	1102	2.06	0.16	7.78	2.89	0.62
118.0	692	2.36	0.15	8.26	2.89	0.68
122.8	271	2.77	0.15	8.57	2.89	0.70
128.2	131	3.08	0.18	9.01	2.89	0.67
132.9	72.4	3.34	0.18	9.34	2.90	0.69
137.2	40.5	3.59	0.17	9.60	2.89	0.73
143.7	21.3	3.87	0.19	10.13	2.90	0.73
148.8	12.1	4.12	0.20	10.51	2.90	0.74
153.7	8.48	4.27	0.21	10.83	2.90	0.74
160.3	5.23	4.48	0.22	11.10	2.91	0.75
<u>0.70 M o-Dichlorobenzene in a Polystyrene Matrix</u>						
80.2	137	3.07	0.17	15.68	2.56	0.70
83.8	79	3.30	0.16	16.42	2.55	0.75
88.7	27.7	3.76	0.16	17.28	2.54	0.79
90.8	17.5	3.95	0.16	17.71	2.54	0.81
93.8	10.5	4.18	0.18	18.55	2.54	0.80
97.1	7.03	4.36	0.20	19.26	2.55	0.79
100.9	3.77	4.63	0.21	19.79	2.56	0.79
102.7	2.97	4.73	0.21	20.09	2.56	0.81
<u>0.63 M o-Dichlorobenzene in o-Terphenyl</u>						
80.4	709	2.35	0.18	11.89	2.74	0.60
85.4	341	2.67	0.15	12.70	2.73	0.70
91.4	110	3.16	0.16	13.65	2.72	0.73
95.8	45.0	3.55	0.18	14.32	2.73	0.72
99.5	27.0	3.77	0.20	15.06	2.73	0.72
102.2	16.4	3.99	0.21	15.56	2.74	0.72
106.4	9.63	4.22	0.22	16.21	2.74	0.73
110.2	6.17	4.41	0.23	16.54	2.74	0.74
114.1	3.91	4.61	0.24	16.91	2.75	0.74

TABLE IV.1 continued...

T(K)	$10^6 \tau$ (s)	$\log f_{\max}$	β	$10^3 \epsilon''_{\max}$	ϵ_{∞}	μ (D)
<u>0.56 M o-Dichlorobenzene in Polyphenyl Ether</u>						
80.5	1726	1.97	0.18	15.79	2.95	0.71
84.0	1054	2.18	0.17	16.96	2.92	0.77
89.5	347	2.66	0.17	17.85	2.88	0.82
94.0	120	3.12	0.18	18.87	2.88	0.84
96.3	78.9	3.30	0.19	19.48	2.88	0.84
100.9	30.8	3.71	0.18	20.17	2.87	0.90
103.4	19.7	3.91	0.19	20.81	2.88	0.90
107.9	10.1	4.20	0.21	21.81	2.89	0.90
112.9	5.43	4.47	0.23	22.65	2.89	0.89
114.8	3.83	4.62	0.25	23.09	2.90	0.88

0.66 M Nitrobenzene in a Polystyrene Matrix

92.5	1066	2.17	0.14	19.27	2.79	0.90
102.4	344	2.66	0.14	22.15	2.79	1.00
108.6	114	3.14	0.15	23.87	2.80	1.03
112.1	104	3.24	0.15	23.97	2.80	1.06
123.8	13.2	4.08	0.17	27.95	2.80	1.12
134.0	7.32	4.34	0.20	29.90	2.82	1.12
114.5	3.15	4.70	0.21	30.93	2.83	1.15

0.67 M Nitrobenzene in o-Terphenyl

117.8	493	2.51	0.14	8.50	2.79	0.67
122.5	276	2.76	0.15	8.97	2.79	0.68
131.1	123	3.11	0.15	9.73	2.79	0.73
139.8	45.5	3.54	0.15	10.50	2.79	0.79
147.1	19.8	3.80	0.16	11.20	2.79	0.81
153.6	14.4	4.04	0.21	11.84	2.81	0.75
161.4	8.47	4.27	0.21	12.41	2.80	0.77

TABLE IV.2 continued...

T (K)	$10^6 \tau$ (s)	$\log f_{\max}$	β	$10^3 \epsilon''_{\max}$	ϵ_{∞}	μ (D)
<u>0.48 M Nitrobenzene in Polyphenyl Ether</u>						
110.4	1221	2.12	0.14	8.94	2.99	0.76
116.4	458	2.54	0.15	9.37	2.99	0.84
122.0	220	2.86	0.14	9.91	2.99	0.89
127.4	97.9	3.21	0.14	10.39	2.99	0.99
133.4	47.9	3.52	0.12	10.95	2.98	0.96
138.4	24.8	3.81	0.14	11.47	2.99	0.98
145.0	11.5	4.14	0.15	12.16	2.98	1.00
151.9	5.09	4.50	0.15	12.66	2.99	1.01
<u>0.77 M Benzonitrile in o-Terphenyl</u>						
166.2	1097	2.16	0.19	14.49	2.80	0.83
172.9	702	2.36	0.18	15.59	2.80	0.90
177.8	379	2.62	0.18	16.18	2.80	0.93
184.0	174	2.96	0.19	17.13	2.80	0.95
190.1	101	3.19	0.19	18.06	2.80	0.99
196.3	52.1	3.49	0.19	18.85	2.80	1.02
204.2	25.6	3.79	0.19	19.96	2.80	1.07
211.4	14.8	4.03	0.20	20.95	2.80	1.09
219.8	8.20	4.29	0.19	22.03	2.80	1.12
<u>0.64 M Benzonitrile in Polyphenyl Ether</u>						
160.0	1071	2.17	0.17	15.49	2.99	0.94
163.6	689	2.36	0.18	16.15	2.99	0.94
168.1	410	2.59	0.17	16.64	2.99	0.99
174.8	178	2.95	0.18	17.62	2.99	1.02
180.6	89.9	3.25	0.17	18.39	2.99	1.08
185.7	53.6	3.47	0.18	18.95	2.99	1.09
190.5	29.8	3.73	0.19	20.08	3.00	1.10
196.0	18.1	3.94	0.20	20.86	3.00	1.11
201.9	10.5	4.18	0.21	21.90	3.00	1.13
208.8	5.39	4.47	0.21	23.03	3.00	1.15

TABLE IV.2 continued...

T(K)	$10^6 \tau$ (s)	$\log f_{\max}$	β	$10^3 \epsilon''_{\max}$	ϵ_{∞}	μ (D)
<u>0.52 M 1-Chloro-naphthalene in o-Terphenyl</u>						
100.4	1672	1.98	0.21	5.36	2.73	0.46
105.0	698	2.36	0.21	5.75	2.73	0.49
109.8	501	2.60	0.18	6.11	2.73	0.55
114.6	189	2.82	0.19	6.45	2.73	0.57
119.5	102	3.19	0.21	6.78	2.73	0.57
124.5	44.2	3.56	0.19	7.04	2.72	0.62
129.6	20.9	3.80	0.20	7.40	2.72	0.64
133.9	18.3	3.94	0.23	7.73	2.73	0.62
138.7	10.3	4.19	0.25	8.08	2.73	0.61
146.1	4.76	4.53	0.25	8.30	2.73	0.64
<u>0.66M 1-Chloro-naphthalene in Polyphenyl Ether</u>						
103.4	1380	2.06	0.19	9.21	2.88	0.56
109.6	601	2.42	0.17	9.83	2.88	0.63
114.4	208	2.88	0.19	10.29	2.88	0.62
119.6	98.2	3.21	0.20	10.80	2.89	0.63
123.9	50.0	3.50	0.20	11.20	2.88	0.66
129.0	23.3	3.83	0.21	11.70	2.89	0.67
133.2	13.5	4.07	0.22	12.17	2.89	0.67
137.7	9.06	4.25	0.23	12.61	2.89	0.68
145.3	3.94	4.61	0.24	13.12	2.89	0.70
<u>0.65 M p-Chlorotoluene in o-Terphenyl</u>						
204.7	1195	2.12	0.22	17.77	2.72	0.84
210.6	887	2.26	0.20	19.35	2.72	1.16
218.2	382	2.62	0.22	20.41	2.72	1.16
244.9	281	2.75	0.19	21.35	2.71	1.29
230.7	182	2.94	0.16	24.90	2.70	1.34
240.6	51.4	3.29	0.23	32.81	2.71	1.50

T(K)	$10^6 \tau$ (s)	$\log f_{\max}$	β	$10^3 \epsilon''_{\max}$	ϵ_{∞}	μ (D)
<u>0.36 M p-Chlorotoluene in Polyphenyl Ether</u>						
197.3	934	2.20	0.20	11.40	2.95	1.11
203.6	652	2.39	0.19	11.86	2.95	1.18
209.0	428	2.57	0.18	11.97	2.95	1.23
214.2	240	2.82	0.19	12.31	2.95	1.24
218.9	166	2.98	0.19	12.45	2.95	1.26
222.4	93.5	3.23	0.20	12.83	2.95	1.25
228.9	67.9	3.37	0.19	12.91	2.95	1.30
234.2	44.4	3.56	0.17	13.17	2.94	1.41
239.7	23.3	3.80	0.19	14.20	2.95	1.40

FIGURE IV.10 Loss versus Temperature (K) for o-dichlorobenzene

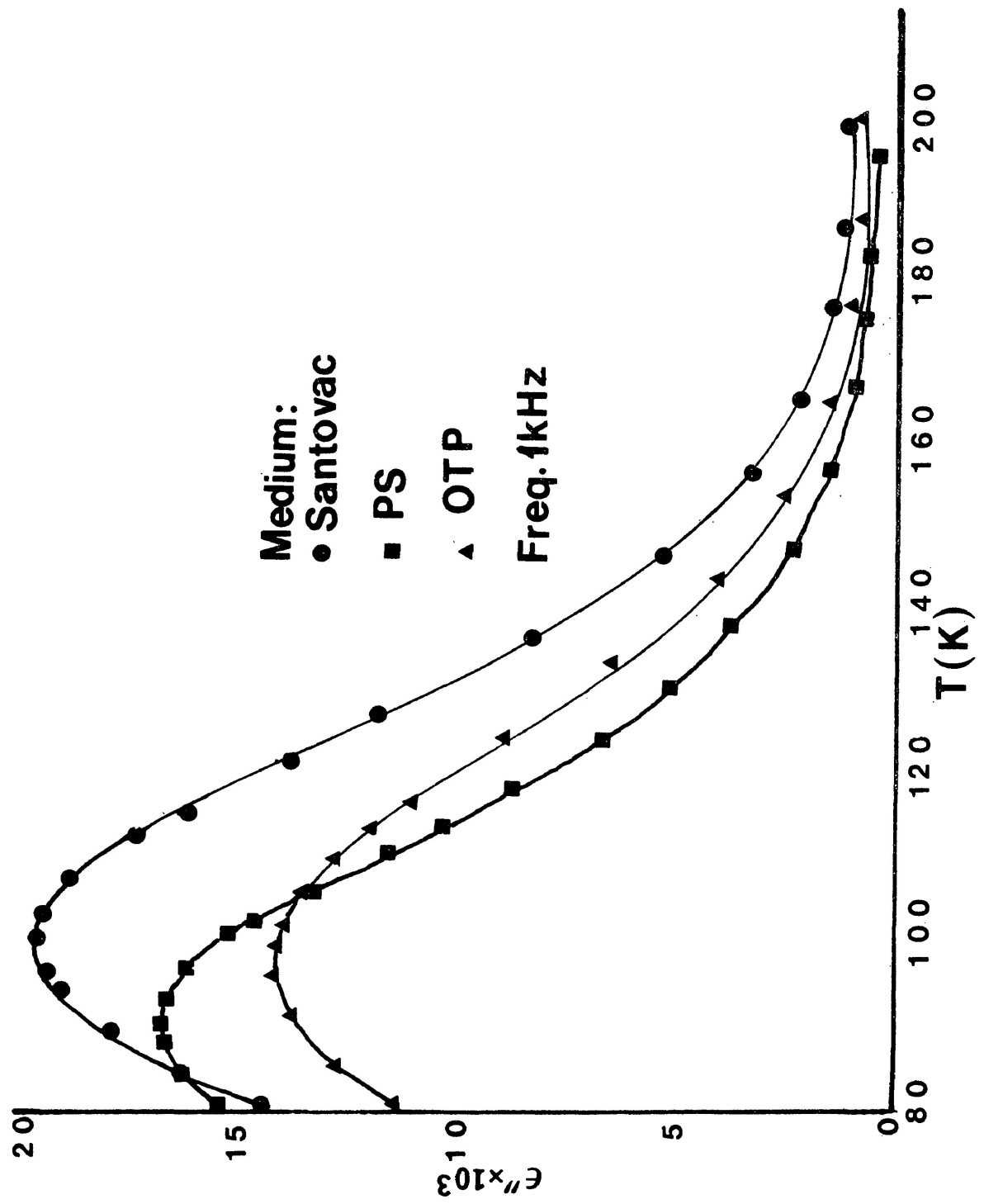
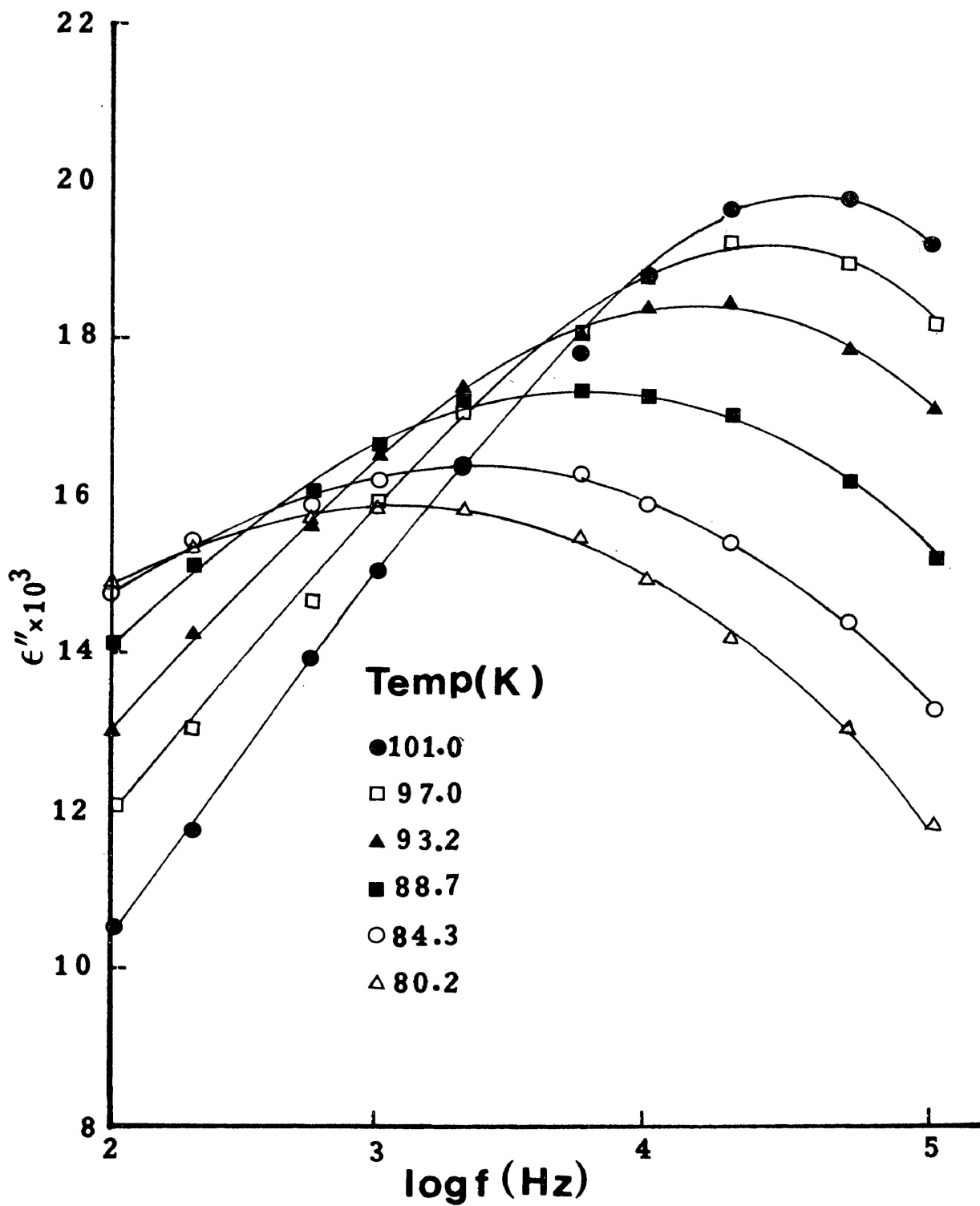


FIGURE IV.11 Loss versus log frequency for o-dichlorobenzene in a polystyrene matrix



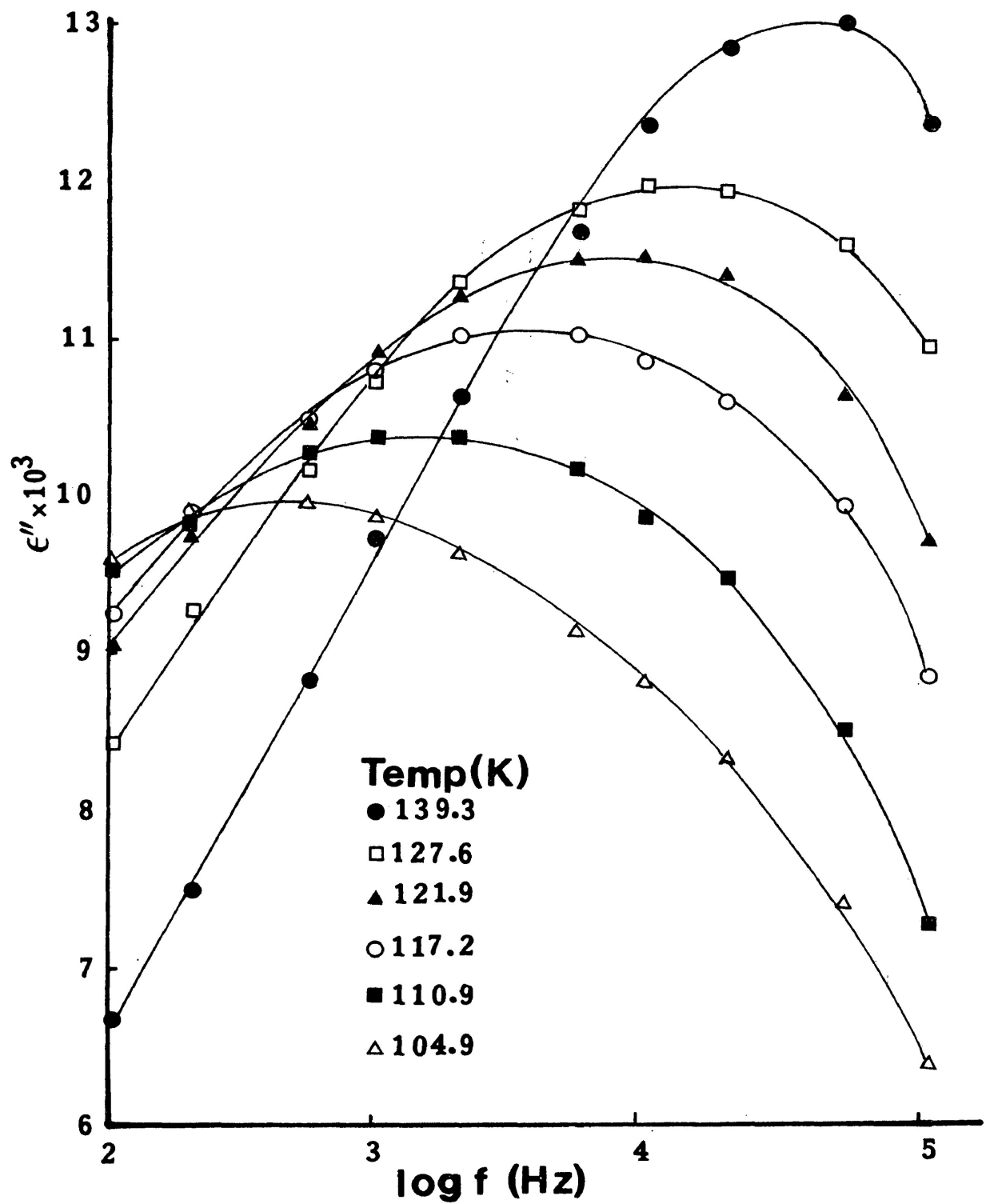


FIGURE IV.12 Loss versus Log frequency for chlorobenzene in o-terphenyl

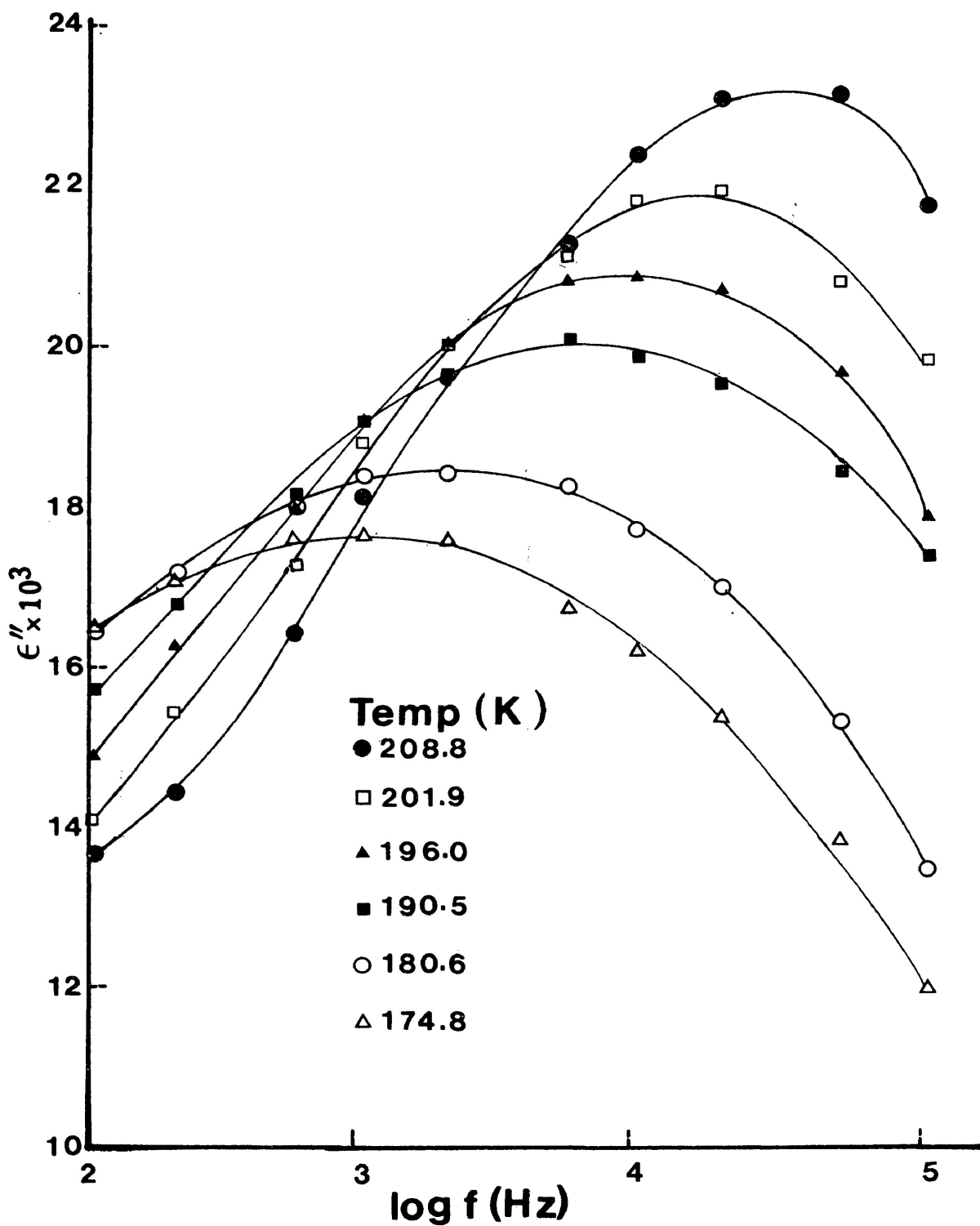


FIGURE IV.13 Loss versus log frequency for benzonitrile in polyphenyl ether

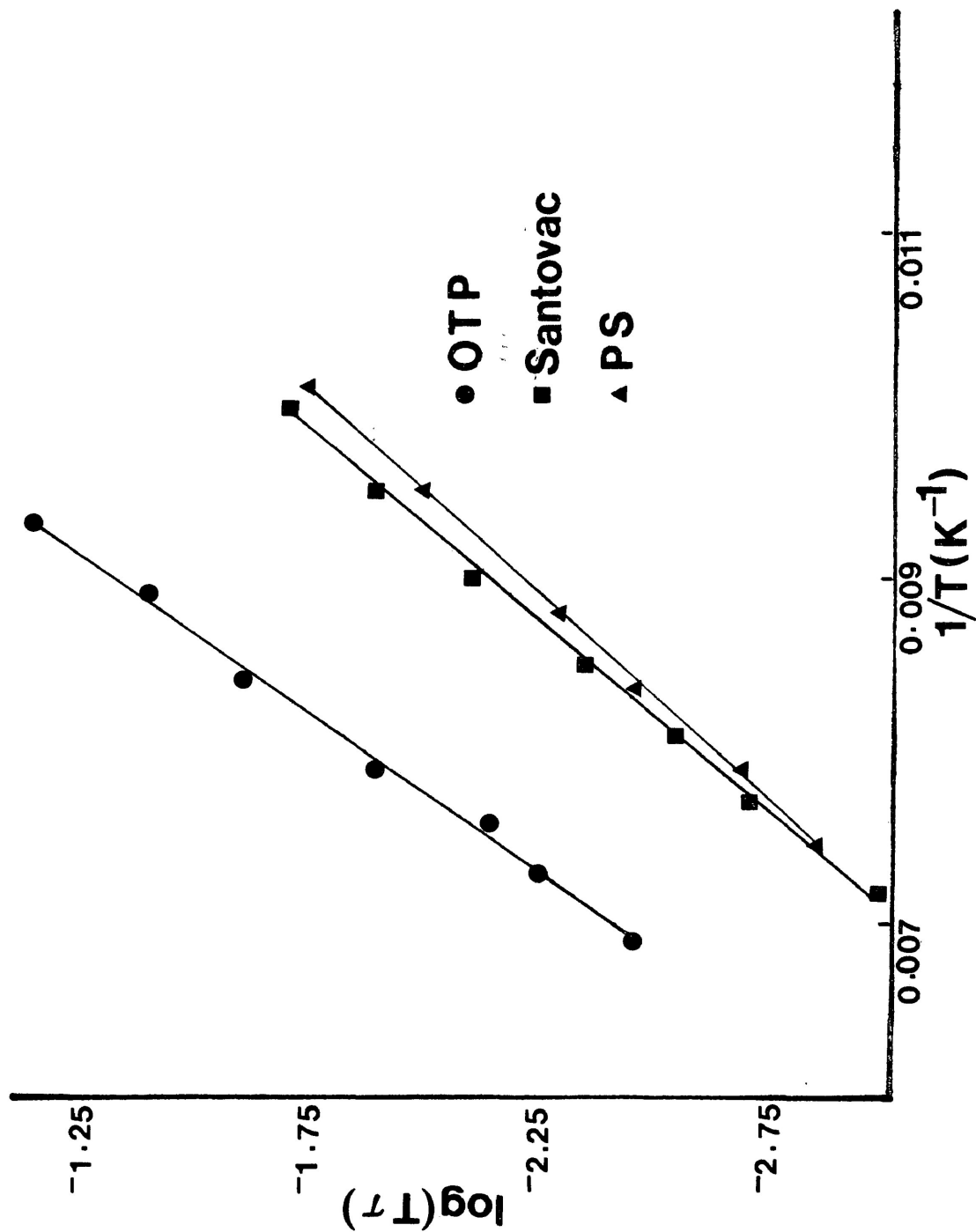
FIGURE IV.14 Eyring plots of $\log(T\tau)$ versus $1/T$ (K^{-1}) for bromoform

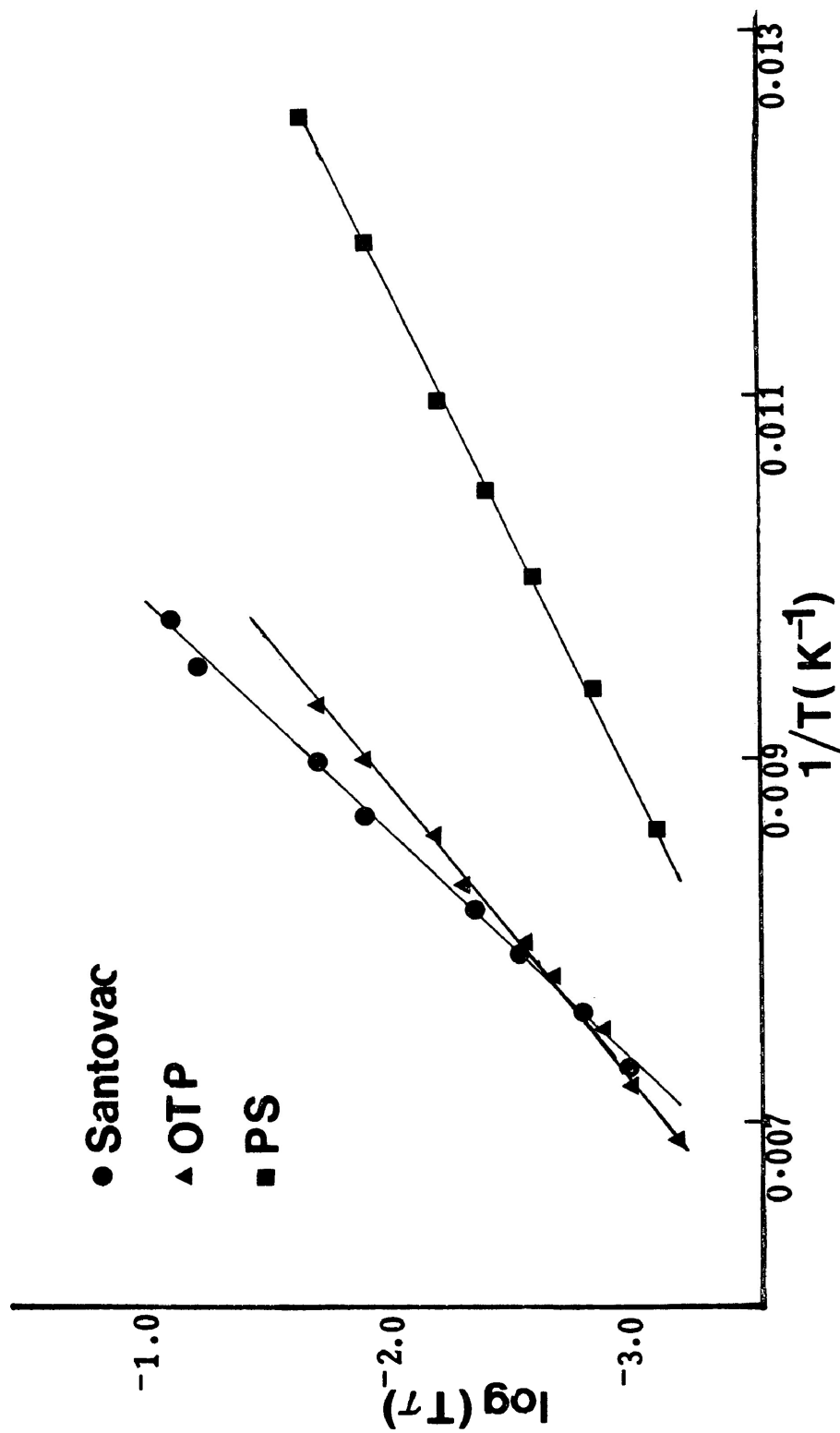
FIGURE IV.15 Eyring plot of $\log(\tau)$ versus $1/T$ (K^{-1}) for trichloroethylene

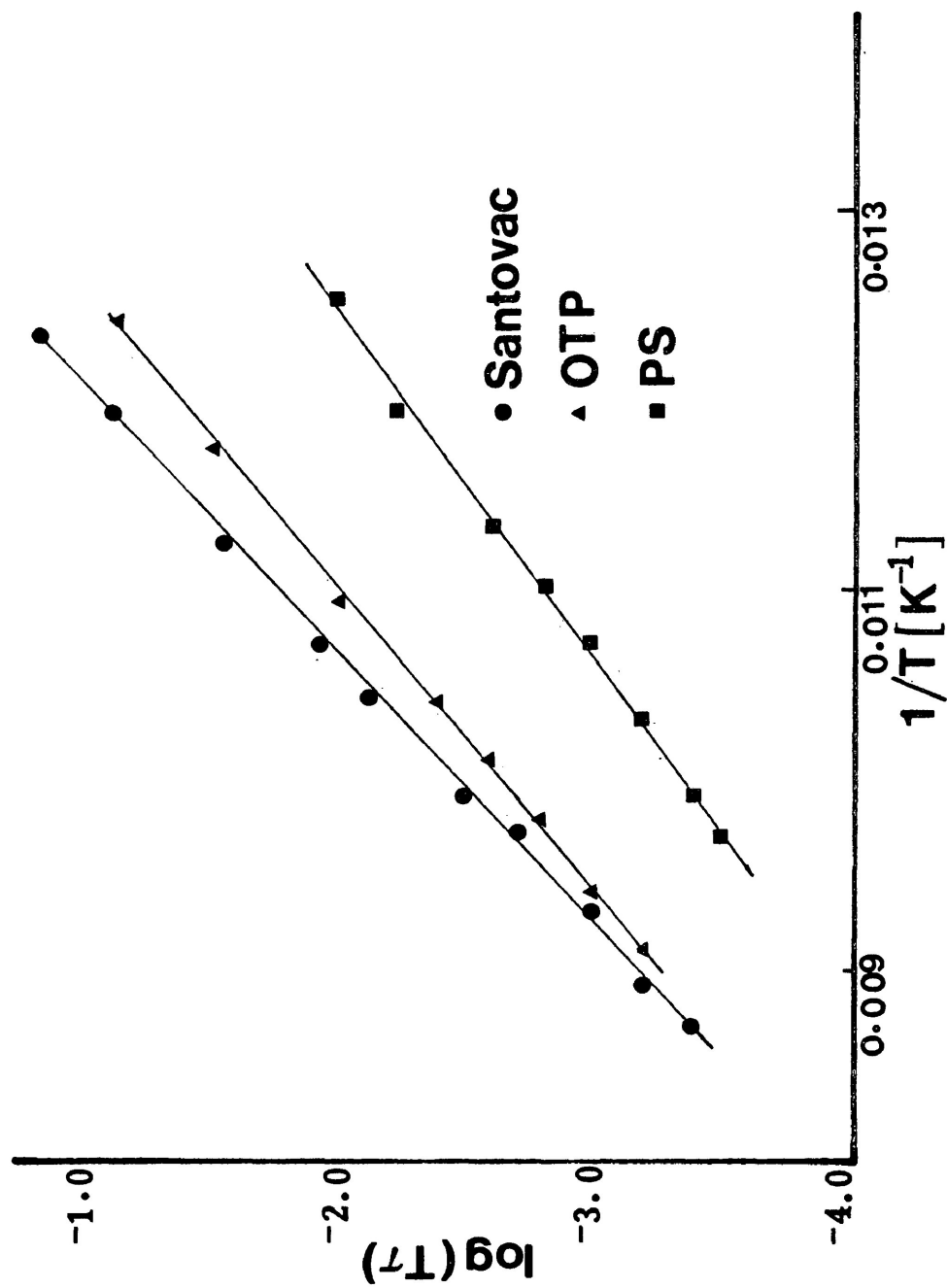
FIGURE IV.16 Eyring plot of $\log(\tau)$ versus $1/T$ (K^{-1}) for o-dichlorobenzene

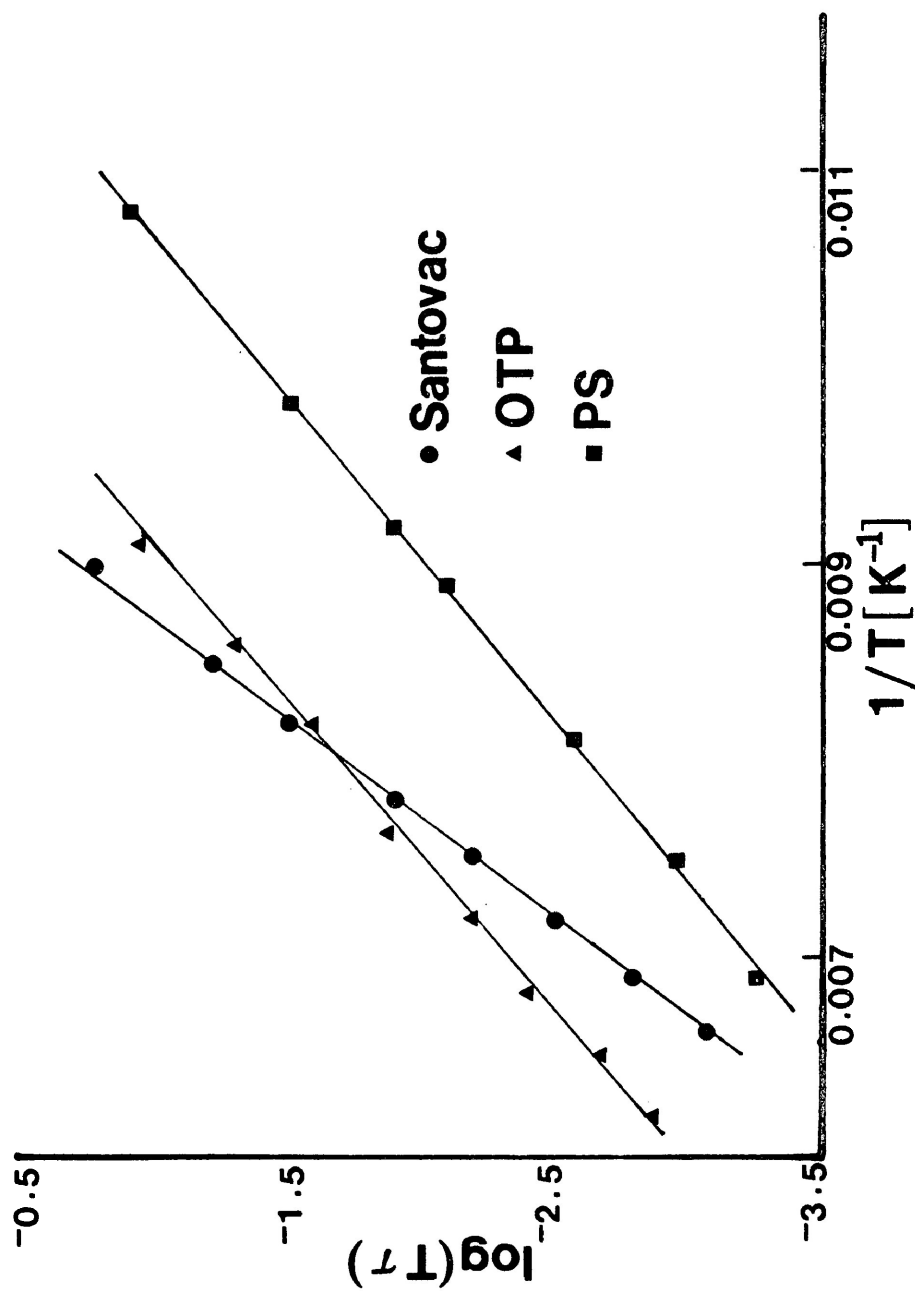
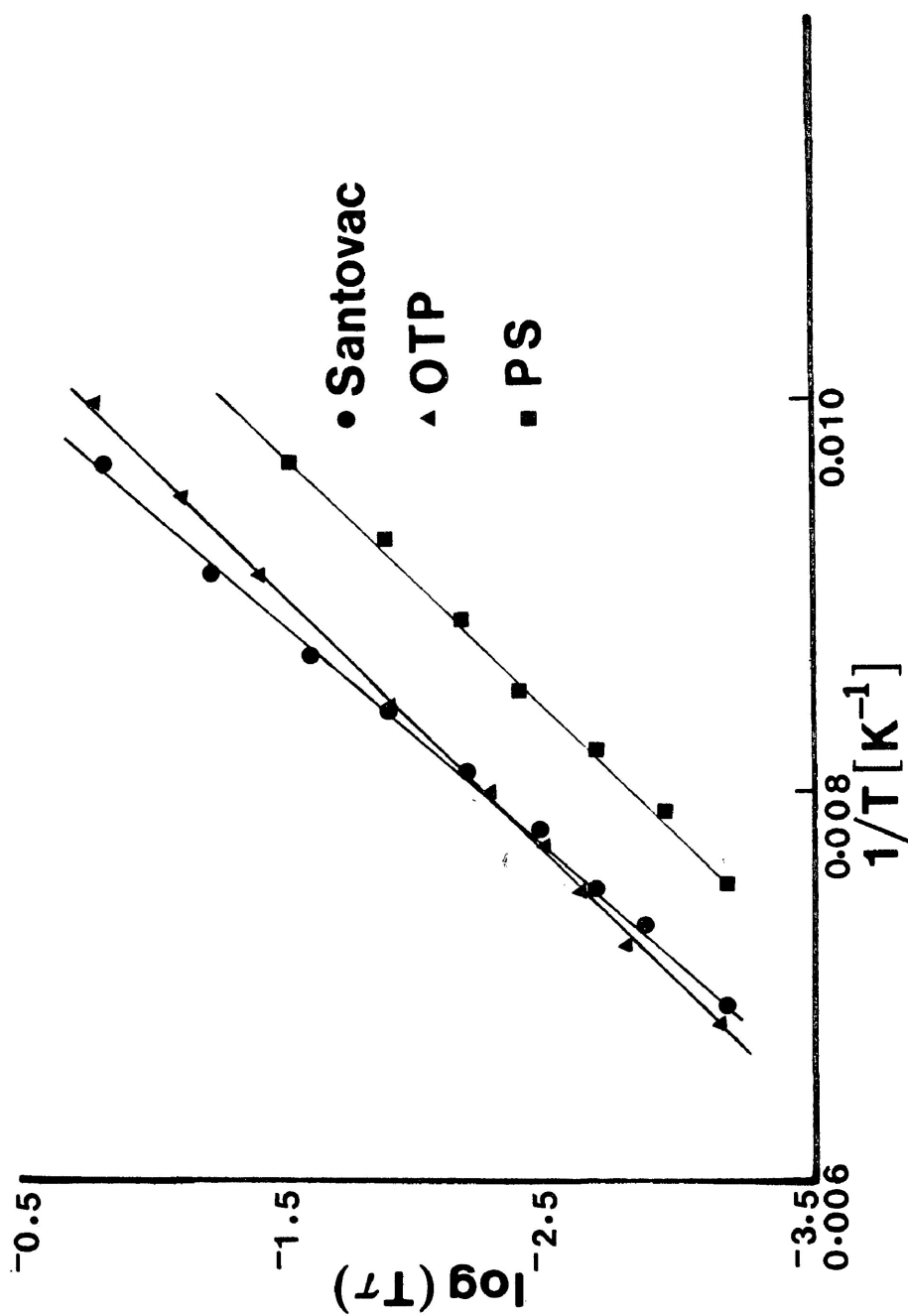
FIGURE IV.17 Eyring plot of $\log(\tau)$ versus $1/T$ (K^{-1}) for nitrobenzene

FIGURE IV.18 Eyring plot of $\log(T\tau)$ versus $1/T$ (K^{-1}) for 1-chloronaphthalene



CHAPTER V

RELAXATION PROCESSES OF SOME

ANISOLES AND ACETOPHENONES

INTRODUCTION

Dielectric absorption techniques have variously been used for the study of molecular and/or intramolecular motions of numerous molecules containing rotatable polar groups, particularly in dilute solutions of non-polar solvents. Such studies have often been complicated by the overlap of the molecular and the intramolecular processes, requiring a Budo analysis which in a number of cases, is now known to be unsatisfactory (1) for the interpretation of relaxation data. However, by dispersing the polar molecules in a polymer matrix such as in polystyrene, it has been found possible by Davies et al (2,3) and Walker et al (4-14) that in a number of cases the intramolecular absorption process can be separated completely from the molecular relaxation owing to the high viscosity of the medium.

In recent years, considerable interest has been shown in establishing accurate energy barriers to methoxy and acetyl groups rotation and in examining the factors such as steric and conjugative effects which influence their barrier. Molecules which have a methoxy group attached to an aromatic ring have been widely studied

by dielectric techniques (15-18). The molecules have been examined either as a pure liquid or as a solute in a dilute solution of a non-polar solvent and the absorption has been observed in the microwave region. In all cases the molecular and group absorptions have overlapped and the relaxation time obtained for the group rotation (deduced from a Budó analysis (1)) indicate that the methoxy group has a high degree of mobility. Mazid et al (8), from their dielectric studies in a polystyrene matrix, concluded that "in the absence of appreciable steric or mutual conjugative effects the barrier to methoxy group relaxation, attached to a conjugated system, is low and of the order of 10 kJ mol^{-1} ."

The energy barrier to acetyl group rotation, when the acetyl group is attached to an aromatic ring, has also received some attention. McLellan and Walker (4) studied the acetyl group relaxation in some aromatic ketones dispersed in a polystyrene matrix and determined the energy barrier for the intramolecular process in a few cases. For example, for both 4-acetylbiphenyl and 2-acetylfluorene the acetyl group relaxation was completely separated from the molecular process, and accurate

enthalpies of activation for each process were obtained. Recently Mazid et al (11) studied eight phenyl-alkyl ketones of the type C_6H_5COR where R is varied from CH_3 to $C_{10}H_{21}$ in a polystyrene matrix. He found an intramolecular relaxation process in each case with an enthalpy of activation of the same order of magnitude ($\Delta H_E = \sim 30 \text{ kJ mol}^{-1}$) as that for acetyl group relaxation in acetophenone, 4-acetylbiphenyl and 1,4-diacetylbenzene (4).

Thus, the foregoing review indicates that the energy barrier for acetyl group rotation differ considerably from that for methoxy group rotation and merit further examination. Therefore, it seemed worthwhile to investigate dielectrically a number of anisoles and acetophenones (listed in Figure V.1) dispersed in (i) a polystyrene matrix, (ii) o-terphenyl and (iii) polyphenyl ether. Such a procedure has proved successful in the study of suitable intramolecular motion and also in the determination of the energy barrier for an intramolecular and/or molecular relaxation process separately.

V.2

EXPERIMENTAL RESULTS

The dielectric measurements of a number of

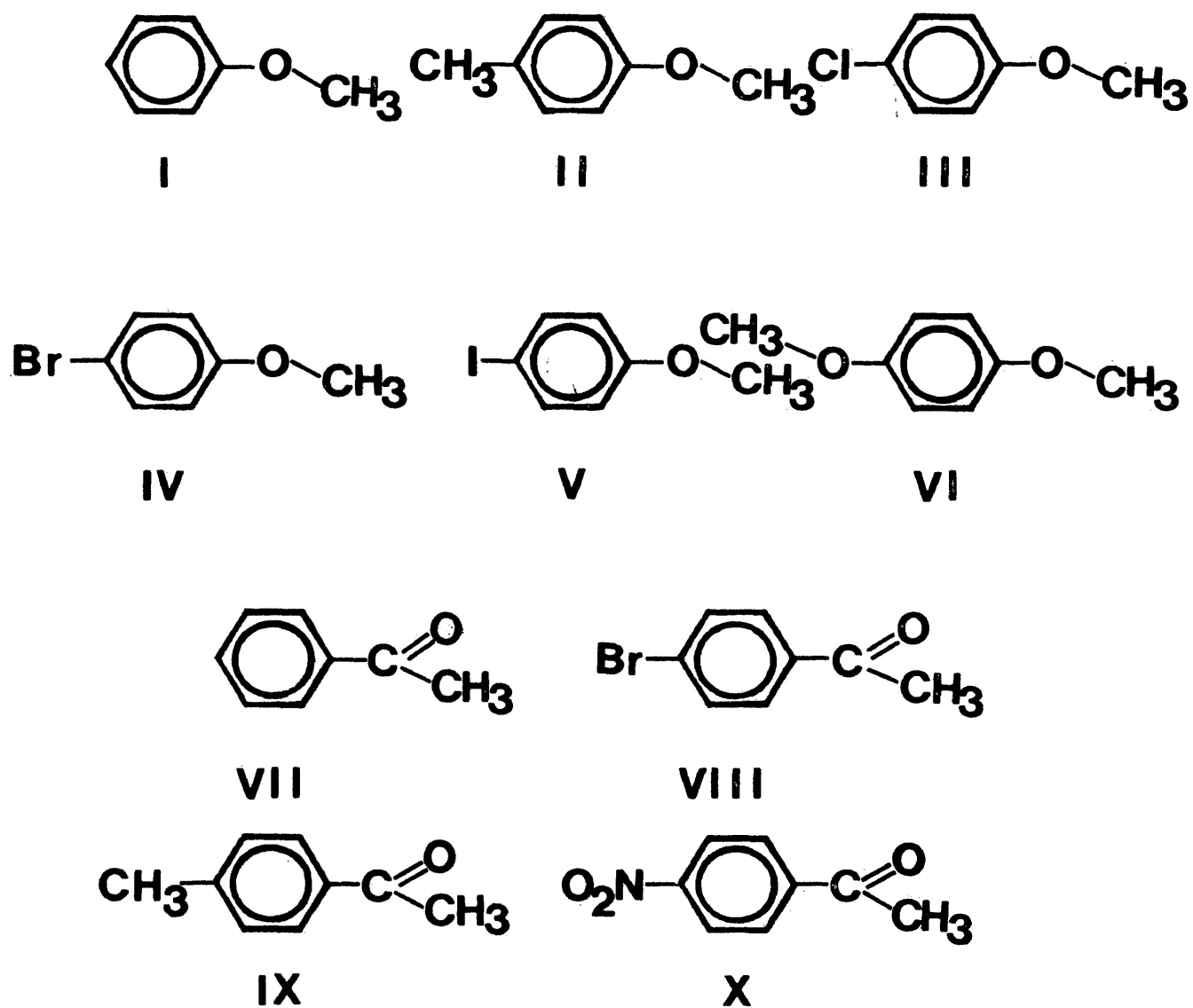


FIGURE: V.1

I	anisole	II	para-methylanisole
III	para-chloroanisole	IV	para-bromoanisole
V	para-iodoanisole	VI	para-dimethoxybenzene
VII	acetophenone	VIII	para-bromoacetophenone
IX	para-methylacetophenone	X	para-nitroacetophenone

methoxy and acetyl groups containing molecules (listed in Figure V.1) have been made in the frequency range of 10^2 to 10^5 Hz by the use of a General Radio bridge, the procedure being described in Chapter III. The solvents used are: (i) polystyrene, (ii) o-terphenyl and (iii) polyphenyl ether.

Sample plots of loss factor ($\epsilon'' = \epsilon''(\text{obs}) - \epsilon''(\text{solvent})$) versus logarithm (frequency) are shown in Figures V.2 to V.4, while Figures V.5 and V.6 show the plots of loss factor, ϵ'' , versus temperature, T(K). Figures V.7 to V.11 show the sample plots of $\log T\tau$ versus $1/T$.

Table V.1 lists the results from Eyring analyses, while Table V.2 summarizes the Fuoss-Kirkwood analysis parameters together with the values of ϵ_∞ and the experimental dipole moments.

V.3 DISCUSSION

The Eyring analysis results and the Fuoss-Kirkwood analysis parameters for the molecules listed in Figure V.1 have been presented in Tables V.1 and V.2,

respectively. Table V.2 also gives the values of ϵ_{∞} and apparent dipole moments corresponding to the dispersion at a particular temperature. The relaxation times and the free energies of activation have been shown at temperatures which are close to the individual absorptions.

Figure V.7 shows the plot of $\log T\tau$ versus $1/T$ for anisole in *o*-terphenyl and the Eyring analysis of which gave $\Delta H_E = 11.0 \pm 0.5 \text{ kJ mol}^{-1}$, $\Delta G_{E(100 \text{ K})} = 15.3 \text{ kJ mol}^{-1}$, $\tau_{100 \text{ K}} = 4.9 \times 10^{-5} \text{ s}$, and $\Delta S_E = -43.3 \pm 5.6 \text{ J K}^{-1} \text{ mol}^{-1}$ (Table V.1). There may be two relaxation candidates in this molecule, one being the molecular relaxation and the other methoxy group relaxation. But bromobenzene, a molecule which Courtald models indicate is slightly smaller in size, gave higher values of ΔH_E ($= 17.4 \pm 1.1 \text{ kJ mol}^{-1}$), $\Delta G_{E(100 \text{ K})}$ ($= 20.7 \text{ kJ mol}^{-1}$), $\tau_{100 \text{ K}} = 3.3 \times 10^{-2} \text{ s}$, and ΔS_E ($= -33.3 \pm 8.1 \text{ J K}^{-1} \text{ mol}^{-1}$) in the same solvent (Chapter IV). On the other hand, the observed value of ΔH_E ($= 11.0 \text{ kJ mol}^{-1}$) is in good agreement with the value of 11 kJ mol^{-1} obtained by Griendley et al (19) from a somewhat empirical approach for methoxy group rotation in anisole. Therefore, these results suggest that the observed process in anisole may contain maximum contribution from the methoxy group rotation. Earlier investigators

(15,17,20,21) also indicated that methoxy group rotation contributes to the total dielectric absorption of anisole.

para-Methyl anisole has been chosen as an important molecule for this study because the methyl group moment is directed into the ring and opposes the resultant fixed component of the moment from the anisole part of the molecule on the long axis so this molecule has virtually no component of the dipole moment along this axis and consequently the only process to be detected is group relaxation. Farmer and Walker (15), from their dielectric studies of para-methylanisole in para-xylene at 25°C at microwave frequencies, suggested that methoxy group relaxation predominates in this molecule. Table V.1 shows that para-methylanisole gave one absorption process in a polystyrene matrix. However, two absorption processes were found in both o-terphenyl and polyphenyl ether. The process in the liquid nitrogen temperature region is common in all the three media and yielded almost identical values of ΔH_E , $\Delta G_E(100\text{ K})$, $\tau_{100\text{ K}}$, and ΔS_E (see Table V.1). These observed values of ΔH_E ($\sim 8\text{ kJ mol}^{-1}$) and other parameters for this molecule seems to be too low for the molecular process when compared to the corresponding

values obtained for para-chlorotoluene, a rigid molecule of smaller size, in all these three media (Chapter IV). Mazid et al (8) obtained ΔH_E values of $\sim 10 \text{ kJ mol}^{-1}$ for methoxy group rotation in substituted anisoles. Thus, the enthalpies of activation ($\Delta H_E = \sim 8 \text{ kJ mol}^{-1}$) obtained for para-methylanisole for the low temperature process is consistent with the values reported by Mazid et al (8) and indicates that the process is methoxy group rotation.

The high temperature process of para-methylanisole in o-terphenyl yielded $\Delta H_E = \sim 210 \text{ kJ mol}^{-1}$, $\Delta S_E = \sim 710 \text{ J K}^{-1} \text{ mol}^{-1}$, $\Delta G_E(200 \text{ K}) = 37.6 \text{ kJ mol}^{-1}$, $\tau_{200 \text{ K}} = 1.7 \times 10^{-3} \text{ s}$. These parameters for this process were evaluated by linear regression of the equation (11 - 22). The measured glass transition temperature, T_g , of the sample was found to be $\sim 211 \text{ K}$. All these results suggest a cooperative motion of the whole molecule together with the associated solvent molecules. Similarly the value of $\Delta H_E = \sim 213 \text{ kJ mol}^{-1}$, $\Delta S_E = \sim 651 \text{ J K}^{-1} \text{ mol}^{-1}$, $\Delta G_E(200 \text{ K}) = 45.6 \text{ kJ mol}^{-1}$ and $\tau_{200 \text{ K}} = 2.4 \times 10^{-2} \text{ s}$, evaluated for the higher temperature process of para-methylanisole in polyphenyl ether with $T_g = 252 \text{ K}$

may be ascribed to the cooperative motion of the whole molecule together with the segments of the polymer chain (see Chapter VI-VII).

Table V.1 shows that para-chloro-, para-bromo-, and para-iodoanisoles in o-terphenyl absorbed in almost the same temperature region and yielded identical values of Eyring parameters, within the limits of experimental error. The temperature region and the values of ΔH_E ($= \sim 8 \text{ kJ mol}^{-1}$), $\Delta G_{E(100 \text{ K})}$ ($= \sim 15 \text{ kJ mol}^{-1}$), and $\tau_{100 \text{ K}}$ ($= 3-4 \times 10^{-5} \text{ s}$) for these para-haloanisoles are of the same order of magnitude for group rotation in para-methyl anisole.

para-Dimethoxybenzene was studied in o-terphenyl and polyphenyl ether and absorption process was found in the region of liquid nitrogen temperature in both the media. Figure V.9, gives the sample plot of $\log T\tau$ against $1/T$ for para-dimethoxy benzene in polyphenyl ether. The Eyring analysis gave $\Delta H_E = 3.3 \pm 0.3$ and $5.4 \pm 0.4 \text{ kJ mol}^{-1}$; $\Delta S_E = -101.9$ and $-80.8 \text{ J K}^{-1} \text{ mol}$; $\Delta G_{E(100 \text{ K})} = 13.6$ and 13.6 kJ mol^{-1} ; and $\tau_{100 \text{ K}} = 6.0 \times 10^{-6}$ and $6.3 \times 10^{-6} \text{ s}$ in o-terphenyl and polyphenyl ether, respectively. These low barriers for this molecule

may be attributed to group rotation. Previous workers (15-17) have examined para-dimethoxy-benzene in cyclohexane and benzene at microwave frequencies. They obtained unusually short relaxation time for this molecule and concluded that the principal mechanism of relaxation is the rotation of the two OCH_3 groups about their bonds to the ring. Recently, Mazid et al (8), from their dielectric studies in a polystyrene matrix, characterize methoxy group rotation in a similar molecule, i.e. 2,6-dimethoxynaphthalene, with comparable values of activation parameters ($\Delta H_E = 11 \pm 1 \text{ kJ mol}^{-1}$, $\Delta G_E(150 \text{ K}) = 14 \text{ kJ mol}^{-1}$ and $\tau_{150 \text{ K}} = 1.5 \times 10^{-5} \text{ s}$).

Therefore, it would seem likely that methoxy group rotation predominantly contributes to the dielectric relaxation of the above mentioned anisoles. Also, the results of para-methyl-, and para-haloanisoles clearly indicates that the barrier to methoxy group rotation is insensitive to para-substituents and virtually remains the same, i.e., of the order of $\sim 8 \text{ kJ mol}^{-1}$.

Acetophenone, a molecule where the keto group is conjugated with the π -electrons of the benzene ring, has been extensively studied in order to gain some

appreciation of the behaviour of acetyl group relaxation.

A far-infrared study (22) of acetophenone in the gas phase gave a value of 13.0 kJ mol^{-1} for acetyl group relaxation. Ab initio calculations (23) yielded 18.4 kJ mol^{-1} . Grindley et al (19) have estimated from n.m.r. data on para-substituted acetophenones that the energy barrier to group rotation in acetophenone is 26 kJ mol^{-1} . A detailed dielectric study has been made for acetophenone and the results are given in Table V.1 at two different molar concentrations in all the three media, i.e. polystyrene matrices, o-terphenyl and polyphenyl ether. The data in polystyrene matrices are provided for comparison through the courtesy of (i) McLellan and Walker (4) for 0.27 M solution, and (ii) Mazid et al (11) for 0.48 M solution. It should be noted that these workers, from their dielectric studies of acetophenone and different substituted acetophenones, concluded that the barrier to acetyl group rotation is of the order of $\sim 30 \text{ kJ mol}^{-1}$.

Sample plots of dielectric loss versus logarithm (frequency) are shown in Figure V.3 for 0.23 M acetophenone in polyphenyl ether, while Figure V.10

shows the plots of $\log T\tau$ versus $1/T$ for acetophenone (at mentioned molar concentrations) in all the three media. Table V.1 shows that the enthalpies of activation, ΔH_E ($\sim 30 \text{ kJ mol}^{-1}$), and other relaxation parameters obtained by this work for acetophenone in o-terphenyl and polyphenyl ether are in good agreement, well within the estimated experimental error, with the corresponding values reported by earlier workers (4,11) for acetyl group rotation in acetophenone in a polystyrene matrix.

The effect of concentration on the relaxation parameters of acetophenone in different media seems to be more interesting. Borisova and Chirkov (24) from a limited study found that the energy barrier for molecular relaxation of small molecules in a polystyrene matrix increased with concentrations of solute above about 5 to 7 mol percent. Hains and Williams (25) have reported a similar result, concluding that this effect is linked to the fact that, as solute concentration is increased, the surroundings of a given molecule are altered from simple polymer segments to some mixture of polymer segments and other solute molecules. The present results indicate that the change of the concentration of the solute

from ~ 0.2 M to ~ 0.9 M does not change appreciably the magnitude of the intramolecular energy barriers and other relaxation parameters except the dielectric loss factor (Table V.1 and V.2). Thus, it would seem more likely that the group relaxation is less sensitive to environment than molecular relaxation. However, it was found that the dielectric loss factor, ϵ'' , increases proportionally with the increase of solute concentration. Table V.3 shows that in each medium the quantity $(\epsilon''_{\text{maximum}}/\text{concentration})$ at a particular value of $\log(\text{frequency})_{\text{maximum}}$ remains almost constant irrespective of the solute concentration.

para-Bromoacetophenone showed only one family of absorption curves (Figure V.4) which occurred in the temperature range 187-209 K in o-terphenyl. An Eyring plot of the data is given in Figure V.11 which yielded $\Delta H_E = 32.9 \pm 3.1 \text{ kJ mol}^{-1}$, $\Delta G_E(200 \text{ K}) = 30.9 \text{ kJ mol}^{-1}$, $\tau_{200 \text{ K}} = 2.9 \times 10^{-5} \text{ s}$, and $\Delta S_E = 13.2 \pm 16.0 \text{ J K}^{-1} \text{ mol}^{-1}$. Table V.1 shows that these parameters obtained for para-bromoacetophenone are almost similar, within the limits of experimental error, to the corresponding values obtained for acetyl group rotation in acetophenone.

This indicates that the insertion of a para-bromo group does not appreciably influence the acetyl barrier, which is consistent with the behaviour of para-methyl and para-halo groups in anisoles.

para-Methyl- and para-nitroacetophenones were examined in o-terphenyl from liquid nitrogen temperature up to above the glass transition temperature, T_g (≈ 243 K (26)), of the solvent. Figures V.5 and V.6 show the plots of dielectric loss versus temperature, $T(K)$, at 1 kHz frequency for para-methyl- and para-nitroacetophenones, respectively. These plots indicate no sign of any detectable absorption process in the temperature/frequency range available in the glassy o-terphenyl; but only the cooperative process of the solvent above its T_g was observed. The absence of intramolecular or molecular absorption process for these molecules in o-terphenyl may be attributed either to weak absorptions or the process has merged with the high loss cooperative process of the solvent. The asymmetric nature of the curves in the temperature range 220-240 K (Figures V.5 and V.6) suggest the latter is the case. This is also supported by the fact that the

perpendicular component of the dipole moment for these molecules is virtually the same as for acetophenone and para-bromoacetophenone and there is no good reason why the acetyl group relaxation should not be observed unless it were overlapped by the more intense absorption of the co-operative process.

REFERENCES

1. J. Crossley, S.P. Tay and S. Walker, Adv. Mol. Relax. Proc., 6(1974)79.
2. M. Davies and A. Edwards, Trans. Faraday, Soc., 63(1967)2163.
3. M. Davies and J. Swain, Trans. Faraday Soc., 67(1971)1637.
4. C.K. McLellan and S. Walker, Can. J. Chem., 55 55(1977)583.
5. S.P. Tay, S. Walker and E. Wyn-Jones, Adv. Mol. Relax. Inter. Proc., 13(1978)47.
6. J. Crossley, M.A. Mazid, C.K. McLellan, P.F. Mountain and S. Walker, Can. J. Chem., 56(1978)567.
7. Ibid., Adv. Mol. Relax. Inter. Proc., 12(1978)239.
8. M.A. Mazid, J.P. Shukla and S. Walker, Can. J. Chem., 56(1978)1800.
9. A. Lakshmi, S. Walker, N.A. Weir and J.H. Calderwood, J. Phys. Chem., 82(1978)1091.
10. Ibid., J. Chem. Soc. Trans. Faraday II, 74(1978)727.
11. M.A. Mazid, S. Walker and N.A. Weir, Adv. Mol. Relax. Inter. Proc., 19(1981)249.
12. H.A. Khwaja, M.A. Mazid and S. Walker, Z. Phys. Chem. Neue Folge, 128(1981)147.
13. H.A. Khwaja and S. Walker, Adv. Mol. Relax. Inter. Proc., 22(1982)27.

14. J.P. Shukla, J. Warren and S. Walker,
Z. Phys. Chem. Neue, 125(1981)67.
15. D.B. Farmer and S. Walker, Can. J. Chem.,
47(1969)4645.
16. D.M. Roberti and C.P. Smyth, J. Am. Chem.
Soc., 82(1960)2106.
17. E. Forest and C.P. Smyth, J. Am. Chem. Soc.,
86(1964)3474.
18. S.K. Garg and C.P. Smyth, J. Chem. Phys.,
46(1967)373.
19. T.B. Grindley, A.R. Katritzky, and R.D.
Topsom, J. Chem. Soc. Perkin
Trans. II, (1974)289.
20. E.L. Grubb and C.P. Smyth, J. Am. Chem.
Soc., 83(1961)4873.
21. E. Fischer, Z. Naturforsch, 9a(1954)909.
22. F.A. Miller, W.G. Fateley, and R.E. Witkowski,
Spectrochim, Acta, 23A(1967)891.
23. W.J. Hehre, L. Radom, and J.A. Pople, J. Am.
Chem. Soc., 94(1972)1496.
24. T.I. Borisova and V.N. Chrikov, Russian J. Phys.
Chem., 47(1973)949.
25. P.J. Hains and G. Williams, Polymer,
16(1975)725.
26. J. Crossley, D.L. Gourlay, M. Rujimethabhas,
S.P. Tay, and S. Walker, J. Chem.
Phys., 71(1979)10.

TABLE V.1
EYRING ANALYSIS RESULTS FOR SOME ANISOLES AND ACETOPHENONES IN ORGANIC CLASSES

MOLECULE	MEDIUM	ΔT (K)	Relaxation Time τ (s)			ΔG_E (kJ mol ⁻¹)			ΔH_E kJ mol ⁻¹	ΔS_E J K ⁻¹ mol ⁻¹
			100 K	200 K	300 K	100 K	200 K	300 K		
Anisole	o-Terphenyl	82-120	4.9×10^{-5}	3.3×10^{-8}		15.3	19.7		11.0 ± 0.5	-43.3 ± 5.6
para-Methylanisole	Polystyrene Matrix	79-111	1.7×10^{-5}	6.1×10^{-7}		14.4	21.7		7.2 ± 0.5	-72.8 ± 5.3
	o-Terphenyl	79-110 200-213	9.9×10^{-6}	3.4×10^{-8} 1.7×10^{-3}	2.5×10^{-5}	14.0	19.7 37.6	30.4	8.3 ± 0.4 ~ 210	-57.2 ± 4.6 ~ 710
	Polyphenyl ether	80-107 257-268	1.0×10^{-5}	3.3×10^{-8} 2.4×10^{-2}	4.5×10^{-5}	14.0	19.7 45.6	33.6	8.4 ± 0.6 ~ 213	-56.4 ± 7.9 ~ 651
para-Chloroanisole	o-Terphenyl	80-110	2.6×10^{-5}	1.5×10^{-7}		14.8	22.2		7.5 ± 0.6	-73.5 ± 6.9
para-Bromoanisole	o-Terphenyl	87-118	3.9×10^{-5}	1.3×10^{-7}		15.2	22.0		8.3 ± 0.3	-68.1 ± 3.3
para-Iodoanisole	o-Terphenyl	79-111	4.1×10^{-5}	2.3×10^{-7}		15.2	22.9		7.5 ± 0.4	-76.5 ± 4.7
para-Diethoxybenzene	o-Terphenyl	79-106	6.0×10^{-6}	4.4×10^{-7}		13.6	23.9		3.3 ± 0.3	-101.9 ± 2.3
	Polyphenyl ether	79-104	6.3×10^{-6}	1.1×10^{-7}		13.6	21.7		5.4 ± 0.4	-80.8 ± 4.4

TABLE V.1 EYRING ANALYSIS RESULTS FOR SOME ANISOLES AND ACETOPHENONES IN ORGANIC GLASSES

MOLECULE	MEDIUM	ΔT (K)	Relaxation time τ (s)			ΔG_E (kJ mol ⁻¹)			ΔH_E kJ mol ⁻¹	$-\Delta S_E$ J K ⁻¹ mol ⁻¹
			100 K	200 K	300 K	100 K	200 K	300 K		
Acetophenone	Polystyrene Matrix	143-213 (a) (0.27 M)	2.8×10^2	6.9×10^{-9}		26	24		29.6 \pm 0.6	26.3 \pm 3.3
		162-181 (b) (0.48 M)	6.2×10^1	1.2×10^{-6}		27.2	25.6		30	23
	o-Terphenyl	173-223 (0.19 M)	2.1×10^3	2.3×10^{-5}		29.9	30.5		29.3 \pm 1.1	-6.4 \pm 5.6
		174-223 (0.88 M)	2.6×10^4	3.5×10^{-5}		32.0	31.0		30.8 \pm 0.7	7.8 \pm 3.8
	Polyphenyl ether	165-218 (0.23 M)	1.0×10^3	1.2×10^{-5}		29.3	29.5		29.2 \pm 1.6	-1.5 \pm 8.2
		172-219 (0.81 M)	2.8×10^4	2.8×10^{-5}		32.1	30.9		31.3 \pm 0.9	11.8 \pm 4.9
para-Bromoaceto- phenone	o-Terphenyl	187-209	3.0×10^2	2.9×10^{-5}		32.5	30.9		32.9 \pm 3.1	13.2 \pm 16

NOTE: Data provided through the courtesy of (a) McLellan and Walker (Ref. 4) and (b) Mazid et al (Ref. 11)

TABLE V.2

Tabulated Summary of Fuoss-Kirkwood Analysis
Parameters, ϵ_{∞} , and Effective Dipole Moments
(μ) for some Anisoles and Acetophenones

T(K)	$10^6 \tau$ (s)	$\log f_{\max}$	β	$10^3 \epsilon''_{\max}$	ϵ_{∞}	μ (D)
<u>0.80 M Anisole in o-Terphenyl</u>						
82.0	992	2.21	0.22	3.00	2.69	0.25
84.7	587	2.43	0.22	3.23	2.69	0.26
89.6	286	2.74	0.19	3.44	2.69	0.30
94.7	124	3.11	0.19	3.66	2.68	0.32
98.4	61.7	3.41	0.19	3.85	2.68	0.33
102.2	43.0	3.57	0.23	4.00	2.69	0.31
105.8	23.2	3.84	0.23	4.17	2.69	0.33
109.0	14.3	4.04	0.23	4.33	2.69	0.34
115.1	9.74	4.31	0.25	4.50	2.69	0.34
120.2	3.86	4.61	0.20	4.47	2.69	0.38
<u>1.03 M para-Methylanisole in Polystyrene Matrix</u>						
79.2	205	2.89	0.21	1.71	2.66	0.17
84.6	82.5	3.21	0.23	1.84	2.66	0.17
86.8	76.0	3.32	0.30	1.87	2.66	0.15
88.8	59.1	3.43	0.32	1.89	2.66	0.15
94.0	19.2	3.75	0.25	1.89	2.66	0.18
97.5	14.1	3.90	0.25	1.97	2.65	0.18
102.9	11.3	4.05	0.33	1.96	2.65	0.16
105.8	9.28	4.15	0.34	1.91	2.65	0.16
110.5	6.24	4.41	0.35	1.93	2.65	0.16
<u>0.74 M para-Methylanisole in o-Terphenyl Low Temperature Process</u>						
79.2	177	2.95	0.21	1.77	2.75	0.20
84.8	77.5	3.31	0.23	1.91	2.75	0.20
86.7	48.8	3.51	0.22	1.95	2.75	0.21
89.8	30.8	3.70	0.23	1.96	2.72	0.21
94.1	18.7	3.93	0.25	2.01	2.72	0.21
97.6	12.1	4.12	0.25	2.07	2.71	0.22
102.6	8.52	4.33	0.28	2.07	2.72	0.21
106.7	5.29	4.48	0.29	2.07	2.72	0.21
110.4	4.57	4.64	0.33	2.04	2.72	0.20

TABLE V.2 continued...

T(K)	$10^6 \tau$ (s)	$\log f_{\max}$	β	$10^3 \epsilon''_{\max}$	ϵ_{∞}	μ (D)
<u>0.74 M para-Methylanisole in o-Terphenyl</u>						
<u>High Temperature Process</u>						
199.9	1685	1.98	0.28	21.85	2.63	0.97
201.6	1041	2.18	0.25	22.58	2.62	1.05
203.4	365	2.64	0.25	22.48	2.62	1.05
205.0	137	3.06	0.27	22.59	2.63	1.02
206.8	52.3	3.48	0.29	22.39	2.63	0.99
207.6	38.6	3.61	0.30	23.22	2.63	0.99
209.4	11.9	4.13	0.35	21.80	2.64	0.90
210.2	9.42	4.23	0.37	22.05	2.65	0.88
213.4	3.50	4.66	0.49	20.39	2.67	0.83

0.76 M para-Methylanisole in Polyphenyl Ether
Low Temperature Process

79.8	312	2.97	0.18	3.12	2.82	0.28
85.0	172	3.32	0.18	3.23	2.82	0.29
89.8	75.6	3.72	0.17	3.40	2.82	0.31
91.4	24.8	3.81	0.19	3.64	2.82	0.31
94.2	22.8	3.88	0.24	3.81	2.83	0.29
97.5	17.3	4.10	0.26	3.87	2.83	0.28
99.5	10.8	4.21	0.22	3.87	2.83	0.31
102.4	8.44	4.29	0.25	3.87	2.83	0.30
106.8	5.81	4.46	0.28	3.85	2.83	0.29

High Temperature Process

257.0	348	2.66	0.47	530.71	3.11	3.52
259.3	112	3.15	0.52	524.80	3.21	3.30
262.3	29.6	3.73	0.61	502.93	3.24	3.01
265.6	10.4	4.18	0.73	508.16	3.40	2.72
267.5	6.20	4.41	0.74	516.59	3.41	2.73

TABLE V.2

continued...

T(K)	$10^6 \tau$ (s)	$\log f_{\max}$	β	$10^3 \epsilon''_{\max}$	ϵ_{∞}	μ (D)
<u>0.49 M para-Chloroanisole in o-Terphenyl</u>						
80.2	368	2.74	0.18	0.96	2.80	0.19
86.3	96.4	3.12	0.20	1.05	2.80	0.20
92.1	62.0	3.41	0.28	1.11	2.80	0.18
96.8	46.4	3.57	0.30	1.15	2.80	0.18
99.8	28.8	3.74	0.28	1.15	2.80	0.19
105.0	15.2	4.02	0.27	1.18	2.80	0.20
110.0	9.88	4.21	0.27	1.18	2.80	0.20
<u>0.43 M para-Bromoanisole in o-Terphenyl</u>						
87.2	608	2.91	0.20	1.07	2.78	0.21
91.7	191	3.15	0.22	1.09	2.78	0.21
96.7	102	3.44	0.26	1.12	2.79	0.20
100.5	60.3	3.63	0.28	1.14	2.79	0.20
104.7	36.2	3.84	0.29	1.17	2.79	0.21
108.8	25.1	4.01	0.31	1.19	2.79	0.20
113.4	17.2	4.19	0.30	1.17	2.79	0.21
118.2	10.4	4.31	0.31	1.16	2.80	0.21
<u>0.37 M para-iodoanisole in o-Terphenyl</u>						
79.3	523	2.48	0.21	0.51	2.69	0.15
84.5	207	2.80	0.22	0.54	2.69	0.16
87.9	158	3.00	0.33	0.55	2.69	0.13
92.4	105	3.20	0.30	0.58	2.69	0.13
97.4	55.1	3.46	0.31	0.59	2.69	0.15
100.4	44.0	3.56	0.30	0.62	2.69	0.15
106.5	21.5	3.87	0.29	0.59	2.69	0.16
110.7	14.1	4.04	0.31	0.59	2.69	0.16

TABLE V.2

continued...

T(K)	$10^6 \tau$ (s)	$\log f_{\max}$	β	$10^3 \epsilon''_{\max}$	ϵ_{∞}	μ (D)
<u>0.63 M para-Dimethoxybenzene in o-Terphenyl</u>						
79.2	21.1	3.88	0.21	2.24	2.68	0.24
82.0	17.0	3.97	0.22	2.27	2.68	0.24
84.3	11.0	4.01	0.22	2.31	2.68	0.25
88.5	9.71	4.18	0.24	2.32	2.68	0.25
93.0	8.71	4.26	0.25	2.27	2.69	0.24
95.0	7.48	4.33	0.27	2.27	2.69	0.24
99.6	6.25	4.41	0.26	2.16	2.69	0.24
102.7	5.64	4.45	0.28	2.03	2.69	0.23
106.0	4.50	4.55	0.29	2.03	2.69	0.23

0.67 M para-Dimethoxybenzene in Polyphenyl Ether

79.3	46.9	3.53	0.18	4.52	2.86	0.35
83.2	26.4	3.78	0.20	4.70	2.86	0.35
85.1	23.3	3.83	0.21	4.78	2.86	0.34
89.0	14.4	4.00	0.22	4.96	2.86	0.35
91.0	12.3	4.06	0.22	4.97	2.86	0.36
94.0	10.6	4.17	0.23	5.03	2.87	0.36
95.8	9.09	4.24	0.23	5.03	2.87	0.36
99.2	6.88	4.36	0.23	4.92	2.87	0.36
103.8	4.39	4.56	0.23	4.91	2.87	0.37

0.19 M Acetophenone in o-Terphenyl

172.5	503	2.50	0.18	4.66	2.73	1.01
177.6	236	2.83	0.19	4.88	2.73	1.02
182.1	128	3.09	0.20	5.12	2.73	1.04
188.2	72.1	3.34	0.20	5.31	2.73	1.07
192.6	43.8	3.56	0.20	5.50	2.73	1.10
197.3	27.1	3.77	0.20	5.71	2.73	1.14
202.1	19.7	3.91	0.22	5.91	2.73	1.12
206.7	11.5	4.14	0.22	6.08	2.73	1.15
211.9	7.88	4.31	0.20	6.07	2.73	1.21
216.7	5.84	4.44	0.23	6.25	2.73	1.16
222.8	3.57	4.65	0.24	6.36	2.74	1.16

TABLE V.2

continued...

T(K)	$10^6 \tau$ (s)	$\log f_{\max}$	β	$10^3 \epsilon''_{\max}$	ϵ_{∞}	μ (D)
<u>0.88 M Acetophenone in o-Terphenyl</u>						
174.4	745	2.33	0.20	22.12	2.80	0.96
179.0	403	2.60	0.20	22.94	2.80	0.99
185.5	178	2.95	0.20	24.03	2.80	1.03
190.1	101	3.20	0.21	24.87	2.80	1.07
195.7	50.9	3.50	0.21	25.81	2.80	1.05
200.4	34.3	3.67	0.23	26.73	2.81	1.05
205.6	19.5	3.91	0.24	27.53	2.81	1.08
210.7	12.2	4.11	0.24	28.33	2.82	1.09
217.6	7.18	4.35	0.26	30.30	2.81	1.19
223.1	3.90	4.61	0.24	32.67	2.81	1.18
<u>0.23 M Acetophenone in Polyphenyl Ether</u>						
165.0	651	2.39	0.21	6.61	2.95	0.95
171.6	275	2.76	0.21	6.87	2.95	0.99
178.1	119	3.13	0.20	7.09	2.95	1.05
183.9	62.1	3.41	0.20	7.35	2.95	1.08
191.8	22.3	3.85	0.19	7.84	2.95	1.17
197.4	13.8	4.06	0.22	8.25	2.95	1.13
203.7	7.30	4.34	0.22	8.59	2.97	1.17
208.9	6.22	4.41	0.24	8.81	2.96	1.14
214.4	4.17	4.59	0.27	9.07	2.97	1.15
218.3	2.65	4.78	0.26	9.18	2.97	1.16
<u>0.81 M Acetophenone in Polyphenyl Ether</u>						
171.5	832	2.28	0.22	24.21	2.97	0.95
178.5	377	2.63	0.21	25.40	2.97	1.02
184.8	171	2.99	0.21	26.48	2.97	1.06
190.4	83.3	3.28	0.22	27.75	2.97	1.07
197.3	38.1	3.62	0.23	28.96	2.98	1.09
202.7	21.3	3.87	0.23	29.98	2.98	1.12
207.2	14.3	4.04	0.24	30.98	2.98	1.13
211.9	8.60	4.27	0.24	31.62	2.98	1.15
218.7	4.37	4.56	0.25	32.37	2.99	1.16

TABLE V.2

continued...

T(K)	$10^6 \tau$ (s)	$\log f_{\max}$	β	$10^3 \epsilon''_{\max}$	ϵ_{∞}	μ (D)
<u>0.34 M para-Bromoacetophenone in o-Terphenyl</u>						
186.5	106	3.12	0.20	2.59	2.76	0.55
190.1	86.5	3.24	0.26	2.66	2.77	0.50
193.4	65.2	3.42	0.24	2.76	2.77	0.53
194.8	37.5	3.55	0.22	2.72	2.77	0.55
199.2	24.2	3.73	0.21	2.79	2.77	0.58
204.2	18.8	3.96	0.20	2.85	2.78	0.60
209.3	10.1	4.15	0.19	2.96	2.78	0.64

TABLE V.3

$\log f_{\max}$	$10^3 \chi \epsilon''_{\max}$	$\frac{10^3 \chi \epsilon''_{\max}}{\text{conc.}}$
<u>0.27 M Acetophenone in a Polystyrene Matrix</u>		
2.21	11.39	42.98
2.62	11.84	44.68
2.99	12.22	46.11
3.32	12.69	47.89
3.60	13.09	49.40
3.94	13.49	50.91
4.17	13.74	51.84
<u>0.49 M Acetophenone in a Polystyrene Matrix</u>		
3.17	22.08	46.10
3.55	22.95	47.91
3.82	24.07	50.25
4.05	24.62	51.40
4.26	25.54	53.32
<u>0.19 M Acetophenone in o-Terphenyl</u>		
2.50	4.65	24.64
2.82	4.87	25.80
3.09	5.11	27.08
3.34	5.31	28.12
3.55	5.50	29.12
3.76	5.71	30.21
3.90	5.90	31.26
4.13	6.07	32.14
4.30	6.19	32.76
4.43	6.25	33.08
4.64	6.36	33.68
<u>0.88 M Acetophenone in o-Terphenyl</u>		
2.32	22.11	25.05
2.59	22.94	25.98
2.95	24.03	27.22
3.19	24.87	28.17
3.49	25.80	29.23
3.66	26.72	30.27
3.91	27.53	31.18
4.11	28.32	32.08
4.34	30.30	34.32
4.61	32.66	36.99

TABLE V.3 CONTINUED...

$\log f_{\max}$	$10^3 \kappa \epsilon''_{\max}$	$\frac{10^3 \kappa \epsilon''_{\max}}{\text{conc.}}$
<u>0.23 M Acetophenone in Polyphenyl Ether</u>		
2.38	6.61	29.38
2.76	6.86	30.52
3.12	7.09	31.53
3.41	7.35	32.67
3.85	7.84	34.86
4.05	8.25	36.67
4.33	8.59	38.20
4.41	8.81	39.17
4.58	9.07	40.31
4.77	9.18	40.80
<u>0.81 M Acetophenone in Polyphenyl Ether</u>		
2.28	24.21	30.04
2.62	25.39	31.51
2.98	26.48	32.85
3.28	27.75	34.43
3.62	28.96	35.93
3.87	29.97	37.20
4.04	30.97	38.43
4.26	31.61	39.22
4.56	32.36	40.16

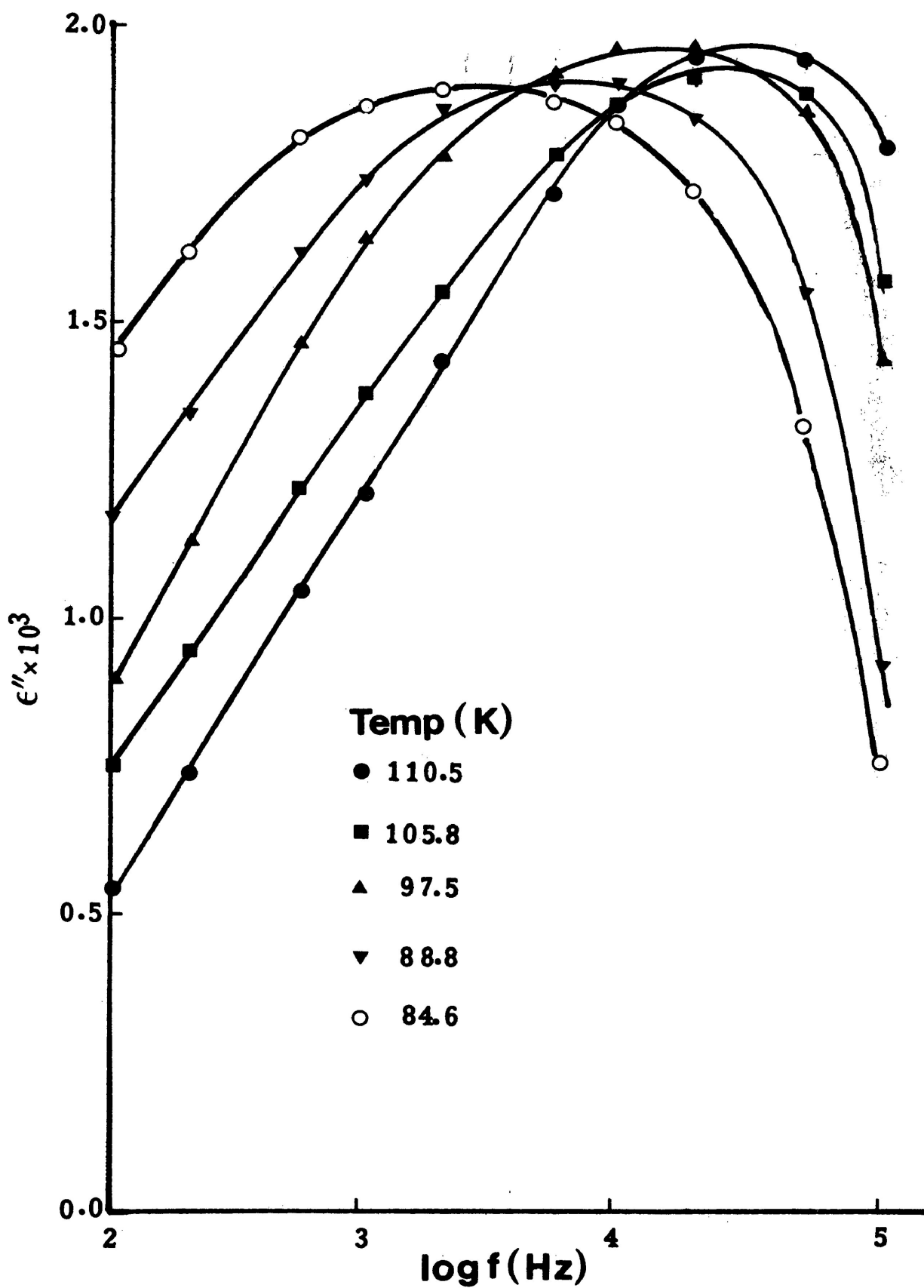


FIGURE V.2

Plot of dielectric loss versus $\log(\text{frequency})$ for para-methyl anisole in a polystyrene matrix

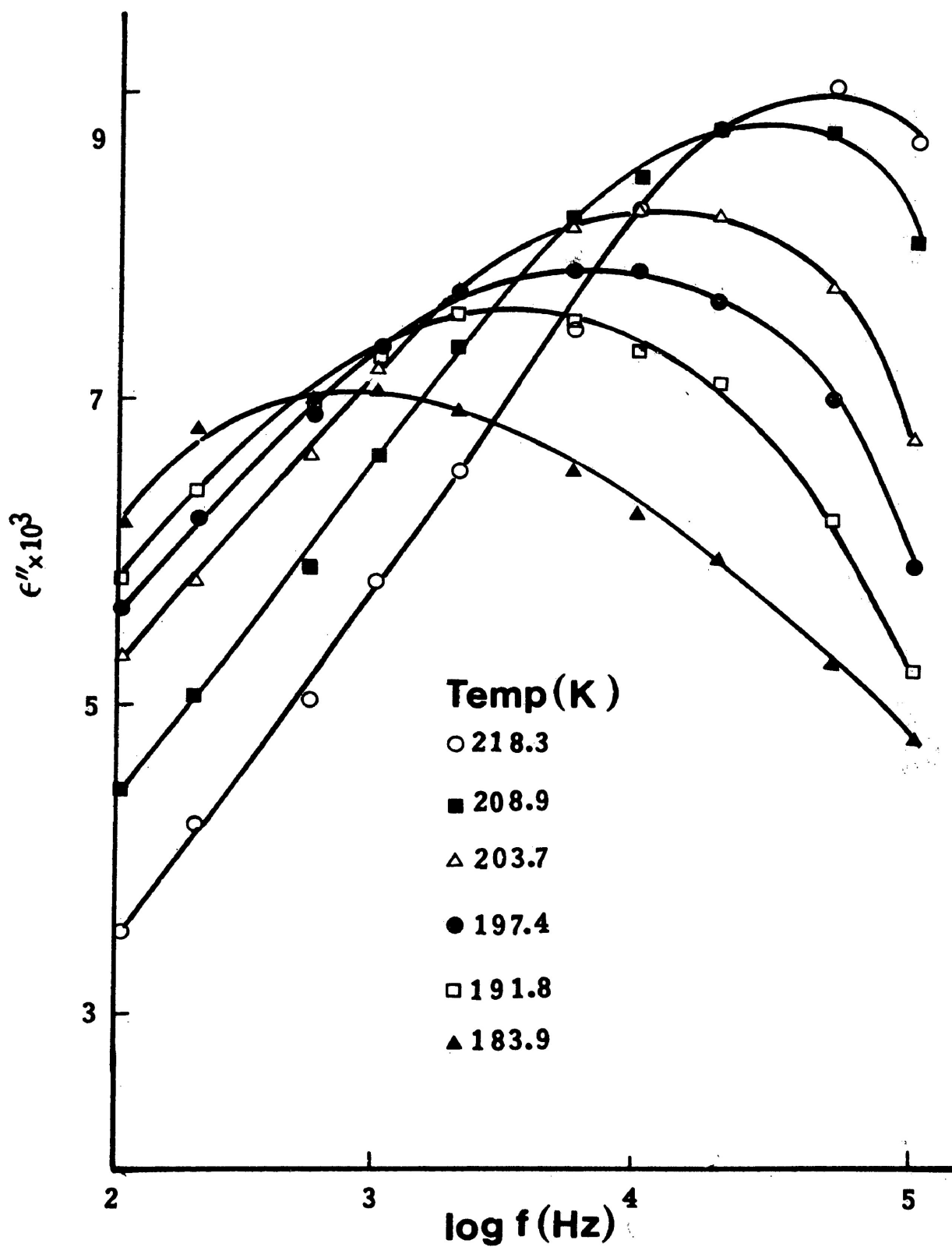


FIGURE V.3

Plot of dielectric loss versus $\log(\text{frequency})$ for acetophenone in polyphenyl ether (conc. 0.23 M)

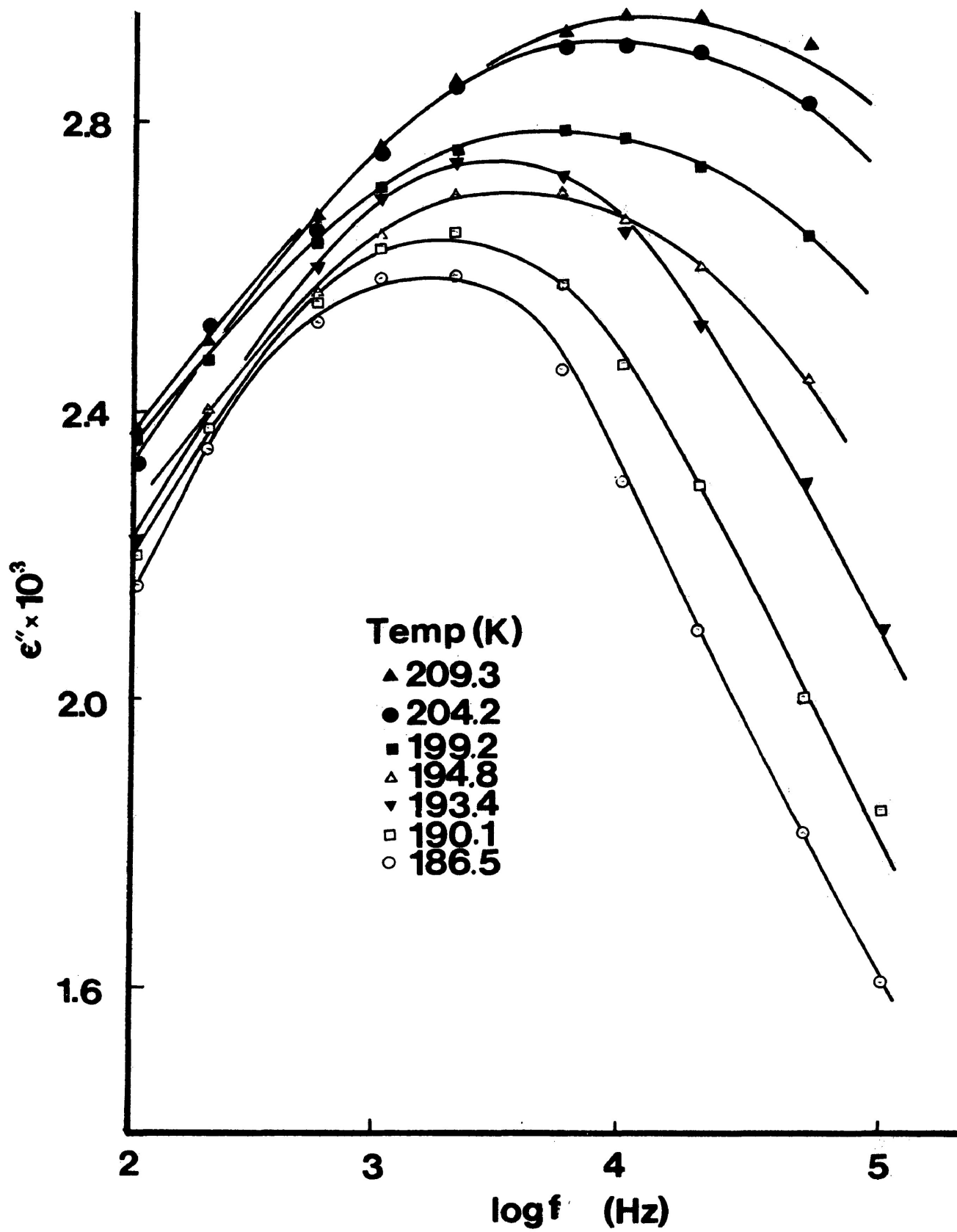


FIGURE V.4 Plot of dielectric loss versus log(frequency) for para-bromoacetophenone in o-terphenyl

FIGURE V.5 Plot of dielectric loss (at 1 kHz) versus temperature (K) for para-methylacetophenone in o-terphenyl

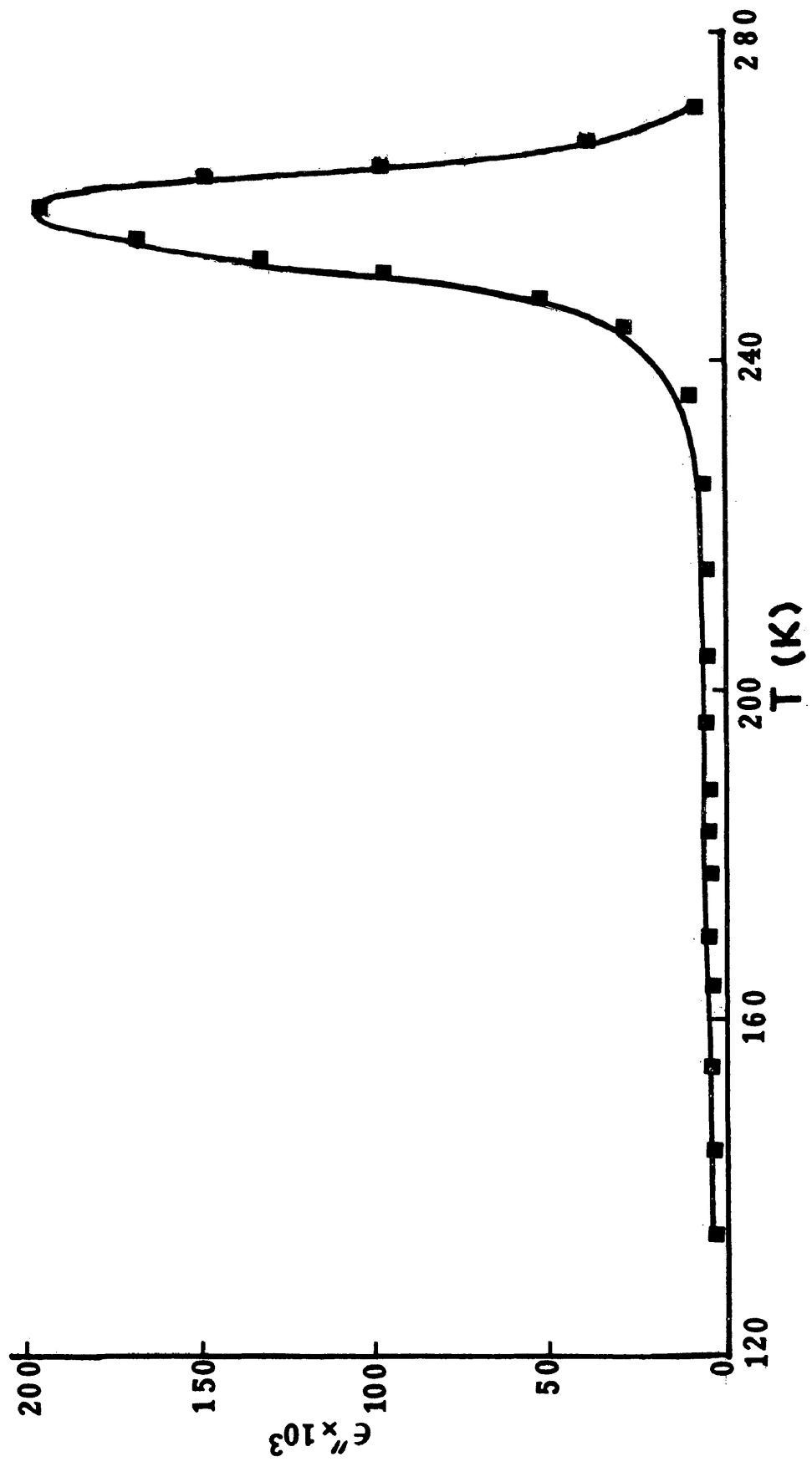


FIGURE V.6 Plot of dielectric loss (at 1 kHz) versus temperature (K) for para-nitroacetophenone in o-terphenyl

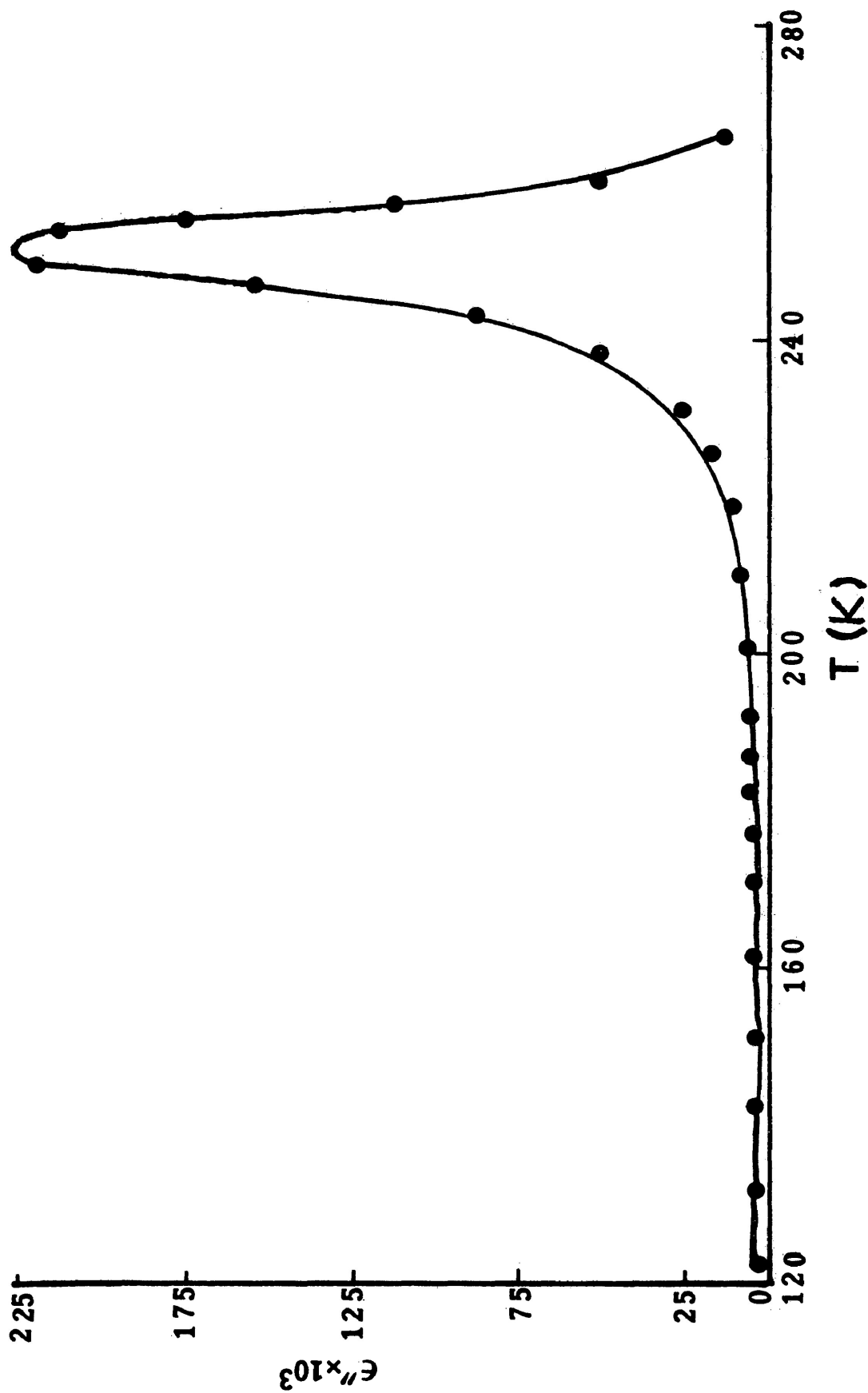
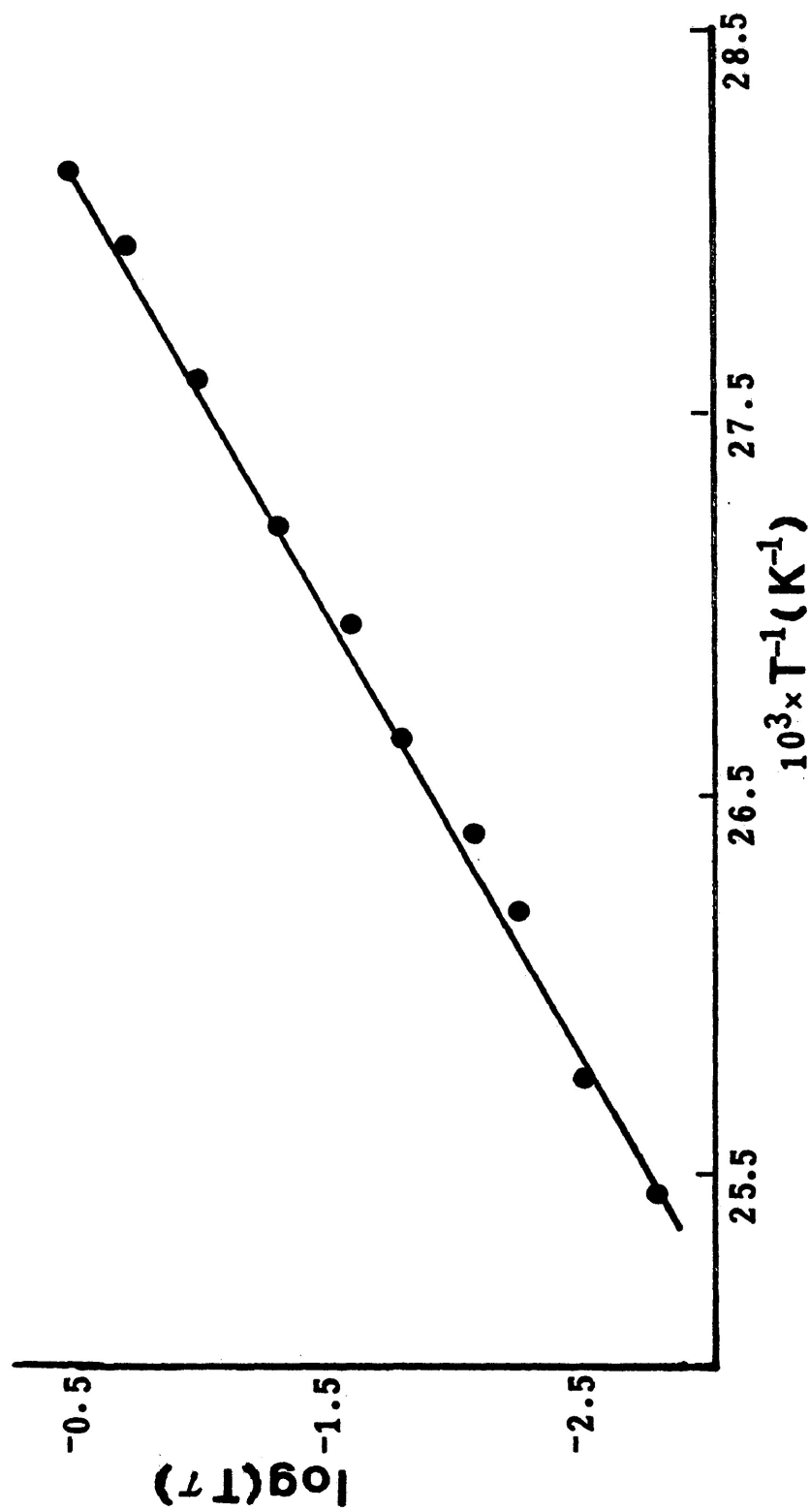


FIGURE V.7 Plot of $\log(\tau\tau)$ versus $1/T$ for anisole in o-terphenyl

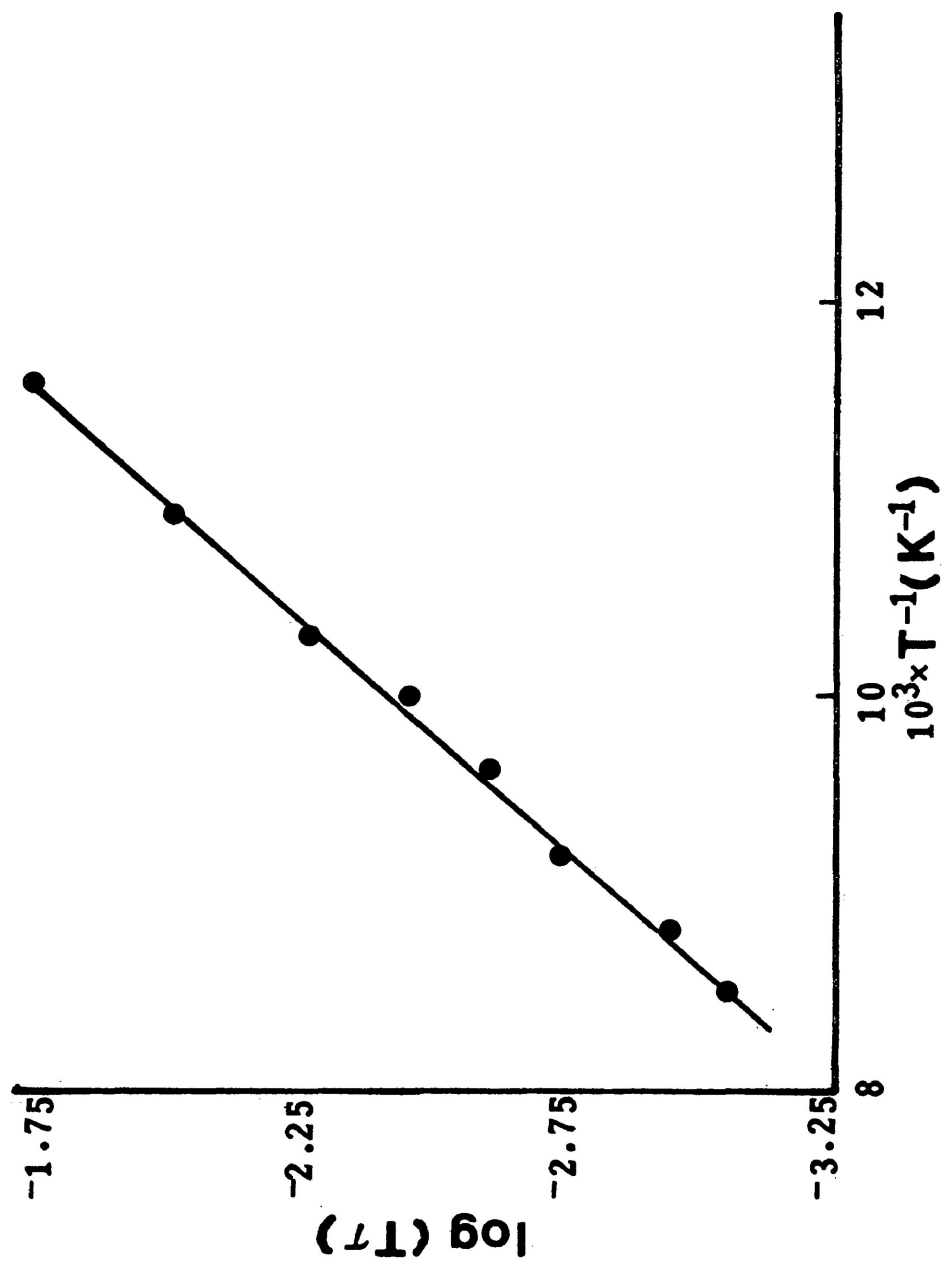


FIGURE V.8 Plot of $\log(T\tau)$ versus $1/T$ for para-bromoanisole in o-terphenyl

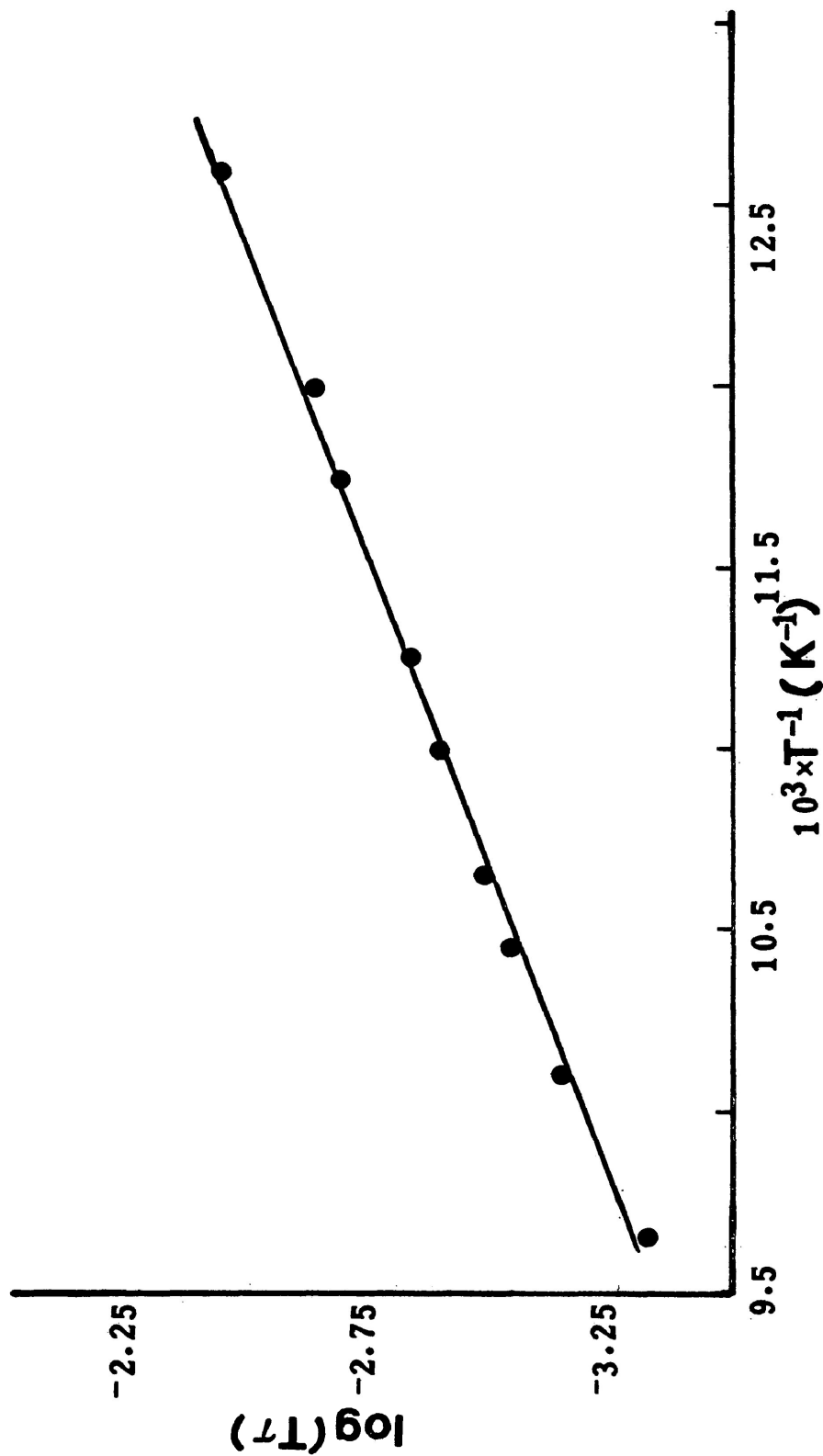


FIGURE V.9 Plot of $\log(TT)$ versus $1/T$ for para-dimethoxy benzene in polyphenyl ether

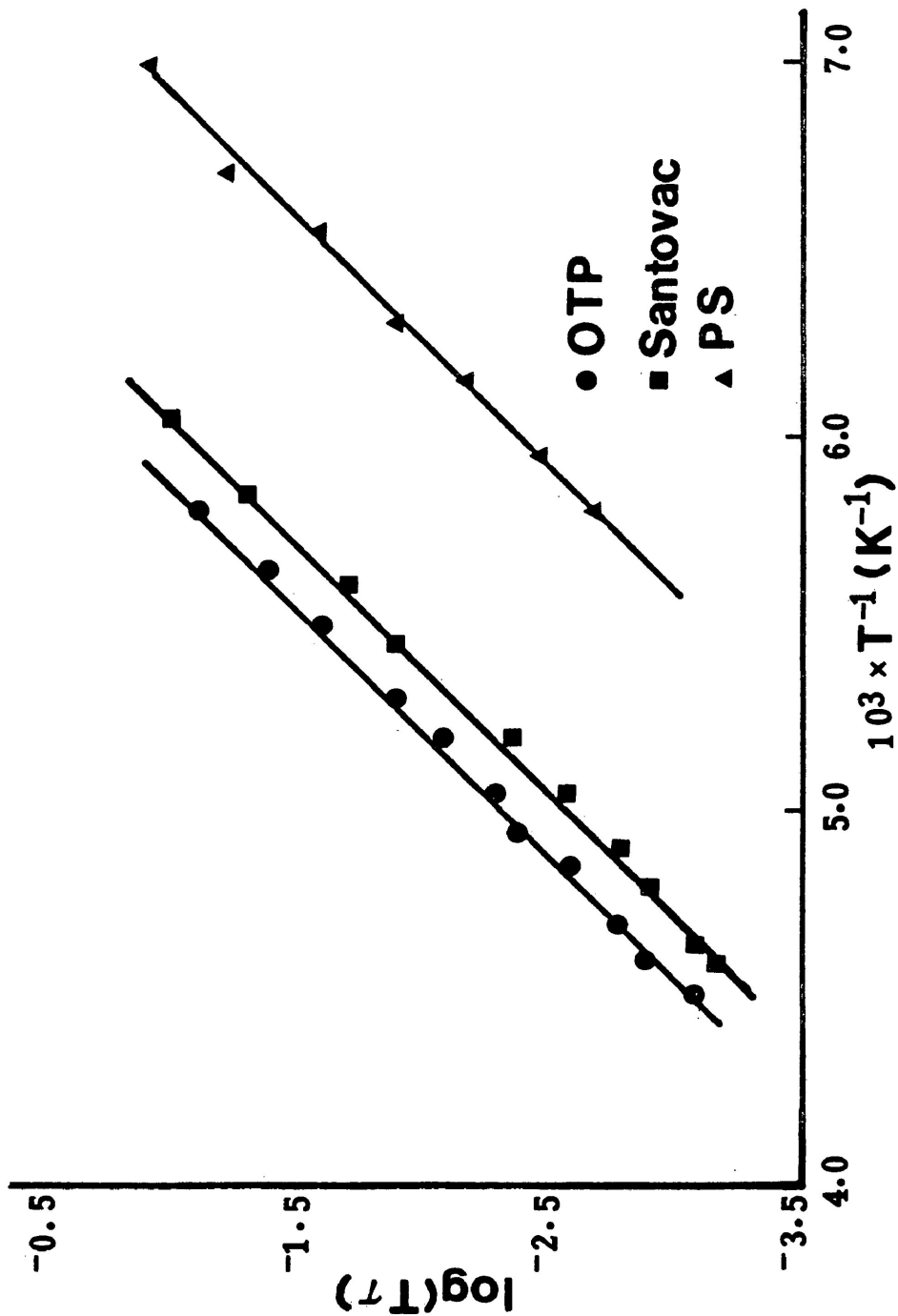


FIGURE V.10 Plot of $\log(T\tau)$ versus $1/T$ for acetophenone in ▲ polystyrene matrix (0.27 M), ● o-terphenyl (0.19 M) and ■ polyphenyl ether (0.23 M).

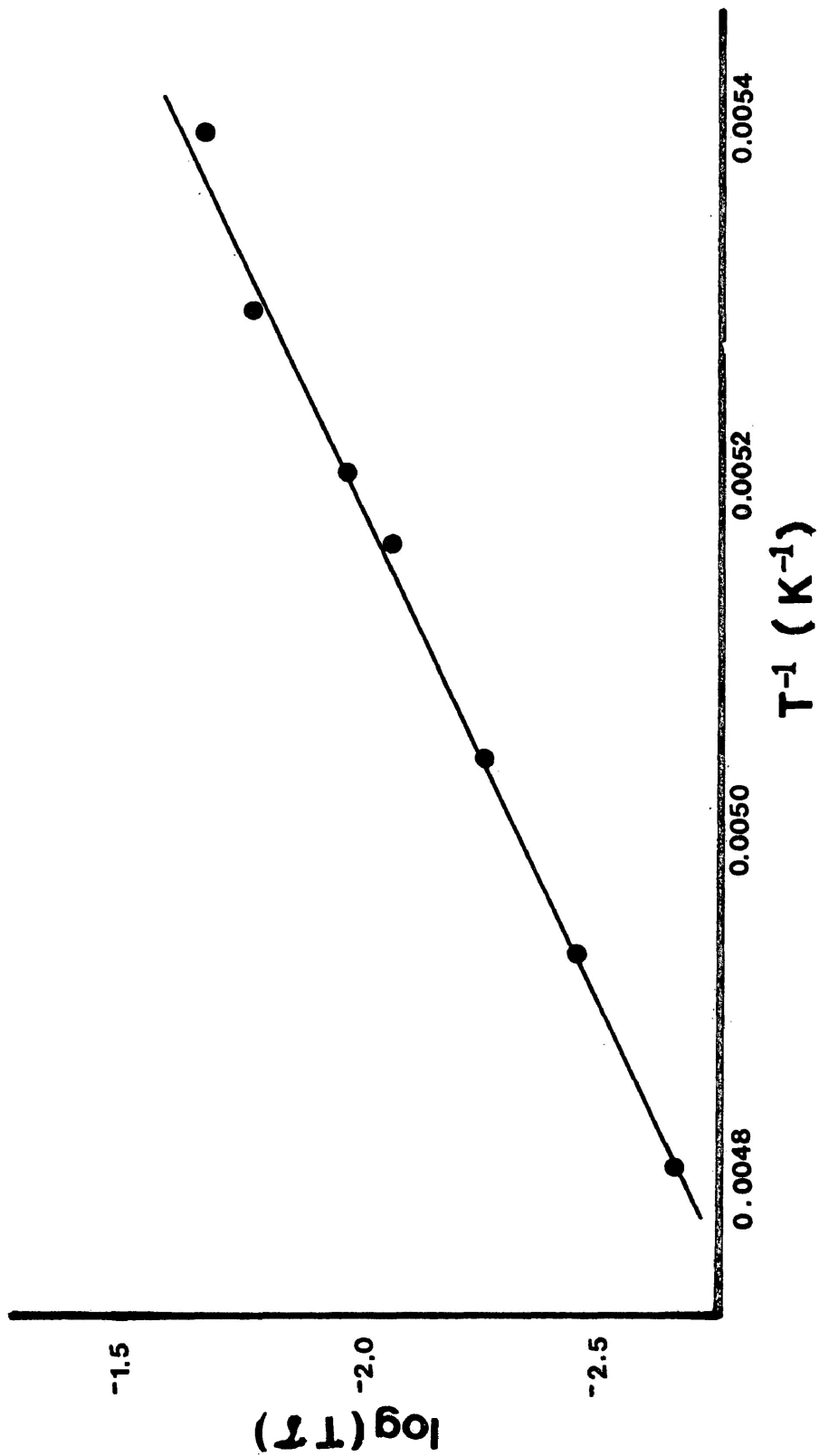


FIGURE V.11 Plot of $\log(T)$ versus $1/T$ for para-bromoacetophenone in o-terphenyl

CHAPTER VI

DIELECTRIC RELAXATION OF ALIPHATIC
E S T E R S

VI.1

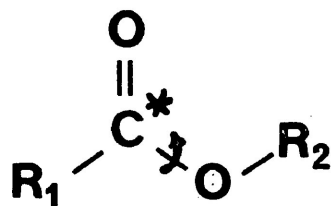
INTRODUCTION

The dielectric behaviour of aliphatic polar molecules has recently been the subject of extensive study by a variety of experimental and theoretical means. Using the dielectric absorption technique in the microwave region, Crossley et al have reported the flexibility of straight-chain aliphatic amines (1), ketones (2), bromides (3), and alkenes (4). The size of the alkyl group R and the location of the polar group X on the carbon skeleton of these compounds RX was varied, and in some instances(5) the effect of solvent viscosity was investigated. The relaxation data for 1-bromoalkanes (3) led them to suggest that dipolar reorientation involves a variety of molecular segments containing the $-\text{CH}_2\text{Br}$ group, whereas it was inferred that a polar end group rotation makes a predominant contribution to the absorption of 1-aminoalkanes (1) and 2-alkanones (2) and that the mean relaxation times are almost independent of the size of the alkyl group. Madan (6,7) has made dielectric measurements on solutions of aliphatic ketones in different non-polar solvents. He interpreted his results in terms of overall molecular rotation and/or

by intramolecular rotation around R-C or R'-C bonds. Recently, Walker et al (8) identified two absorption regions from the dielectric study of long chain aliphatic aldehydes in a polystyrene matrix. They also interpreted the results in terms of molecular and intramolecular motions. The relaxation data for the lower temperature process (around 100 K region) "has been identified with segmental rotation and probably, with rotation about the C-CHO bond as well."

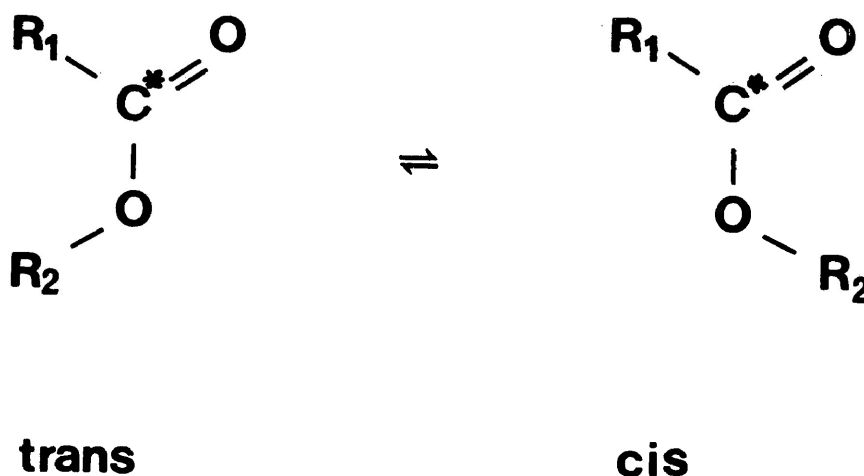
Although these molecules containing a rotatable polar group have so far been studied extensively, little attention seems to have been paid to aliphatic esters. McGreer et al (9), from their dielectric studies on esters in the pure liquid state, suggested the relaxation of polar molecular segments presumably by rotation around C-C* bonds. A detailed dielectric study of ten alkyl acetates in benzene solution has been carried out by Higasi et al (10). From their results they suggested that there were more than two dispersions corresponding to segmental reorientation and to molecular rotation as a whole, while Crossley and Koizumi (11), from the dielectric relaxation studies of aliphatic esters $R_1C^*OOR_2$

in cyclohexane solution at microwave frequencies, considered that the dipole orientation of the methoxy



and ethoxy groups around C*-O is very important particularly in methyl and ethyl esters. Kano et al (12) studied the same esters in cyclohexane at 25°C at the frequency of 100 GHz. They also indicated that the dielectric absorption of these esters is dominated by intramolecular mechanism. But, in contrast to Crossley and Koizumi (11) who considered "that the dipole orientation of the methoxyl and ethoxyl groups around their C*-O bonds is very important especially for a few esters, the present authors reached the conclusion that rotations of groups around C-C bonds/or the O-C bond play the dominant role in the dielectric absorption of the aliphatic esters."

The method of acoustic measurements is the earliest technique used for studying the relaxations of esters associated with conformational equilibria (13). Based on ultrasonic results it was concluded that simple esters of the lower carboxylic acids exhibit (14-18) an ultrasonic relaxation process in the frequency region 1-30 MHz. The relaxation is caused by perturbation of the equilibrium between two planar rotational isomers of the form:



The planar conformations are stabilized by the partial double bond character of the central C*-O bond. Bailey

et al (19-20), from their ultrasonic relaxation study of simple aliphatic esters, concluded that the energy difference between the trans (low energy state) and transition state is roughly constant in all the esters ($36.8 \pm 5.9 \text{ kJ mol}^{-1}$).

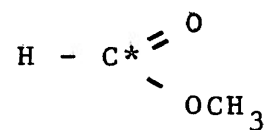
The lack of adequate and systematic dielectric relaxation data and values for the energy barriers to internal rotation in esters led us to examine dielectrically a number of aliphatic esters in different organic glasses, namely, polystyrene, o-terphenyl, and polyphenyl ether. The object was to gain insight into the types of relaxation processes which can take place, if feasible, to separate completely one process from another by changing the solvent viscosity, i.e., by studying the molecules in highly viscous solvents. In earlier microwave studies (11,12) of aliphatic esters in dilute solutions of low viscous solvents no such separation of processes has ever been achieved, whereas in this work such a separation of processes has been effected in most of the cases. The effect of conjugation on Eyring parameters for intramolecular motions in esters was also examined by studying some $\alpha\beta$ -unsaturated and vinyl esters. In some instances

the conjugative effect on dielectric behaviour was attempted to relate with the vibrational frequencies of the esters, i.e., C*=O and C*-O stretching frequencies. All the experimentally observed results indicate that the dipole relaxations of these esters $R_1C^*OOR_2$ is dominated by intramolecular rotation around the C-C* bond and/or the C*-O bond.

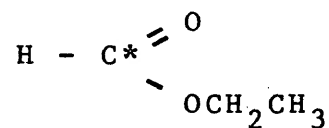
VI.2 EXPERIMENTAL RESULTS

The dielectric measurements for several aliphatic esters in (a) polystyrene matrices, (b) o-terphenyl and (c) polyphenyl ether have been made over suitable ranges of temperature and frequency by the use of a General Radio capacitance bridge as described in Chapter III. The present study includes the investigation of the following esters:

1. Methyl formate



2. Ethyl formate



3. Propyl formate $\text{H} - \text{C}^* \begin{array}{l} \text{=O} \\ \text{-} \\ \text{OCH}_2\text{CH}_2\text{CH}_3 \end{array}$
4. Methyl acetate $\text{CH}_3 - \text{C}^* \begin{array}{l} \text{=O} \\ \text{-} \\ \text{OCH}_3 \end{array}$
5. Methyl acrylate $\text{CH}_2 = \text{CH} - \text{C}^* \begin{array}{l} \text{=O} \\ \text{-} \\ \text{OCH}_3 \end{array}$
6. Methyl crotonate $\text{CH}_3 - \text{CH} = \text{CH} - \text{C}^* \begin{array}{l} \text{=O} \\ \text{-} \\ \text{OCH}_3 \end{array}$
7. Vinyl crotonate $\text{CH}_3 - \text{CH} = \text{CH} - \text{C}^* \begin{array}{l} \text{=O} \\ \text{-} \\ \text{OCH} = \text{CH}_2 \end{array}$
8. Methyl propiolate $\text{CH} \equiv \text{C} - \text{C}^* \begin{array}{l} \text{=O} \\ \text{-} \\ \text{OCH}_3 \end{array}$
9. Vinyl chloroacetate $\text{Cl} - \text{CH}_2 - \text{C}^* \begin{array}{l} \text{=O} \\ \text{-} \\ \text{OCH} = \text{CH}_2 \end{array}$
10. Vinyl bromoacetate $\text{Br} - \text{CH}_2 - \text{C}^* \begin{array}{l} \text{=O} \\ \text{-} \\ \text{OCH} = \text{CH}_2 \end{array}$

11. Vinyl propionate $\text{CH}_3 - \text{CH}_2 - \text{C}^* \begin{matrix} = \text{O} \\ \diagdown \\ \text{OCH} = \text{CH}_2 \end{matrix}$
12. Vinyl butyrate $\text{CH}_3 - \text{CH}_2 - \text{CH}_2 - \text{C}^* \begin{matrix} = \text{O} \\ \diagdown \\ \text{OCH} = \text{CH}_2 \end{matrix}$
13. Dimethyl oxalate $\begin{matrix} \text{CH}_3 - \text{O} - \text{C}^* \begin{matrix} = \text{O} \\ \diagdown \\ \text{O} \end{matrix} \\ \text{O} = \text{C}^* - \text{O} - \text{CH}_3 \end{matrix}$
14. Methyl chloroformate $\text{Cl} - \text{C}^* \begin{matrix} = \text{O} \\ \diagdown \\ \text{OCH}_3 \end{matrix}$
15. Ethyl chloroformate $\text{Cl} - \text{C}^* \begin{matrix} = \text{O} \\ \diagdown \\ \text{OCH}_2\text{CH}_3 \end{matrix}$
16. Butyl chloroformate $\text{Cl} - \text{C}^* \begin{matrix} = \text{O} \\ \diagdown \\ \text{OCH}_2\text{CH}_2\text{CH}_2\text{CH}_3 \end{matrix}$
17. iso-Butyl chloroformate $\text{Cl} - \text{C}^* \begin{matrix} = \text{O} \\ \diagdown \\ \text{OCH}_2\text{CH}(\text{CH}_3)\text{CH}_3 \end{matrix}$

Sample plots of loss factor ($\epsilon'' = \epsilon''_{(\text{obs})} - \epsilon''_{(\text{solvent})}$) against logarithm (frequency) are shown in Figures VI-2 to VI-4, while Figures VI-5 to VI-9 show the plots of $\log T\tau$ versus T^{-1} . Figures VI-10 to VI-12 show the sample plots of "Cole-Cole", while Figures VI-13 to VI-15 show the plots of loss factor, ϵ'' , versus temperature, T (K)/or $\ln T$.

Table VI-1 gives the values of " ΔH_E " and " ΔS_E " evaluated from dielectric data as well as " ΔG_E " and τ values at 100 K, 150 K and 200 K for every system. The values of $C^*=O$ and C^*-O stretching frequencies for these esters are also presented in the Table VI-1. The Fuoss-Kirkwood analysis parameters for several aliphatic esters at various temperatures are listed in Table VI-2.

VI-3. DISCUSSION

The relaxation data and activation parameters for seventeen aliphatic esters, $R_1C^*OOR_2$, are presented in Table VI-1. Formates are the first of the series in which dipole relaxation may occur either by the rotation of the alkoxy group around C^*-O bond or the molecule as a whole or both. The infrared bands at $1160-1214 \text{ cm}^{-1}$ in

formates (21-22) and the ultrasonic relaxations in these simple carboxylic esters (14,19-20) have been attributed to rotational isomers which arise from restricted rotation about the C*-O bond owing to its partial double bond character.

For asymmetrical barriers such as one in Figure VI-1 both ultrasonic and dielectric absorption techniques

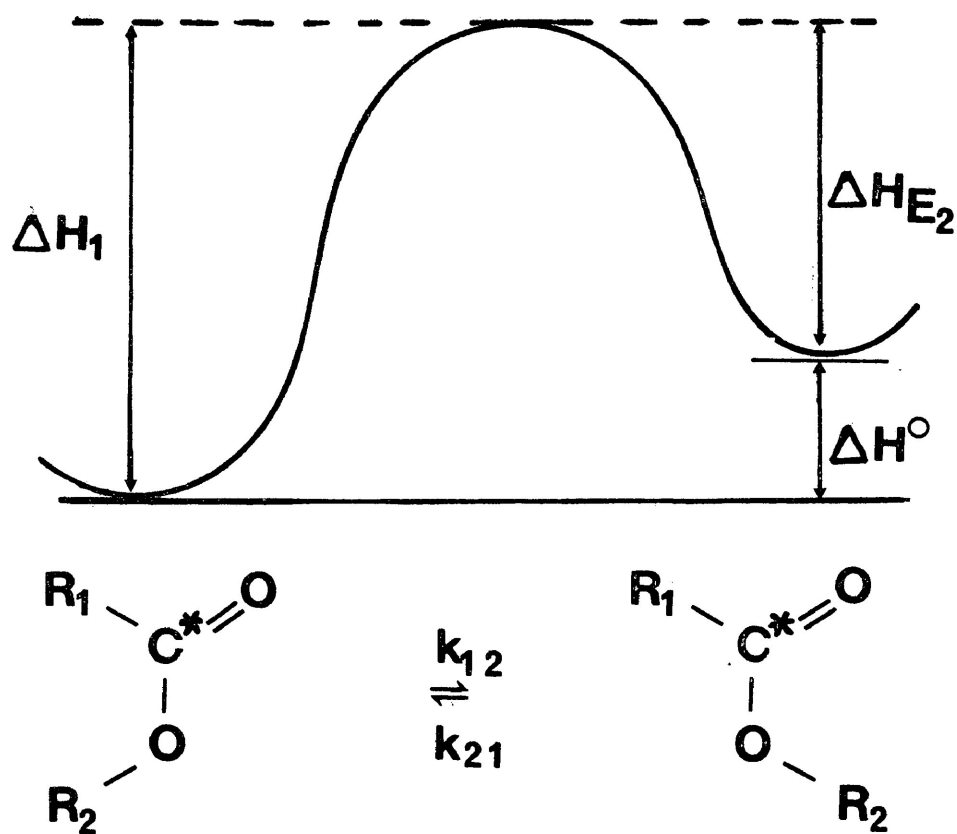


Figure VI-1 Enthalpy of activation diagram for an isomerization of an aliphatic ester.

yield a ΔH_{E2} corresponding to the switch from the isomer with the higher energy to that of the lower (30). It would be expected that both methods would yield similar ΔH_{E2} -values providing the difference in medium does not influence the value. The ultrasonic method also yields ΔH° .

Methyl formate examined in polyphenyl ether showed two dielectric absorption regions. The low temperature process was in the region of liquid nitrogen temperature (84 - 109 K) and yielded values for the enthalpy of activation ($\Delta H_E = 4.2 \pm 1.1 \text{ kJ mol}^{-1}$), and entropy of activation ($\Delta S_E = \sim -95.0 \text{ J K}^{-1} \text{ mol}^{-1}$), while the high temperature absorption process (233 - 246 K) yielded $\Delta H_E = 146 \text{ kJ mol}^{-1}$ and $\Delta S_E = \sim 310 \text{ J K}^{-1} \text{ mol}^{-1}$. The parameters for the high energy process were evaluated by linear regression of the equation (II-22). It is to be noted (Table VI-1) that the relaxation time ($\tau = 2.6 \times 10^{-4} \text{ s}$), free energy of activation ($\Delta G_{E(200 \text{ K})} = 36 \text{ kJ mol}^{-1}$), and the enthalpy of activation ($\Delta H_E = 146 \text{ kJ mol}^{-1}$) obtained for this molecule are considerably higher. These values are rather unexpected for a single molecular relaxation of such a small molecule or for the rotation

about the C*-O bond. However, since the dielectric absorption occurs at a much higher temperature (>230 K), it appears that the absorption might have arisen owing to the lowering of glass transition temperature: indeed, the measured glass transition temperature, T_g , of the sample was found to be at ~ 240 K, whereas the T_g of pure solvent is ~ 270 K (29); i.e., addition of methyl formate lowered the T_g of polyphenyl ether by about 30 K. Therefore, a cooperative motion of the whole molecule together with the segments of the polymer chain is believed to occur for this high temperature process of methyl formate in polyphenyl ether.

The enthalpy of activation ($\Delta H_E = 4.2 \pm 1.1 \text{ kJ mol}^{-1}$) and entropy of activation ($\Delta S_E = -95.0 \text{ J K}^{-1} \text{ mol}^{-1}$) for the low temperature dielectric absorption of methyl formate are not consistent with the ultrasonic results ($\Delta H_E = 32.6 \text{ kJ mol}^{-1}$) (19-20) for the barrier to internal rotation about the C*-O bond. The ultrasonic results of ΔS_E , however, are not known. Although barriers obtained by two different techniques may differ, yet the value of 4.2 kJ mol^{-1} seems to be too low compared to 32.6 kJ mol^{-1} . On the other hand, these low barriers for the low

temperature dielectric absorption of methyl formate may be compared with the relaxation parameters of similar-sized rigid polar molecules. For example, bromoform, which is slightly bigger in size than methyl formate, exhibits dielectric relaxation in a similar range of temperature (~ 100 K) in the same medium (Chapter IV) yielding $\Delta H_E = \sim 8$ kJ mol⁻¹, $\Delta S_E = \sim -80$ J K⁻¹ mol⁻¹. Compared to size, the relaxation time, τ ($= 2.0 \times 10^{-4}$ s), and ΔG_E ($= 16.5$ kJ mol⁻¹) at 100 K for bromoform in polyphenyl ether seems to be consistent with the values of methyl formate in the same solvent ($\tau_{100 \text{ K}} = 5.0 \times 10^{-6}$ s, $\Delta G_E(100 \text{ K}) = 13.4$ kJ mol⁻¹). Another rigid molecule of about similar size, that is pyridine, also showed dielectric absorption in the temperature range (78 - 99 K) in o-terphenyl and yielded comparable relaxation data and barriers (Chapter IV), i.e., $\Delta G_E(100 \text{ K}) = 12.8$ kJ mol⁻¹, $\tau_{100 \text{ K}} = 2.3 \times 10^{-6}$ s, $\Delta H_E = 8.4 \pm 1.1$ kJ mol⁻¹, and $\Delta S_E = -59$ J K⁻¹ mol⁻¹. All these results, however, suggest that the low temperature dielectric absorption of methyl formate in polyphenyl ether may be due to the molecular process. The intramolecular process about the C*-O bond was not detected. It is probable that this process was merged with the tail of the high loss

cooperative process. This molecule was tried to examine in polystyrene matrix in order to detect the intramolecular process around the C*-O bond. But due to the low boiling point (~ 307 K) of methyl formate polystyrene disk could not be made.

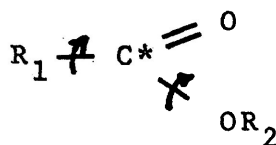
The dielectric absorption of ethyl formate in polyphenyl ether was observed in the temperature range 115 - 141 K. Table VI-1 shows the values of $\Delta H_E = 21.8 \pm 2$ kJ mol⁻¹, $\Delta S_E = 17.2$ J K⁻¹ mol⁻¹, $\tau_{100\text{ K}} = 1.5 \times 10^{-2}$ s, $\Delta G_{E(100\text{ K})} = 20.1$ kJ mol⁻¹, while the next higher molecule, propyl formate, exhibited dielectric absorption in polystyrene matrix in the temperature range 94 - 143 K, yielding $\Delta H_E = 14.2 \pm 1.0$ kJ mol⁻¹, $\Delta S_E = -24.0$ J K⁻¹ mol⁻¹, $\Delta G_{E(100\text{ K})} = 14.5$ kJ mol⁻¹, and $\tau_{100\text{ K}} = 2.3 \times 10^{-4}$ s. Although there may be some variation in the values of energy barrier for the molecular relaxation in different media, yet the value of ΔH_E (=21.8 kJ mol⁻¹) for ethyl formate seems to be quite high for the single molecular process, and it is quite reasonable to suggest that both molecular and intramolecular dipole orientation contribute to the dielectric relaxation of ethyl formate in polyphenyl ether. But the ultrasonic

results for the same molecule ($\Delta H_E = 25.5 \text{ kJ mol}^{-1}$) (19-20,28) indicate that the observed process contains maximum contribution from the intramolecular motion around C*-O bond. Ethyl formate, like methyl formate, could not be studied in polystyrene matrix due to its low boiling point ($\sim 325 \text{ K}$).

The enthalpy of activation for propyl formate, $\Delta H_E = 14.2 \text{ kJ mol}^{-1}$, and other parameters (Table VI-1) for the low temperature process (94 - 143 K) in polystyrene matrix are comparable with the values of $\Delta H_E (= 14 \text{ kJ mol}^{-1})$, $\Delta S_E (= -19 \text{ J K}^{-1} \text{ mol}^{-1})$, $\Delta G_E(100 \text{ K}) (= 15.8 \text{ kJ mol}^{-1})$, and $\tau_{100 \text{ K}} (= 8.5 \times 10^{-5} \text{ s})$ for 4-methyl pyridine (31) in the same solvent. Moreover, the energy barrier obtained by the ultrasonic technique for propyl formate for the rotation about the C*-O bond is $\Delta H_E = 28.0 \text{ kJ mol}^{-1}$ (19,20), which is a quite large value compared to 14.2 kJ mol^{-1} . Thus, this observed dielectric relaxation process of propyl formate is possibly due to the rotation of the whole molecule rather than to intramolecular motion; the group rotation about the C*-O bond, being sterically more hindered in this molecule, therefore requires more energy.

Table VI-1 shows that propyl formate in a polystyrene matrix exhibited another higher temperature absorption process (231 - 249 K) in a polystyrene matrix and gave values of activation enthalpy and entropy of $136.5 \text{ kJ mol}^{-1}$ and $295 \text{ J K}^{-1} \text{ mol}^{-1}$, respectively. These values would seem to be too high either for a molecular or group process and may be accounted for by the cooperative motion of the molecule with the polymer chain. A number of other systems exhibiting similar behaviour in polystyrene matrices have been carefully examined by Mazid (31) and Khwaja (35) in this laboratory, and a relation of the form, $\Delta S_E \text{ (J K}^{-1} \text{ mol}^{-1}) = -150 + 3.24 \Delta H_E \text{ (kJ mol}^{-1})$, has been derived. According to this equation, the calculated ΔS_E value of $292 \text{ J K}^{-1} \text{ mol}^{-1}$ is in good agreement with that obtained from the Eyring analysis.

In other aliphatic esters, except the formates, there is a possibility of internal rotation about the C*-O as well as the C-C* bonds in addition to the rotation of the whole molecule.



It has been mentioned that the barrier to internal rotation about the C*-O bond in most simple esters is between 25 to 50 kJ mol⁻¹ (32(a)), whereas, microwave spectroscopic results suggest that the barriers to internal rotation about the single, C-C*, bond in acetic acid and methyl acetate are about ~2 kJ mol⁻¹ (32(b)).

Dielectric studies of methyl acetate gave two absorption regions in a polystyrene matrix, while only one absorption process was found in both o-terphenyl and polyphenyl ether. Table VI-1 shows that although the low temperature process observed in a polystyrene matrix and the process observed in the other two media are almost in the same temperature range, yet the energy barriers differ quite significantly. However, the value of ΔH_E ($= 2.4 \text{ kJ mol}^{-1}$) in a polystyrene matrix may be considered as a rough estimate, since the process could not be studied over the whole frequency range of the measurements as even at the lowest temperature the absorption process started from $\log f_{\max}$ value of 3.43 (Table VI-2). And these low values ($\Delta H_E = 2.4 \pm 0.4 \text{ kJ mol}^{-1}$, $\Delta S_E = -124.0 \text{ J K}^{-1} \text{ mol}^{-1}$, $\Delta G_E(100 \text{ K}) = 14.5 \text{ kJ mol}^{-1}$)

in a polystyrene matrix are comparable to the corresponding values in o-terphenyl ($\Delta H_E = 6.9 \pm 0.46 \text{ kJ mol}^{-1}$, $\Delta G_{E(100 \text{ K})} = 14.8 \text{ kJ mol}^{-1}$, $\Delta S_E = -78.9 \text{ J K}^{-1} \text{ mol}^{-1}$). In addition, the values of relaxation time, τ , at 100 K are $2.5 \times 10^{-5} \text{ s}$ and $2.7 \times 10^{-5} \text{ s}$ in polystyrene and in o-terphenyl, respectively, which are identical. When it is borne in mind that the barriers for internal rotation about the C-C* single bond obtained by microwave spectroscopy are $\sim 2 \text{ kJ mol}^{-1}$ (32(b)) this low energy dielectric absorption process in polystyrene and in o-terphenyl may be interpreted as due to the rotation about the C-C* bond. On the other hand, the possibility of the rotation of the whole molecule cannot be ruled out, since bromoform, which is a similar-sized rigid molecule but bigger than methyl formate (considered earlier), yielded values of $\Delta H_E = 10.4 \text{ kJ mol}^{-1}$ in o-terphenyl and 7.9 kJ mol^{-1} in a polystyrene matrix (Chapter IV).

The results obtained in polyphenyl ether, i.e., $\Delta H_E = 18.4 \pm 0.4 \text{ kJ mol}^{-1}$; $\Delta S_E = -2.1 \text{ J K}^{-1} \text{ mol}^{-1}$; $\Delta G_{E(100 \text{ K})} = 18.6 \text{ kJ mol}^{-1}$; and $\tau_{100 \text{ K}} = 2.5 \times 10^{-3} \text{ s}$ for the relaxation process of methyl acetate are significantly higher for the single molecular motion, which

may involve some contribution from the high energy relaxation about the C*-O bond.

Table VI-1 shows the values of ΔH_E ($= 27.1 \pm 1.5$ kJ mol⁻¹), ΔS_E ($= -23.6$ J K⁻¹ mol⁻¹), $\Delta G_E(200$ K) ($= 30.6$ kJ mol⁻¹); τ_{200 K ($= 5.0 \times 10^{-5}$ s) obtained for the higher temperature relaxation process of methyl acetate in a polystyrene matrix. The high beta (0.32 - 0.46) values indicate also that it is more likely an intramolecular reorientation process (33). The most probable intramolecular process with such a high energy barrier ($\Delta H_E = \sim 27$ kJ mol⁻¹) would be the relaxation of the methoxy group around the C*-O bond. The ultrasonic value of ΔH_E ($= 24.7$ kJ mol⁻¹) (19-20) is also consistent with this proposed relaxation process.

In order to explore the effect of conjugation on the internal rotation about the C*-O/or the C-C* bond in aliphatic esters, the dielectric behaviour of $\alpha\beta$ -unsaturated and vinyl esters was examined. In $\alpha\beta$ -unsaturated esters the C-C* bond acquires some partial double bond character with the resultant increase of barrier to rotation about the bond, but in cases where

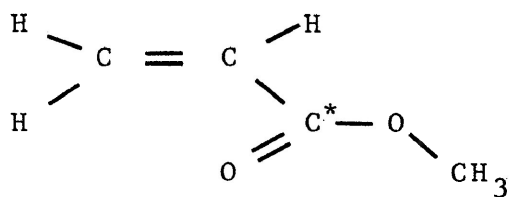
this barrier becomes almost identical with that for the rotation about the C*-O bond, the separation of the two intramolecular relaxation processes would be impossible.

Methyl acrylate and methyl crotonate were studied in a polystyrene matrix, o-terphenyl, and in polyphenyl ether. Both the molecules exhibited a dielectric absorption process in almost the same temperature region irrespective of the media. Figure VI-5 presents the plot of $\log T\tau$ versus $1/T$ for methyl acrylate in polystyrene matrix, which indicated the presence of two absorption processes and yielded an overall enthalpy of activation, $\Delta H_E = 20.1 \pm 1.1 \text{ kJ mol}^{-1}$. However, when the two portions of this plot were analyzed separately, the values of 18.6 and 23.6 kJ mol^{-1} were obtained for the enthalpies of activation. This suggests that the observed intramolecular process is largely influenced by the two overlapping intramolecular processes, where the barriers to rotation differ slightly, but no such observation was found from the plots of $\log T\tau$ versus $1/T$ for methyl acrylate in the other two media and also for methyl crotonate in all the three media. Figure VI-3 shows some typical plots of ϵ'' versus $\log f$ for methyl acrylate

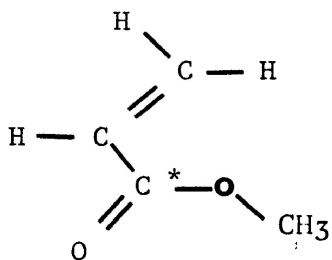
in polyphenyl ether, while Figure VI-6 shows the plots of $\log T\tau$ versus $1/T$ for methyl crotonate in the three media (polystyrene, o-terphenyl and polyphenyl ether).

Table VI-1 gives the values of dielectric relaxation parameters along with the infrared stretching frequencies of $C^*=O$ and C^*-O bonds for methyl acrylate and methyl crotonate. For saturated esters the $C^*=O$ bond stretching frequencies are in the range of 1750-1735 cm^{-1} (21), but the lower values of 1729 and 1728 cm^{-1} (23) for methyl acrylate and methyl crotonate, respectively, reflect the effect of conjugation. The Table VI-1 shows that the values of enthalpy of activation (ΔH_E in kJ mol^{-1}), entropy of activation (ΔS_E in $\text{J K}^{-1} \text{mol}^{-1}$), free energy of activation (ΔG_E at 150 K and 200 K in kJ mol^{-1}), and also the relaxation times (τ at 150 K and 200 K in s) are all quite similar in magnitude within the limits of experimental error for both the molecules. The results are also seen to be independent of the media, which suggests intramolecular motion. Therefore, these high energy barriers ($\Delta H_E = 23 \pm 3 \text{ kJ mol}^{-1}$) for methyl acrylate and methyl crotonate are probably due to the reorientational motion around the $C-C^*/$ or the C^*-O bond, or an overlap of both.

Feairheller and Katon (34) have examined the infrared spectrum of methyl acrylate, and their findings are consistent with the presence of two rotamers (shown below):



cis



trans

Bowles et al (23) have carried out intensity measurements on certain infrared bands between 163 K and 473 K for methyl acrylate and methyl (trans) crotonate. They interpreted their results in terms of an equilibrium between cis and trans forms

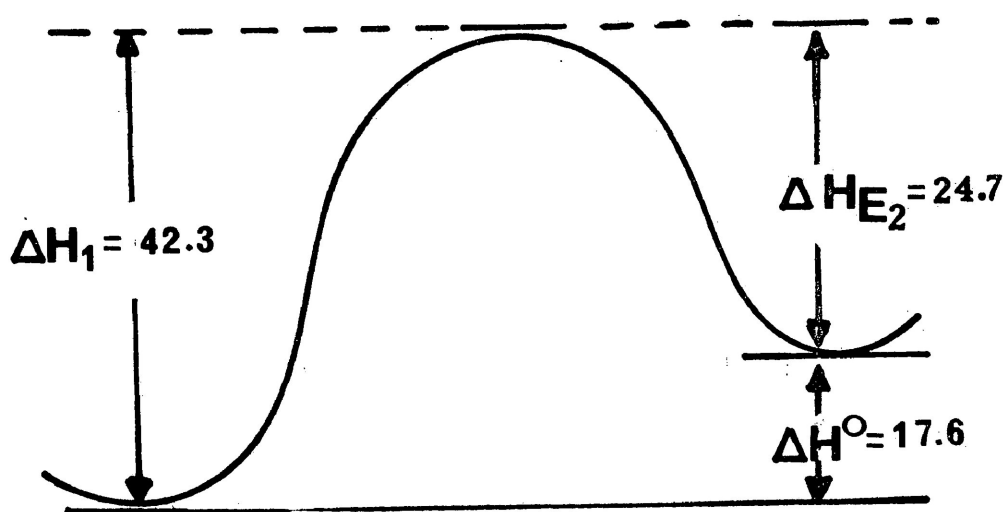
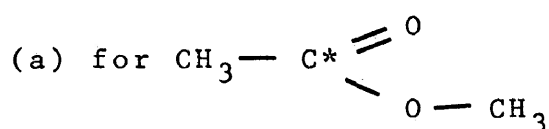
in both cases. They also mentioned that the infrared bands (Table VI-1) in the region of $1178 - 1202 \text{ cm}^{-1}$ probably contain a contribution from both the $\text{C}-\text{C}^*:\text{O}$ and $\text{O}:\text{C}^*-\text{O}$ bond stretching motions.

Thus, it is quite reasonable to interpret the dielectric absorption results for methyl acrylate and methyl crotonate assuming a maximum contribution from the intramolecular motion around the $\text{C}-\text{C}^*$ bond rather than the C^*-O bond, but the low β values (~ 0.2) for both the molecules and also the plot of $\log T\tau$ versus $1/T$ for methyl acrylate in a polystyrene matrix (Figure VI-5) support the presence of more than one intramolecular process.

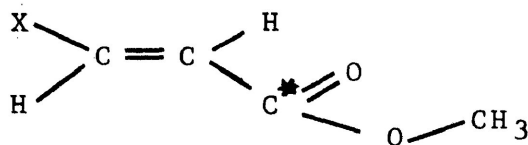
Although conjugation in vinyl crotonate (26-27) may be different from that in methyl crotonate, yet dielectric study showed that vinyl crotonate absorbed in *o*-terphenyl in the temperature range (152 - 193 K) and yielded values of ΔH_E ($= 22.0 \pm 1.6 \text{ kJ mol}^{-1}$), $\Delta G_E(200 \text{ K})$ ($= 28.7 \text{ kJ mol}^{-1}$), $\tau_{200 \text{ K}}$ ($= 7.7 \times 10^{-6} \text{ s}$), ΔS_E ($= -33.5 \text{ J K}^{-1} \text{ mol}^{-1}$) and β ($= \sim 0.2$), which are almost identical with the corresponding values of methyl crotonate in the same medium.

Therefore, a similar interpretation can be drawn for the dielectric absorption of vinyl crotonate, i.e., in terms of likely contributions from both the internal rotations about the C-C* and C*-O bonds.

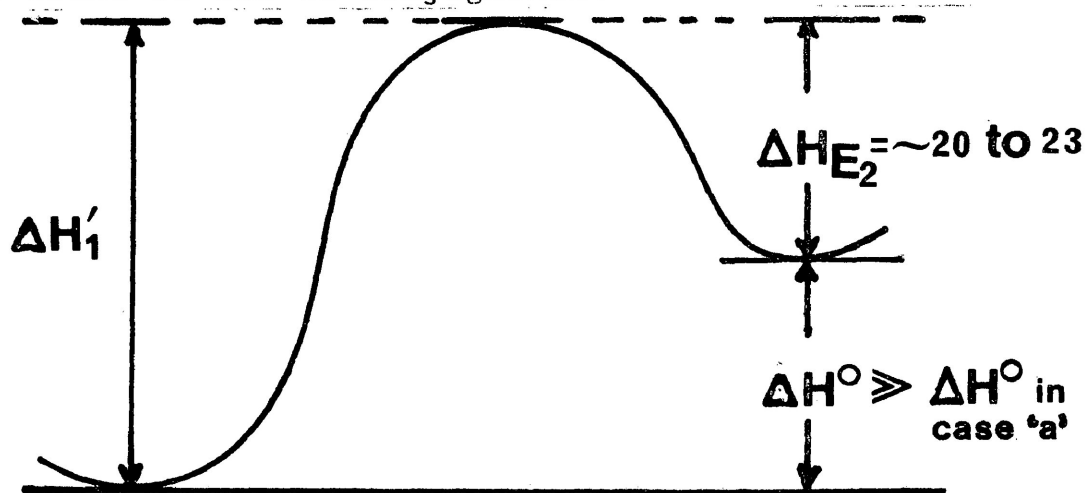
The barrier ($\Delta H_E = 20 \pm 3 \text{ kJ mol}^{-1}$) for intramolecular motion in methyl acrylate and methyl crotonate (also vinyl crotonate) is lower than that observed in methyl acetate ($\Delta H_E = 27.1 \text{ kJ mol}^{-1}$) in a polystyrene matrix. This discrepancy probably may be explained with the help of Figure VI-1. Considering the ultrasonic values of enthalpies of activation (kJ mol^{-1}) for methyl acetate (19-20) the diagram (Figure VI-1) can be redrawn as:



(b) whereas for:



the case could be due to conjugation:



although $\Delta H'_1 > \Delta H_1$ in case (a), the much more increased value of ΔH° (in case (b)) reduced the ΔH_{E_2} value in case (b). The values of ΔH° estimated from the dielectric data by the use of the following equation, as employed by Meakins (43), are shown in Table VI.1

$$\epsilon''_{\max} = \frac{B}{kT} \exp(-\Delta H^\circ/RT), \text{ where } B = \text{constant}$$

However, it is to be noted that in most cases the ΔH° values are less than the mean thermal energy and therefore, according to Meakins, could not be considered reliably to be different from zero.

Conjugation in methyl propiolate is higher than that in methyl crotonate which is reflected in the values

of the infrared stretching frequencies of C*#O and C*-O bonds (Table VI-1) as reported by Allan et al (24). The results of dielectric measurements are shown in Table VI-1 and in Table VI-2. In a polystyrene matrix there were two absorption regions, whereas in o-terphenyl and in polyphenyl ether only the low temperature absorption process was observed.

For the low temperature process, Table VI-1 shows that the temperature region (85 - 125 K), values of ΔH_E ($= \sim 5.0 \pm 1 \text{ kJ mol}^{-1}$), and all other parameters for methyl propiolate are identical within the limits of experimental error in all the three media. This low temperature process may be identified by means of the molecular relaxation process.

The high temperature (165 - 198 K) dielectric absorption process in a polystyrene matrix yielded values of $\Delta H_E = 45.0 \text{ kJ mol}^{-1}$, $\Delta G_E(200 \text{ K}) = 33.8 \text{ kJ mol}^{-1}$, $\Delta S_E = 74.5 \text{ J K}^{-1} \text{ mol}^{-1}$ and $\tau_{200 \text{ K}} = 2.0 \times 10^{-1} \text{ s}$. These high energy barriers are rather interesting. The most likely interpretation for this process could be the result of the overlapping of two intramolecular motions around the highly conjugated C*-C and C*-O bonds. The process

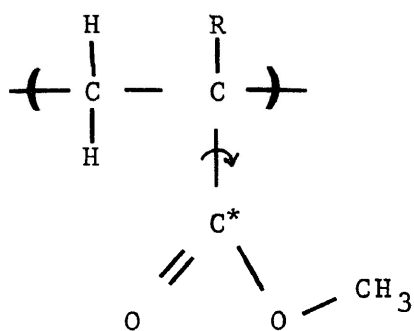
was not observed in o-terphenyl and in polyphenyl ether, the reason for which may be attributed to the overlap of the intramolecular process with the high loss cooperative process of these two solvents at such high temperatures. Figure VI-13 shows the sample plot of ϵ'' versus T(K) at 10^4 Hz frequency for methyl propiolate in o-terphenyl.

The dielectric behaviour observed for vinyl chloroacetate, vinyl bromoacetate, vinyl propionate and vinyl butyrate is quite different from that observed for vinyl crotonate. Table VI-1 shows that all these four molecules exhibited low temperature (79 - 133 K) dielectric absorption process in o-terphenyl. The enthalpies of activation for vinyl chloroacetate and vinyl bromoacetate are 2.5 ± 0.1 and 2.0 ± 0.1 kJ mol⁻¹, respectively, while the corresponding values for vinyl propionate and vinyl butyrate are 8.7 ± 0.1 and 9.1 ± 0.5 kJ mol⁻¹, also the values of $\Delta G_E(100 \text{ K})$, $\tau_{100 \text{ K}}$ and other parameters are almost similar. These results indicate that the observed absorption process for these four molecules cannot be identified with the molecular process, since for the molecular process the enthalpy of activation for these

identical-sized molecules should be the same. Moreover, vinyl crotonate, almost the similar in size, gave higher values ($\Delta H \sim 22 \text{ kJ mol}^{-1}$), which is quite a reasonable value for the intramolecular process of the conjugated system. However, these results may be compared with the low temperature process observed for methyl acetate in polystyrene matrix and in o-terphenyl. The relatively lower values ΔH_E ($\sim 2 \text{ kJ mol}^{-1}$) for vinyl chloroacetate and vinyl bromoacetate may be due to the fact that the presence of halogen (electron withdrawing atom) in the carbon atom, which is attached to the unsaturated ester carbon atom, may decrease the C-C* bond-order, thus permitting an increased flexibility to rotation about the bond. Therefore, on comparison of all these results for the low temperature process in vinyl esters as well as in methyl acetate, it may be suggested that in these esters the reorientational motion about the C-C* bond is more facile and requires low energy barrier, though this barrier to rotation about the C-C* bond depends to some extent on the conjugative and steric effects.

More recently Shukla (41) studied dielectric absorption of alkyl methacrylate polymers (polymethyl and

polyethyl methacrylate) in the solid state and observed a low temperature process with the enthalpies of activation, ΔH_E , of about 8 - 12 kJ mol⁻¹ which could possibly be due to ester group rotation, i.e., rotation about the C-C* bond.



where R = CH₃ or C₂H₅

The plot of ϵ'' versus T(K) at 1 kHz frequency (Figure VI-14) shows that vinyl butyrate in o-terphenyl also exhibited another high temperature (196 - 206 K) process with values of $\Delta H_E = 115$ kJ mol⁻¹, $\Delta S_E = 230$ J K⁻¹ mol⁻¹, $\Delta G_E(200 \text{ K}) = 30.9$ kJ mol⁻¹ and $\tau_{200 \text{ K}} = 3.6 \times 10^{-3}$ s. The glass transition temperature of the sample was recorded as ~ 228 K, whereas the T_g of the pure solvent is ~ 243 K (36). The parameters (ΔH_E and ΔS_E) for this high energy process were evaluated by linear regression of the equation (11-22). This high

energy process would seem to be the result of a cooperative motion of the molecule with associated solvent molecules.

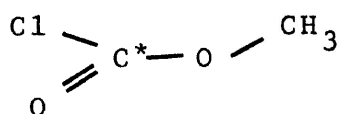
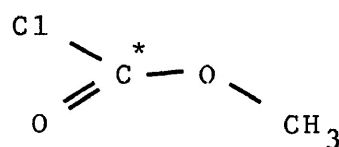
The dimethyl ester of oxalic acid was studied in a polystyrene matrix, and two absorption regions were detected. The low temperature (101 - 143 K) process gave $\Delta H_E = 7.2 \pm 0.5 \text{ kJ mol}^{-1}$, $\Delta G_{E(100 \text{ K})} = 18.9 \text{ kJ mol}^{-1}$, and $\Delta S_E = -116.7 \text{ J K}^{-1} \text{ mol}^{-1}$. These results may be compared with that of trichloroethylene, which is a rigid molecule of about the same size and shows absorption (Chapter IV) in the temperature range, 79 - 117 K, in a polystyrene matrix. For trichloroethylene the observed values of $\Delta H_E (= 7.0 \pm 0.3 \text{ kJ mol}^{-1})$, $\Delta G_{E(100 \text{ K})} (= 14.8 \text{ kJ mol}^{-1})$, and $\Delta S_E (= -77.7 \text{ J K}^{-1} \text{ mol}^{-1})$ are almost identical with those of dimethyl oxalate, and, therefore, it would seem that the whole molecular rotation is responsible for the low temperature dielectric absorption in dimethyl oxalate.

Figure VI-8 shows the plot of $\log T\tau$ versus $1/T$ for the higher temperature (231 - 291 K) process of dimethyl oxalate in a polystyrene matrix. The enthalpy of activation, $\Delta H_E (= 45.3 \pm 1.6 \text{ kJ mol}^{-1})$, and entropy

of activation, ΔS_E ($= -8.2 \text{ J K}^{-1} \text{ mol}^{-1}$), and other parameters (Table VI-1) obtained for this process are comparable to those of the high temperature (165 - 198 K) process of methyl propiolate in the same polystyrene matrix. Though the conjugation in these two molecules may not be the same, yet owing to both dipole-dipole and lone pair-lone pair interactions of the two adjacent ester groups in dimethyl oxalate, the dipole reorientation about the C*-C*/or the C*-O bond is hindered as in the case of methyl propiolate. Therefore, a similar suggestion may be made for this high energy ($\Delta H_E \approx 45 \text{ kJ mol}^{-1}$) process of dimethyl oxalate which results from the overlapping of two hindered intramolecular motions about the C*-C* and the C*-O bonds.

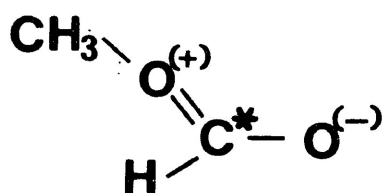
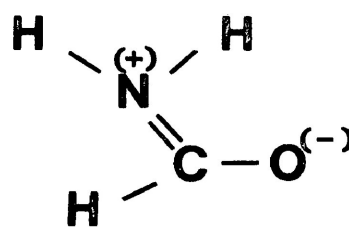
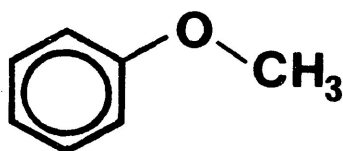
Dielectric measurements of methyl, ethyl, butyl and iso-butyl chloroformate were carried out to explore the relaxation processes associated with these molecules. Mizushima and Kubo (37), from their dipole moment measurements data for methyl and ethyl chloroformate, interpreted that the presence of halogen decreases the central C*-O bond-order, thus permitting an increased flexibility to torsion about that bond which results in larger amplitudes of

motion. Oki and Nakanishi (38) studied the infrared and n.m.r. spectra of methyl chloroformate (as well as ethyl and isopropyl chloroformates), and they concluded that both cis and trans forms are present in the solution phase with the trans rotamer as the more stable isomer.

transcis

Methyl and ethyl chloroformates exhibited a single relaxation process in a polystyrene matrix, o-terphenyl, and in polyphenyl ether. Table VI-1 gives the values of ΔH_E and other parameters for both the molecules in the three media. For methyl chloroformate the values of ΔH_E ($\sim 22 \pm 2 \text{ kJ mol}^{-1}$) and other parameters are almost similar in magnitude (within the limits of experimental error) in the three media. Figures VI-4 shows the sample plot of ϵ'' versus $\log(\text{freq.})$ for methyl

chloroformate in *o*-terphenyl, while Figure VI-9 presents the plots of $\log T\tau$ versus $1/T$ for the same molecule in all the three media. All these results suggest an intramolecular relaxation process about the C*-O bond, i.e., methoxy group relaxation in methyl chloroformate. The barrier being $\sim 22 \pm 2 \text{ kJ mol}^{-1}$, which is higher than that observed by Walker et al (39) and also by the present work (Chapter V) for methoxy group relaxation. The higher energy barrier for methoxy group relaxation in esters may be interpreted as evidence that the rotation about the C*-O bond in esters is hindered owing to its partial double bond character (as may be seen from the quinonoid structure), whereas the

**Ester****Amide****Anisole**

value of $\sim 10 \text{ kJ mol}^{-1}$ was observed for the same group relaxation in cases where there is no mutual conjugation or steric effect. Shukla et al (42) obtained high energy barrier ($\sim 50 \text{ kJ mol}^{-1}$) for internal rotation in amides which can be compared with that in esters, where $\text{CH}_3\text{O-}$ and $\text{H}_2\text{N-}$ groups are both strong +M groups.

The energy barriers and other parameters for ethyl chloroformate are not similar in all the three media. The results in a polystyrene matrix were obtained by Enayetullah (40). The values of $27.1 \pm 1.1 \text{ kJ mol}^{-1}$ in o-terphenyl and 23.3 kJ mol^{-1} in a polystyrene matrix for the enthalpy of activation may be considered to be the barrier to rotation about the C^*-O bond (ethoxy group rotation). A comparatively higher barrier ($\Delta H_E = 33.0 \pm 1.5 \text{ kJ mol}^{-1}$) for ethoxy group relaxation in ethyl chloroformate in polyphenyl ether possibly involves some contribution from the high energy cooperative motion of polymer segments. The glass transition temperature, T_g , of the sample was recorded to be $\sim 231 \text{ K}$.

Butyl and isobutyl chloroformate, both in polyphenyl ether, showed two absorption regions. The

enthalpies of activation, $14 \pm 1 \text{ kJ mol}^{-1}$ and $19.1 \pm 1.9 \text{ kJ mol}^{-1}$ for butyl and isobutyl chloroformate, respectively, are for the low temperature process (Table VI-1). These results and other parameters may be ascribed to the molecular, dielectric absorption process.

The higher temperature (250 - 263 K) process observed for butyl chloroformate in polyphenyl ether with $\Delta H_E = 168 \text{ kJ mol}^{-1}$, $\Delta S_E = 392 \text{ J K}^{-1} \text{ mol}^{-1}$, and $T_g = \sim 248 \text{ K}$ may be attributed to a cooperative process. On the other hand, the values of ΔH_E ($= 38.5 \text{ kJ mol}^{-1}$) and other parameters (Table VI-1) for the higher temperature process of iso-butyl chloroformate, when compared to the corresponding values obtained by Enayetullah (40) for butyl and iso-butyl chloroformate in a polystyrene matrix, seem to be appreciably higher for internal rotation about the C*-O bond. The influence of high energy cooperative motion ($T_g = \sim 245 \text{ K}$) may increase the barrier to rotation about the C*-O bond in polyphenyl ether.

In conclusion, it may be said that the energy barriers as well as the relaxation times obtained for the dielectric absorptions of different aliphatic esters

suggest the rotation of groups around the central C-C* and/or C*-O bond. The barrier to rotation about the central C-C* bond in simple cases is found to be significantly lower (about 6 - 10 kJ mol⁻¹ in the absence of conjugative effect) than that about the C*-O bond (~22 ± 2 kJ mol⁻¹ for methoxy group rotation in esters). It is also observed that the barriers to internal rotation are almost independent of the three types of media (polystyrene, o-terphenyl and polyphenyl ether).

VI. REFERENCES

1. S. P. Tay and J. Crossley, *J. Chem. Phys.*, 56(1972)4303.
2. J. Crossley, *J. Chem. Phys.*, 56(1972)2549.
3. S. P. Tay and J. Crossley, *Can. J. Chem.*, 50(1972)2031.
4. J. Crossley, *J. Chem. Phys.*, 58(1973)5315.
5. J. Crossley, *Can. J. Chem.*, 51(1973)2671.
6. M. P. Madan, *Can. J. Phys.*, 53(1975)23.
7. M. P. Madan, *Can. J. Phys.*, 54(1976)794.
8. H. A. Khwaja and S. Walker, *Adv. Mol. Relax. & Inter. Process.*, 22(1982)27.
9. P. L. McGreer, A. J. Curtis, G. B. Rathman, and C. P. Smyth, *J. Am. Chem. Soc.*, 74(1952)3541.
10. Y. Koga, H. Takahashi, and K. Higasi, *Bull. Chem. Soc., Japan*, 47(1974)84.
11. J. Crossley and N. Koizumi, *J. Chem. Phys.*, 60(1974)4800.
12. Y. Kano, R. Minami and H. Takahashi, *Bull. Chem. Soc., Japan*, 53(1980)642.
13. P. Biquard, *Ann. Phys.*, 6(1936)195.
14. J. Karpovich, *J. Chem. Phys.*, 22(1954)1767.
15. D. N. Hall and J. Lamb, *Trans. Faraday Soc.*, 55(1959)784.
16. V. F. Nøzdrev, "The Use of Ultrasonics in Molecular Physics", Pergaman, London and New York, (1965).

VI. REFERENCES continued...

17. J. E. Piercy and S. V. Subrahmanyam, J. Chem. Phys., 42(1965)1475.
18. S. V. Subrahmanyam and J. E. Piercy, J. Acoust. Soc. Amer., 37(1965)340.
19. J. Baily and A.M. North, Trans. Faraday Soc., 64(1968)1499.
20. J. Bailey, S. Walker and A. M. North, J. Mol. Structure, 6(1970)53.
21. H. W. Thompson and P. Torkington, J. Chem. Soc., (1945)640.
22. R. A. Russel and H. W. Thompson, J. Chem. Soc., (1955)479.
23. A. J. Bowles, W. O. George, and D. B. Cunliffe-Jones, J. Chem. Soc., B(1970)1070.
24. J. L. H. Allan, G. D. Meakins and M. C. Whiting, J. Chem. Soc., (1955)1874.
25. J. K. Wilmshurst, J. F. Horwood, J. Mol. Spectroscopy, 21(1966)48.
26. R.B. Barnes, R.C. Gore, U. Liddel and V.Z. Williams, Infrared Spectroscopy, Reinhold, (1944).
27. L.J. Bellamy, J. Chem. Phys., 28(1955)4221.
28. D. Tabuchi, J. Chem. Phys., 28(1958)1014.
29. A. J. Barlow, J. Lamb, and N. S. Taskoprülü, J. Acoust. Soc. Am., 46(1969)569.
30. S. P. Tay, S. Walker and E. Wyn-Jones, Adv. Mol. Relax. & Inter. Process., 13(1978)47.

VI. REFERENCES continued...

31. M. A. Mazid, M.Sc. Thesis, Lakehead University, Thunder Bay, Ontario, Canada, (1977).
- 32(a). D. G. Lister, J. N. Macdonald and N. L. Owen, "Internal Rotation and Inversion", Academic Press, London, New York, San Francisco, (1978)88.
- 32(b). Ibid., p. 131.
33. M. Davies and J. Swain, Trans. Faraday Soc., 67(1971)1637.
34. W. R. Fairheller and J. E. Katon, J. Mol. Spectroscopy, 1(1957)239.
35. H.A. Khwaja, M.Sc. Thesis, Lakehead University, Thunder Bay, Ontario, Canada, (1977).
36. J. Crossley, D. Gourlay, M. Rujimethabhas, S. P. Tay and S. Walker, J. Chem. Phys., 71(1979)4095.
37. S. Mizushima and Kubo, Bull. Chem. Soc. Japan, 14(1938)15.
38. M. Oki and H. Nakanishi, Bull. Chem. Soc. Japan, 45(1972)1552.
39. M. A. Mazid, J. P. Shukla and S. Walker, Can. J. Chem., 56(1978)1800.
40. M. A. Enayetullah, Personal Communication, this laboratory.
41. J. P. Shukla, Personal Communication, this laboratory.
42. J. P. Shukla, B. Chan and S. Walker, Z. Phys. Chem. Neue Folge., Germany, to be published.
43. R.J. Meakins, Trans. Faraday Soc., 51(1955)371.

TABLE VI-1 INFRARED STRETCHING FREQUENCIES AND DIELECTRIC RELAXATION DATA OF ALIPHATIC ESTERS

Molecule	IR Stretching Frequencies		Medium	ΔT (K)	Relaxation times τ (s)			ΔG_E (kJ mol ⁻¹)			ΔH_E (kJ mol ⁻¹)	ΔS_E (J K ⁻¹ mol ⁻¹)
	C*-O	C*-O			100 K	150 K	200 K	100 K	150 K	200 K		
Methyl formate	1724 (21)	1161 (22)	Poly-Phenyl ether	84-109 233-246	5.0x10 ⁻⁶	6.8x10 ⁻⁷	2.6x10 ⁻⁴	13.4	18.2	36.1	4.2	0.97 -95.0
		1214										146.0
Ethyl formate	1724 (21)	1155 (22)	Poly-Phenyl ether	115-141	1.5x10 ⁻²	1.7x10 ⁻⁶		20.1	19.3		21.8	2.40 17.2
		1195										
Propyl formate	1724 (21)	1154 (22)	Poly-styrene matrix	94-143 231-249	2.3x10 ⁻⁴	5.1x10 ⁻⁷	4.8x10 ⁻⁴	16.6	17.8	37.2	14.2	1.65 -24.0
		1190										136.5
Methyl acetate	1748 (21)	1253 (23)	Poly-styrene matrix	89-115 171-218	2.5x10 ⁻⁵	6.4x10 ⁻⁶	5.0x10 ⁻⁵	14.5	19.8	31.8	2.4	1.26 -124.0
												27.1
			o-ter-phenyl	79-121	2.7x10 ⁻⁵	1.1x10 ⁻⁶		14.8	18.8		6.9	1.65 -78.9
			Poly-phenyl ether	103-144	2.5x10 ⁻³	1.1x10 ⁻⁶		18.6	18.7		18.4	1.33 -2.1

TABLE VI-1 INFRARED STRETCHING FREQUENCIES AND DIELECTRIC RELAXATION DATA OF ALIPHATIC ESTERS continued...

Molecule	IR Stretching Frequencies (cm^{-1})		Medium	ΔT (K)	Relaxation times τ (s)			ΔG_E (kJ mol^{-1})			ΔH_E (kJ mol^{-1})	ΔH° (kJ mol^{-1})	ΔS_E ($\text{J K}^{-1} \text{mol}^{-1}$)
	C*=0	C*-O			100 K	150 K	200 K	100 K	150 K	200 K			
Vinyl crotonate	1745*	1142* 1170	o-ter-phenyl	152-193	8.5×10^{-4}	7.7×10^{-6}	27.1	28.7	22.0	3.56	-33.1		
Methyl propiolate	1718 ⁽²⁴⁾	1169*	Poly-styrene matrix	84-111 165-198	1.5×10^{-5} 2.0×10^{-1}	1.9×10^{-6} 1.8×10^{-5}	14.3	19.4 33.8	4.1 45.0	1.12 1.86	-102.2 74.5		
			o-ter-phenyl	87-115	2.1×10^{-5}	1.5×10^{-6}	14.6	19.2	5.6	1.63	-90.7		
			Poly-phenyl ether	90-125	1.1×10^{-4}	1.0×10^{-5}	16.0	21.6	4.9	1.90	-111.0		
Vinyl chloroacetate	1770*	1153*	o-ter-phenyl	83-110	2.7×10^{-5}	6.6×10^{-6}	14.8	21.0	2.5	1.47	-123.4		
Vinyl bromoacetate	1763*	1145*	o-ter-phenyl	79-118	2.7×10^{-5}	7.9×10^{-6}	14.8	21.2	2.0	1.13	-128.1		
Vinyl propionate	1763*	1158*	o-ter-phenyl	82-127	5.2×10^{-5}	1.1×10^{-6}	15.4	18.7	8.7	1.75	-67.1		
Vinyl butyrate	1760*	1158*	o-ter-phenyl	87-133 196-206	6.2×10^{-5}	1.1×10^{-6}	15.5	18.7	9.1	1.25	-63.9		
					3.6×10^{-3}		30.9	115.0			232.0		

*spectra recorded in this laboratory

TABLE VI-1 INFRARED STRETCHING FREQUENCIES AND DIELECTRIC RELAXATION DATA OF ALIPHATIC ESTERS continued...

Molecule	IR Stretching Frequencies (cm^{-1})		Medium	ΔT (K)	Relaxation times τ (s)			ΔG_E (kJ mol^{-1})			ΔH_E (kJ mol^{-1})	ΔH° (kJ mol^{-1})	ΔS_E ($\text{J K}^{-1} \text{mol}^{-1}$)
	C*=0	C*-O			100 K	150 K	200 K	100 K	150 K	200 K			
Dimethyl oxalate	1775 (25)	1189 (25)	Poly-styrene matrix	101-143 231-291	3.7×10^{-3} 1.3×10^{-4}	5.1×10^3 4.4×10^{-1}	18.9	24.8	7.2	1.60	-116.7		
	1750	1216						46.4	45.3	4.86		-8.6	
Methyl chloroformate	1782*	1151*	Poly-styrene matrix	151-183	8.5×10^{-4}	5.9×10^{-6}	27.0	28.3	23.3	4.32	-24.8		
		1205											
			o-ter-phenyl	130-181	4.2×10^{-5}	5.5×10^{-7}	23.3	24.4	20.2	2.78	-20.9		
			Poly-phenyl ether	142-177	7.6×10^{-5}	4.3×10^{-7}	24.0	23.9	24.4	2.42	2.3		
Ethyl chloroformate	1782*	1165*	Poly-styrene matrix (40)	127-147	3.0×10^{-5}	2.1×10^{-7}	22.9	22.7	23.3		2.9		
			o-ter-phenyl	156-205	2.3×10^{-3}	7.4×10^{-6}	28.3	28.6	27.1	3.77	-79		
			Poly-phenyl ether	163-210	8.0×10^{-3}	8.1×10^{-3}	29.9	28.8	33.0	3.61	20.9		

TABLE VI-1 INFRARED STRETCHING FREQUENCIES AND DIELECTRIC RELAXATION DATA OF ALIPHATIC ESTERS continued...

Molecule	IR Stretching Frequencies (cm ⁻¹)	Medium	ΔT (K)	Relaxation times τ (s)			ΔG_E (kJ mol ⁻¹)			ΔH_E (kJ mol ⁻¹)	ΔH^0 (kJ mol ⁻¹)	ΔS_E (J K ⁻¹ mol ⁻¹)
				100 K	150 K	200 K	100 K	150 K	200 K			
Butyl chloroformate	1784*	Poly-styrene matrix (40)	159-205	3.0×10^{-3}	8.6×10^{-6}	28.6	28.9	27.8	-5.7			
iso-butyl chloroformate	1782*	poly-styrene matrix (40)	98-135	5.0×10^{-4}	8.8×10^{-7}	17.3	18.5	14.8	1.60	-24.5	392.0	
			184-219			22.1	23.6	19.1	2.18	-29.3	25.5	

* spectra recorded in this laboratory

TABLE VI.2

Tabulated Summary of Fuoss-Kirkwood
Analysis Parameters and Effective Dipole
Moments (μ) for Aliphatic Esters

T(K)	$10^6 \tau$ (s)	$\log f_{\max}$	β	$10^3 \epsilon''_{\max}$	ϵ_{∞}	μ (D)
<u>1.05 M Methyl formate in Polyphenyl ether</u>						
<u>Low Temperature Process</u>						
84.5	13.9	4.06	0.20	20.78	2.94	0.57
96.5	12.1	4.21	0.22	21.24	2.95	0.59
101.9	4.74	4.53	0.18	20.91	2.93	0.67
109.9	2.82	4.75	0.24	22.33	2.97	0.62
<u>High Temperature Process</u>						
232.9	305	2.72	0.49	617.20	3.50	2.79
237.3	54.5	3.47	0.57	601.50	3.55	2.58
240.2	25.5	3.80	0.64	583.29	3.66	2.38
242.7	14.6	4.04	0.74	583.70	3.78	2.24
244.5	6.90	4.36	0.74	576.83	3.80	2.19
<u>0.89 M Ethyl formate in Polyphenyl ether</u>						
114.8	995	2.21	0.16	20.68	2.98	0.80
122.8	101	3.20	0.21	21.57	2.99	0.74
129.5	28.9	3.74	0.17	24.16	2.98	0.89
133.8	13.5	4.07	0.18	25.10	2.99	0.89
140.5	6.18	4.41	0.20	26.38	3.00	0.89
<u>0.86 M Propyl formate in Polystyrene Matrix</u>						
<u>Low Temperature Process</u>						
94.2	698	2.36	0.21	6.88	2.44	0.42
100.3	227	2.85	0.20	7.19	2.45	0.45
107.5	70.4	3.35	0.18	7.59	2.45	0.50
113.3	21.8	3.86	0.18	8.03	2.46	0.54
121.4	81.5	4.29	0.19	8.55	2.48	0.55
126.3	5.52	4.46	0.19	8.73	2.47	0.57
133.8	2.51	4.80	0.18	8.87	2.48	0.61
<u>High Temperature Process</u>						
231.0	733.04	2.34	0.23	17.75	2.62	0.97
234.9	295.88	2.73	0.21	16.99	2.62	1.00
238.9	95.02	3.22	0.21	17.15	2.61	1.01
243.3	23.66	3.83	0.21	16.87	2.61	1.02
248.5	4.81	4.52	0.19	17.00	2.59	1.08

TABLE VI.2

continued...

T(K)	$10^6 \tau$ (s)	$\log f_{\max}$	β	$10^3 \epsilon''_{\max}$	ϵ_{∞}	μ (D)
<u>0.98 M Methyl acetate in Polystyrene Matrix</u>						
<u>Low Temperature Process</u>						
88.6	59.8	3.43	0.14	0.42	2.49	0.12
93.2	45.7	3.54	0.15	0.45	2.49	0.12
100.7	22.0	3.86	0.18	0.47	2.49	0.11
108.4	5.69	4.45	0.09	0.50	2.49	0.17
114.7	4.41	4.56	0.08	0.47	2.49	0.18
<u>High Temperature Process</u>						
171.3	947	2.23	0.45	14.03	2.50	0.51
176.2	568	2.45	0.44	14.08	2.50	0.52
181.8	269	2.77	0.46	15.06	2.51	0.54
187.3	145	3.04	0.43	14.93	2.51	0.56
192.2	96.1	3.22	0.44	15.27	2.51	0.57
197.4	62.2	3.41	0.41	15.42	2.51	0.60
202.0	37.8	3.62	0.44	16.00	2.51	0.60
209.4	22.8	3.84	0.38	16.71	2.51	0.67
218.1	13.6	4.07	0.32	18.83	2.50	0.79
<u>0.94 M Methyl acetate in o-Terphenyl</u>						
79.4	308	2.71	0.10	5.65	2.77	0.45
86.1	112	3.15	0.12	6.25	2.78	0.45
91.8	62.0	3.41	0.15	6.67	2.79	0.43
99.4	25.5	3.79	0.13	7.36	2.78	0.50
101.2	24.8	3.81	0.16	7.53	2.79	0.46
109.0	12.5	4.10	0.16	8.03	2.80	0.50
114.6	9.28	4.23	0.19	8.34	2.81	0.47
120.7	4.82	4.52	0.17	8.72	2.81	0.53
<u>0.91 M Methyl acetate in Polyphenyl ether</u>						
102.8	1359	2.07	0.13	8.35	2.97	0.53
108.0	441	2.55	0.15	9.54	2.97	0.54
114.7	313	3.08	0.12	9.90	2.97	0.64
133.2	77.6	4.31	0.17	12.30	3.02	0.64
144.0	19.9	4.90	0.17	13.18	3.01	0.69

T (K)	$10^6 \tau$ (s)	$\log f_{\max}$	β	$10^3 \epsilon''_{\max}$	ϵ_{∞}	μ (D)
<u>0.84 M Methyl acrylate in Polystyrene Matrix</u>						
111.4	1142	2.14	0.20	3.14	2.73	0.30
114.6	668	2.38	0.22	3.28	2.73	0.30
118.7	332	2.68	0.25	3.31	2.73	0.29
124.0	151	3.02	0.21	3.40	2.73	0.34
127.7	92.1	3.24	0.20	3.46	2.72	0.33
131.7	43.0	3.57	0.22	3.55	2.72	0.34
136.7	19.8	3.90	0.22	3.59	2.72	0.34
141.8	8.95	4.25	0.23	3.67	2.72	0.35
149.0	3.64	4.64	0.20	3.69	2.72	0.36
<u>0.87 M Methyl acrylate in o-Terphenyl</u>						
114.3	1984	1.90	0.17	9.83	2.77	0.57
119.5	911	2.24	0.16	10.39	2.77	0.62
125.4	297	2.73	0.19	11.05	2.77	0.60
131.0	119	3.13	0.20	11.56	2.78	0.61
137.0	51.4	3.49	0.21	12.05	2.78	0.62
139.8	34.8	3.66	0.22	12.28	2.78	0.62
143.4	15.6	4.01	0.21	12.68	2.78	0.65
149.5	9.91	4.21	0.24	13.10	2.79	0.63
156.3	4.02	4.60	0.23	13.39	2.79	0.66
<u>0.84 M Methyl acrylate in Polyphenyl ether</u>						
129.0	783	2.31	0.19	14.76	2.92	0.69
138.2	126	3.10	0.19	15.80	2.92	0.74
144.6	38.0	3.62	0.20	16.63	2.92	0.76
151.8	14.6	4.04	0.20	17.26	2.90	0.79
162.0	4.51	4.55	0.20	18.24	2.90	0.83
<u>0.66 M Methyl crotonate in Polystyrene Matrix</u>						
141.1	679	2.37	0.19	9.75	3.42	0.60
145.1	326	2.69	0.21	9.99	3.42	0.58
149.6	176	2.96	0.22	10.32	3.42	0.59
155.8	75.5	3.32	0.24	10.64	3.43	0.59
162.8	40.0	3.60	0.20	10.98	3.42	0.67
169.7	20.4	3.89	0.22	11.34	3.43	0.66
175.4	10.3	4.19	0.19	11.55	3.42	0.73
182.9	5.10	4.49	0.14	11.65	3.40	0.79

TABLE VI.2

continued...

T(K)	$10^6 \tau$ (s)	$\log f_{\max}$	β	$10^3 \epsilon''_{\max}$	ϵ_{∞}	μ (D)
<u>0.89 M Methyl crotonate in o-Terphenyl</u>						
135.5	703	2.36	0.14	9.31	2.77	0.66
138.6	374	2.63	0.15	9.41	2.77	0.65
142.6	182	2.94	0.17	9.80	2.78	0.63
148.3	77.5	3.31	0.19	10.18	2.78	0.62
153.6	38.8	3.61	0.20	10.55	2.79	0.62
158.1	27.0	3.77	0.23	10.88	2.79	0.60
163.3	14.6	4.04	0.23	11.28	2.79	0.62
167.2	9.18	4.24	0.23	11.56	2.80	0.63
172.2	6.87	4.37	0.26	11.82	2.81	0.61
177.1	3.40	4.67	0.23	11.98	2.80	0.65
<u>0.83 M Methyl crotonate in Polyphenyl ether</u>						
134.9	1099	2.16	0.17	9.69	2.93	0.61
139.7	603	2.42	0.16	9.89	2.92	0.65
144.1	263	2.78	0.18	10.24	2.93	0.63
149.2	118	3.13	0.19	10.59	2.93	0.63
153.8	63.3	3.40	0.18	10.88	2.93	0.67
158.7	35.6	3.65	0.20	11.31	2.94	0.66
161.9	28.1	3.75	0.22	11.56	2.94	0.64
166.5	15.0	4.02	0.22	11.92	2.95	0.66
171.2	9.78	4.21	0.23	12.25	2.95	0.67
178.7	5.77	4.44	0.23	12.67	2.95	0.69
182.3	3.24	4.69	0.20	12.65	2.95	0.71
<u>0.81 M Vinyl crotonate in o-Terphenyl</u>						
151.6	711	2.35	0.20	3.83	2.78	0.38
157.6	328	2.69	0.26	3.98	2.78	0.36
162.9	172	2.96	0.28	4.17	2.79	0.36
167.2	130	3.09	0.27	4.27	2.78	0.37
174.4	67.9	3.37	0.20	4.59	2.78	0.46
179.4	42.6	3.54	0.19	4.83	2.78	0.49
186.1	21.6	3.87	0.24	5.00	2.79	0.48
193.2	10.2	4.15	0.22	5.29	2.79	0.49

TABLE VI.2

continued...

T(K)	$10^6 \tau$ (s)	$\log f_{\max}$	β	$10^3 \epsilon''_{\max}$	ϵ_{∞}	μ (D)
<u>0.90 M Methyl propiolate in Polystyrene Matrix</u>						
<u>Low Temperature Process</u>						
83.6	46.5	3.53	0.20	1.16	2.45	0.16
94.1	21.9	3.86	0.18	1.23	2.45	0.19
103.0	13.4	4.07	0.17	1.28	2.45	0.21
110.9	7.83	4.31	0.13	1.28	2.45	0.24
120.5	4.03	4.45	0.14	1.33	2.46	0.25
<u>0.89 M Methyl propiolate in Polystyrene Matrix</u>						
<u>High Temperature Process</u>						
164.6	10625	1.30	0.10	1.51	2.55	0.36
172.9	1297	2.09	0.14	1.52	2.55	0.32
176.0	672	2.37	0.16	1.41	2.55	0.29
177.9	564	2.46	0.18	1.56	2.55	0.29
181.9	354	2.66	0.20	1.57	2.55	0.28
187.4	144	3.04	0.17	1.57	2.55	0.30
193.0	43.3	3.57	0.14	1.54	2.55	0.33
198.3	22.1	3.86	0.15	1.55	2.55	0.33
<u>0.86 M Methyl propiolate in o-Terphenyl</u>						
86.7	71.2	3.35	0.13	3.20	2.77	0.33
89.1	51.3	3.49	0.15	3.30	2.77	0.32
95.5	31.8	3.70	0.14	3.55	2.77	0.35
102.0	16.7	3.98	0.15	3.81	2.78	0.36
109.2	10.7	4.17	0.15	4.04	2.78	0.38
115.8	7.30	4.31	0.17	4.21	2.78	0.38
<u>0.89 M Methyl propiolate in Polyphenyl ether</u>						
89.5	254	2.80	0.12	4.68	2.92	0.38
97.3	145	3.04	0.12	5.18	2.92	0.44
104.5	70.4	3.35	0.12	5.67	2.92	0.47
112.3	47.9	3.50	0.15	6.16	2.93	0.46
118.4	40.9	3.63	0.17	6.52	2.94	0.45
124.7	29.9	3.73	0.16	6.92	2.94	0.49

TABLE VI.2

continued...

T(K)	$10^6 \tau$ (s)	$\log f_{\max}$	β	$10^3 \epsilon''_{\max}$	ϵ_{∞}	μ (D)
<u>0.70 M Vinyl chloroacetate in o-Terphenyl</u>						
83.4	59.4	3.43	0.20	1.38	2.80	0.19
86.4	48.7	3.50	0.20	1.38	2.80	0.19
92.4	23.3	3.63	0.29	1.48	2.80	0.18
98.6	17.9	3.74	0.32	1.57	2.79	0.17
103.5	10.7	3.83	0.33	1.63	2.79	0.17
110.4	6.15	3.93	0.35	1.74	2.79	0.18
<u>0.51 M Vinyl bromoacetate in o-Terphenyl</u>						
79.0	64.5	3.39	0.22	1.12	2.80	0.18
85.2	46.4	3.53	0.24	1.16	2.80	0.19
92.1	40.9	3.63	0.26	1.19	2.79	0.19
96.2	32.8	3.72	0.25	1.20	2.79	0.20
102.2	26.4	3.80	0.22	1.23	2.79	0.22
109.0	17.8	3.90	0.23	1.28	2.79	0.22
117.6	12.2	4.01	0.20	1.34	2.79	0.24
<u>0.79 Vinyl propionate in o-Terphenyl</u>						
82.3	524	2.48	0.14	2.09	2.77	0.26
87.3	290	2.74	0.14	2.22	2.77	0.27
91.7	171	2.97	0.15	2.34	2.77	0.28
95.7	64.2	3.29	0.20	2.45	2.77	0.25
100.3	40.6	3.50	0.21	2.59	2.77	0.26
105.3	26.5	3.75	0.20	2.73	2.77	0.28
110.0	12.9	3.99	0.19	2.99	2.77	0.30
115.8	10.9	4.19	0.18	3.13	2.77	0.33
122.3	5.62	4.36	0.18	3.17	2.77	0.34
127.4	3.29	4.59	0.17	3.18	2.77	0.36

TABLE VI.2 continued...

T(K)	$10^6 \tau$ (s)	$\log f_{\max}$	β	$10^3 \epsilon''_{\max}$	ϵ_{∞}	μ (D)
<u>0.74 M Vinyl butyrate in o-Terphenyl</u>						
<u>Low Temperature Process</u>						
86.9	390	2.61	0.20	2.43	2.76	0.25
91.4	204	2.89	0.21	2.54	2.76	0.25
100.3	58.8	3.43	0.21	2.69	2.76	0.27
105.6	28.1	3.75	0.23	2.86	2.76	0.27
109.5	20.8	3.88	0.24	2.94	2.76	0.28
114.9	11.0	4.16	0.25	2.99	2.76	0.28
119.3	9.08	4.24	0.27	3.00	2.76	0.28
126.3	5.43	4.47	0.27	2.89	2.76	0.28
132.7	3.37	4.67	0.30	2.78	2.77	0.27
<u>High Temperature Process</u>						
196.1	135	3.07	0.25	21.46	2.78	0.98
199.7	36.5	3.64	0.26	20.57	2.79	0.95
200.5	27.9	3.76	0.28	21.11	2.79	0.93
202.8	15.0	3.97	0.30	21.25	2.79	0.91
204.0	9.25	4.20	0.34	20.92	2.80	0.85
206.0	4.11	4.59	0.35	20.48	2.81	0.83
<u>0.38 M Dimethyl oxalate in Polystyrene Matrix</u>						
<u>Low Temperature Process</u>						
100.8	3665	1.64	0.14	0.26	3.14	0.14
110.6	1146	2.04	0.12	0.27	3.14	0.16
117.0	826	2.29	0.11	0.28	3.14	0.17
124.0	521	2.49	0.15	0.29	3.14	0.15
128.3	395	2.60	0.23	0.30	3.14	0.13
133.4	298	2.72	0.16	0.31	3.14	0.16
138.4	248	2.81	0.14	0.31	3.14	0.17
142.8	240	2.88	0.13	0.32	3.14	0.19

TABLE VI.2

continued...

T(K)	$10^6 \tau$ (s)	$\log f_{\max}$	β	$10^3 \epsilon''_{\max}$	ϵ_{∞}	μ (D)
<u>High Temperature Process</u>						
231.1	10638	1.18	0.17	79.30	3.05	3.18
237.0	5573	1.46	0.17	82.20	3.04	3.29
241.4	3135	1.71	0.17	84.91	3.02	3.37
245.4	2047	1.89	0.18	87.45	3.03	3.35
251.6	1244	2.11	0.18	91.96	3.02	3.44
258.2	710	2.35	0.19	96.55	3.03	3.47
265.4	470	2.58	0.20	101.05	3.04	3.50
272.4	246	2.81	0.21	106.81	3.04	3.54
281.4	122	3.11	0.21	112.32	3.03	3.60
291.0	57.7	3.44	0.23	119.00	3.04	3.75
<u>0.90 M Methyl chloroformate in Polystyrene Matrix</u>						
150.9	763	2.32	0.34	3.51	2.59	0.28
157.7	296	2.73	0.35	3.73	2.59	0.28
162.6	199	2.90	0.27	4.05	2.58	0.29
170.2	78.2	3.31	0.30	4.90	2.59	0.29
176.3	71.9	3.35	0.36	4.92	2.59	0.30
179.9	41.4	3.58	0.27	5.31	2.59	0.30
183.2	23.7	3.72	0.36	4.89	2.60	0.32
<u>0.87 M Methyl chloroformate in o-Terphenyl</u>						
130.2	638	2.40	0.16	14.18	2.76	0.75
136.4	238	2.82	0.17	14.86	2.76	0.76
142.8	97.3	3.21	0.16	15.65	2.76	0.82
148.4	43.5	3.56	0.15	16.17	2.75	0.84
152.6	28.9	3.74	0.18	16.81	2.76	0.83
158.3	16.8	3.97	0.19	17.50	2.77	0.84
163.7	10.0	4.20	0.20	18.17	2.77	0.85
169.3	6.10	4.42	0.20	18.46	2.78	0.87
180.6	2.46	4.81	0.22	19.30	2.79	0.87

TABLE VI.2

continued...

T(K)	$10^6 \tau$ (s)	$\log f_{\max}$	β	$10^3 \epsilon''_{\max}$	ϵ_{∞}	μ (D)
<u>0.85 M Methyl chloroformate in Polyphenyl ether</u>						
142.3	241	2.82	0.17	25.34	2.98	0.98
147.5	112	3.15	0.16	26.31	2.96	1.05
151.9	60.8	3.42	0.16	26.90	2.96	1.08
156.8	28.6	3.74	0.17	28.13	2.96	1.08
163.9	11.4	4.14	0.18	29.65	2.97	1.10
169.2	7.60	4.32	0.19	30.60	2.98	1.11
176.8	3.66	4.64	0.21	32.15	2.99	1.10
<u>0.86 M Ethyl chloroformate in o-Terphenyl</u>						
155.9	915	2.24	0.18	11.73	2.80	0.71
162.4	371	2.63	0.17	12.64	2.80	0.77
171.3	146	3.04	0.17	13.71	2.80	0.82
180.5	47.3	3.53	0.17	14.87	2.80	0.88
187.4	25.0	3.80	0.17	15.67	2.80	0.92
192.9	14.5	4.04	0.17	16.38	2.79	0.95
198.8	8.42	4.28	0.17	17.15	2.79	0.99
205.2	4.24	4.58	0.16	18.12	2.79	1.06
<u>0.74 M Ethyl chloroformate in Polyphenyl ether</u>						
162.8	877	2.26	0.17	16.56	2.91	0.93
172.8	234	2.83	0.17	17.79	2.79	1.01
182.8	57.1	3.45	0.16	18.99	2.80	1.10
186.0	39.7	3.60	0.17	19.08	2.81	1.08
189.8	22.9	3.84	0.18	20.21	2.82	1.09
197.0	9.45	4.23	0.19	21.94	2.82	1.13
202.0	7.12	4.35	0.18	22.26	2.81	1.18
209.7	3.18	4.70	0.18	22.79	2.81	1.22

TABLE VI.2

continued...

T(K)	$10^6 \tau$ (s)	$\log f_{\max}$	β	$10^3 \epsilon''_{\max}$	ϵ_{∞}	μ (D)
<u>0.71 M Butyl chloroformate in Polyphenyl ether</u>						
<u>Low Temperature Process</u>						
97.6	755	2.32	0.30	5.06	2.90	0.31
107.2	180	3.03	0.25	5.44	2.91	0.37
113.3	61.8	3.41	0.24	5.85	2.91	0.40
119.8	20.4	3.89	0.23	6.09	2.91	0.43
125.4	9.63	4.22	0.23	6.24	2.91	0.44
129.7	7.02	4.36	0.24	6.17	2.91	0.44
134.6	3.83	4.62	0.21	6.18	2.91	0.47
<u>High Temperature Process</u>						
249.9	714	2.35	0.36	615.81	3.36	4.14
254.2	86.0	3.27	0.44	596.48	3.43	3.72
257.6	24.3	3.82	0.57	592.86	3.70	3.18
262.5	6.74	4.37	0.67	577.35	3.90	2.85
<u>0.65 M iso-Butyl chloroformate in Polyphenyl ether</u>						
<u>Low Temperature Process</u>						
130.4	565	2.45	0.24	5.57	2.92	0.44
136.8	264	2.78	0.20	5.81	2.92	0.49
143.7	85.0	3.31	0.23	6.12	2.92	0.49
148.6	49.5	3.35	0.16	6.17	2.91	0.59
155.0	27.2	3.77	0.16	6.48	2.91	0.63
<u>High Temperature Process</u>						
184.6	844	2.28	0.16	11.32	2.94	0.89
192.6	307	2.72	0.16	12.00	2.94	0.94
197.2	204	2.89	0.16	12.42	2.94	0.97
204.5	78.4	3.31	0.17	12.98	2.94	0.98
211.3	33.2	3.68	0.17	13.79	2.94	1.02
218.8	14.4	4.04	0.18	15.45	2.94	1.07

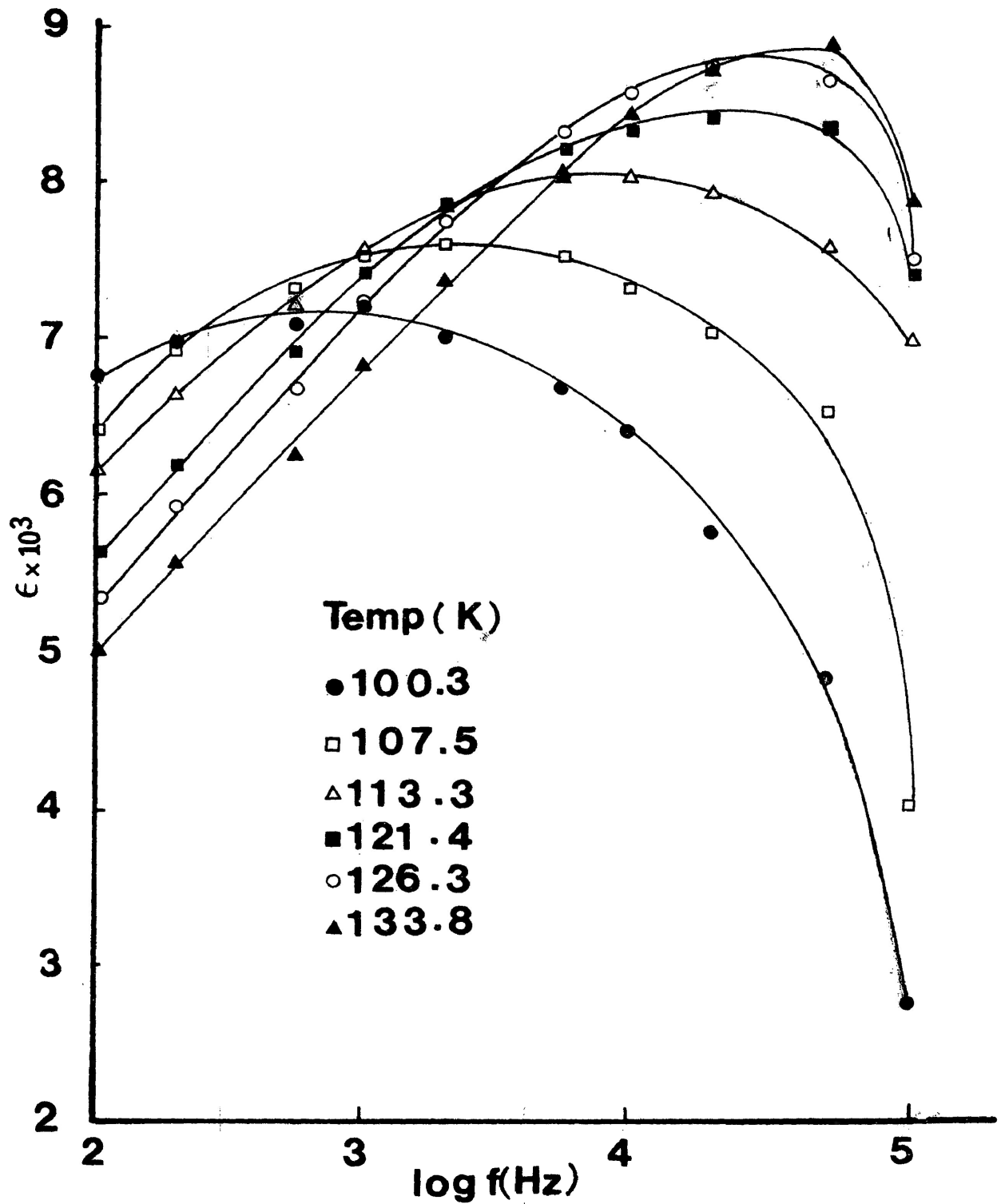


FIGURE VI.2

Plot of dielectric loss versus log(frequency)
for propyl formate in a polystyrene matrix

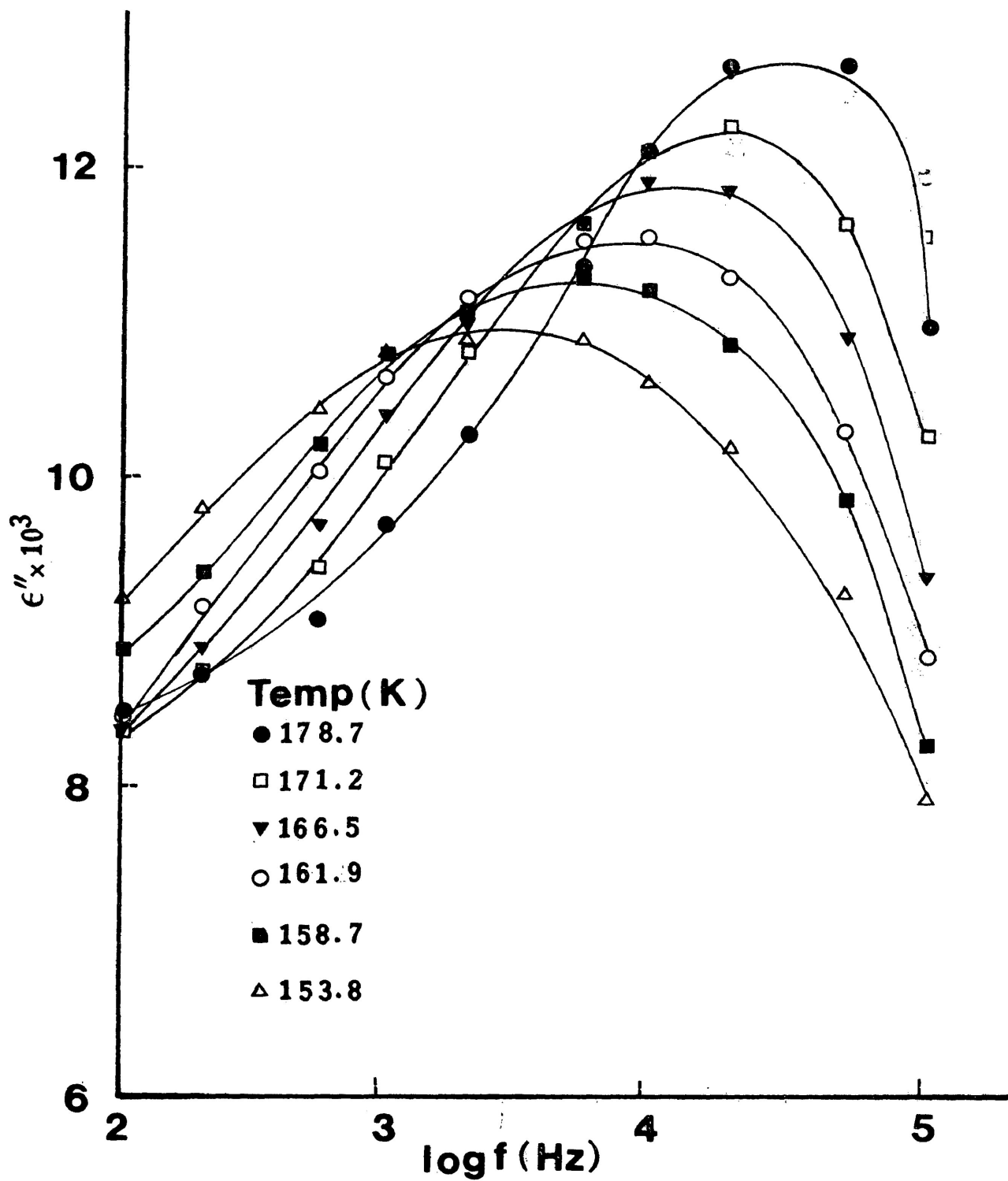


FIGURE VI.3

Plot of dielectric loss versus $\log(\text{frequency})$ for methyl crotonate in polyphenyl ether

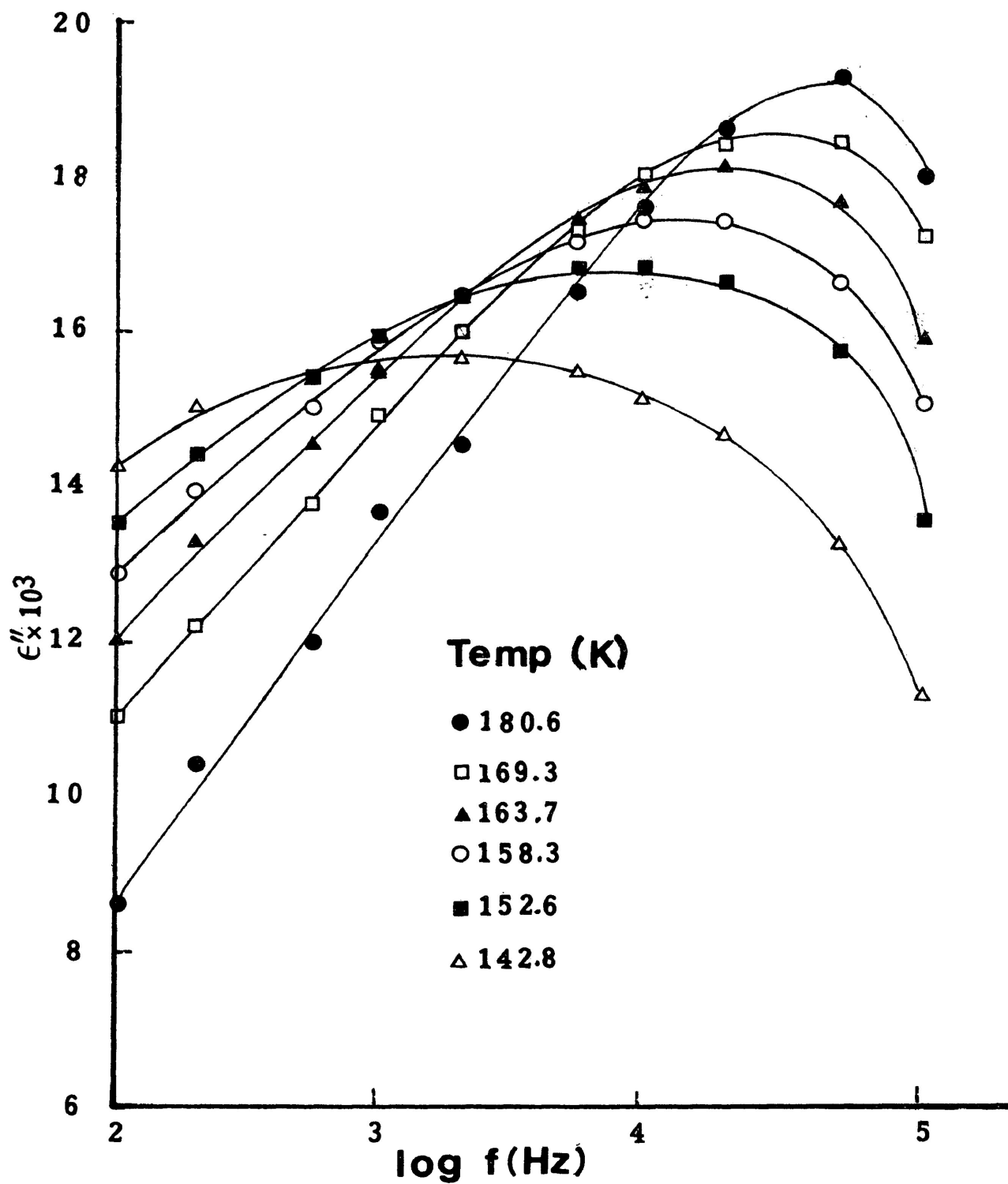


FIGURE VI.4

Plot of dielectric loss versus $\log(\text{frequency})$ for methyl chloroformate in o-terphenyl

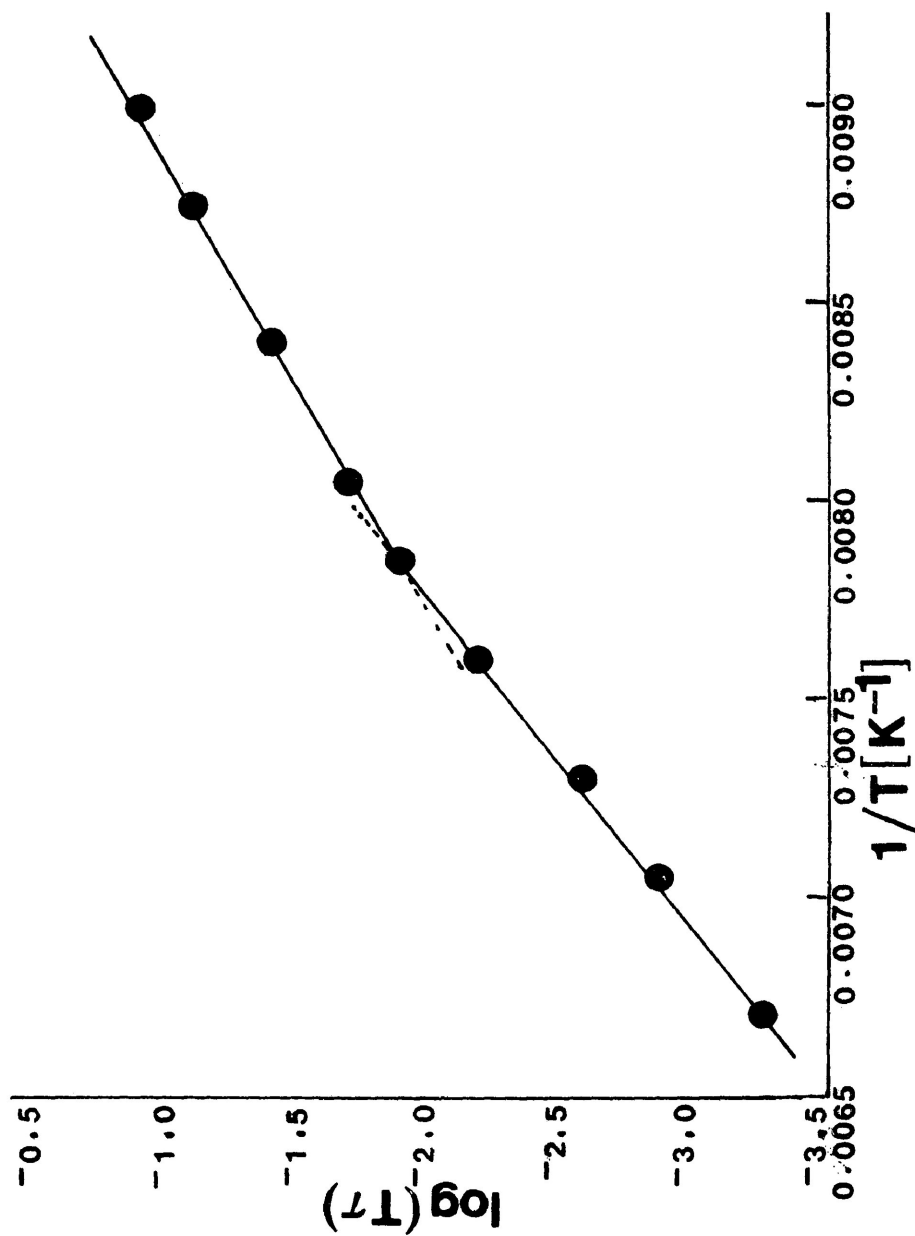


FIGURE VI.5 Plot $\log(T\tau)$ versus $1/T$ for methyl acrylate in a polystyrene matrix

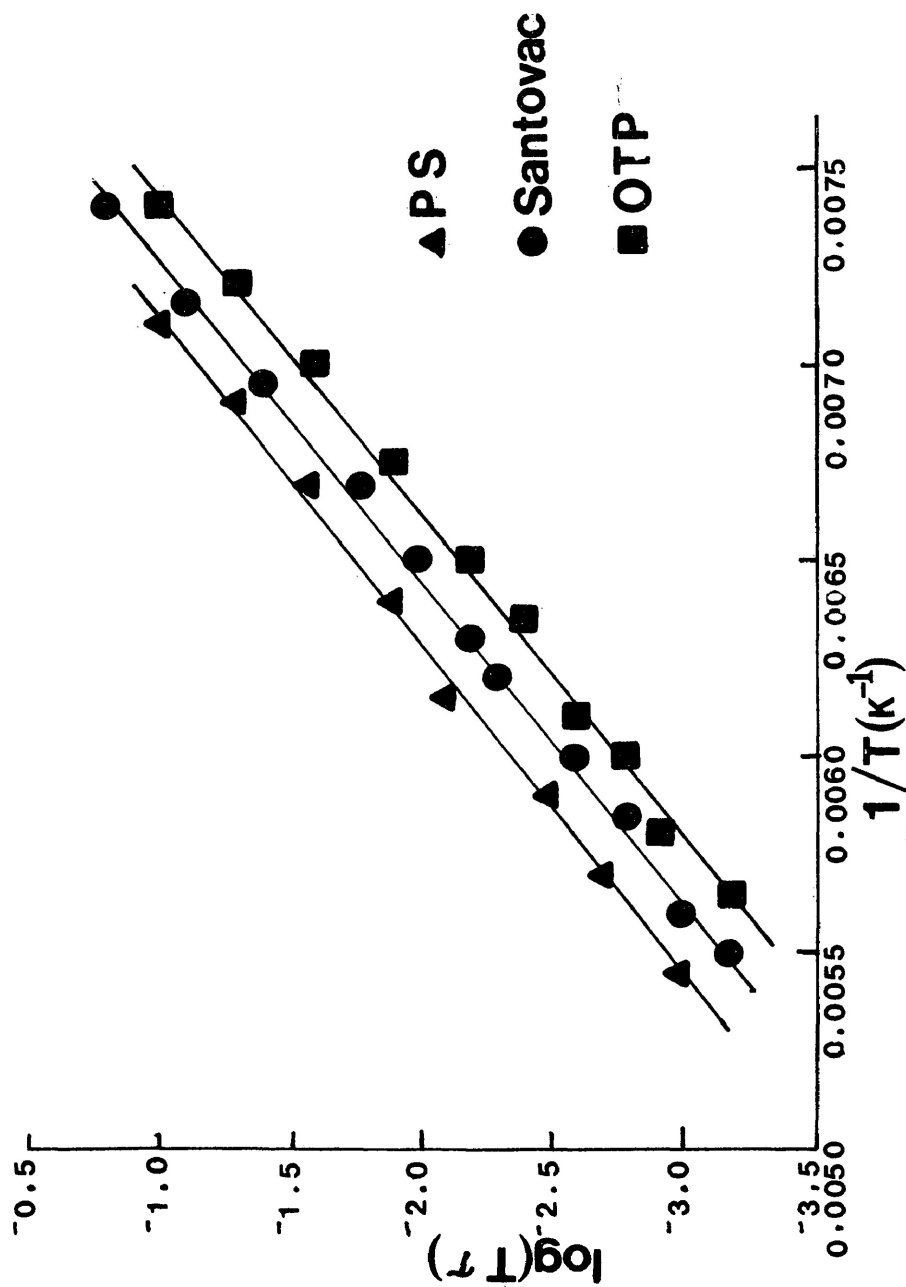


FIGURE VI.6 Plot of $\log(T\tau)$ versus $1/T$ for methyl crotonate in a polystyrene matrix (PS); ● polyphenyl ether (Santovac); and ■ o-terphenyl (OTP).

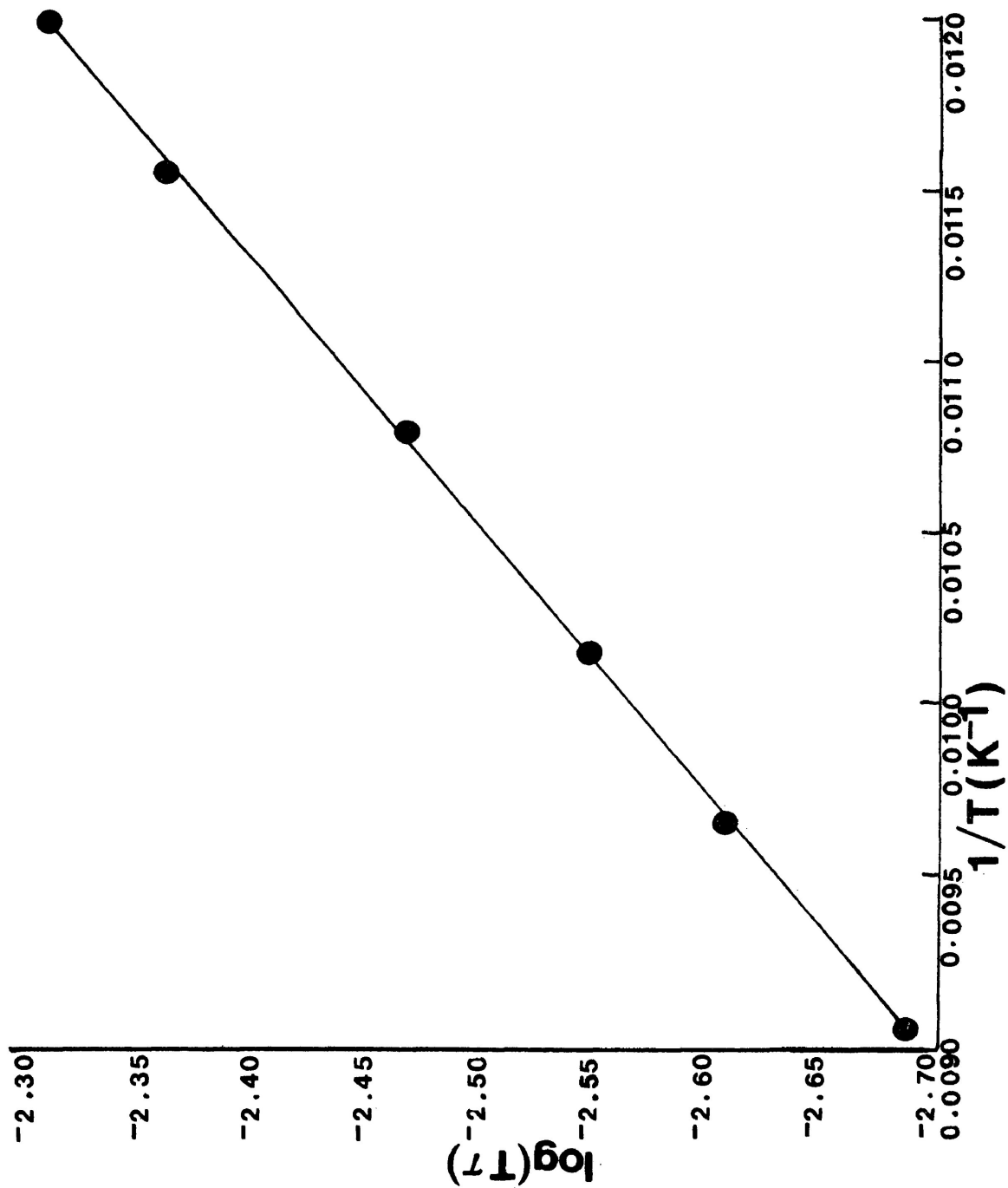


FIGURE VI.7 Plot of $\log(TT)$ versus $1/T$ for vinyl chloroacetate in o-terphenyl

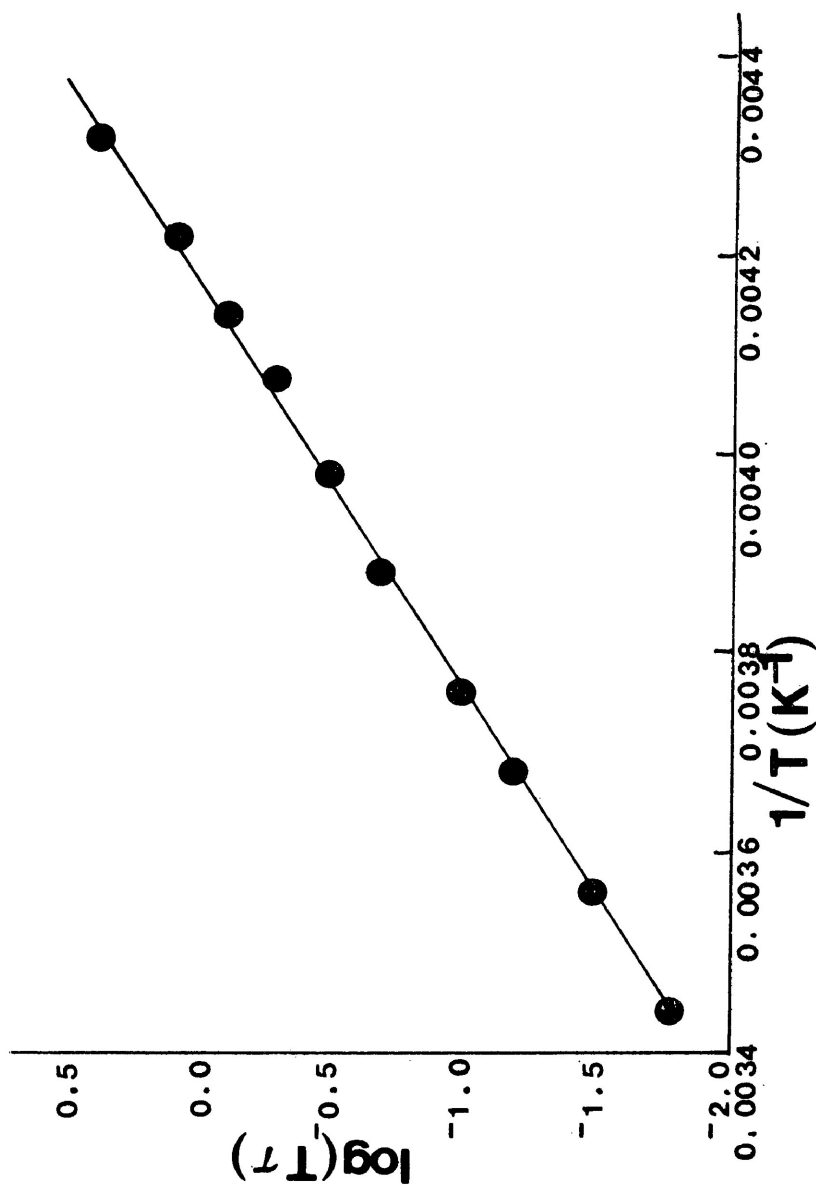


FIGURE VI.8 Plot of $\log(T_T)$ versus $1/T$ for dimethyl Oxalate in a polystyrene matrix

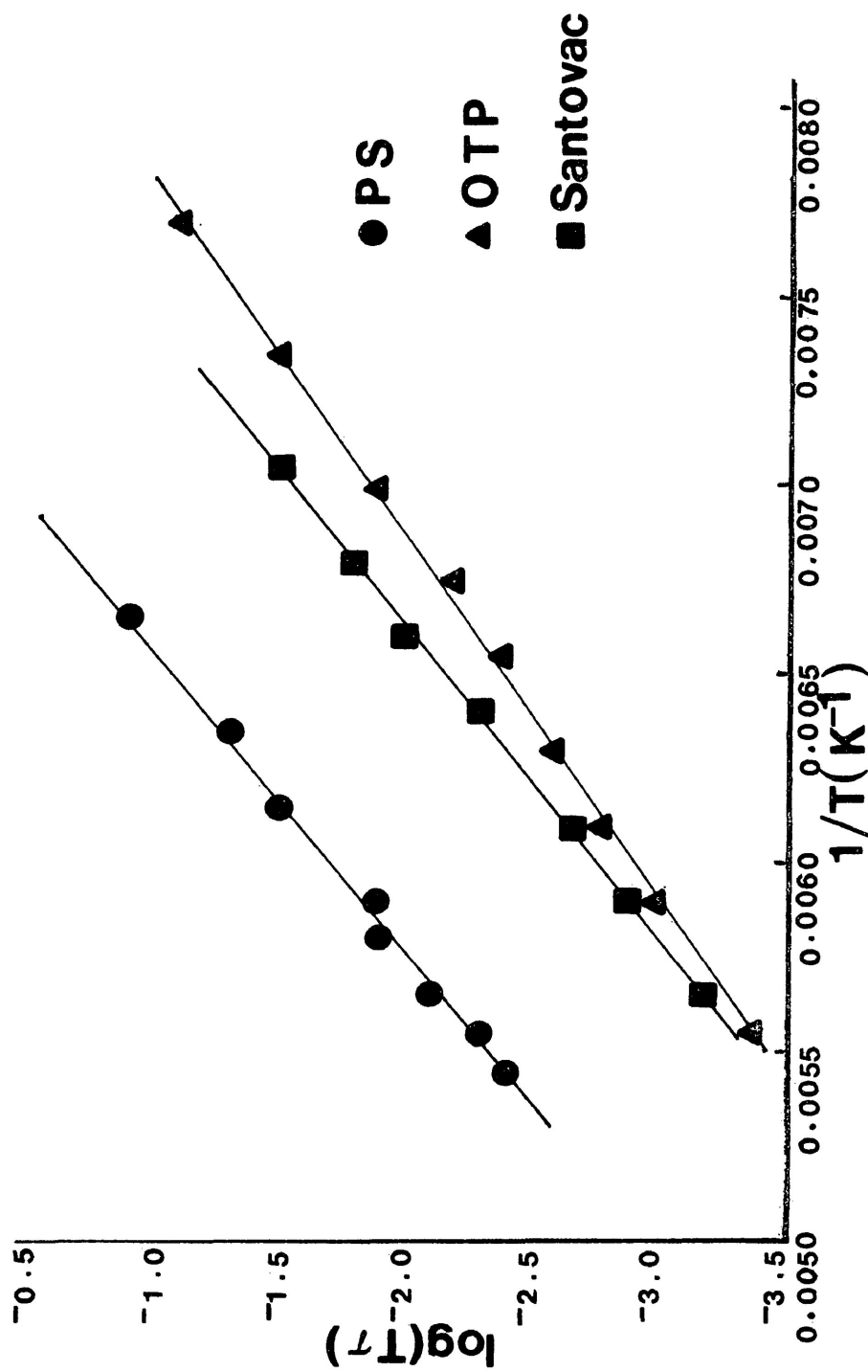


FIGURE VI.9 Plot of $\log(T\tau)$ versus $1/T$ for methyl chloroformate in
 ● a polystyrene matrix (PS); ▲ o-terphenyl (OTP); and
 ■ polyphenyl ether (Santovac)

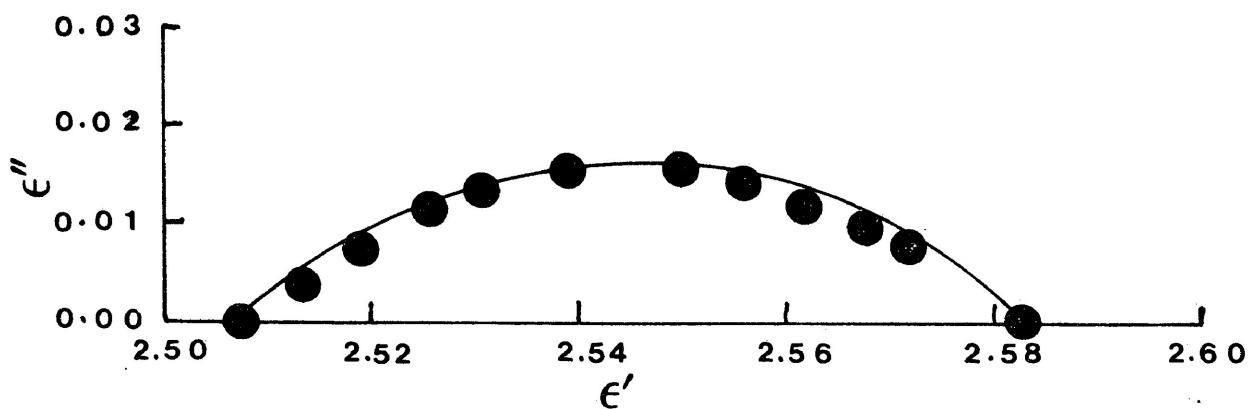


FIGURE VI.10 Cole-Cole plot for methyl acetate in a polystyrene matrix at 197.4 K

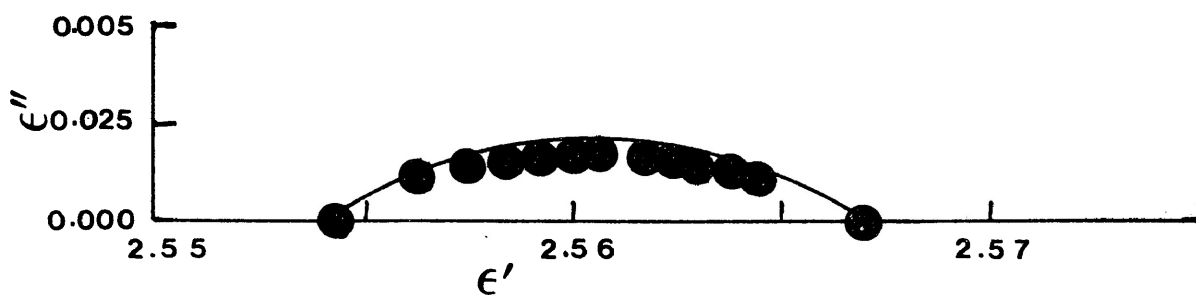


FIGURE VI.11 Cole-Cole plot for methyl propiolate in a polystyrene matrix at 181.9 K

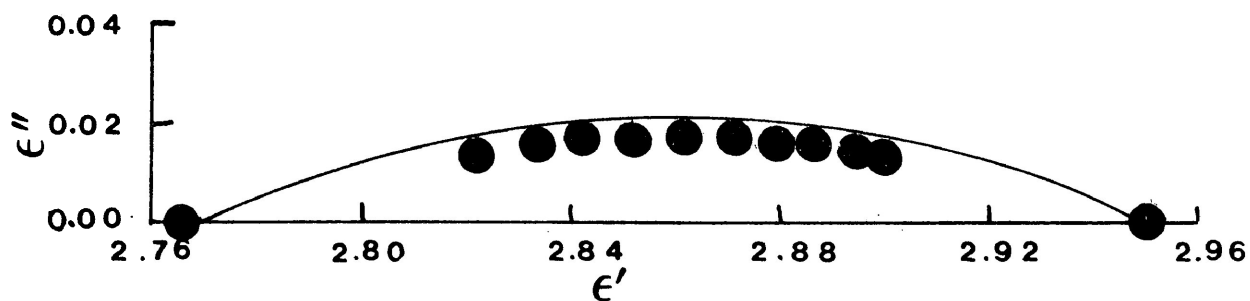
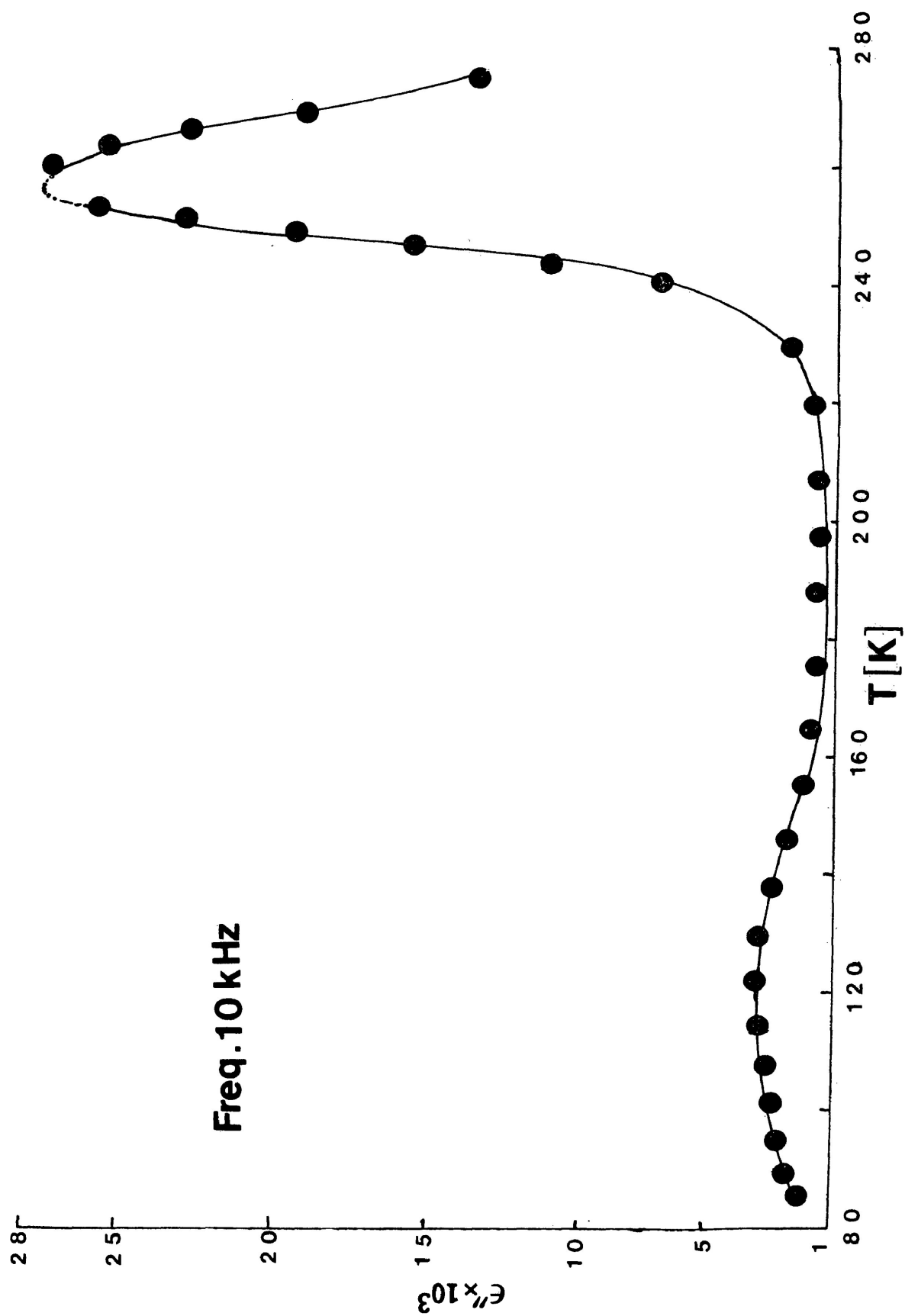


FIGURE VI.12 Cole-Cole plot for methyl chloroformate in o-terphenyl at 152.6 K

FIGURE VI.13 Plot of dielectric loss versus $T(K)$ for methyl propiolate in o-terphenyl

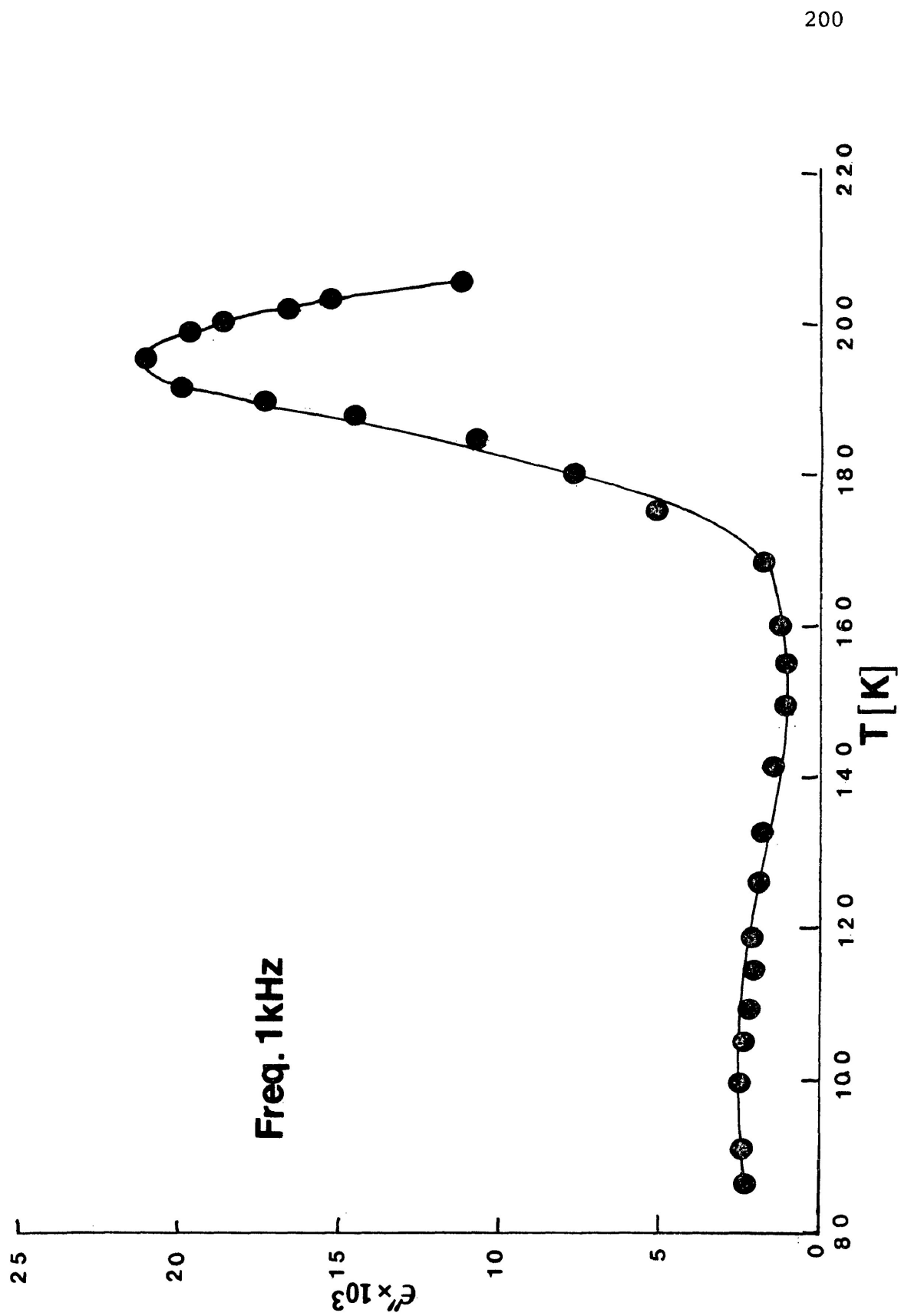


FIGURE VI.14. Plot of dielectric loss versus T (K) for vinyl butyrate in o-terphenyl

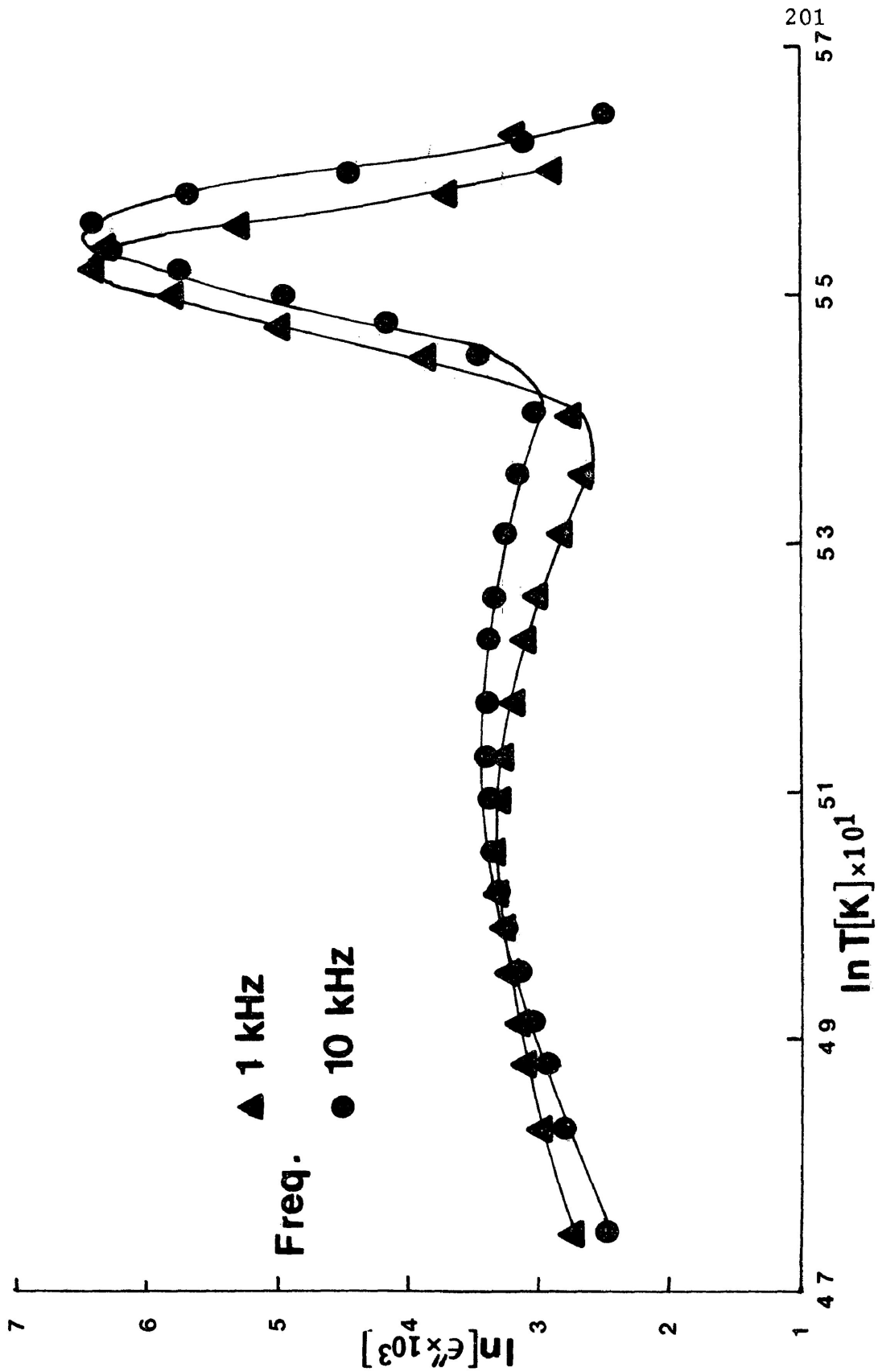


FIGURE VI.15 Plot of $\ln(\text{dielectric loss})$ versus $\ln(T)$ for methyl chloroformate in polyphenyl ether

CHAPTER VII

DIELECTRIC RELAXATION OF AROMATIC
AND
RELATED ESTERS

VII.1 INTRODUCTION

In the preceeding chapter, dielectric absorption of several aliphatic esters in polystyrene matrices, o-terphenyl and polyphenyl ether has been considered. It was indicated that the dipole relaxation of these esters, $R_1C^*OOR_2$, dominated by intramolecular rotation around the C-C* bond and/or the C*-O bond. And also it was observed that the barrier to intramolecular rotation involving the ester group (around C-C* bond), in particular, depends to some extent on the conjugative effect in $\alpha\beta$ -unsaturated esters. It is also of interest to investigate the behaviour of the ester group in aromatic and related molecules. In the literature there appears to be disagreement among investigators as to whether or not there is electronic interaction between the aromatic ring and the attached carbonyl group in alkyl benzoates. Smyth (1) and Krishna et al (2) suggested that the dipole moments of aromatic esters give no evidence of interaction between the polar group and the aromatic ring. Guryanova and Grishko (3) stated that free rotation about the $C_{Ar}-C^*$ bond was unlikely because of the presence of π -electrons at C_{Ar} and C^* carbon atoms.

Le Fèvre and Sundaram (4) stated that the "effective" conformation appeared to be that in which maximum π -electron overlap or the conjugation between the benzene ring and the carbonyl group occurred with the $C^*=O$ atoms in the plane of the ring, and this corresponded to a potential energy minimum.

Pinkus and Ellen (5) interpreted the increase in the electric dipole moments of a series of alkyl benzoates over the corresponding alkyl acetates in terms of conjugative interaction with the phenyl ring and supplying electrons to the electron-deficient carbonyl carbon, C^* . Hasan et al (6,7), from their dielectric studies of some monocarboxylic esters in the liquid state, observed that, although the dielectric data in benzyl formate, benzyl acetate, etc. could be analyzed in terms of both molecular and group relaxation, in the methyl- and ethyl benzoates the data were consistent with one relaxation process only. They proposed that in the methyl- and ethyl benzoates, $(PH \cdots \overset{O}{\underset{\cdot\cdot\cdot}{C^*}}-OR)$, $C^*=O$ dipole is adjacent to the benzene ring and that it imparts double bond character to the C^*-O bond owing to resonance, thus inhibiting the rotation of the OR group around the C^*-OR linkage. Further investigation by later workers (8)

of propyl- and butyl benzoates in the microwave region indicates no group rotation in these molecules. This supports the hypothesis of these workers (6,7) in the cases of methyl- and ethyl benzoates. While Grindley et al (9) have estimated the energy barriers to rotation about the $C_{Ar}-C^*$ bond to be 22.2 and 24.7 kJ mol^{-1} for the C^*O_2Me and C^*O_2Et groups in methyl benzoate and ethyl benzoate, respectively; they assumed the strain energy to be zero.

Krishna et al (10) made a dielectric study of methyl-p-nitrobenzoate, methyl-m-nitrobenzoate, ethyl-m-nitrobenzoate, ethyl-o-nitrobenzoate and methyl-o-aminobenzoate in benzene solution at 303 K. They reported barrier heights (ΔH_E) as 9.6, 9.2, 10.0, 8.4, and 9.2 kJ mol^{-1} , respectively. Comparing the observed and theoretically calculated dipole moment values, they proposed the absence of intramolecular rotation in these esters except for methyl- and ethyl-m-nitrobenzoate. And the observed relaxation process in these molecules and the corresponding ΔH_E -values were ascribed to overall rotation of the molecule in the solvent. Krishna et al (2) from dipole moment measurements of benzyl benzoate, 2-naphthyl benzoate,

and o-hydroxy-benzyl benzoate, obtained ΔH_E -values of 8.3, 8.2, and 8.8 kJ mol⁻¹, respectively. They interpreted these results in terms of restricted rotation of the -OR group about the position of minimum potential energy.

Recently, Khwaja (11) studied several aromatic esters in the frequency range 10² to 10⁵ Hz. He observed both molecular and intramolecular relaxation processes; and the intramolecular relaxation process was suggested to be due to rotation of the ester group.

From the foregoing review it seems that the information about the characterization of intramolecular relaxation process in aromatic esters is indecisive. Therefore, it seemed desirable to examine dielectrically a variety of aromatic and related esters (listed in Figure VII.1(a) and VII.1(b)) in polystyrene matrices, o-terphenyl and polyphenyl ether, as such an investigation has proved successful in a variety of cases in determining the energy barriers and also to characterize the intramolecular process in aliphatic esters (Chapter VI).

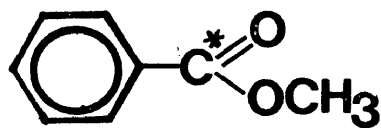
VII.2 EXPERIMENTAL

The dielectric measurements of a variety of aromatic and related esters (listed in Figure VII.1(a) and VII.1(b)) have been made over suitable ranges of temperature and frequency (usually 10^2 to 10^5 Hz) by the use of General Radio 1615 and 1621 bridges, the procedure being described in Chapter III. The solvents used are: (a) polystyrene, (b) o-terphenyl, and (c) polyphenyl ether.

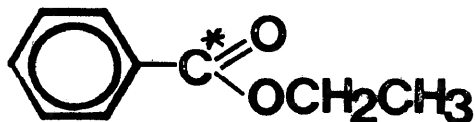
Sample plots of loss factor ($\epsilon'' = \epsilon''_{(\text{obs})} - \epsilon''_{(\text{solvent})}$) versus logarithm (frequency) are shown in Figures VII.2 to VII.4, while Figure VII.5 shows the sample plot of loss factor against T(K). Figures VII.6 to VII.12 show the sample plots of $\log T\tau$ versus $1/T$ (K^{-1}).

Table VII.1 gives the values of " ΔH_E " and " ΔS_E " evaluated from dielectric data as well as " ΔG_E " and " τ " values at 100 K, 200 K and 300 K. Tabulated summary of Fuoss-Kirkwood analysis parameters, " ϵ_∞ ", and effective dipole moments for a variety of aromatic and related esters at various experimental temperatures are presented in Table VII.2.

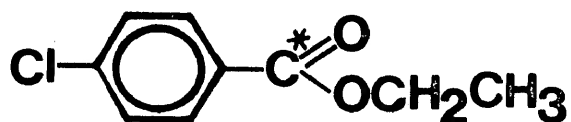
1. Methyl benzoate



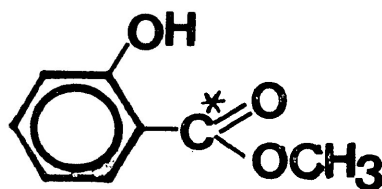
2. Ethyl benzoate



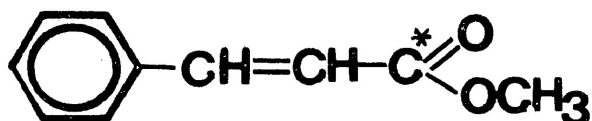
3. Ethyl-p-chloro benzoate



4. Methyl salicylate



5. Methyl cinnamate



6. Dimethyl-
2,6-naphthalene
dicarboxylate

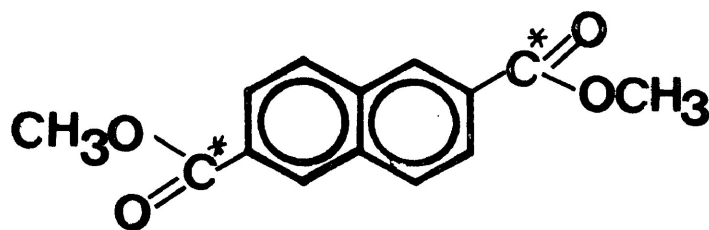
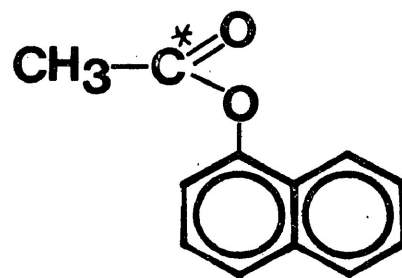
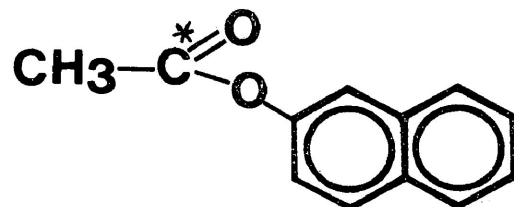


FIGURE VII.1(a)

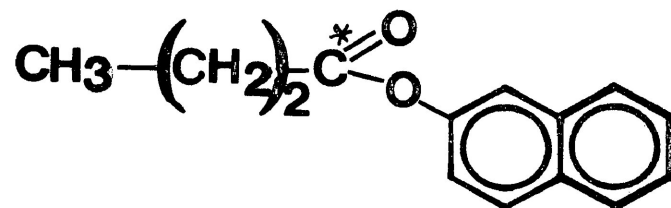
7. alpha-Naphthyl acetate



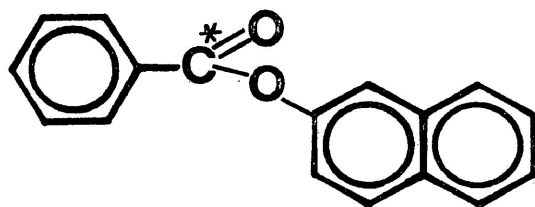
8. beta-Naphthyl acetate



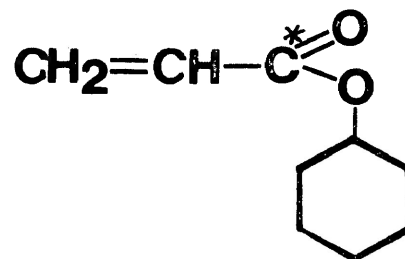
9. beta-Naphthyl butyrate



10. beta-Naphthyl benzoate



11. Cyclohexyl acrylate



12. Cyclohexyl cinnamate

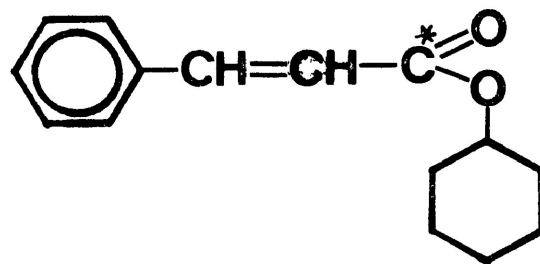


FIGURE VII.1(b)

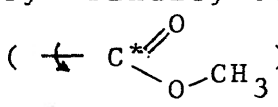
VII.3 DISCUSSION

The Eyring analysis results for the different aromatic and related esters are given in Table VII.1. It can be seen that methyl benzoate and ethyl benzoate showed absorptions in almost the same temperature range (160 - 210 K) in a polystyrene matrix and in polyphenyl ether. In polystyrene matrices both the molecules gave similar values of ΔH_E , ΔS_E and ΔG_E and τ values at 200 and 300 K. Table VII.1 shows that in polyphenyl ether both the molecules exhibited another high temperature process and yielded values of $\Delta H_E = 234.0$ and 257 kJ mol^{-1} , $\Delta S_E = 720$ and $810 \text{ J K}^{-1} \text{ mol}^{-1}$ for methyl- and ethyl benzoate, respectively. The parameters for this high energy process were evaluated by linear regression of the equation (II.22). A co-operative motion of the whole molecule together with the segments of polymer chain may be the cause of this high energy process in methyl- and ethyl benzoates. The measured glass transition temperature, T_g , of the two samples 246 and 241 K, respectively, are also consistent with this hypothesis.

Table VII.1 shows that the values of ΔH_E and

other relaxation parameters for methyl benzoate are almost identical in a polystyrene matrix and polyphenyl ether, while the corresponding values of ethyl benzoate differs in the two media for the low temperature absorption process. The ΔH_E -values for methyl benzoate are 31 and 31.4 ± 3.1 kJ mol⁻¹, and that of ethyl benzoate are 33 and 26.8 ± 2.1 kJ mol⁻¹ in a polystyrene matrix and polyphenyl ether, respectively. The results in a polystyrene matrix were obtained by an earlier worker (11) in this laboratory. It appears that there would be two possible sources of dielectric absorption in these aromatic esters, one being intramolecular and the other molecular relaxation. Khwaja (11) calculated μ_{\parallel} (the component of the substituent ester group dipole moment along the long axis of the molecule) and μ_{\perp} (the component of the dipole moment perpendicular to this axis, responsible for group relaxation) and found values of 0.65 D and 1.71 D, respectively, for methyl benzoate. This calculation produced a molecular weighting factor, $C_1 = 0.13$ and a group weighting factor $C_2 = 0.87$, which suggested that there may be a little contribution from molecular relaxation. Moreover, the plot of $\log T\tau$ versus $1/T$ (Figure VII.6)

for methyl benzoate in polyphenyl ether indicated the presence of two absorption processes and yielded an overall enthalpy of activation, $\Delta H_E = 31.4 \pm 3.1 \text{ kJ mol}^{-1}$. When the two portions of this plot were analyzed separately, the values of 22 and 33 kJ mol^{-1} were obtained for the enthalpies of activation. This suggests that the observed process is largely influenced by two overlapping processes, but no such separation was found from the plots of $\log T\tau$ versus $1/T$ for methyl benzoate in a polystyrene matrix and for ethyl benzoate in the two media.

The ΔH_E value of 22 kJ mol^{-1} obtained for the lower temperature portion of the plot (Figure VII.2) may be compared with the value of 22.2 kJ mol^{-1} obtained by Grindley et al (9) for rotation about the $C_{Ar}-C^*$ () bond. On the other hand, α,α,α -trichlorotoluene, an approximately similar sized rigid molecule, gave ΔH_E value of 20 kJ mol^{-1} in a polystyrene matrix (12). Thus, these results and the small magnitude of the weight factor for the molecular process ($C_1 = 0.13$) seem to indicate that either the molecular process is too weak to be detected or it overlaps with ester group relaxation about $C_{Ar}-C^*$ bond.

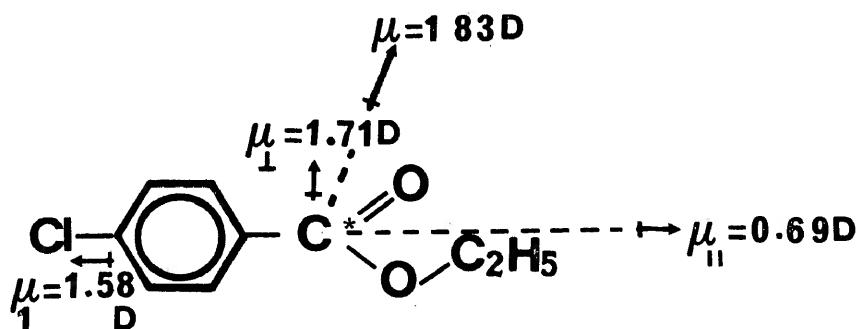
For methyl benzoate in a polystyrene matrix and for ethyl benzoate in both the media it may so happen that the molecular absorption occurred within a temperature region similar to that of the group process and with a similar energy, so that both the molecular and group processes overlapped. But again the small magnitude of the weight factor $C_1 = 0.13$ seem to indicate that predominantly group relaxation contributes to the dielectric absorption of methyl- and ethyl benzoates. The group relaxation may be owing to the intramolecular motion either about the $C_{Ar}-C^*$ or C^*-O bond or both.

Ethyl-p-chlorobenzoate exhibited only one family of absorption curves in a polystyrene matrix and in polyphenyl ether in the same temperature region (153 - 211 K) yielding almost identical values, within the limits of experimental error, of ΔH_E and other parameters (Table VII.1). The ΔH_E value of 24 and 25.2 kJ mol^{-1} for ethyl-p-chlorobenzoate in a polystyrene matrix and in polyphenyl ether, respectively, when compared to the value of $\Delta H_E = 42 \text{ kJ mol}^{-1}$ obtained for a slightly smaller-sized rigid molecule (i.e. p-iodotoluene (11)) in a polystyrene matrix suggest that the

intramolecular relaxation is responsible for the observed process in the former molecule. Moreover, the enthalpies of activation for ethyl-p-chlorobenzoate in the two media are lower than that obtained for methyl- and ethyl benzoates, which are quite reasonable for an intramolecular motion. As it is to be expected that the para-substituent chlorine atom, which is known as an electron-withdrawing substituent, would lower the electron density between the bond connecting the aromatic benzene ring and the ester group ($C_{Ar}-C^*$). This would in turn lower the enthalpy of activation for ester group relaxation owing to the decreased double bond character. This observation is supported by the results of Miller et al (13), who suggested that para-substituent can influence the barrier height only through electronic interactions.

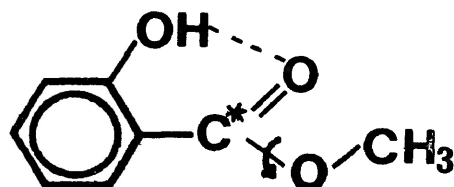
The molecular relaxation process for ethyl-p-chlorobenzoate was not detected. Dipole moment calculation by Khwaja (11) gave values of $\mu_{||}$ (the component of the substituent ester group dipole moment along the long axis of the molecule) = 0.69 D, μ_{\perp} (the component of the dipole moment perpendicular to this axis, responsible

for group relaxation) = 1.71 D, and μ_2 ($= \mu_1 - \mu_{II}$) = 0.89 D. This calculation also produced a molecular



weighting factor, $C_1 = 0.22$, and a group weighting factor, $C_2 = 0.78$, which suggested that there may be a little contribution from molecular relaxation.

Methyl salicylate may be considered an interesting molecule for this work, where owing to strong intramolecular hydrogen bonding the ester group rotation about the $C_{Ar}-C^*$ bond is ruled out, and consequently the methoxy group relaxation about the C^*-O bond becomes the only feasible intramolecular motion.



Methyl salicylate

This molecule was studied in polyphenyl ether and in pure compressed solid (14). Table VII.1 shows that the values of ΔH_E and ΔS_E are 20.7 ± 3.5 and 24.2 ± 4.1 kJ mol^{-1} , and -49.8 and $-17.1 \text{ J K}^{-1} \text{ mol}^{-1}$ in compressed solid and polyphenyl ether, respectively. In pure compressed solid the molecular process is unlikely and only the intramolecular relaxation could be expected to occur. In addition, o-nitrophenol (20), a rigid molecule of slightly smaller size, yielded values of $\Delta H_E = 12.2$ kJ mol^{-1} , $\Delta S_E = -37.3 \text{ J K}^{-1} \text{ mol}^{-1}$, $\Delta G_E(200 \text{ K}) = 19.7$ kJ mol^{-1} , and $\tau_{200 \text{ K}} = 3 \times 10^{-8} \text{ s}$ in a polystyrene matrix.

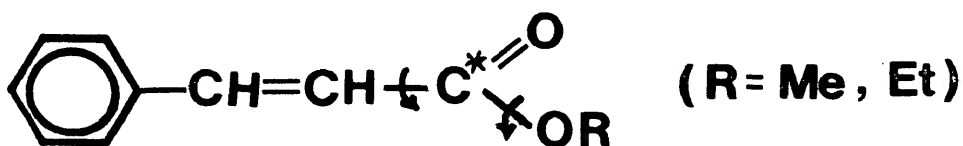
Therefore, the observed process for methyl salicylate in polyphenyl ether and in pure compressed solid may be most likely attributed to methoxy group

rotation about the C*—O bond. The value of $\Delta H_E = 24.4 \text{ kJ mol}^{-1}$ obtained for methoxy group rotation in methyl chloroformate in polyphenyl ether (Chapter VI) is consistent with that of methyl salicylate ($\Delta H_E = 24.2 \text{ kJ mol}^{-1}$) in the same medium.

Methyl cinnamate (a molecule where the ester group is not directly attached to the benzene ring) exhibited two distinctly separate regions of dielectric absorption in a polystyrene matrix, while only one absorption process was observed in o-terphenyl and in polyphenyl ether. An earlier worker (11) also observed two absorption processes for ethyl cinnamate in a polystyrene matrix, the results are presented in Table VII.1 for comparison.

The low temperature dielectric absorption in methyl- and ethyl cinnamate in a polystyrene matrix yielded ΔH_E and ΔS_E values of 25.2 ± 1.7 and 30 kJ mol^{-1} ; and -7 and $22 \text{ J K}^{-1} \text{ mol}^{-1}$, respectively. However, it is to be noted that the plot of $\log T\tau$ versus $1/T$ for methyl cinnamate in a polystyrene matrix (Figure VII.7) show a divergence in the plot, which might be described by

two straight lines of limiting slopes to account for an overlapped absorption due to two intramolecular motions. When the two portions of this plot were analyzed separately they yielded ΔH_E values of ~ 16 and $\sim 36 \text{ kJ mol}^{-1}$, respectively. The Eyring plots of methyl cinnamate in o-terphenyl and polyphenyl ether, and also that of ethyl cinnamate in polystyrene matrices showed no such separation, but yielded similar values of ΔH_E ($\Delta H_E = 29.3 \pm 1.4$, 29.0 ± 1.4 , and 30 kJ mol^{-1} , respectively), which are much too small to be ascribed to molecular relaxation and must be attributed to intramolecular relaxation. Therefore, we can suggest that the low temperature dielectric absorption of methyl- and ethyl cinnamate contains contribution from the intramolecular motions around C-C* and C*-O bonds.



The high temperature absorption process (258 - 288 K) of methyl cinnamate in a polystyrene matrix yielded $\Delta H_E = 80.3 \pm 11 \text{ kJ mol}^{-1}$ and $\Delta S_E = 116.6 \pm 29 \text{ J K}^{-1} \text{ mol}^{-1}$ (Table VII.1). The observed entropy of activation for methyl cinnamate, $\Delta S_E = 116 \text{ J K}^{-1} \text{ mol}^{-1}$, agrees well within the limits of experimental error with that of $\Delta S_{E(\text{calculated})} = 106 \text{ J K}^{-1} \text{ mol}^{-1}$ obtained from the relation: $\Delta S_E (\text{J K}^{-1} \text{ mol}^{-1}) = -70 + 2.2 \Delta H_E$ (kJ mol^{-1}) (cf: Chapter IV) corresponding to a molecular relaxation process. Moreover, the extrapolation of the observed dipole moment at 300 K for the low temperature process gives $\mu_{\perp} = 1.06 \text{ D}$, whereas for the high temperature process the extrapolated value of observed dipole moment at 300 K is $\mu_{\parallel} = 1.48 \text{ D}$. Thus, the resultant dipole moment $\sqrt{(1.06)^2 + (1.48)^2} = 1.82 \text{ D}$, which is in good agreement with the literature value of $\sim 1.95 \text{ D}$ (15) for a benzene solution at 288 K. Khwaja (11) obtained almost similar values of temperature range (286 - 311), ΔH_E and other parameters (Table VII.1) for the molecular process of ethyl cinnamate in a polystyrene matrix. Thus, all these results suggest that the high temperature process observed for methyl cinnamate in a polystyrene matrix may be attributed to the motion of the whole molecule. This high energy

process was not observed in o-terphenyl and in polyphenyl ether, the reason is most likely this process would occur above the T_g and be obscured by the cooperative process.

Dimethyl-2,6-naphthalene dicarboxylate also showed two regions of dielectric absorptions. The low temperature process with $\Delta H_E = 35 \text{ kJ mol}^{-1}$ and $\Delta S_E = 36 \text{ J K}^{-1} \text{ mol}^{-1}$, was studied by Khwaja (11) of this laboratory. He interpreted this low temperature process for dimethyl-2,6-naphthalene dicarboxylate is due to the ester group relaxation.

Figure VII.5 shows the plot of ϵ'' (loss factor) versus $\log f$ while the plot of $\log T\tau$ versus $1/T$ are shown in Figure VII.8 for the high temperature process of dimethyl-2,6-naphthalene dicarboxylate in a polystyrene matrix. This process yielded $\Delta H_E = 90.1 \pm 2.9 \text{ kJ mol}^{-1}$, $\Delta S_E = 148.3 \pm 9.8 \text{ J K}^{-1} \text{ mol}^{-1}$, $\Delta G_E(200 \text{ K}) = 52.4 \text{ kJ mol}^{-1}$, and $\tau_{200 \text{ K}} = 1.1 \times 10^{-7} \text{ s}$, which are almost similar to the corresponding values obtained for molecular relaxation process in methyl- and ethyl cinnamates. The experimental entropy of activation, $\Delta S_E = 148.3 \text{ J K}^{-1} \text{ mol}^{-1}$

also agrees well with $\Delta S_E(\text{calculated}) = -128 \text{ J K}^{-1} \text{ mol}^{-1}$ calculated from the relation (cf: Chapter IV) for a molecular relaxation process. Also the measured glass transition temperature, $T_g = 340 \text{ K}$, of the sample rules out the possibility of a cooperative motion and thus, the observed high temperature (226 - 268 K) dielectric absorption of dimethyl-2,6-naphthalene dicarboxylate may be ascribed to a molecular relaxation process.

Table VII.1 shows that α -naphthyl acetate in a polystyrene matrix exhibited two dielectric absorption regions. The low temperature (81 - 128 K) process yielded $\Delta H_E = 3.8 \pm 0.3 \text{ kJ mol}^{-1}$, $\Delta S_E = -123.2 \text{ J K}^{-1} \text{ mol}^{-1}$, $\Delta G_E(100 \text{ K}) = 16.1 \text{ kJ mol}^{-1}$, and $\tau_{100 \text{ K}} = 1.2 \times 10^{-4} \text{ s}$. Such low values of ΔH_E and $\Delta G_E(100 \text{ K})$ with a large negative entropy of activation obtained for this molecule immediately suggests an intramolecular process. There may be two intramolecular relaxation processes in this molecule, one being the rotation about the C*-O bond and the other around the O-C_{Ar} bond. But the value of 3.8 kJ mol^{-1} for the enthalpy of activation seems to be significantly low for the rotation about

the C*-O bond, which has partial double bond character. On the other hand, these low values of ΔH_E , ΔG_E , and ΔS_E for this molecule are comparable to the corresponding values for methoxy group rotation about the O-C_{Ar} bond in an aromatic system such as 2,6-dimethoxy naphthalene, in a polystyrene matrix (16). Therefore, the observed low temperature dielectric absorption of α -naphthyl acetate may be attributed to the intramolecular motion about the O-C_{Ar} bond.

The high temperature (179 - 222 K) process for α -naphthyl acetate gave the values of $\Delta H_E = 43.3 \pm 2.1 \text{ kJ mol}^{-1}$, $\Delta S_E = 41.3 \pm 10.4 \text{ J K}^{-1} \text{ mol}^{-1}$, $\Delta G_{E(200 \text{ K})} = 35.3 \text{ kJ mol}^{-1}$, and $\tau_{200 \text{ K}} = 3.9 \times 10^{-4} \text{ s}$. β -Naphthyl acetate in the same polystyrene matrix only showed the high temperature process (207 - 242 K) and yielded values of $\Delta H_E = 60.2 \pm 6.7 \text{ kJ mol}^{-1}$, $\Delta S_E = 65.1 \pm 28.0 \text{ J K}^{-1} \text{ mol}^{-1}$, $\Delta G_{E(200 \text{ K})} = 56.5 \text{ kJ mol}^{-1}$, and $\tau_{200 \text{ K}} = 1.3 \times 10^{-2} \text{ s}$. These parameters for the higher temperature process of β -naphthyl acetate are comparable to the corresponding values ($\Delta H_E = 52.4 \pm 5.3 \text{ kJ mol}^{-1}$, $\Delta S_E = 38 \pm 21 \text{ J K}^{-1} \text{ mol}^{-1}$, $\Delta G_{E(200 \text{ K})} = 45 \text{ kJ mol}^{-1}$ and

$\tau_{200\text{ K}} = 1 \times 10^{-1}$ s) for 2-iodonaphthalene (17), a slightly smaller-sized rigid molecule, in a polystyrene matrix.

In 2-iodonaphthalene the process is only that of molecular relaxation. Earlier investigation (17) also indicates that the barrier for the molecular relaxation of a α -naphthyl derivative is usually lower than that of the corresponding β -naphthyl one, which is in good agreement with the ΔH_E values of 43.3 and 60.2 kJ mol⁻¹ obtained for α - and β -naphthyl acetates, respectively. The possibility of a cooperative motion of the molecules with the polymer segments was also ruled out by measuring the glass transition temperature, T_g , of the samples of α - and β -naphthyl acetates in the polystyrene matrix; the measured T_g were 345 and 351 K, respectively.

All these results suggest that the molecular relaxation is responsible for the higher temperature dielectric absorption in α - and β -naphthyl acetate in a polystyrene matrix.

Table VII.1 shows that β -naphthyl butyrate gave two absorption processes in a polystyrene matrix.

The values of $\Delta H_E = 10.8 \pm 0.8 \text{ kJ mol}^{-1}$, $\Delta S_E = -45 \pm 8.8 \text{ J K}^{-1} \text{ mol}^{-1}$, $\Delta G_{E(100 \text{ K})} = 15.3 \text{ kJ mol}^{-1}$, and $\tau_{100 \text{ K}} = 4.8 \times 10^{-5} \text{ s}$, obtained for the low temperature (79-113 K) process of β -naphthyl butyrate may be owing to the intramolecular motion about the $\text{O}-\text{C}_{\text{Ar}}$ bond as in the case of α -naphthyl acetate and 2,6-dimethoxy naphthalene (16). The high temperature (275-311 K) process for β -naphthyl butyrate yielded $\Delta H_E = 57.5 \pm 3.7 \text{ kJ mol}^{-1}$, $\Delta S_E = 72.5 \pm 9.7 \text{ J K}^{-1} \text{ mol}^{-1}$, $\Delta G_{E(200 \text{ K})} = 54.9 \text{ kJ mol}^{-1}$, $\tau_{200 \text{ K}} = 5.4 \times 10^1 \text{ s}$ and $T_g = 349 \text{ K}$. These results for β -naphthyl butyrate would seem reasonable on comparison with the corresponding results for molecular relaxation of α - and β -naphthyl acetate in the same medium.

β -Naphthyl benzoate in a polystyrene matrix gave only one absorption process in the temperature range 157-195 K and yielded values of $\Delta H_E = 33.7 \pm 2.5 \text{ kJ mol}^{-1}$, $\Delta G_{E(200 \text{ K})} = 30.1 \text{ kJ mol}^{-1}$, $\Delta S_E = 17.9 \pm 12.9 \text{ J K}^{-1} \text{ mol}^{-1}$, and $\tau_{200 \text{ K}} = 1.7 \times 10^{-5} \text{ s}$ (Table VII.1). Compared to the above results for the molecular relaxation of α - and β -naphthyl acetates as well as β -naphthyl butyrate in the same medium, it is apparent that the observed process in β -naphthyl benzoate is more likely an intramolecular relaxation process. But ΔH_E value of 33.7 kJ mol^{-1}

seems to be significantly higher for the rotation about the $O-C_{Ar}$ bond, as is observed in α -naphthyl acetate and β -naphthyl butyrate at liquid nitrogen temperatures. On the other hand, the temperature range, and the other relaxation parameters for β -naphthyl benzoate are almost identical (Table VII.1) with the corresponding values obtained for the intramolecular motion in ethyl cinnamate and dimethyl-2,6-naphthalene dicarboxylate. Therefore, a similar conclusion (the probability of both the ester group rotation and the rotation about the C^*-O bond) can be made for the dielectric absorption of β -naphthyl benzoate in a polystyrene matrix.

In order to investigate further the behaviour of ester group relaxation, cyclohexyl acrylate and cyclohexyl cinnamate were studied in a polystyrene matrix. The plot of loss factor (ϵ'') versus $T(K)$ at 1 kHz (Figure VII.5) indicates that cyclohexyl acrylate exhibited two distinct absorption processes. Also good straight line plots of $\log T\tau$ versus $1/T$ (Figures VII.11 and VII-12) yielded values of $\Delta H_E = 21.2 \pm 0.7$ and $46.9 \pm 1.4 \text{ kJ mol}^{-1}$, and $\Delta S_E = 5.3 \pm 4.9$ and $22.7 \pm 5.4 \text{ J K}^{-1} \text{ mol}^{-1}$ for the low temperature (118-155 K) and high temperature (227-290 K) absorption processes,

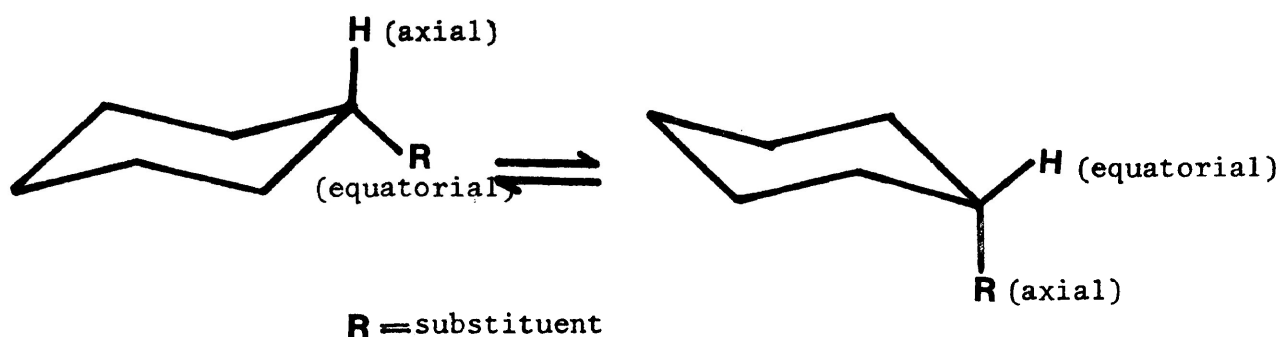
respectively.

For the low energy ($\Delta H_E = 21.2 \pm 0.7$ kJ mol⁻¹) process there may be two relaxation candidates for this molecule, one being the molecular relaxation and the other ester group rotation. The values of $\Delta H_E = 20.1$ kJ mol⁻¹ and $\Delta S_E = -1$ J K⁻¹ mol⁻¹ obtained for the ester group relaxation (rotation about C-C* or C*-O bond/or both) in methyl acrylate (Chapter VI) seem to be in good agreement with the corresponding values obtained for cyclohexyl acrylate. On the other hand, cyclohexyl acrylate and cyclohexyl iodide (12) (a slightly smaller-sized rigid molecule) yielded comparable values of $\Delta H_E = 21.2 \pm 0.7$ and 22 kJ mol⁻¹, $\Delta S_E = 5.3 \pm 4.9$ and 19 J K⁻¹ mol⁻¹, $\Delta G_{E(200\text{ K})} = 20.1$ and 17.9 kJ mol⁻¹, and $\tau_{200\text{ K}} = 4.4 \times 10^{-8}$ and 1.2×10^{-8} s, respectively. In addition, cyclohexyl iodide absorbed in almost the same temperature range, i.e. 115-145 K (12). Thus, both molecular and ester group relaxation processes are equally probable for the low temperature relaxation process of cyclohexyl acrylate in a polystyrene matrix.

The higher temperature absorption of cyclohexyl acrylate (227-290 K) is clearly due to the intra-

molecular chair-chair conversion for which the results are in good agreement with those observed by Davies and Swain (18) for cyclohexyl chloride and cyclohexyl bromide with ΔH_E values of 42 and 43 kJ mol^{-1} , respectively. Similar values of enthalpies of activation, 48 and 50 kJ mol^{-1} , for cyclohexyl iodide and cyclohexyl methyl ketone, respectively, observed by Mazid (12) are also consistent with this hypothesis.

The ring inversion of the cyclohexyl derivatives can be represented by the following diagram showing the two low energy chair conformations in equilibrium which, of course, involve a number of possible intermediates (12).



Cyclohexyl cinnamate in a polystyrene matrix also exhibited two absorption processes, one in the temperature range 172-218 K and the other in 235-255 K. The values of $\Delta H_E = 33.6 \pm 2.6 \text{ kJ mol}^{-1}$, $\Delta S_E = 8.5 \pm 12.2 \text{ J K}^{-1} \text{ mol}^{-1}$, $\Delta G_E(200 \text{ K}) = 31.9 \text{ kJ mol}^{-1}$, $\tau_{200 \text{ K}} = 5.0 \times 10^{-5} \text{ s}$, for the low temperature process of cyclohexyl cinnamate would seem reasonable for ester group relaxation on comparison with the corresponding values for the low temperature process of ethyl cinnamate in the same polystyrene matrix. Similarly, the high temperature absorption process (235-255 K) for cyclohexyl cinnamate with values of $\Delta H_E = 107.1 \text{ kJ mol}^{-1}$ and $\Delta S_E = 180 \text{ J K}^{-1} \text{ mol}^{-1}$, may be attributed to the molecular relaxation process. Moreover, the calculated value of entropy of activation $\Delta S_{E(\text{calculated})} = 165 \text{ J K}^{-1} \text{ mol}^{-1}$ obtained from the relation (cf. Chapter IV), agrees well within the limits of experimental accuracy with the observed value of $180 \text{ J K}^{-1} \text{ mol}^{-1}$.

The intramolecular ring inversion process for this molecule was not detected or alternatively the process has overlapped with the observed molecular process. The reason may be the result of increase in the energy barrier to intramolecular ring inversion for this molecule due to larger size of the substituent. There is evidence (19)

from n.m.r. studies that the substituent effects upon the energy barriers to ring inversion depend directly on the effective size of the substituents. The observed values of enthalpies of activation, 42, 43, 48, 46.9, and 50 kJ mol⁻¹ for cyclohexyl chloride (18), cyclohexyl bromide (18), cyclohexyl iodide (12), cyclohexyl acrylate, and cyclohexyl methyl ketone (12), respectively, also support the substituent effects upon intramolecular ring inversion.

REFERENCES

1. C.P. Smyth, "Dielectric Behaviour and Structure", McGraw-Hill, New York, (1955)319.
2. B. Krishna, and R.K. Upadhyay, J. Chem. Soc., A, (1970)3144.
3. E.N. Guryanova and N.I. Grishko, Zh. Strukt. Khim., 40(1963)368. (J. Struct. Chem. USSR, 5(1964)339).
4. R.J.W. Le Fèvre and A. Sundaram, J. Chem. Soc., (1962)3904.
5. A.G. Pinkus and Ellen Y. Lin, J. Mol. Struct., 24(1975)9.
6. A. Hasan, A. Das, and A. Ghatak, Indian J. Phys., 45(1971) 443.
7. A. Hasan, A. Das, and A. Ghatak, Indian J. Phys., (1973).
8. A. Hasan, A. Das, and A. Ghatak, Indian J. Phys., 47(1973)701.
9. T. Bruce Grindley, Allan R. Katritzky, and Ronald D. Topsom, J. Chem. Soc., Perkin II, (1974)289.
10. B. Krishna, B. Prakash and S.V. Mahadane, J. Phys. Chem., 73(1969)3697.
11. H.A. Khwaja, M.Sc. Thesis, Lakehead University, Thunder Bay, Ontario, Canada, (1977).
12. M.A. Mazid, M.Sc. Thesis, Lakehead University, Thunder Bay, Ontario, Canada, (1977).
13. F.A. Miller, W.G. Fately and R.E. Wtikowski, Spectrochim Acta, 23A(1967)891.

14. M.A. Enayetullah, personal communication, this laboratory.
15. A.L. McLellan, "Tables of Experimental Dipole Moments"; Vol. 2, Rahara Enterprises, Calif., U.S.A., (1974).
16. M.A. Mazid, J.P. Shukla, and S. Walker, Can. J. Chem., 56(1978)1800.
17. S.P. Tay, Ph.D. Thesis, University of Salford, Lancashire, U.K., (1977).
18. M. Davies and J. Swain, Trans. Faraday Soc., 67(1971)1637.
19. I.O. Sutherland, Ann. Rep. n.m.r. Spectroscopy, 4(1971)71.
20. S.P. Tay, J. Kraft and S. Walker, J. Phys. Chem., 80(1976)303.

TABLE VII.1: EYRING ANALYSIS RESULTS FOR A VARIETY OF AROMATIC AND RELATED ESTERS IN SOME ORGANIC GLASSES

MOLECULE	MEDIUM	ΔT (K)	Relaxation Time τ (s)				ΔG_E (kJ mol ⁻¹)			ΔH_E kJ mol ⁻¹	ΔS_E J K ⁻¹ mol ⁻¹
			100 K	200 K	300 K	100 K	200 K	300 K			
Methyl benzoate	Polystyrene matrix	165-205 ^(a)	3.3x10 ⁻⁶	3.3x10 ⁻⁶	4.4x10 ⁻⁹	27	25	31	18		
			172-211	3.5x10 ⁻⁵	4.3x10 ⁻⁸	31.2	31.2	31.4 ±3.1	1.1 ±13.3		
Ethyl benzoate	Polystyrene matrix	171-203 ^(a)	3.8x10 ⁻³	3.6x10 ⁻⁶	3.4x10 ⁻⁹	27	25	33	26		
			255-273	3.6x10 ⁻³	3.4x10 ⁻⁸	73.2	26.9	~234.0	~720		
Ethyl-p-chloro-benzoate	Polystyrene matrix	163-204	3.1x10 ⁻³	3.1x10 ⁻³	3.4x10 ⁻⁸	29.3	30.6	26.8 ±2.1	-12.8 ±10.6		
			259-271	3.6x10 ⁻³	4.2x10 ⁻⁶	99.7	11.2	~257.0	~810		
Methyl salicylate	Compressed solid	170-205 ^(b)	1.7x10 ⁻⁵	2.5x10 ⁻⁵	2.6x10 ⁻⁷	28	29	24	-17		
			216-236	1.7x10 ⁻⁵	2.6x10 ⁻⁵	30.1	32.5	25.2 ±1.7	-24.4 ±7.6		
Methyl cinnamate	Polystyrene matrix	140-191	2.6x10 ⁻³	2.3x10 ⁻⁶	9.8x10 ⁻⁹	30.7	35.7	20.7 ±3.5	-49.8 ±18.0		
			258-288	1.8x10 ⁻¹	9.9x10 ⁻¹	1.1x10 ⁻⁶	38.4	45.6	24.2 ±4.1	-17.1 ±11.6	
o-Terphenyl	Polystyrene matrix	162-208	2.3x10 ⁻⁶	9.3x10 ⁻⁶	1.7x10 ⁻⁸	26.7	27.5	25.2 ±1.7	-7 ±11		
			160-212	9.9x10 ⁻¹	1.1x10 ⁻⁵	2.1x10 ⁻⁸	55.9	39.3	80.3 ±11	116 ±29	
Polyphenyl ether	Polystyrene matrix	160-212	9.3x10 ⁻⁶	1.1x10 ⁻⁵	2.1x10 ⁻⁸	29.0	28.9	29.3 ±1.5	1.2 ±7.9		
			160-212	1.1x10 ⁻⁵	2.1x10 ⁻⁸	29.3	29.4	29.0 ±1.4	-1.5 ±7.8		

TABLE VII.1: continued...

MOLECULE	MEDIUM	ΔT (K)	Relaxation Time τ (s)				ΔG_E (kJ mol ⁻¹)	ΔH_E kJ mol ⁻¹	ΔS_E J K ⁻¹ mol ⁻¹
			100 K	200 K	300 K	300 K			
Ethyl cinnamate	Polystyrene matrix	159-188 286-311 (a)	1.5x10 ⁻⁶	2.3x10 ⁻⁹	26	24	30	22	
			5.1x10 ⁻³	3.9x10 ⁻⁵	63	48	91	143	
Dimethyl-2,6- naphthalene dicarboxylate	Polystyrene matrix	170-213 226-268 (a)	3.6x10 ⁻⁶	2.3x10 ⁻⁹	27	24	35	36	
			1.1x10 ⁻¹	1.1x10 ⁻⁷	52.4	33.6	90.1 ± 2.9	148.3 ± 9.8	
α -Naphthyl acetate	Polystyrene matrix	81-128 179-222	1.2x10 ⁻⁴	1.2x10 ⁻⁴	16.1	28.4	3.8 ± 0.3	-123.2 ± 2.3	
			3.9x10 ⁻⁴	4.2x10 ⁻⁸	35.3	31.1	43.3 ± 2.1	41.3 ± 10.4	
β -Naphthyl acetate	Polystyrene matrix	207-242	1.3x10 ⁻²	3.5x10 ⁻⁸	56.5	30.6	60.2 ± 6.7	65.1 ± 28.0	
β -Naphthyl butyrate	Polystyrene matrix	79-113 275-311	4.8x10 ⁻⁵	3.7x10 ⁻⁸	15.3	19.9	10.8 ± 0.8	-45.5 ± 8.8	
			5.4x10 ⁻¹	3.6x10 ⁻⁴	54.9	53.7	57.5 ± 3.7	72.5 ± 9.7	
β -Naphthyl benzoate	Polystyrene matrix	157-195	1.7x10 ⁻⁵	1.4x10 ⁻⁸	30.1	28.3	33.7 ± 2.5	17.9 ± 12.9	
Cyclohexyl acrylate	Polystyrene matrix	118-155 227-290	3.0x10 ⁻²	4.4x10 ⁻⁸	20.7	20.1	21.2 ± 0.7	5.3 ± 4.9	
				2.7x10 ⁻²	42.3	40.0	46.9 ± 1.4	22.7 ± 5.4	
Cyclohexyl cinnamate	Polystyrene matrix	172-218 235-255	5.9x10 ⁻⁴	5.0x10 ⁻⁵	32.7	31.9	33.6 ± 2.6	8.5 ± 13.3	
				5.3x10 ⁻³	56.8	48.5	107.1	~180.0	

NOTE: Data provided through the courtesy of H.A. Khwaja (a) (Ref. 11) and M.A. Enayetulillah (b) (Ref. 14) of this laboratory.

TABLE VII.2: Tabulated Summary of Fuoss-Kirkwood Analysis Parameters, ϵ_{∞} , and Effective Dipole Moments (μ) for a variety of Aromatic and Related Esters

T(K)	$10^6 \tau$ (s)	$\log f_{\max}$	β	$10^3 \epsilon''_{\max}$	ϵ_{∞}	μ (D)
<u>0.61 M Methyl benzoate in Polyphenyl Ether</u>						
<u>Low Temperature Process</u>						
171.6	768	2.32	0.20	8.24	2.95	0.68
177.9	405	2.59	0.19	8.62	2.95	0.72
185.2	210	2.88	0.18	9.14	2.95	0.78
191.8	95.4	3.22	0.18	9.66	2.95	0.82
197.4	50.2	3.50	0.17	10.07	2.94	0.87
204.4	21.9	3.86	0.17	10.61	2.94	0.91
211.2	10.3	4.20	0.18	10.72	2.95	0.90
<u>High Temperature Process</u>						
255.2	1049	2.18	0.56	506.69	3.27	3.44
259.3	464	2.53	0.46	596.69	3.26	4.09
263.6	65.3	3.39	0.54	589.36	3.33	3.78
266.9	20.4	3.89	0.67	580.73	3.53	3.97
273.5	7.61	4.32	0.66	577.55	3.61	4.12
<u>0.60 M Ethyl benzoate in Polyphenyl Ether</u>						
<u>Low Temperature Process</u>						
163.4	543	2.47	0.20	4.69	2.94	0.51
168.4	238	2.82	0.21	4.85	2.94	0.51
172.4	193	2.91	0.20	4.95	2.94	0.53
177.1	85.4	3.27	0.20	5.23	2.94	0.56
183.4	51.5	3.49	0.20	5.40	2.94	0.58
192.0	21.2	3.88	0.20	5.93	2.94	0.62
198.0	11.0	4.16	0.19	6.27	2.94	0.66
204.4	9.30	4.23	0.21	6.41	2.95	0.64

TABLE VII.2: continued...

T(K)	$10^6 \tau$ (s)	$\log f_{\max}$	β	$10^3 \epsilon''_{\max}$	ϵ_{∞}	μ (D)
<u>High Temperature Process</u>						
258.9	745	2.33	0.43	600.64	3.17	4.32
262.8	91.8	3.24	0.54	583.27	3.28	3.80
265.7	26.8	3.77	0.59	579.21	3.32	3.64
268.8	10.4	4.19	0.61	567.22	3.37	3.54
271.4	4.47	4.55	0.69	552.02	3.52	3.24
<u>0.49 M Ethyl-p-Chlorobenzoate in Polyphenyl Ether</u>						
163.5	584	2.44	0.27	1.65	2.92	0.29
172.1	244	2.81	0.23	1.71	2.93	0.33
178.2	115	3.14	0.22	1.74	2.93	0.34
184.8	60.3	3.42	0.27	1.88	2.93	0.33
192.5	35.7	3.65	0.24	2.02	2.93	0.45
197.2	25.2	3.80	0.24	2.10	2.93	0.37
204.4	10.5	4.18	0.25	2.25	2.93	0.39
211.3	6.85	4.37	0.24	2.32	2.94	0.41
<u>0.61 M Methyl salicylate in Polyphenyl Ether</u>						
216.8	745	2.33	0.25	10.24	2.98	0.77
223.8	540	2.47	0.24	11.39	2.98	0.83
230.2	338	2.67	0.22	12.44	2.98	0.91
236.0	235	2.83	0.20	13.58	2.95	1.02

TABLE VII.2: continued...

T(K)	$10^6 \tau$ (s)	$\log f_{\max}$	β	$10^3 \epsilon''_{\max}$	ϵ_{∞}	μ (D)
<u>0.60 M Methyl cinnamate in Polystyrene Matrix</u>						
<u>Low Temperature Process</u>						
140.8	1050	2.18	0.20	8.61	2.57	0.69
149.9	575	2.44	0.18	9.69	2.58	0.79
160.7	202	2.90	0.15	10.69	2.59	0.93
170.0	65.3	3.39	0.14	11.52	2.58	1.03
175.3	29.0	3.74	0.15	12.01	2.67	1.01
181.8	10.8	4.17	0.15	12.95	2.69	1.10
191.2	2.36	4.83	0.14	13.83	2.70	1.17
<u>High Temperature Process</u>						
257.8	539	2.47	0.15	11.70	2.66	1.22
265.7	112	3.15	0.12	11.95	2.63	1.41
268.5	74.4	3.33	0.15	12.20	2.67	1.26
273.1	24.6	3.81	0.11	12.21	2.62	1.50
288.6	5.47	4.46	0.16	13.49	2.68	1.34
<u>0.51 M Methyl cinnamate in o-Terphenyl</u>						
161.7	617	2.41	0.22	5.22	2.77	0.57
167.0	405	2.59	0.20	5.43	2.77	0.62
173.0	182	2.94	0.21	5.71	2.74	0.63
179.7	80.3	3.30	0.21	6.01	2.74	0.66
185.5	39.5	3.60	0.21	6.28	2.74	0.69
191.5	20.7	3.88	0.23	6.55	2.75	0.68
196.4	12.8	4.09	0.23	6.77	2.75	0.70
202.8	7.56	4.32	0.25	7.06	2.75	0.70
208.2	4.08	4.59	0.24	7.28	2.75	0.73

TABLE VII.2: continued...

T(K)	$10^6 \tau$ (s)	$\log f_{\max}$	β	$10^3 \epsilon''_{\max}$	ϵ_{∞}	μ (D)
<u>0.57 M Methyl cinnamate in Polyphenyl Ether</u>						
159.5	993	2.21	0.22	5.49	2.91	0.53
169.1	305	2.72	0.23	5.84	2.91	0.54
176.5	126	3.10	0.21	6.21	2.91	0.60
188.3	34.8	3.66	0.23	6.86	2.91	0.62
193.6	20.7	3.88	0.24	7.21	2.92	0.64
197.8	13.4	4.07	0.24	7.33	2.92	0.64
204.8	7.17	4.35	0.26	7.70	2.93	0.64
212.2	3.01	4.72	0.25	7.99	2.93	0.68

0.33 M Dimethyl-2, 6-naphthalene dicarboxylate in Polystyrene Matrix

225.9	18338	0.94	0.40	23.67	2.34	1.59
230.7	9052	1.25	0.33	24.51	2.34	1.63
235.6	2950	1.73	0.31	23.43	2.34	1.66
240.2	1094	2.16	0.29	22.05	2.34	1.68
246.9	323	2.69	0.28	20.47	2.33	1.68
251.7	117	3.13	0.29	19.16	2.34	1.61
255.9	58.9	3.43	0.31	18.37	2.34	1.54
260.2	33.1	3.68	0.34	17.73	2.34	1.46
264.9	15.9	4.00	0.34	16.41	2.34	1.44
268.4	9.55	4.22	0.34	15.21	2.34	1.37

0.48 M α -Naphthyl acetate in Polystyrene Matrix Low Temperature Process

81.2	413	2.59	0.14	1.25	2.30	0.28
88.0	267	2.78	0.15	1.36	2.31	0.30
98.5	197	2.91	0.13	1.52	2.31	0.36
111.2	71.9	3.34	0.11	1.66	2.31	0.43
118.5	49.6	3.51	0.09	1.75	2.31	0.50
127.2	35.7	3.65	0.10	1.86	2.32	0.51

TABLE VII.2: continued...

T(K)	$10^6 \tau$ (s)	$\log f_{\max}$	β	$10^3 \epsilon''_{\max}$	ϵ_{∞}	μ (D)
<u>High Temperature Process</u>						
179.0	10864	1.17	0.10	3.37	2.29	0.82
186.3	2798	1.76	0.12	3.50	2.30	0.78
191.7	1449	2.04	0.11	3.63	2.30	0.83
198.6	482	2.51	0.13	3.80	2.30	0.80
204.2	260	2.79	0.12	3.93	2.30	0.86
212.2	83.3	3.28	0.10	4.09	2.30	0.97
218.0	36.3	3.64	0.10	4.21	2.30	1.00
222.1	25.8	4.50	0.10	4.32	2.30	1.02

0.55 M β -Naphthyl acetate in Polystyrene Matrix

207.5	3700	1.63	0.09	3.22	2.40	0.82
216.2	864	2.27	0.08	3.36	2.39	0.91
224.7	174	2.96	0.09	3.50	2.40	0.90
230.1	60.4	3.42	0.10	3.60	2.40	0.87
232.6	54.4	3.47	0.12	3.70	2.40	0.81
237.5	35.3	3.65	0.13	3.77	2.40	0.80
241.6	23.4	3.83	0.12	3.79	2.40	0.84

0.38 M β -Naphthyl-n-butyrate in Polystyrene Matrix
Low Temperature Process

79.0	1892	1.93	0.17	3.14	2.54	0.43
84.2	783	2.31	0.17	3.29	2.55	0.45
86.2	430	2.57	0.18	3.37	2.54	0.45
93.1	116	3.10	0.18	3.59	2.55	0.48
98.2	49.5	3.50	0.20	3.72	2.54	0.48
102.4	26.4	3.68	0.22	3.88	2.56	0.48
106.1	25.5	3.80	0.23	3.91	2.55	0.47
113.1	12.6	4.20	0.27	3.90	2.55	0.48

TABLE VII.2: continued...

T(K)	$10^6 \tau$ (s)	$\log f_{\max}$	β	$10^3 \epsilon''_{\max}$	ϵ_{∞}	μ (D)
<u>High Temperature Process</u>						
275.3	2156	1.69	0.18	3.43	2.55	0.81
280.4	1941	1.91	0.15	3.46	2.54	0.89
286.2	1069	2.17	0.14	3.47	2.54	0.94
292.2	655	2.39	0.13	3.49	2.53	0.99
300.7	357	2.65	0.14	3.53	2.53	0.99
311.2	121	3.02	0.12	3.56	2.52	1.00
<u>0.34 M β-Naphthyl benzoate in Polystyrene Matrix</u>						
156.5	5746	1.44	0.12	3.62	2.46	0.83
165.8	1590	2.00	0.13	3.79	2.46	0.84
170.0	825	2.29	0.14	3.89	2.46	0.83
175.0	338	2.67	0.16	4.00	2.47	0.79
179.4	168	2.98	0.16	4.07	2.46	0.81
185.2	87.9	3.26	0.18	4.24	2.47	0.79
190.4	50.5	3.50	0.19	4.36	2.48	0.79
195.1	33.2	3.68	0.21	4.50	2.47	0.78
<u>0.59 M Cyclohexyl acrylate in Polystyrene Matrix</u>						
<u>Low Temperature Process</u>						
117.5	623	2.41	0.18	5.82	2.45	0.56
123.5	183	2.94	0.19	6.07	2.45	0.57
127.8	89.1	3.25	0.20	6.30	2.46	0.58
132.7	42.2	3.58	0.21	6.52	2.45	0.59
136.7	23.0	3.84	0.21	6.72	2.45	0.60
141.7	10.7	4.17	0.22	7.01	2.46	0.61
146.5	6.95	4.36	0.23	7.31	2.45	0.62
151.5	3.26	4.69	0.23	7.58	2.45	0.64
155.4	2.33	4.84	0.23	7.72	2.45	0.66

TABLE VII.2: continued...

T(K)	$10^6 \tau$ (s)	$\log f_{\max}$	β	$10^3 \epsilon''_{\max}$	ϵ_{∞}	μ (D)
<u>High Temperature Process</u>						
226.5	1024	2.19	0.31	9.90	2.52	0.77
231.4	529	2.48	0.34	9.53	2.52	0.73
237.6	241	2.82	0.40	9.44	2.52	0.68
243.3	138	3.06	0.40	9.35	2.51	0.68
248.3	89.1	3.25	0.40	9.12	2.51	0.68
252.5	59.0	3.43	0.42	9.06	2.51	0.67
260.0	32.4	3.69	0.44	8.76	2.51	0.67
266.8	16.8	3.98	0.41	8.54	2.50	0.68
274.9	8.87	4.25	0.39	8.27	2.50	0.69
282.8	5.37	4.47	0.44	7.86	2.50	0.66
289.5	3.27	4.69	0.42	7.42	2.50	0.65
<u>0.38 M Cyclohexyl cinnamate in Polystyrene Matrix</u>						
<u>Low Temperature Process</u>						
172.1	1113	2.06	0.18	4.32	2.52	0.72
176.1	953	2.22	0.17	4.70	2.52	0.78
184.0	375	2.63	0.16	4.82	2.52	0.83
192.0	123	3.11	0.17	4.92	2.51	0.84
199.4	40.4	3.59	0.14	5.12	2.51	0.95
205.8	27.7	3.76	0.14	5.41	2.50	0.98
211.4	20.5	3.99	0.16	5.74	2.50	1.01
217.6	9.95	4.20	0.15	6.09	2.50	1.06
<u>High Temperature Process</u>						
235.2	659	2.38	0.19	15.06	2.51	1.53
238.3	344	2.67	0.21	14.64	2.52	1.54
241.0	131	3.08	0.19	15.16	2.51	1.55
245.4	54.0	3.47	0.20	15.02	2.51	1.52
248.3	20.2	3.89	0.17	14.66	2.51	1.63
250.1	14.6	4.04	0.18	14.64	2.50	1.60
251.3	9.43	4.23	0.19	14.87	2.49	1.57
253.4	6.20	4.41	0.20	15.03	2.49	1.55
255.2	4.38	4.56	0.21	15.27	2.50	1.53

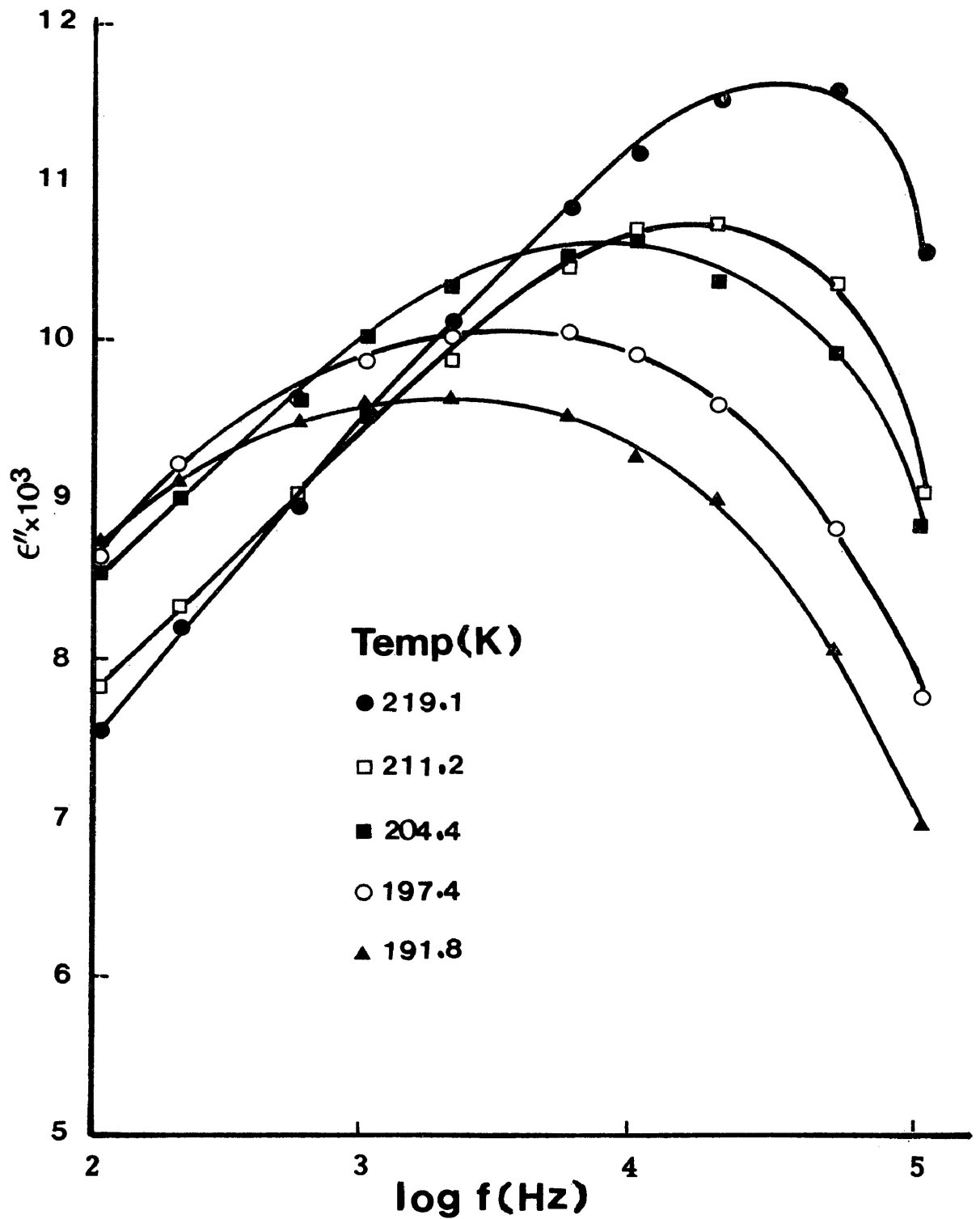


FIGURE VII.2

Plot of dielectric loss versus log frequency for methyl benzoate in polyphenyl ether

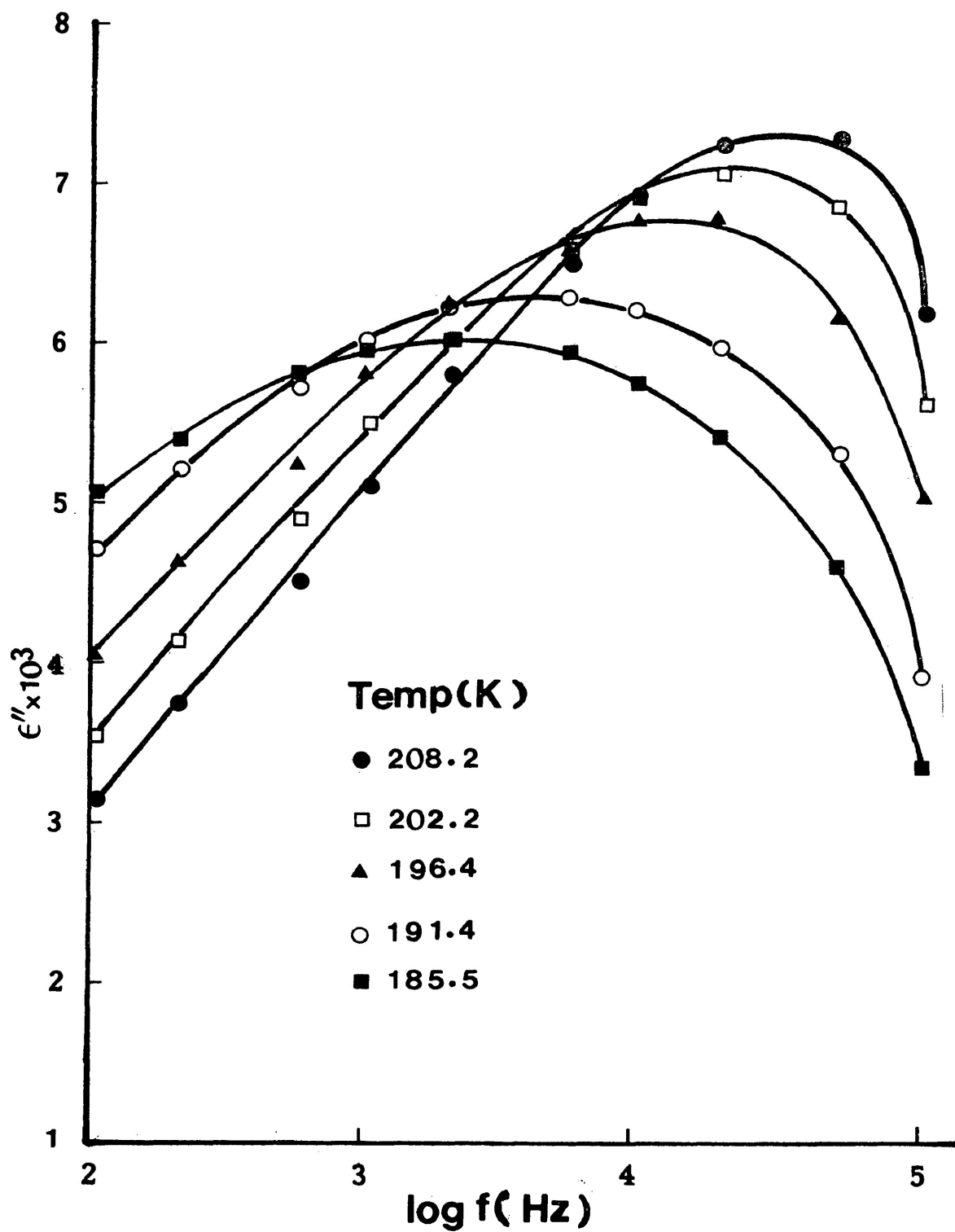


FIGURE VII.3

Plot of dielectric loss versus log frequency for methyl cinnamate in o-terphenyl

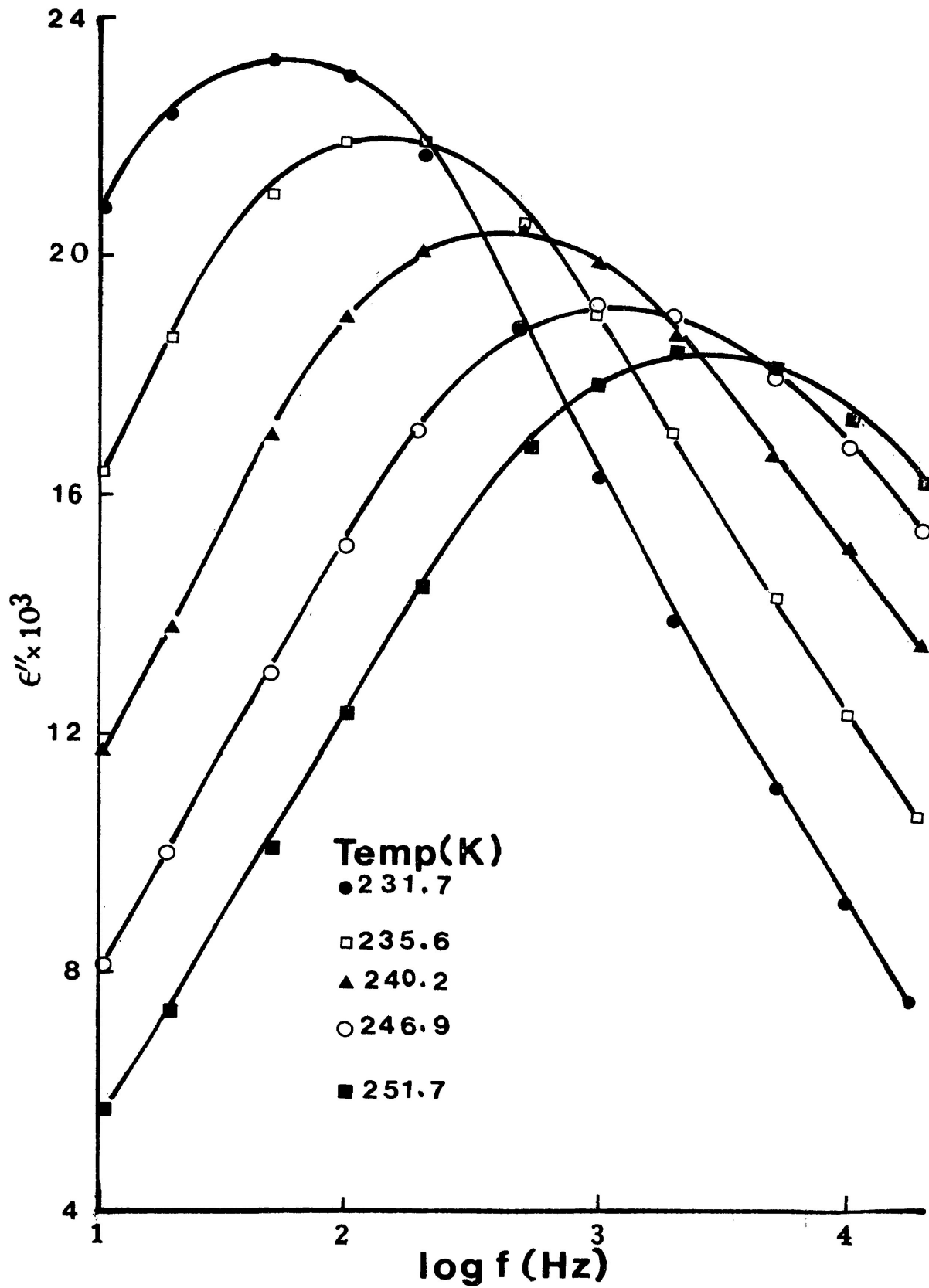


FIGURE VII.4

Plot of dielectric loss versus log frequency for dimethyl-2,6-naphthalene dicarboxylate in polystyrene matrices

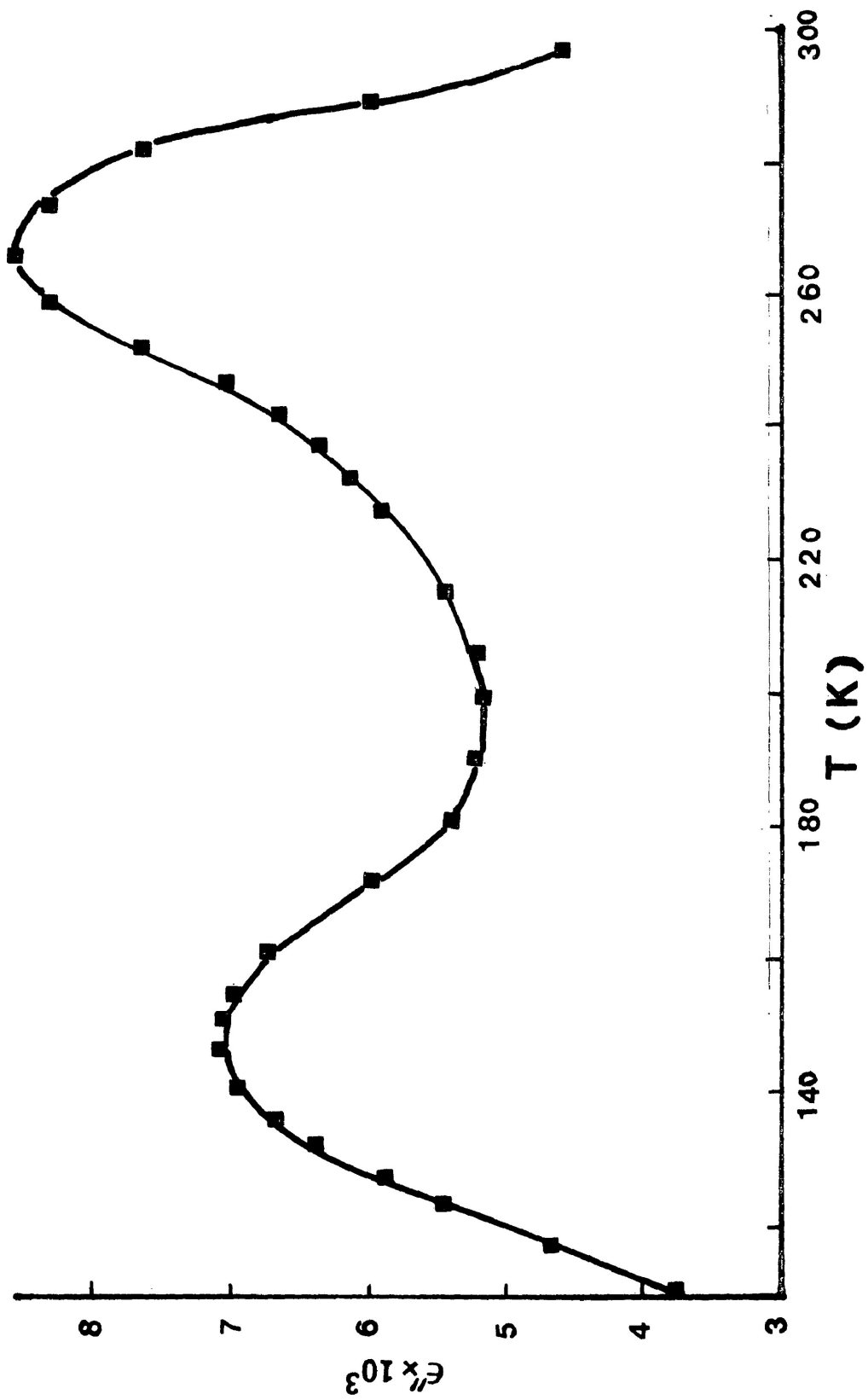


FIGURE VII.5 Plot of dielectric loss (at 10 kHz) versus temperature (K) for cyclohexyl acrylate in polystyrene matrices

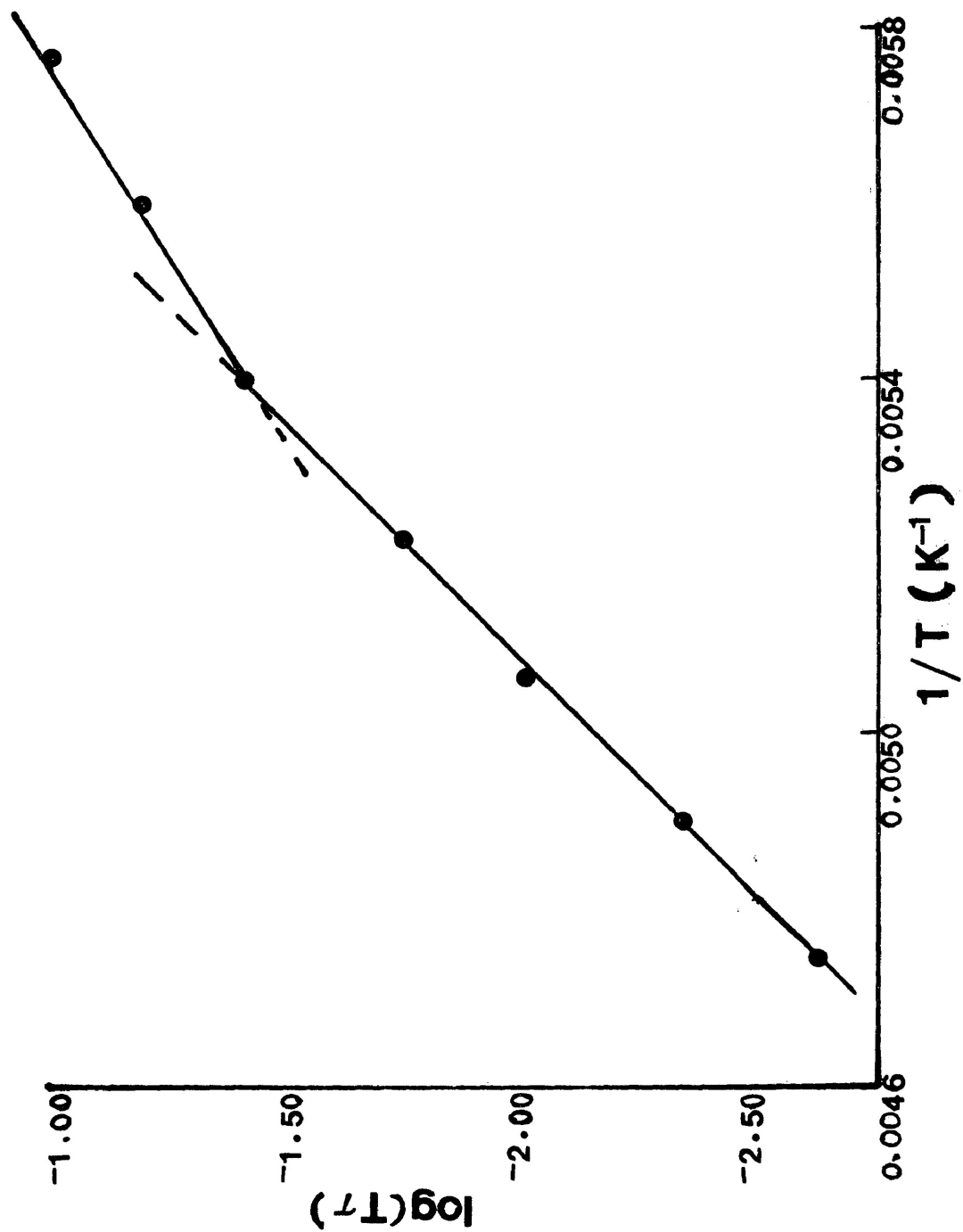


FIGURE VII.6 Plot of $\log(TT)$ versus $1/T \text{ (K}^{-1}\text{)}$ for methyl benzoate in polyphenyl ether

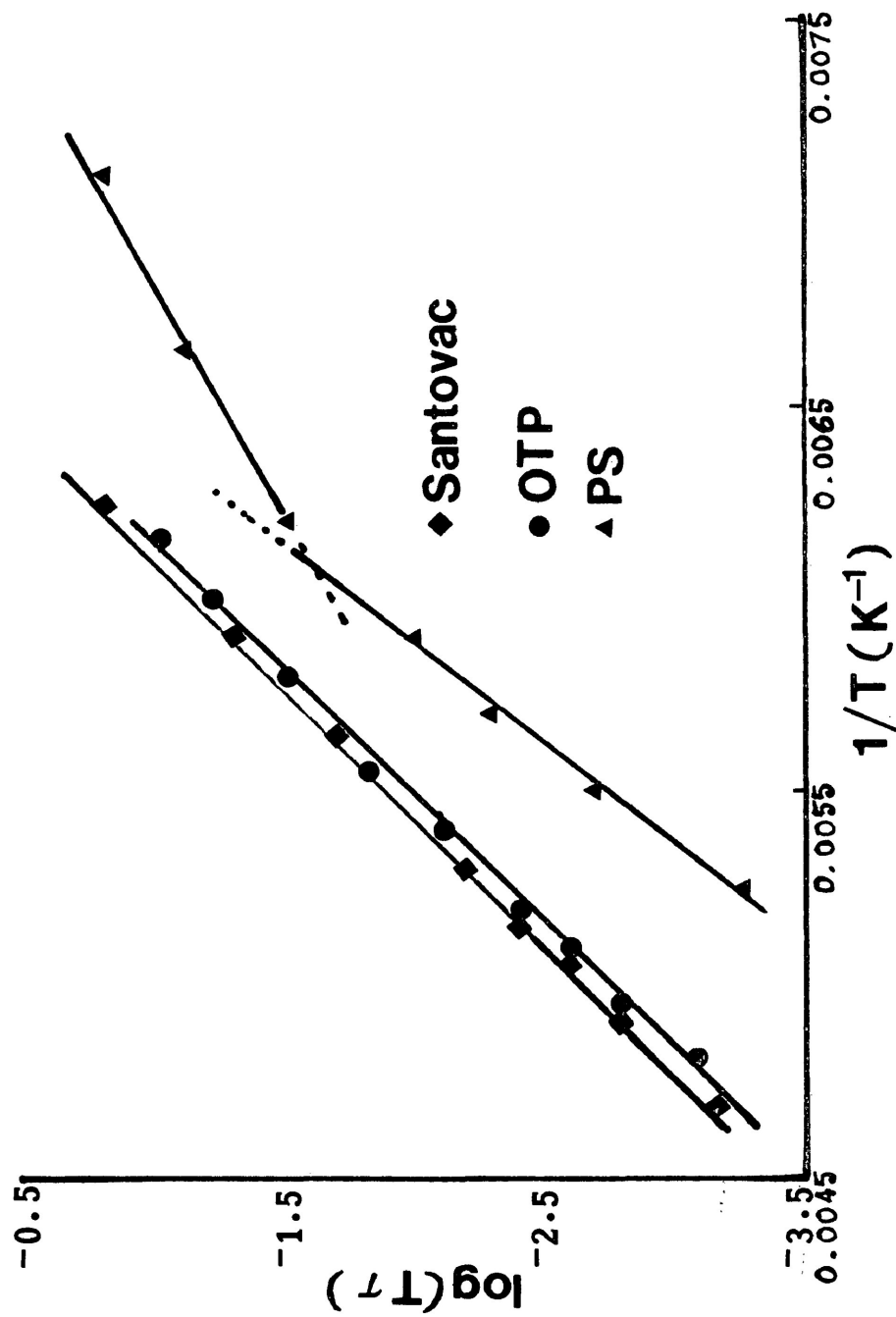


FIGURE VII.7 Plot of $\log(TT)$ versus $1/T$ (K^{-1}) for methyl cinnamate in
 ▲ polystyrene matrices (PS), ● o-terphenyl (OTP), and
 ■ polyphenyl ether (Santovac)

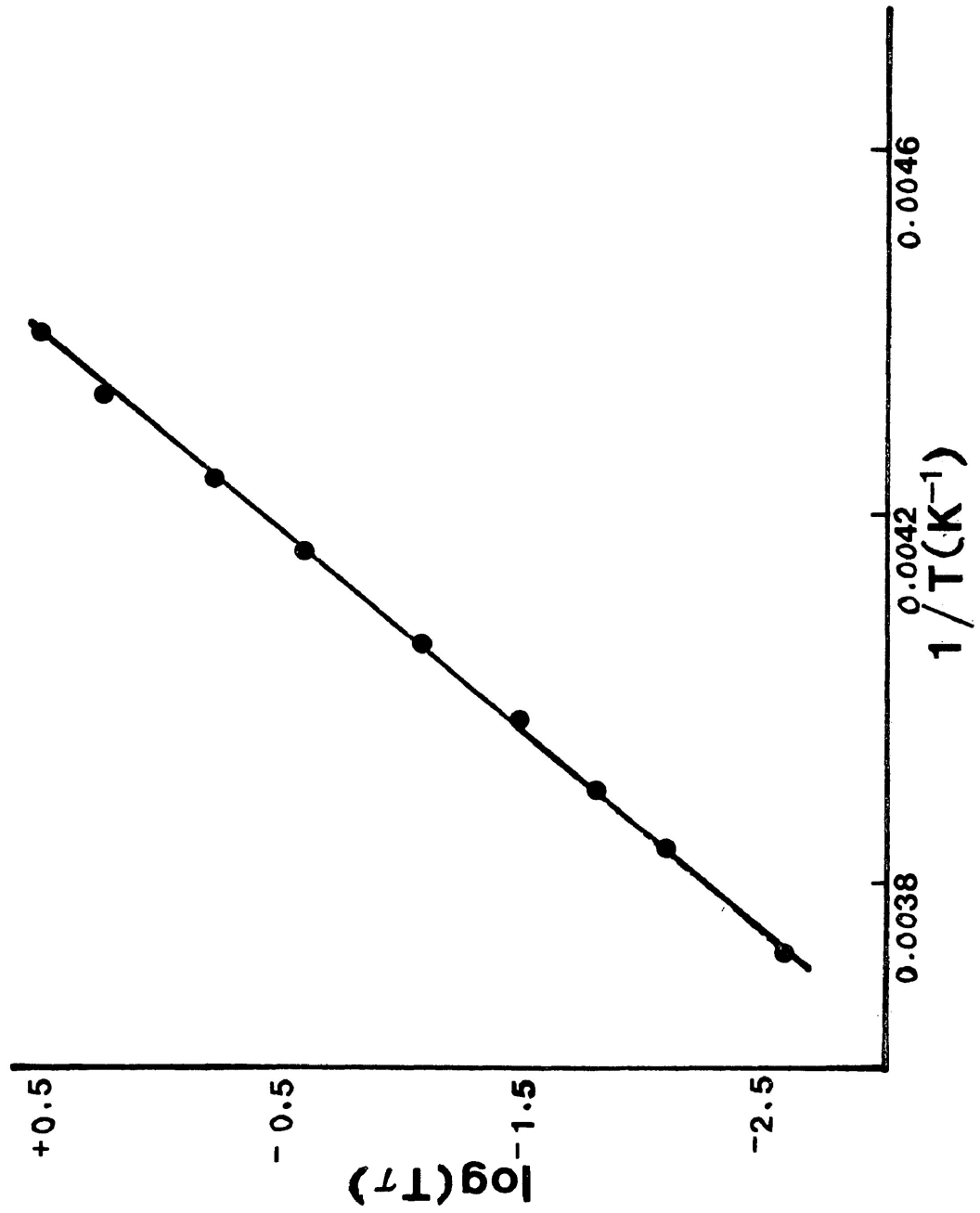


FIGURE VII.8 Plot of $\log(T\tau)$ versus $1/T (\text{K}^{-1})$ for dimethyl-2,6-naphthalene dicarboxylate in polystyrene matrices (High temperature process)

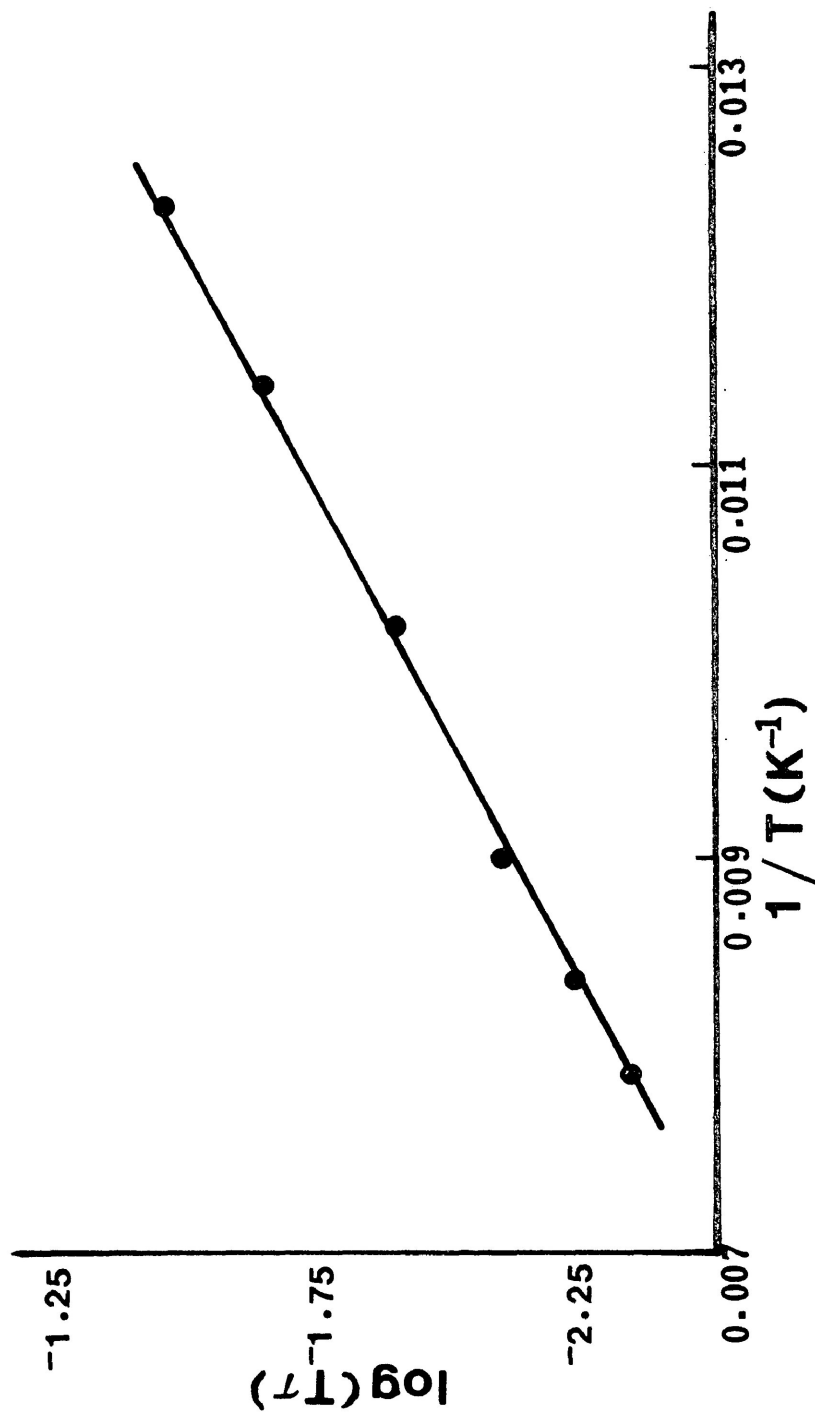


FIGURE VII.9 Plot of $\log(T\tau)$ versus $1/T (\text{K}^{-1})$ for α -naphthyl acetate in polystyrene matrices (Low temperature process)

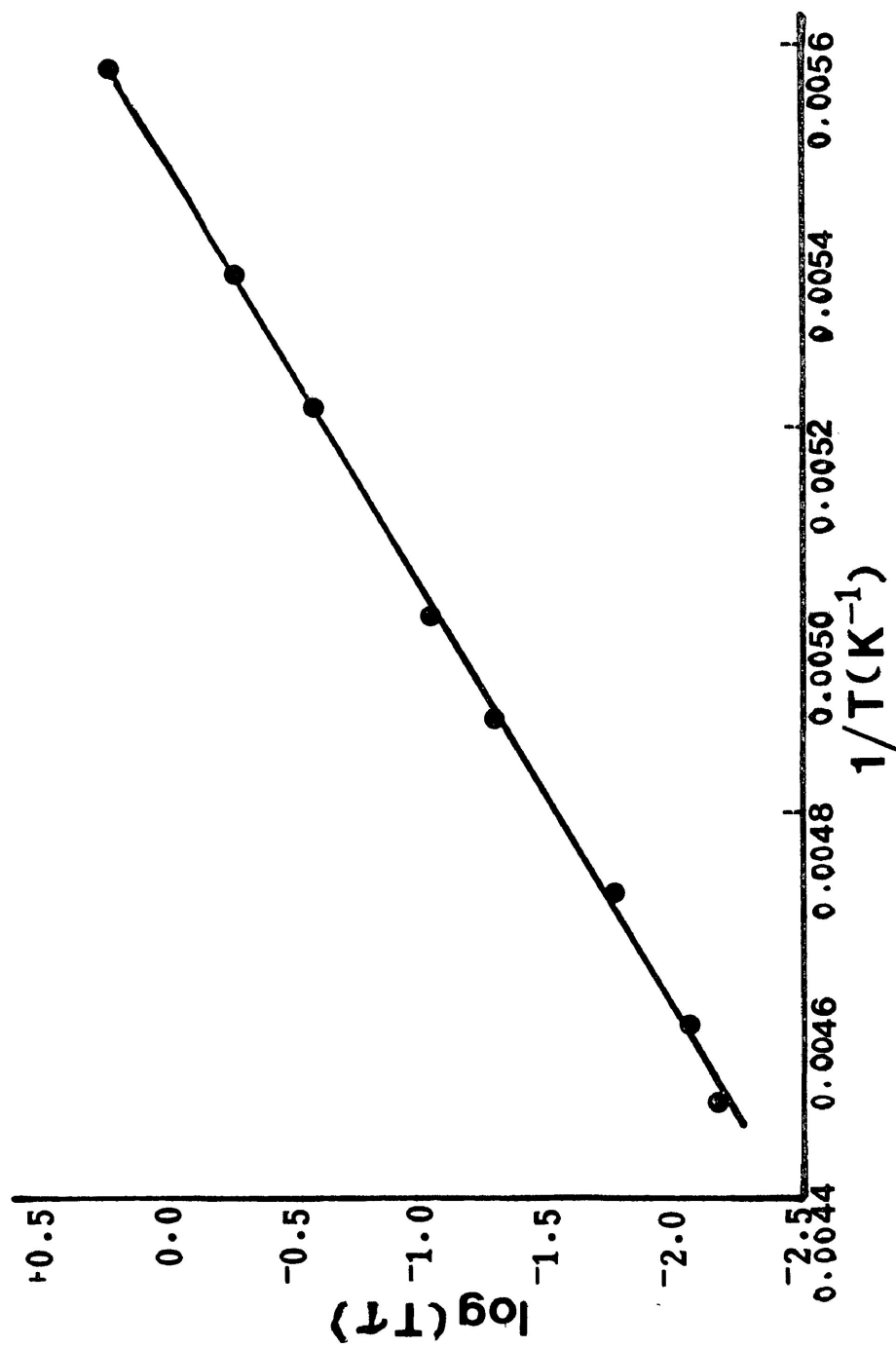


FIGURE VII.10 Plot of $\log(T\tau)$ versus $1/T$ (K^{-1}) for α -naphthyl acetate in polystyrene matrices (High temperature process)

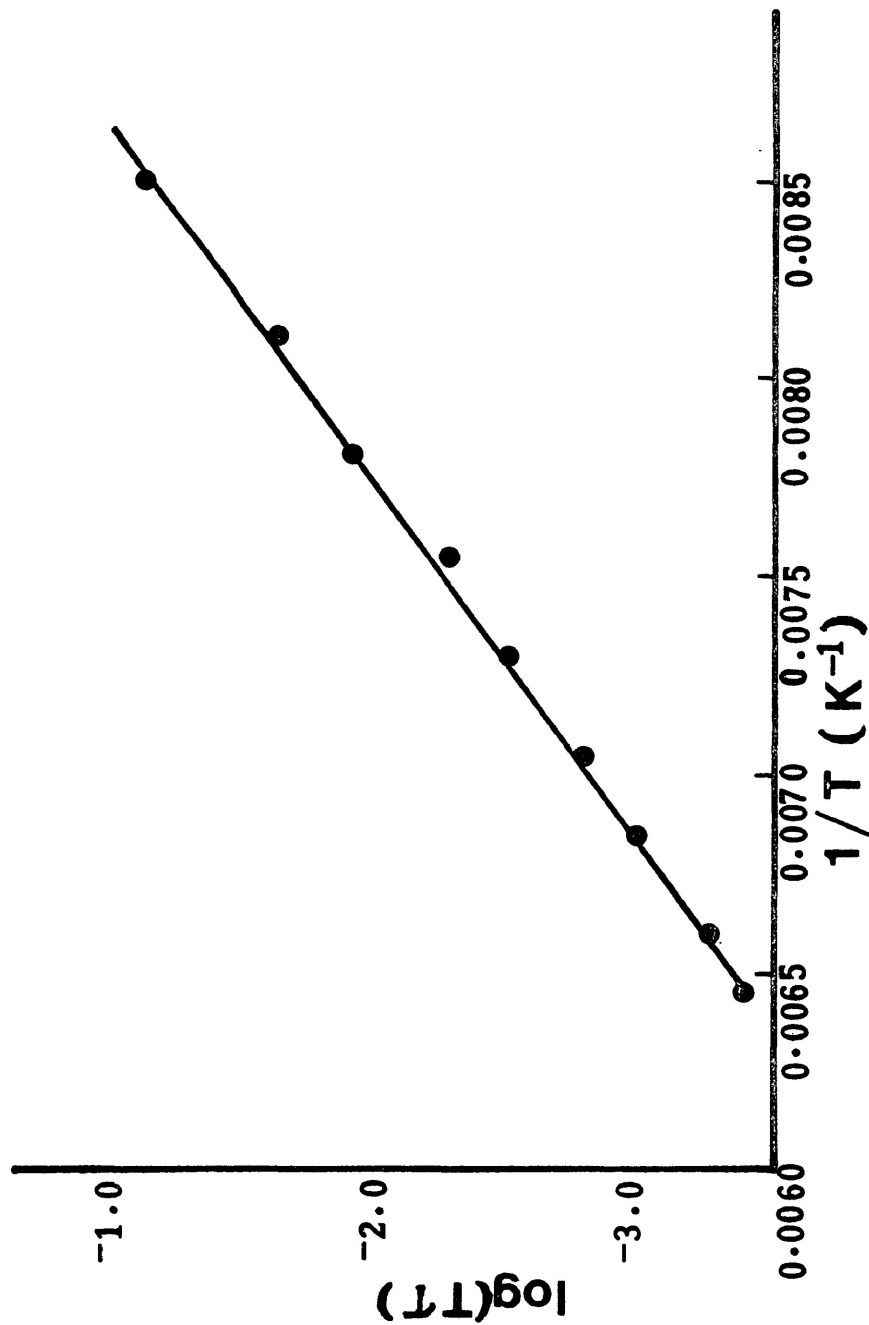


FIGURE VII.11

Plot of $\log(\tau)$ versus $1/T \text{ (K}^{-1}\text{)}$ for cyclohexyl acrylate in polystyrene matrices (Low temperature process)

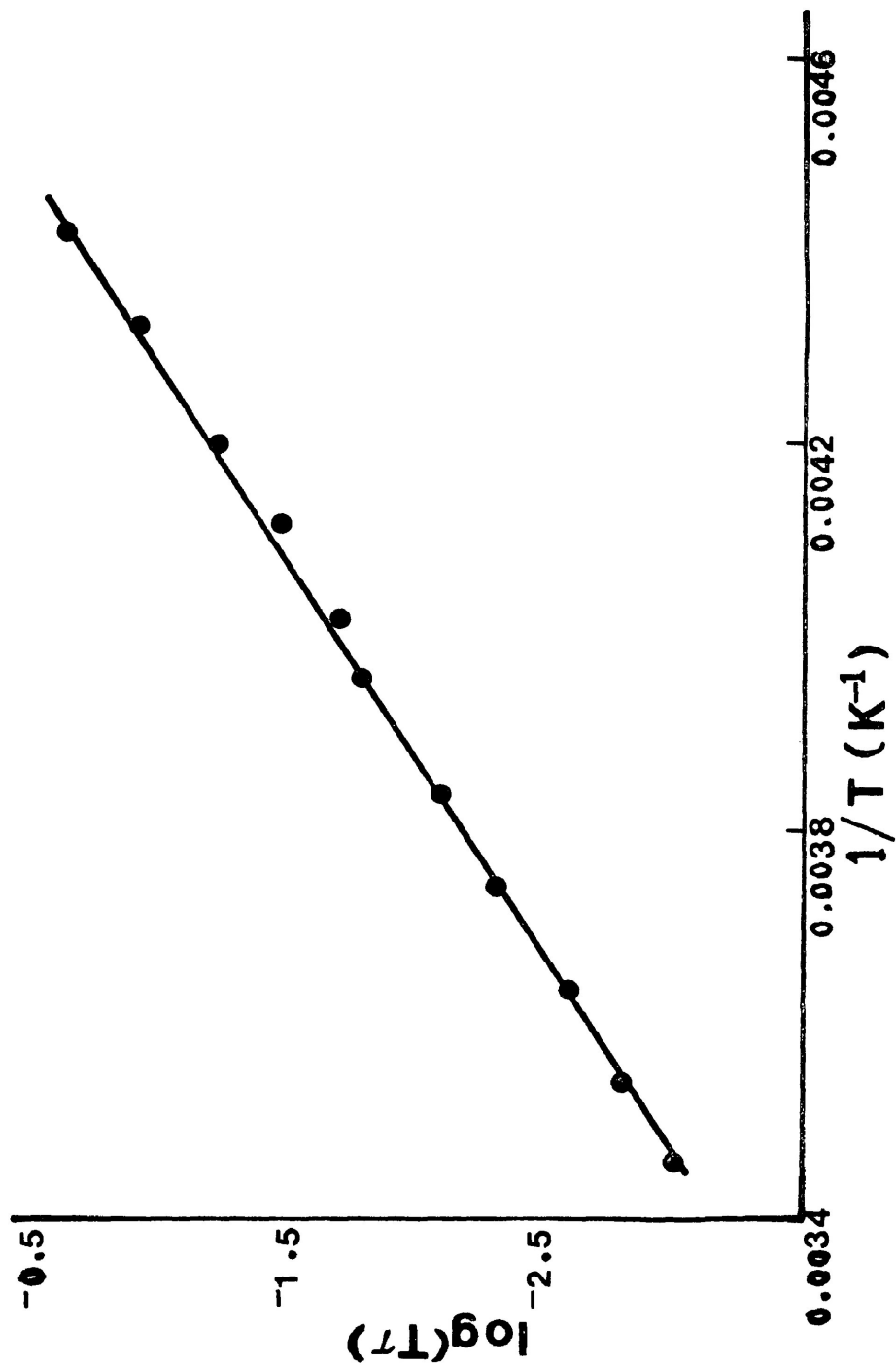


FIGURE VII.12

Plot of $\log(\tau)$ versus $1/T \text{ (K}^{-1}\text{)}$ for cyclohexyl acrylate in polystyrene matrices (High temperature process)